Influenza A Virus Interaction with Complement Factor H

A thesis submitted for the degree of Doctor of Philosophy

By

Iman Hussein Rabeeah

In

Department of Life Sciences

College of Health, Medicine and Life Sciences

Brunel University London

And

The Pirbright Institute

November 2020

Acknowledgements

My profound gratitude goes to Allah, the Almighty God for wisdom and strength, that sustained me throughout this research. Thank you, God, for never leaving me.

My heartfelt thanks go to my husband, Sadiq, for his support, patience, love, prayer and being there for me. Without him, none of this would have been possible. Dear, for sticking with me, I owe you forever. My special appreciation to my sweet children, Noor, Mohammed, Zahraa, and Abbas for their patience. I know I have not been the easiest to be around at times. I am forever appreciative.

I would like to acknowledge my supervisors: Dr Holly Shelton, and Professor Venugopal Nair at the Pirbright Institute and my principal supervisor at Brunel University, Dr Ansar Pathan for their guidance and support.

It would not have been possible to complete this thesis without the help and support of the Director of Postgraduate Research Programmes in the Department of Life Sciences, Dr Predrag Slijepcevic and the PGR Office members: Amanda castle, Joanne Musgrave, and Marie Webb, I am extremely grateful.

I would like to express my deep and sincere gratitude to my sponsor, the Iraqi Ministry of Higher Education and Scientific Research and the University of Basra for giving me the opportunity to undertake this research in the UK and for the provision of financial support.

I would also like to thank my friend Dr Zainab Jawad for her wonderful help during this long journey. To Dr Zainab, I am particularly grateful. Also, Dr Suha and Dr Suleman for their valuable advice at Brunel University London.

I would like to extend a special thanks to Dr Miroslava Novakova for her help and advice.

Finally, my sincere thanks to my brother Ismail who has been there throughout my PhD providing emotional support.

Apologies if I missed anyone out who supported me and thank you from the bottom of my heart.

Declaration

I declare that the research presented in this thesis is wholly my own work, except where otherwise specified, and has not been submitted for any other degree or qualification to any other academic institution.

Iman Hussein Rabeeah

Abstract

Influenza A virus (IAV) is a major causative agent of respiratory tract infection in humans. Human IAVs cause seasonal epidemics, whilst avian IAV strains sporadically cross the host range barrier leading to zoonotic infections. The complement system is a component of the innate immune system that acts to remove pathogens including IAVs. Many pathogens have been reported to actively target components of the complement system to ensure their survival within the host. Therefore, this thesis aims to understand if there is an interaction between IAV and factor H (FH), a critical inhibitor of the complement system and what effect any interaction may have on IAV replication.

Direct interaction between purified human FH protein and purified human H1N1 and H3N2 IAVs and avian H5N3 and H9N2 IAVs, was assessed. An interaction does occur between FH and all the IAV strains tested, and this interaction is mediated by the viral HA and NA surface protein, but not the viral M1 protein. Several technical approaches were performed to confirm that the HA protein mediates IAV binding to FH. Deglycosylation of purified IAV and FH revealed that the interaction of IAV with FH is a protein-to-protein interaction and mediated by protein to carbohydrates. Moreover, removal of glycans increased the ability of HA protein to bind to FH. IAV-FH interaction site mapping was undertaken using different fragments of recombinant FH protein and a panel of biotinylated HA peptides from of H1N1 and H3N2 IAVs. IAV binding to FH occurs in two regions on the surface of the FH protein: domains 5-7 and 15-20. Molecular characterizations of HA binding sites on the surface of the H1 and H3 HA proteins that are involved in the interaction with FH revealed that FH binds to 130-loop and the surrounding area, as well as with residues between 190-helix and 220-loop in RBS pocket of the HAs. Moreover, FH also interacts with several residues involved in fusion peptide pocket in HA1 or HA2 in both H1 and H3 HA protein.

Interestingly the interaction has divergent effects on the replication of the IAV strains, marginally enhancing human H1N1 replication and dramatically restricting H3N2 replication in human A549 and THP-1 cells whilst having no effect on the replication of avian H5N3 or H9N2 viruses. The role of FH at the entry stage of IAV infection in A549 cells was analysed using a variety of different methods and this revealed that FH slowed down but did not completely inhibit H1N1 virus entry during the early stage of the replication cycle, while it completely prevented the entry of H3N2 into A549 target cells. Overall, these findings indicate that different subtypes of human and avian IAVs have binding ability to human FH that reveals a different effect on IAV replication for various strains.

List of Contents

List of Figures

Chapter 1.

Chapter 2.

Chapter 3.

Chapter 4.

Chapter 5.

List of Tables

Chapter 1.

Chapter 2.

Chapter 4.

Abbreviations

AP	Alternative pathway
ATP	Adenosine triphosphate
BSA	Bovine serum albumin
CH	Cholesterol
CNBr	Cyanogen bromide
CPE	Cytopathic effect
CRM1	Cellular chromosomal maintenance 1
cRNP	Complementary ribonucleoprotein
DMSO	Dimethylsulphoxide
dsRNA	Double-stranded RNA
FBS	Fetal bovine serum
FHL-1	Factor H like-1 protein
FHR	Factor H related protein
GAG	glycosaminoglycan
Gal	Galactose
h	Hour
H_2O	Sterile deionised water
HA	Haemagglutinin
HA	Haemagglutination assay
HAU	Haemagglutinin unit
HCl	Hydrochloric acid
HI	Haemagglutination inhibition
HIV	Human immunodeficiency virus
IAV	Influenza A virus

IFN	Interferon
IL	Interleukin
IP	Immunoprecipitation assay
L	Litre
M 2	Matrix 2
M l	Matrix 1
mAb	Monoclonal antibody
MAVS	Mitochondrial antiviral signalling
MBL	Mannose-binding lectin
MDCK	Madin-Darby canine kidney
mg	Milligram
min	Minute
ml	Millilitre
MOI	Multiplicity of infection
MOI	Multiplicity of infection
mRNA	Messenger ribonucleoprotein
NA	Neuraminidase
NEP	Nuclear export protein
NP	Nucleoprotein
NS1	Non-structural protein 1
NS2	Non-structural protein 2
NTHi	Non-typeable Haemophilus influenzae
ºC	Degree Celsius
PAb	Primary antibody
PAMPs	Pathogen associated molecular patterns
PB1	Polymerase basic 1

PB1-F2	Polymerase basic protein 1 frame 2
PB2	Polymerase basic 2
PBS	0.01 M Phosphate buffered saline
PBSTM	PBS tween milk
Pen/Strep	Penicillin/Streptomycin
PFU	Plaque forming units
RBC	Red blood cells
RBS	Receptor binding site
RIG-I	Retinoic acid-inducible gene-I protein
RLU	Relative luminescence unit
RNA	Ribonucleic acid
RT	Room temperature
SAb	Secondary antibody
SD	Standard deviation
SDS-PAGE	Sodium dodecyl sulphate polyacrylamide gel
TEMED	Tetramethylethylenediamine
TLR	Toll-like receptor
TNFα	Tumour necrosis factor-α
TPCK-Trypsin	trypsin treated with N-tosyl-L-phenylalanine chloromethyl ketone
TRBC	Turkey red blood cell
TRIM25	Tripartite motif-containing protein 25
vRNPs	Viral ribonucleoprotein complex
WHO	World Health Organisation

Chapter 1: Introduction

1.1 History of IAV

Influenza viruses pose a great threat to human and animal health. They cause annual influenza epidemics and occasional pandemics, leading to high rates of morbidity, mortality, and enormous economic repercussion. For centuries, epidemics and pandemics of influenza have been occurring as described in Greek writings from 412 BCE which is what historians of medicine believe may be an influenza pandemic (Kuszewski & Brydak, 2000). Influenza epidemics were first reported in the 10^{th} and 11^{th} centuries, where it is most likely that the symptoms described in 1173–4 were symptoms of influenza. However, this outbreak of influenza was not considered a pandemic (Potter, 2001). It is agreed that the first influenza pandemic occurred in 1580 (Potter, 2001; Daly *et al*., 2007). This pandemic started in Asia and within six months reached Africa and Europe, later the infection spread to the Americas (Pyle, 1986). The first report on "influenza" was documented in the scientific literature in 1650 (Potter, 2001). Influenza virus was first isolated in 1901 from chickens infected with fowl plague, which was later diagnosed as influenza in 1955 and recently classified as H7N7 (Shahab & Glezen,1994). The first influenza virus was isolated from swine by Richard Shope in 1930 (Van Epps, 2006). Two years later, the first human influenza virus was isolated in 1933 and successfully transmitted to ferrets by Wilson Smith, Christopher Andrewes and Patric Laidlow (National Institute for Medical Research, London) (Kuszewski & Brydak, 2000; Hannoun, 2013). The first avian influenza virus was isolated after propagation in embryonated chicken eggs by Burnet in 1938. Amplification of the influenza virus in embryonated chicken eggs promoted extensive studies to understand the characteristics of the virus, especially for research that need large quantities of virus and allowed the development of novel drugs and vaccines. This technique led to the production of the inactivated influenza vaccines in the 1940s. Haemagglutination, the ability of the virus to bind to red blood cells holding them in suspension, is another technique that Hirst discovered in 1940, which then facilitated serological experiments with influenza viruses (Glezen & Couch, 1997; Treanor, 2014). The H1N1 global pandemic of 1918, which killed nearly 50 million worldwide remains, a tragic warning of the impact of influenza viruses may have on human health (Taubenberger & David, 2006; Sriwilaijaroen & Suzuki, 2012). It is clear that more extensive research is required to understand influenza epidemiology, transmission, pathogenicity, genomics, receptor binding interactions, host immune factors that modulate influenza replication to develop novel vaccines, therapies and diagnostic methods to better prepare for an unpredictable pandemic (Morse, 2007).

1.2 Classification and nomenclature

The name influenza came from the Latin word Influentia, or "influence" as people in the ancient times believed that the disease was caused by the influence of a star (Broxmeyer, 2006). Influenza viruses are enveloped viruses which belong to the family Orthomyxoviridae. They are classified into four genera, A, B, C, and D based on the diversity of their core proteins, the nucleoprotein (NP) and matrix (M l). Influenza B and C viruses mainly infect humans, causing seasonal epidemics. Influenza D virus was first isolated from pigs, but cows are the natural reservoir. Human infection by influenza D virus has not been reported to date, although ferrets, the gold standard animal model for human IAV infectivity studies, were infected with and transmitted influenza D virus. IAVs infect humans and a wide range of avian and mammalian hosts, Only IAVs have caused pandemics (Wu *et al*., 2014; Su *et al*., 2017; Sreenivasan *et al*, 2019).

The IAV genome undergoes high mutation rates ranging from 1×10^{-3} to 10^{-4} substitutions per site per year. This is due to the lack of proofreading activity of the viral RNA polymerase complex, leading to variations in virus antigens (Shao *et al*., 2017). Minor changes in the amino acid sequence of surface protein HA and NA are referred to as antigenic drift. These changes occur frequently, causing influenza epidemics by evading host immune recognition. Antigenic shift refers to the ability of IAV to undergo reassortment (rearrangement of genetic material), because of the segmented nature of the IAV genome. The scenario where two divergent IAV enter the same cell allows in theory for the substitution of genetic segments between the viruses causing novel genetic constellations to arise. Such changes may have major impacts on the antigenicity of the IAV and in addition virulence and pathogenicity of the virus. These mutated viruses could lead to a novel subtype capable of causing a global pandemic. Based on these frequent changes in the genomic structure, IAVs are classified into different subtypes and clades (Krammer *et al*.,2018). 16 antigenic subtypes of haemagglutinin (H1-H16) and 9 antigenic subtypes of neuraminidase (N1-N9) have been found in IAV isolated from wild waterfowl and poultry throughout the world (Figure 1. 1). The new H17/H18 and N10/N11 subtypes were recently isolated from bats (Tong *et al*., 2012, 2013; Wu *et al*., 2014). Within the subtypes, IAVs are named as strains, such as the A/California/7/2009 strain. The name begins with the type of antigen (A), followed by the host of origin (e.g. duck, swine, chicken, etc.) or is left blank if the virus is isolated from a human, the site of virus isolation (California),

followed by the virus strain number (7), the year of the isolation (2009), and finally, the virus subtype (H1N1) (WHO, 1980).

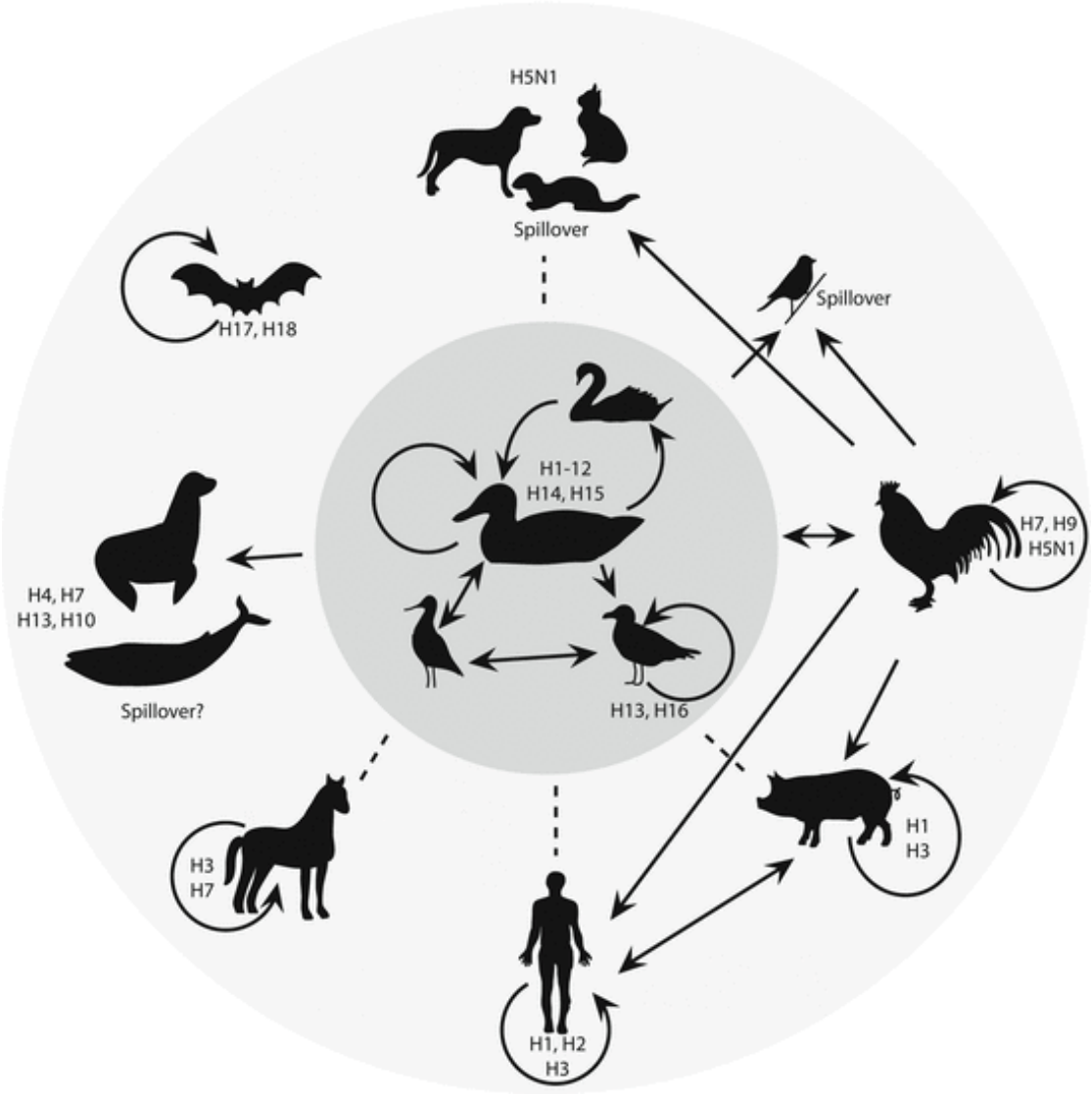

Figure 1. 1: Ecology and interspecies transmission of IAV subtypes. Representative diagram of the genetic variations of HA IAVs protein and their natural hosts, where they have been isolated. Solid arrows indicate direct transmission that has been established in the host species. Dashed arrows represent occasional or limited infection of subtypes where no continuous transmission was detected in the new host. Migratory aquatic birds (dark grey) are the largest natural reservoir of IAVs. They are the origin of a genetic shift, where pandemics emerge. Human IAVs subtypes are genetically different from avian IAVs subtypes. They do not cause efficient infection for both species. Due to the host species barrier, it is difficult for avian IAVs to transmit from birds to humans directly. However, pigs can be infected with both viruses, acting as "mixing vessels" that facilitate the transmission of avian IAVs from the wild bird into other species such as humans and other mammals, causing the emergence of influenza pandemics. All four IAV pandemics in the past century (1918 H1N1, 1957 H2N2, 1968 H3N2, and 2009 H1N1) arose in whole or in part from non-human origin were related to the genetic recombination of avian or other IAV. Poultry can also spread avian viruses such as H5N1 to the humans by direct transmission. An avian IAV could be transmitted to human by genetic reassortment between avian and human viruses. If the host cell infected with both avian and human IAV subtypes, genetic reassortment could occur to produce a new subtype of IAV with a novel combination of genes. IAV transmission between bats and other host groups is unknown (Wille *et al*., 20017).

1.3 IAV virion structure

IAV is surrounded by a lipid bilayer derived from the plasma membrane of the host cell and contains three transmembrane proteins (Dou *et al*., 2018). HA is the most abundant viral membrane protein at approximately 80% (around 500 molecules per virion). NA is a second glycoprotein with an abundance of about 17% of the total proteins in the viral envelopes at approximately 40-50 molecules per virion. The third protein is the ion channel matrix 2 (M2) protein which is found in low abundance on the virion surface with only 16 to 20 molecules per virion. (Samji, 2009; Dou *et al*., 2018; McAuley *et al*., 2019). Beneath the viral membrane is a dense protein layer that supports the viral envelope and encloses the core of the virion. It consists of matrix 1 (M1) protein, the most abundant component of the virus particle. (Kordyukova *et al*., 2019) (Figure 1. 2).

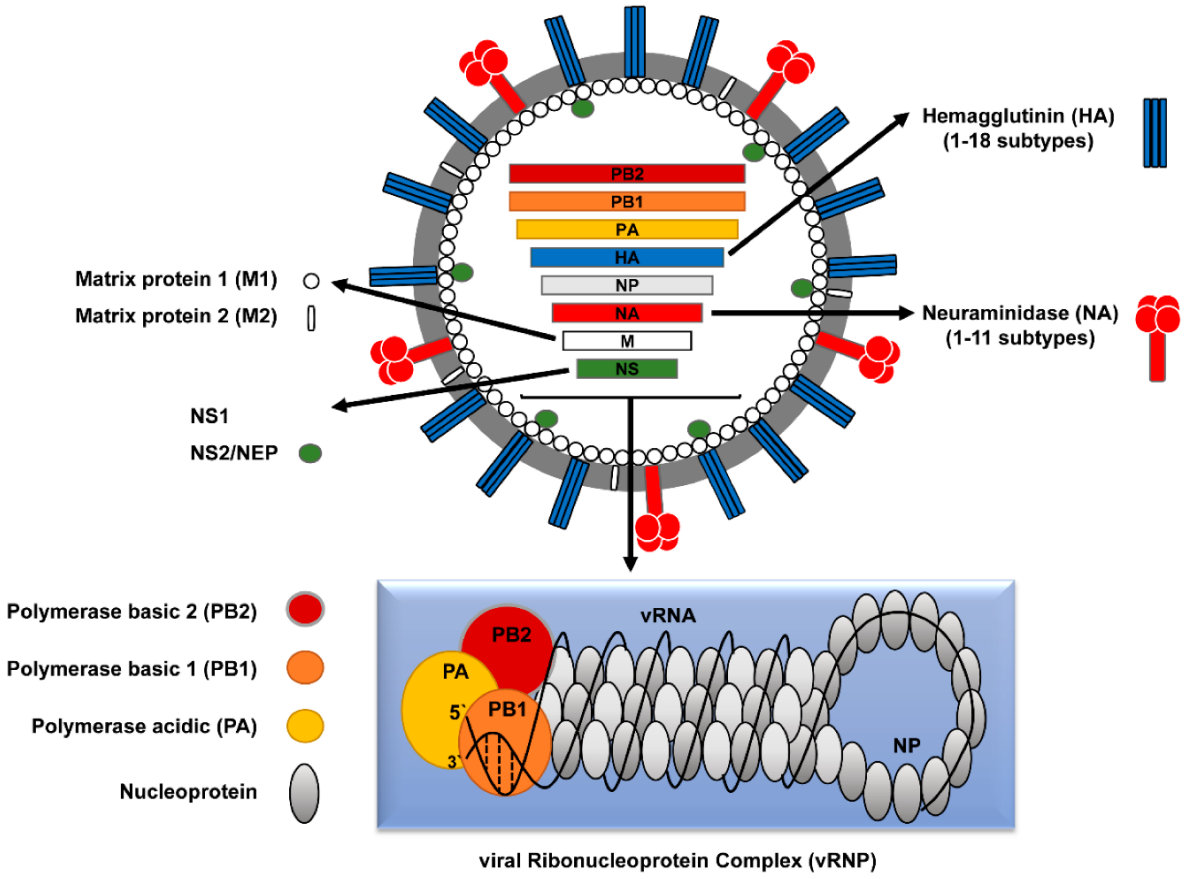

Figure 1. 2: Virion structure. The upper panel shows a whole virion of IAV. Haemagglutinin (HA), neuraminidase (NA) and the ion channel M2 are external proteins on the envelope of the virus that is derived from the host cell membrane. Matrix protein (M1) under the viral envelope. The virion core accommodates a segmented eight viral genome. The lower panel demonstrates the structure of the viral ribonucleoprotein complex (vRNP). Each vRNP consists of a viral RNA (vRNP) segment associated with three polymerase subunits (A, B1, B2), multi copies of nucleoprotein and a small amount of nuclear export protein (NEP) (Mostafa et al., 2018).

The IAV genome is presented as eight individual viral ribonucleoproteins (vRNPs). Each segment is tightly coated with multiple copies of nucleoprotein (NP) along its length. At the 5′ and 3′ termini of vRNA sits a heterotrimer of viral RNA-dependent RNA polymerase consisting of three subunits, polymerase basic protein 1 and 2 (PB1, PB2), and polymerase acidic protein (PA) (Pflug *et al*., 2017; Miyake *et al*., 2017). The virion also includes the non-structural proteins 1 and 2 (NS1 and NS2, also known as nuclear export protein, NEP) (Dawson *et al*., 2018).

1.3.1 Genome organisation

IAVs contain a segmented negative single-stranded RNA genome of about 14000 bases distributed among 8 genome segments to encode for 10 core proteins (PB2, PB1, PA, HA, NP, NA, M1, M2, NS1, and NEP) and several accessory proteins (PB2-S1, PB1-F2, PB1-N40, PA-X, PAN155, PA-N182, M42, and NS3) (Vasin *et al*., 2014). (Figure 1. 3 and table 1. 1). Viral segments are numbered according to their size starting with the largest segments denoted by number 1 that express PB2 protein and ending with number 8. Viral genome segments code viral proteins through various mechanisms. The viral proteins, PB2, PB1, PA, HA, NP, M1, M2, NS1 are expressed by canonical pathway. Segments 7 and 8 encode the splice products M2 and NEP by alternative splicing.

IAV produce accessory proteins using different strategies, such as ribosomal scanning to encode PB1-F2, N40, PAN155, whereas the PA-X protein is expressed by ribosomal skipping (Franci *et al*., 2016). Unlike other RNA viruses, IAVs replicate in the nucleus allowing the virus to exploit the host splicing machinery. Each vRNA genome segment has a semi-complimentary, highly conserved sequences at the 5′ and 3′ termini that are not involved within the coding regions called untranslated regions (UTRs). These UTRs bind together giving the vRNP a double-helical arrangement with a large, twisted panhandle structure (Figure 1. 2). This structure binds to viral polymerase and acts as a promoter for mRNA to transcribe and replicate the genome (Lenartowicz *et al*., 2016; Hutchinson *et al*., 2010).

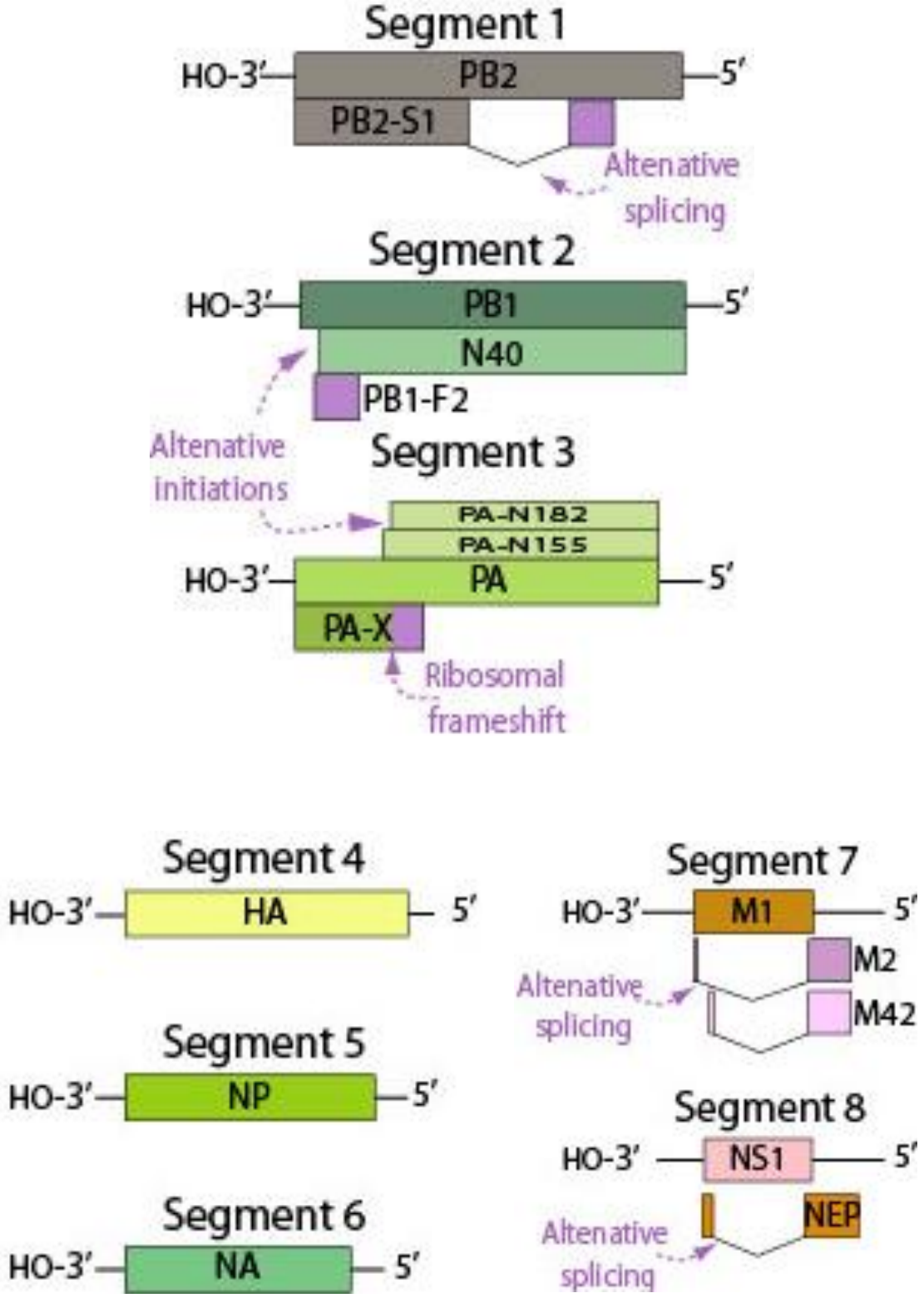

Figure 1. 3: Genome structure of influenza. Boxes represent the expressed proteins and lines at the 5′ and 3′ termini symbolise the non-coding regions. Introns of the spliced mRNAs of segments 1, 7, and 8 are shown in V-shapes (https://viralzone.expasy.org/).

Table 1. 1: The genome segments of IAV, expressed proteins and their functions (Franci *et al*., 2016; Vasin *et al*., 2016).

Gene ID	Segment	Protein Name	Encoding pattern	Protein Function
1	PB2	PB2 PB2-S1	Canonical Alternative splicing	Virus replication (cap recognition) Binds to PB1, inhibits signalling pathways
2	PB1	PB1 PB1-F2 N40	Canonical Alternative initiations Alternative initiations	Virus replication (elongation) Mitochondrial targeting and apoptosis, virulence factor Regulates PB1 and PB1-F2 expression
3	PA	PA PA-X PA-N155 PA-N182	Canonical Ribosomal frameshift Alternative initiations Alternative initiations	Virus replication (endonuclease activity) Modulates host response and virulence. Unknown Unknown
4	HA	HA	Canonical	Integral membrane glycoprotein, viral attachment, fusion function, target of antibodies neutralisation, antigenic determinant, subtype specific (H1-H18)
5	NP	NP	Canonical	Nucleocapsid protein RNA coating, nuclear targeting RNA transcription
6	NA	NA	Canonical	Surface glycoprotein, antigenic determinant, viral release from infected cells, promotion of viral entry subtype specific (N1 through N11)
7	M	M1 M2 M42	Canonical Alternative splicing Alternative splicing	Multiple roles in virion assembly and infection Membrane protein, viral uncoating, pH maintenance Can replace M2 in M2-null viruses
8	NS	NS1 NS2 NS3	Canonical Alternative splicing Alternative splicing	Multifunctional protein, INF antagonist activity Mediates RNP nuclear export Associated to new host adaptation ability

1.3.2 IAV surface glycoproteins

Influenza A virus membrane glycoproteins HA and NA are responsible for viral infection, transmissibility, specificity, affinity for the host cell, major antigenic characteristics, and pathogenic effects. HA is the most abundant surface glycoprotein of IAV. It includes a receptor binding site (RBS), which binds IAV to the target cells by binding to sialic acid receptors on the surface of the host cell to initiate the viral infection.. HA is highly immunogenic, and the variability caused by the high mutation rate enables the virus to evade neutralising antibodies. HA contains a fusion peptide that mediates fusion between viral and endosomal membranes, allowing entry of viral ribonucleoprotein into the host cell to start the replication cycle. NA protein has opposing functions to the HA protein. It cleaves sialic acids to release and allow spread of the progeny virions to complete the infectious cycle. Recently, it has been found that HA and NA work coperatively to transfer virions on the host cell surface, resulting in enhanced viral infection (Sakai *et al*., 2017). Therefore, HA and NA viral proteins are important virulence factors of IAV and monitoring their functions is required to control virus replication (Sriwilaijaroen & Suzuki, 2012; Kosik & Yewdell, 2019).

1.3.2.1 Haemagglutinin

HA is a type I transmembrane glycoprotein molecule which is present as homotrimer of 220 kDa. It is a spike-shaped protein that extends from the surface of the virus. (Figure 1. 2). It is initially synthesised as single polypeptide precursor that is glycosylated and cleaved by trypsin-like protease into sialic acid receptors binding subunit (HA1) and ectodomain (HA2) which maintains the linkage between HA1 and HA2 via the disulphide bond. This bond links both subunits at the residues 14 of HA1 and 137 of HA2 (Figure 1. 4, a) (Das *et al*., 2010; Hamilton *et al*., 2014). The HA trimer protrudes around 135Å from the viral envelope and contains two different regions: the first region is the head that contains sialic acid and the predominant antigenic binding sites and consists of HA1 molecules. The second region presents the stem, the base of the cylindrical trimeric molecules that is composed of residues from both subunits, HA1 and HA2. The stem is a core of HA2, and it forms the protein backbone. (Figure 1. 4a, b) (Cross *et al*., 2001; Das *et al*., 2010). The molecular weight of HA monomer is about 76 kDa and it is 13.5 nm in size. The name haemagglutinin is derived from its ability to agglutinate red blood cells, resulting in aggregation, or clumping of red blood cells together. This agglutination occurs by binding to the sialic acid receptors on the surface of the red blood cells. The primary function of HA is binding influenza A virus to sialic acid molecules on the host cell surface,

initiating viral infection (Nicholls *et al*., 2008; 2011; Kreicova *et al*., 2015). In spite of the fact that only H1 and H3 had caused widespread pandemics and seasonal outbreaks in humans, there are cases of humans being infected by avian HA subtypes as well: H5 (Nasreen *et al*., 2013), H7 (Guo *et al*., 2013), and H9 (Bi *et al*., 2014). HA is the primary target for neutralising antibodies, which work either by inhibiting the attachment to the host cells or interfering with conformational changes of HA, inhibiting viral and endosomal membranes fusion. (Han and Marasco, 2011).

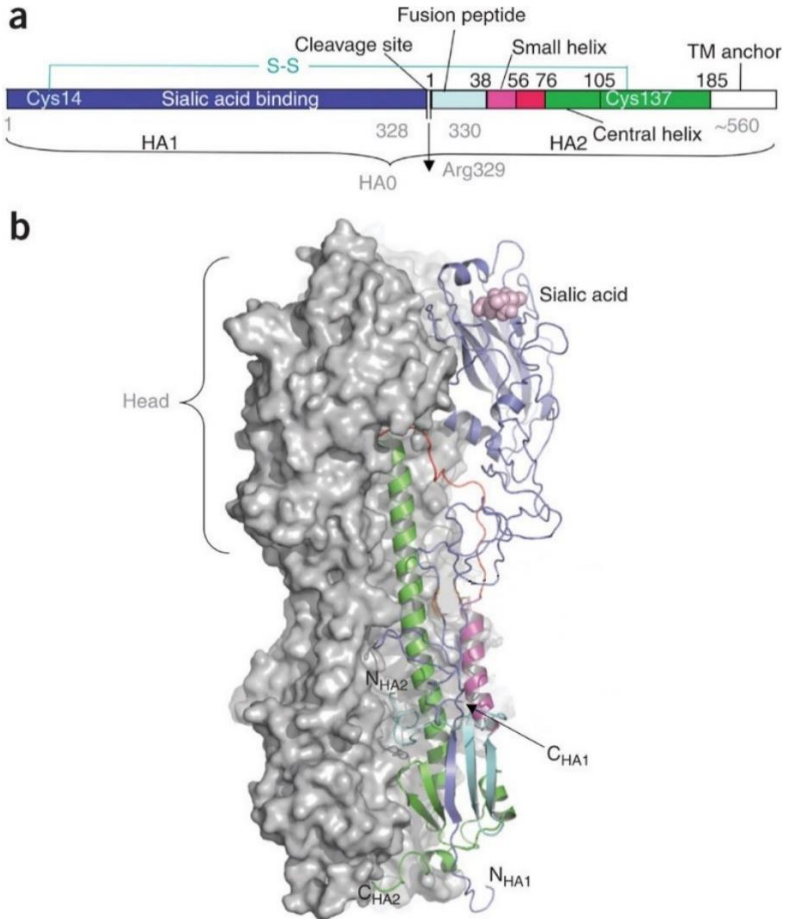

Figure 1. 4: The structure of unfolded and folded haemagglutinin of influenza A virus. **(a)** A single polypeptide chain of unfolded HA0 includes about 560 amino acids and consists of two subunits: HA1 and HA2 linked by binding residue 14 of HA1 to residue 137 of HA2 by the disulphide bond. HA1 includes sialic acid binding site (blue) in the middle of the polypeptide of unfolded HA, whereas its location in the top of the globular head region of the folded HA1which is formed completely from HA1 residues, colour coded as shown in panel a (Figure 1. 4, b). In addition to the sialic acid binding, HA1 contains neutralisation antibodies sites. HA2 is located in the stem of HA trimeric molecule and exhibits on the surface of the viral envelope and contains a fusion peptide at the N-terminal end of HA2 and a transmembrane anchor domain. **(b)** Trimeric molecule of HA protein, and two HA molecules show a folded structure, whereas the third one exists in a ribbon form. The head of the HA polypeptide chain (blue) contains all the three antigenic binding sites and is responsible for binding with sialic acid receptors. The HA head is closely connected with a central helical domain of HA2 (green). Through the fusion of viral and host cell membranes at low pH, the three HA1 molecules move away from HA2. The loop (red) which connected between the central helical domain and fusion peptide is then folded, resulting in forming a helical structure and extending the central coiled coil to expose the fusion peptide which binds to the endosome membrane to start the fusion process (Das *et al*., 2010).

1.3.2.2 Neuraminidase

Neuraminidase is a type II surface glycoprotein, which is also called sialidase. It is coded by RNA segment 6. The antigenic neuraminidase consists of three domains: the largest domain is the box-like head (Figure 1. 5, a – b) which is found as a mushroom-shaped protrusion of a homotetramer molecule, sitting on top thin, variable length stalk domain connecting to a hydrophobic sequence of the transmembrane domain (TMD) near the N-terminal that anchors the enzymatic head in the lipid bilayer of the viral envelope (Figure 1. 5, c). It is thought that the variation in stalk length among influenza virus strains is likely due to regulating the distance between the head domain and the host cell receptors (Smith et al., 2006; Da Silva et al., 2013). The enzymatic protein NA is composed of 470 amino acid residues. The four identical glycoprotein monomers (head) possess antigenic and enzymatic characteristics of viral neuraminidase (Figure 1. 5, a-b) with a molecular mass around 240 kDa and approximately 60 kDa for the monomer. The crystal structure of NA has revealed that every single subunit composes of six four-stranded antiparallel β-sheets arranged in a propeller like shape around a sixfold axis. The active site of this enzyme is located in a deep pocket on the upper corner of each monomer surface (Figure 1. 5, a), which contains a highly conservative region of amino acids from 74 to 390 across all subtypes of influenza A and B viruses (Garman & Laver, 2005; Gong & Zhang, 2007; Shtyrya *et al*., 2009).

The enzyme active site domain is stabilised at low pH and has two calcium-binding sites. The first site of calcium binding is found on the fourfold axis with moderate affinity, whereas the second site of high affinity is situated under the active site in each monomer (Figure 1. 5, b). In the calcium ion site, the calcium cation binds the carboxylate side chain of Asp324 and the carbonyl O atoms of Asp293, Gly297, and Asn347. This binding results in hiding the internal-facing carbohydrate side chain and therefore would be protected from the immune system pressure. The lack of this metal ion has caused sensitivity of the monomer towards the protease (Burmeister *et al*., 1992; Burmeister *et al*., 1994; Lawrenz *et al*., 2010). Smith et al (2006) have shown that the absence of calcium ion leads to conformation of loops surrounding the binding site, causing changes in the substrate binding site structure and therefore this ion is important for stability and activity of neuraminidase. The NA molecule possesses eight disulphide bonds, which are conserved in all subtypes of influenza virus and one more in the N2, N8 and N9 subtypes. Amino acid sequence analysis has shown that NAs include two distinct groups; the first one of N1, N4, N5, N8 and the second group includes N2, N3, N6, N7, and N9. This

classification depends on the difference in the three-dimensional shapes of their active sites (Shtyrya *et al*., 2009; Wu *et al*., 2014).

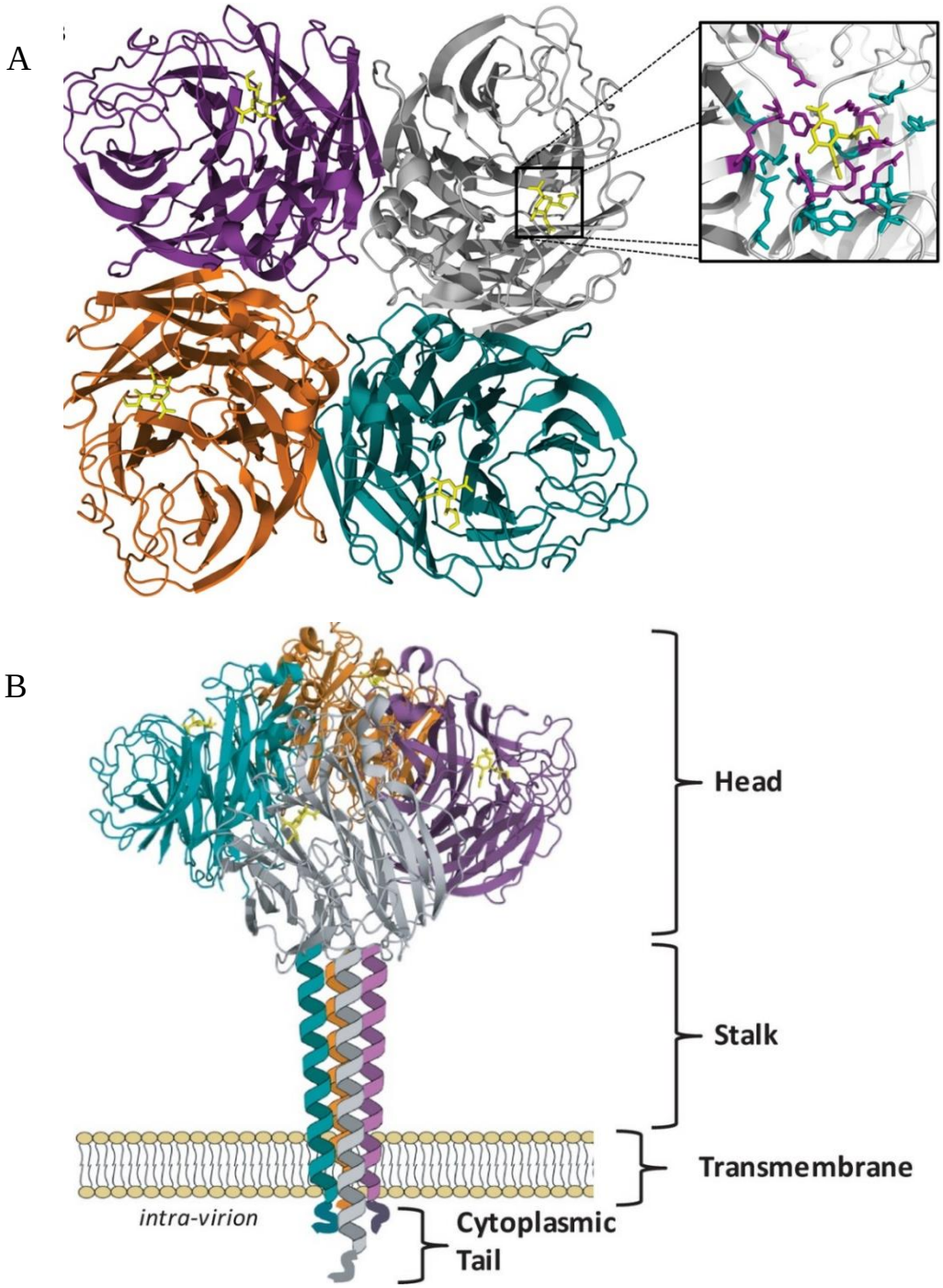

Figure 1. 5: The structure of influenza A virus neuraminidase. (A) The NA head consists of the propeller-like structure with six blades. Each blade includes four anti-parallel β-sheets that are connected by disulfide bonds. The Sialic acid binding site is shown in yellow on the head of each monomer. The magnified boxed region demonstrates the active site containing receptor-binding pocket to which sialic acid (yellow molecule) binds. **(B)** The mushroom-like structure illustrates the enzymatic head domain and the stalk domain (McAuley *et al*., 2019).

The enzyme neuraminidase is an exo-glycohydrolase which cleaves the α-ketosidic linkage between the terminal sialic acid (N-acetylneuraminic) acid and the sugar residue, resulting in essential effects on the spread of progeny virions in the respiratory tract (Gong & Zhang, 2007; Shtyrya *et al*., 2009). First, it cleaves the sialic acid from respiratory tract mucin, cilia and glycocalyx to facilitate virus access to the target cells and therefore it plays an important role in virus invasion of the ciliated epithelial cells of human airways (Matrosovich *et al*., 2004). Second, it prevents virus aggregation after viral release from infected cells by cleaving sialic acid from host cells and newly formed HA and NA of the progeny virions (Gamblin and Skehel, 2010; Shtyrya *et al*., 2009). Finally, there are data suggesting that NA may participate in viral fusion and cell membrane (Wagner *et al*., 2000).

1.4 IAV replication cycle

The epithelial cells of the respiratory tract, alveolar macrophages and dendritic cells are all target cells for human IAV infection. IAVs replicate inside the nucleus of host cells that they infect; hence, they need to enter and move between different cell compartments to deposit their genome into the nucleus for replication. Figure 1.6 presents an overview of the IAV life cycle, which is discussed in detail below**.**

1.4.1 Attachment, entry, and fusion

To initiate infection, IAVs bind to sialic acids on the surface of host cells via the viral HA protein. The nature of the glycosidic linkage between the terminal sialic acid and the galactose of the glycans on the surface of the host cell plays an important role in the specificity of receptor binding site on HA protein. Human IAVs recognise the α 2,6 linked sialic acids found on the surface of the cell membrane in the human upper respiratory tract (Figure 1. 7, A) (Skehel & Wiley, 2000; Samji, 2009), whereas avian IAVs have a predominant preference for sialic acid linked in an α 2-3 linked configuration. The HA precursor (HA0) is subsequently cleaved by extracellular proteases into HA1 and HA2 (Huang *et al*., 2003). Upon binding of HA to sialic acid, the virus is endocytosed by the host cell (Figure 1. 7, step i). The endocytosis can occur in a clathrin-dependent manner, involving dynamin and the adaptor protein Epsin-1 (Roy *et al*., 2000), or by macropinocytosis (Sieczkarski *et al*., 2002). Once the virus enters the cell, it is trafficked to the endosome until the acidification in the late endosome induces structural changes in the HA protein (shaw & Palese, 2013). The acidic environment (about pH 5) in the endosome activates the M2 ion channel, causing a considerable conformational change in HA

protein (Das *et al*., 2010). Opening of the M2 ion channel acidifies the viral core, destabilising the M1 interactions leading to the dissociation of the viral protein capsid (Bui *et al*., 1996).

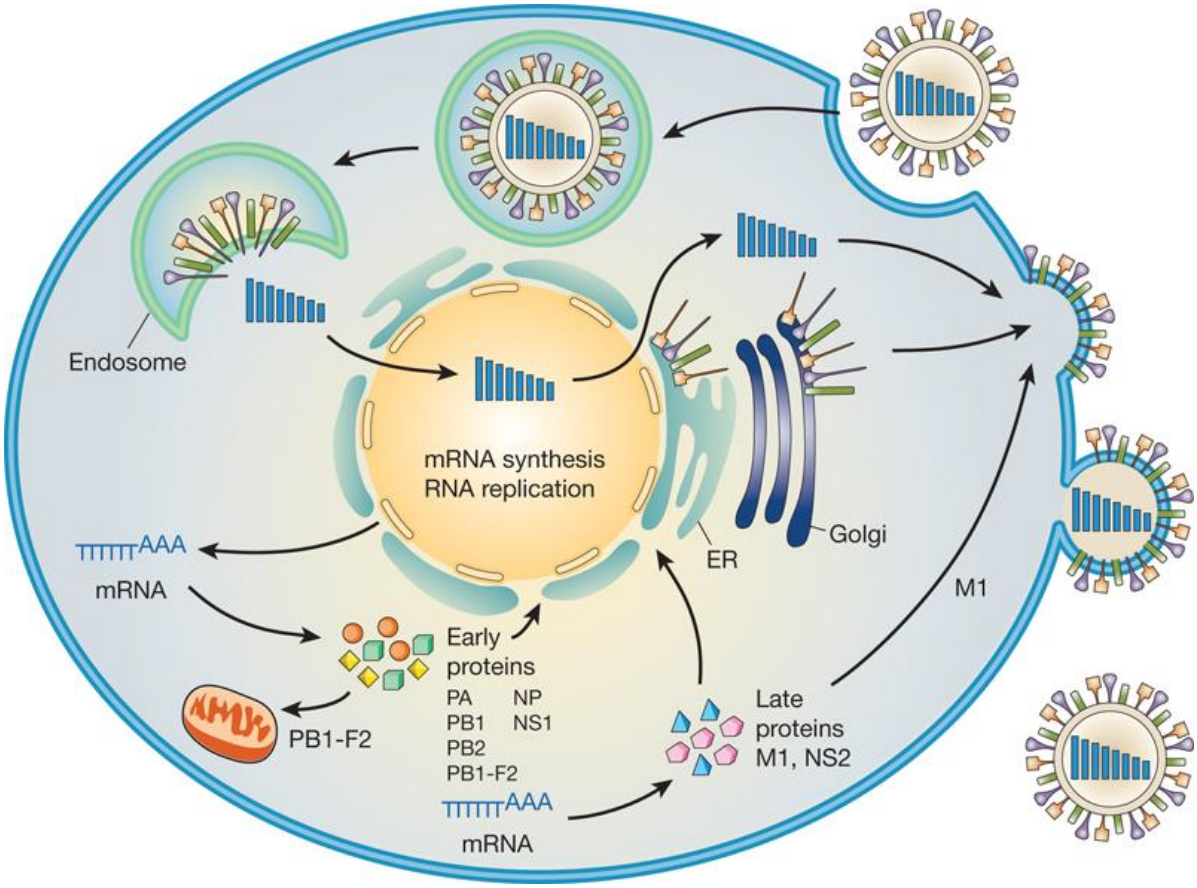

Figure 1. 6: Schematic diagram of the IAV replication cycle. The entry of the virus into the host cell occurs through the binding of HA protein to the cellular receptor. Upon binding, the virus is endocytosed by the host cell. Due to the fusion of viral and endosomal membranes, the vRNPs are then released into the cytoplasm. Then, RNPs are imported into the nucleus, where the transcription and replication occur. The synthesised viral mRNAs are exported out of the nucleus into the cytosol to translate into viral proteins, PA, PB1, PB2, NP, NS1, NS2, M1, M2, HA, and NA. These proteins either are transported to the nucleus and are involved in replication and secondary transcription or are transported with newly synthesized vRNP to the cell membrane to be incorporated into progeny viruses, which are released from the infected cell by sialidase activity of NA (Neumann *et al*., 2009). The details of each stage are described in the text.

The pH changes also lead to a massive conformational change in HA which results in the insertion of the HA fusion peptide into the endosome (Figure 1. 7, step ii "box"). This draws both the viral membrane and host membrane into proximity and thus initiating fusion of these two membranes (Figure 1. 7, step iii and iv "box"), creating a pore that enables the viral

ribonucleoprotein (RNPs) genome segments to exit into the cytoplasm of the infected cell (Figure 1. 7, step v "box") (Bui *et al*., 1996).

1.4.2 IAV genome entry into the host cell nucleus

The vRNPs transport to the nucleus of the host cells because the synthesis and processing of IAV RNAs depend on nuclear functions. Numerous studies suggest that the cytoplasmic vRNPs use the importin-α–importin-β nuclear import pathway to enable their entry to the host cell karyoplasm (the protoplasm inside the nucleus) (Figure 1. 7 B, steps vi and vii) (Chou *et al*., 2013). It is believed that the vRNPs use the nuclear localization sequences (NLS) that are localised on the surface of NP molecules to recruit the adapter protein importin-α. Once importin-α is attached to the vRNP, it is recognised by the importin-β transport receptor, which directs the vRNP to the nuclear pore complex (NPC), where it is imported into the karyoplasm (Wu *et al*., 2007).

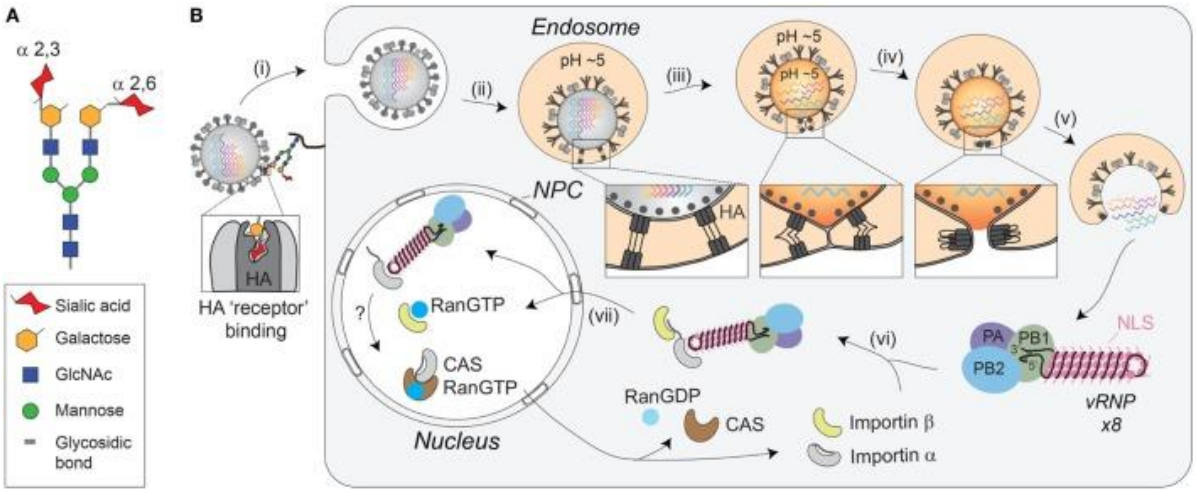

Figure 1. 7: Binding and entry of IAVs. (A) Schematic representation of a N-linked glycan. The terminal sialic acid residues are shown with an α-2,3 linkage and α-2,6 linkage. **(B)** Illustration of IAV cell attachment and entry (Dou *et al*., 2018).

1.4.3 Viral RNA transcription and replication

After entry into the nucleus, the transcription and replication of the vRNAs are carried out by the viral RNA-dependent RNA polymerase (RdRp) (Fodor, 2013; Pflug *et al*., 2017). The parental vRNPs first transcribe viral mRNA via a primer-dependent mechanism. This process needs the cap-snatching activity of the viral PB2 and PA for initiation. The PB2 subunit of viral polymerase bind to the 5′ caps of the cellular RNA polymerase II C-terminal domain (Pol II CTD). The PA subunit acts as an endonuclease domain to cleave the 5′ cap-structure plus 10–13 additional nucleotides from host cell pre-mRNAs (non-coding RNA) (Fodor, 2013). The PB2 cap-binding domain then rotates to place the newly acquired capped primer into the PB1 catalytic centre where it is elongated by using the vRNA as a template (Pflug *et al*., 2014). In the final stage of transcription, each transcript is polyadenylated through a process called reiterative stuttering in which the polymerase encounters the short poly-U sequence at the vRNA 5′ end (Figure 1. 8). It is thought that this process includes multiple cycles of dissociation, repositioning, and reannealing of the mRNA to this region of the vRNA template to accomplish the polyadenylation process (Reich *et al*., 2017). The polyadenylated mRNAs are subsequently exported from the nucleus into the cytoplasm for translation that occurs at the host cell ribosomes. The M and NS mRNA are different from other segments, where they contain splicing sites that correspond with those in the host transcripts. These sites can recruit the cellular spliceosome leading to the production of two distinct mRNAs that encode for the M2 and NEP proteins, respectively (Figure 1. 3) (Lamb Lai, 1980; Zhang *et al*., 2018).

There are two steps involved in the replication of IAV genome. The first step is the transcription of complementary RNA (cRNA (+)) produced by a primer-independent process. In this pathway, the viral polymerase employs the negative-sense vRNA as a template to transcribe the complementary positive-sense RNA (cRNA). The resulting positive-sense (+) cRNA is used in the next step as templates for transcription of the progeny vRNA (-) (Figures 1. 6) (Fodor, 2013; Pflug *et al*., 2017). The progeny vRNA then bind to the newly synthesised NP proteins and one copy of the viral polymerase complex (PB1, PB2, and PA) to produce the progeny vRNP. This latter is either used for additional replication or is exported from the nucleus to the plasma membrane for packaging into the progeny virus (York *et al*., 2013).

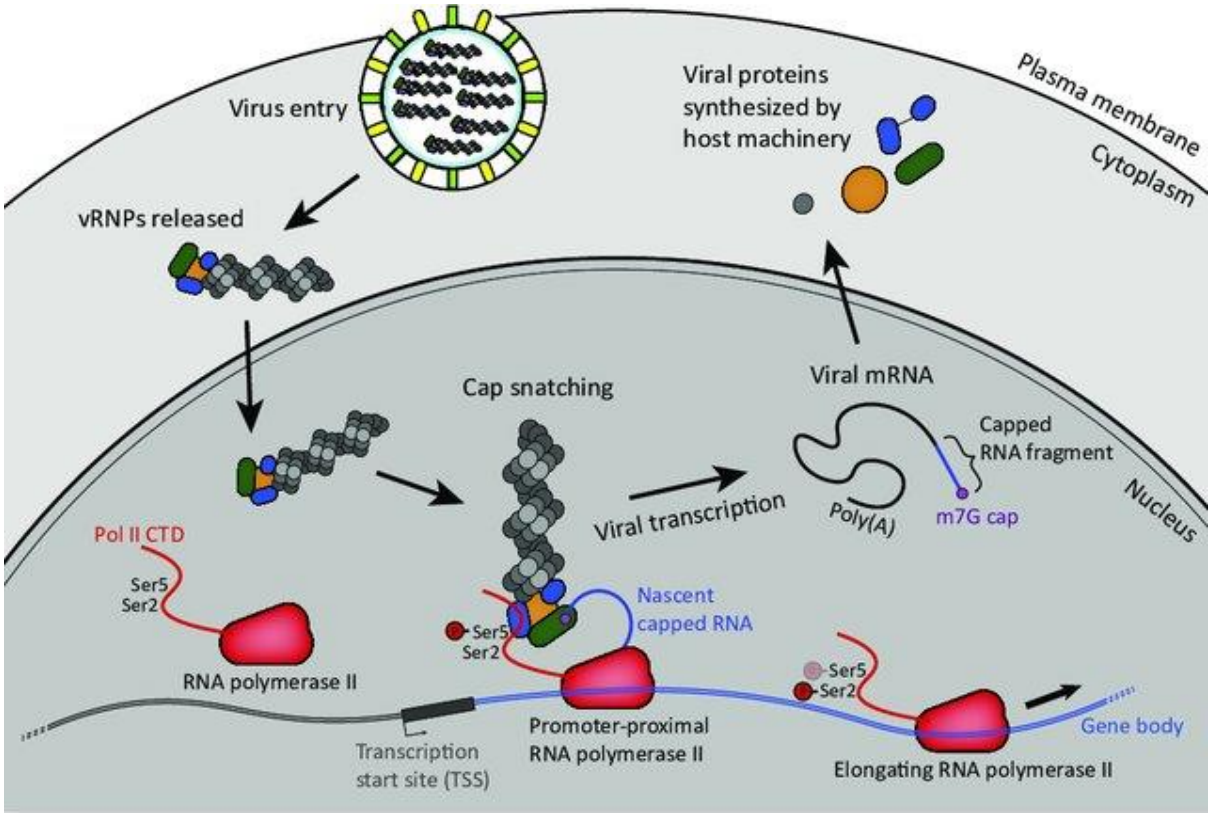

Figure 1. 8: Viral mRNA Transcription. After the vRNPs are transferred to the nucleus, they target the cellular Pol II and bind to 5′ terminal N7-methyl guanosine (m^7G) cap. The CTD of unbound Pol II is hypophosphorylated at Ser2 and Ser5. When Pol II initiates the transcription at the starting site (TSS), Ser5 is phosphorylated early in transcription. In the late stage of transcription and during the elongation, Ser2-phosphorylated and Ser5 is gradually dephosphorylated. The m^7G capped and polyadenylated viral mRNA is exported to the cytoplasm and translated by host machinery (Walker & Fodor, 2019).

The translation of IAV proteins also relies on mechanisms of the host cell. The envelope proteins (HA, NA and M2) are translated and folded on rough endoplasmic reticulum and transferred to the plasma membrane to assemble into progeny viruses. HA and NA proteins undergo glycosylation during their traffic through the endoplasmic reticulum and the Golgi apparatus to the plasma membrane (Meischel *et al*., 2020). The soluble proteins (PB2, PB1, PA, NP, M1, NS1 and NEP) are also synthesised by cytoplasmic ribosomes and can either be transferred to the plasma membrane to form newly synthesised virions or imported back into the nucleus for different functions (Figure 1. 6) (Paterson & Fodor, 2012). PB2, PB1, PA and NP bind to vRNA (-) that is used for secondary transcription and progeny vRNP formation (Lamb *et al*., 1980; Eisfeld *et al*., 2015).

The NS1 protein inhibits the cellular gene expression and prevents the type I interferon system activation (Hale *et al*., 2008). NS1 protein also promotes the translation of viral mRNAs and

may regulate the synthesis of viral RNAs (Marc, 2014). It may participate in viral mRNA nuclear export (Ayllon & García-Sastre, 2014).

1.4.4 Export of vRNPs from the nucleus

After the progeny vRNPs are assembled successfully, they can either engage in mRNA and cRNA synthesis or leave the nucleus to form the newly synthesised virions. The latter occurs via a pathway that includes the cellular chromosome region maintenance 1 protein (CRM1), which is also known as exportin-1 (Figure 1. 9). It is believed to be directed mainly by M1 and NEP proteins (Shaw & Palese, 2013; Cros & Palese, 2003; Boulo *et al*., 2007; Eisfeld *et al*., 2015). However, the interaction with the CRM1 requires a nuclear export signal (NES), which has only recently been recognised on M1 protein (Cao *et al*., 2012). This NES is thought to be used to trigger a CRM1 pathway. There is a belief that the IAV NEP protein mediates the interaction of M1-vRNP complexes with the cellular export machinery. This is because the NEP protein can bind to both exportin-1 protein and the M1 protein (Neumann *et al.*, 2000; Huang *et al*., 2013). Export of vRNPs from the nucleus is facilitated by the CRM1–NEP- M1-vRNP complex that triggers the exportin activity of the CRM1 pathway to direct vRNPs to leave the nucleus. After achieving this process, the NEP protein binds to M1 which blocks its NLS and inhibits re-entry of nascent vRNPs into the nucleus (Li *et al*., 2015).

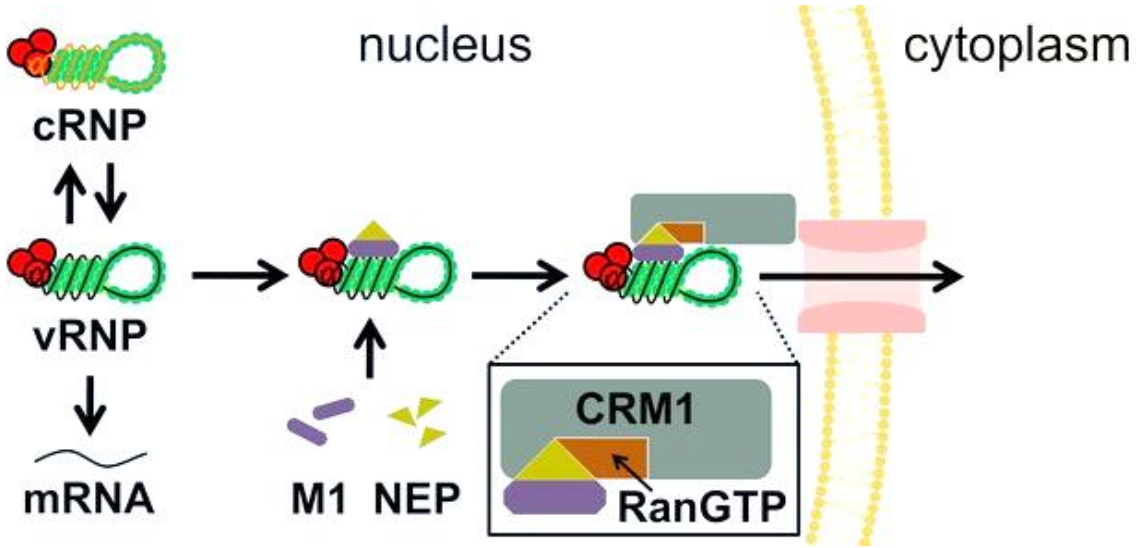

Figure 1. 9: Export of vRNPs from the nucleus to the cytosol. The CRM1 and its cofactor, the GTPase Ran mediates the export of vRNPs. NEP protein facilitates the interaction between the cellular export machinery and M1, while M1 binds to the vRNP (Heldt, 2015).

1.4.5 Assembly, budding and releasing

Compared with the lipid bilayer of the host cell plasma membrane, the IAV envelope is enriched in lipid containing cholesterol and sphingolipids (Gerl *et al*., 2012). This indicates that IAV bud from specific apical plasma membrane domains known as lipid rafts (Lingwood & Simons, 2010). IAVs have mechanisms to direct the eight vRNPs segments, as well as the newly synthesised HA, NA, M1, and M2 proteins to these domains in the membrane (Rossman & Lamb, 2011). HA and NA are thought to be directed to these domains based on fatty acid modifications that occur in the Golgi apparatus (Figure 1. 6) (Zurcher & Palese, 1994; Takeda, 2003). Unlike HA and NA, the M2 protein accumulates at the boundaries of budding domains (Rossman *et al*., 2010). It has been suggested that M1 protein is localised to the budding regions by associating with the transmembrane domains of HA and NA (short cytoplasmic tails) (Ali *et al*., 2000). This indicates that NA and HA proteins have membrane regions that include a unique lipid pattern with high affinity for M1 protein. Finally, the vRNPs are delivered to the cell periphery by Rab11 Protein, a small GTPase molecule that directs the transfer of membrane components to the cell surface. The vRNPs are thought to be localised at the budding site by binding to M1 protein (Zhang et al., 2000; Noton *et al*., 2009).

Accumulation of HA and NA proteins may contribute to bud formation by altering the membrane curvature. M1 protein may also contribute to this process by acting as a membrane-bending protein on the inner leaflet of the lipid rafts (Chen *et al*., 2010; Chlanda *et al*., 2015). During bud formation, M2 has been shown to aggregate at the neck of the budding site where it is thought to facilitate the membrane cutting process (Rossman *et al*., 2010; Rossman & Lamb, 2013).

The release of the progeny virions is highly dependent on the sialidase activity of the NA protein. NA facilitates viral release by catalysing the hydrolysis of the glycosidic linkage that binds sialic acid to the basic sugar molecules. By removing residues of sialic acid, NA prevents HA binding on the cell surface, thus facilitating virus release during budding (Figure 1. 6). The movement of IAVs from cell to cell in the respiratory epithelium is notably different from its movement between the cell lines grown in culture. This is because there are different types of cells and a mucus layer. The mucus layer acts as a protective barrier for the epithelium and is rich in heavily glycosylated mucins that can bind with IAVs and limit cell binding (Cohen *et al*., 2013). Measurement of viral movement through mucus and respiratory epithelial cells have

shown that IAV's motility through the mucus layer and their infectivity are enhanced upon NA-mediated cleavage of sialic acid from mucins (Cohen *et al*., 2013; Yang *et al*., 2014; Matrosovich *et al*., 2004).

1.5 Innate immune response to the IAV infection

The innate immune response is the first line of defence against viral infection which is rapid, but not specific. During the IAV infection, viral conserved molecules known as pathogen associated molecular patterns (PAMPs) are recognised by host pathogen recognition receptors (PRRs), like retinoic acid-inducible gene-I protein (RIG-I) and toll-like receptor (TLR), resulting in activation of innate immune signalling that eventually stimulates the production of various cytokines and antiviral components (Cao, 2016; Ouyang *et al*., 2014). These PAMPs contains certain features of viral RNA that are not involved in cellular RNAs, such as double-stranded RNA (dsRNA), uncapped single-stranded RNA (ssRNA), and viral DNA (Rehwinkel *et al*., 2010; Baum & Garcia-Sastre, 2011).

Host cells recognise pathogens by PRRs that can distinguish self from non-self-molecules within the infected cells. The ssRNA and transcriptional intermediates of IAVs in the infected host cells are recognised by the main receptors, RIG-I (Figure 1. 10). The newly synthesised RNA of IAVs in the cytoplasm of the host cells are also sensed by melanoma differentiation-associated gene 5 (MDA5) (Pichlmair *et al*., 2006). After the pathogen is recognised, RIG-I is activated, and its caspase activation and recruitment domains (CARDs) are revealed. The CARD is then modified by dephosphorylation or ubiquitination by E3 ligases, such as tripartite motif-containing protein 25 (TRIM25) (Munir, 2010). Thus, CARD-dependent association of RIG-I and downstream adaptors mitochondrial antiviral signalling (MAVS) trigger the downstream transduction signalling at the outer membrane of mitochondria (Yoneyama *et al*., 2015). This action leads to activation of the transcription factors, including interferon regulatory factor 3 (IRF3) and IRF7, and nuclear factor kappa-light-chain-enhancer of activated B cells (NF-κB), causing the release of a variety of IFNs and cytokines (Figure 1. 10) (Hiscott *et al*., 2006).

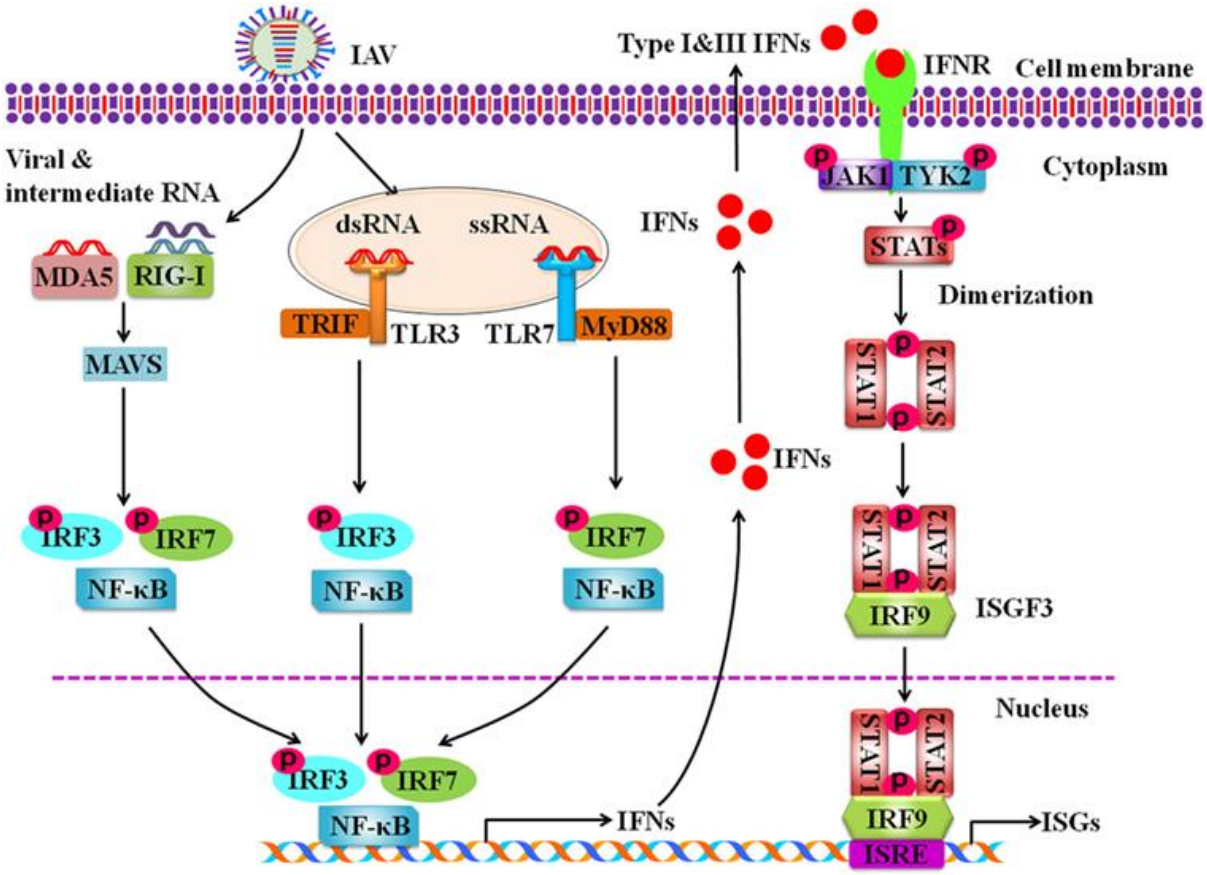

Figure 1. 10: Schematic diagram for innate immune response against IAV infection (Chen *et at*., 2018).

Toll-like receptors are highly sensitive PRRs that recognise IAVs outside and inside of the cell membrane at endosomes and lysosomes (Takeshita *et al*., 2006). The TLR1, 2, 4, 5, and 6 are expressed on the cell membrane and recognise PAMPs derived from bacteria, fungi, and protozoa. On the other hand, TLR3, 7, 8, and 9 are expressed on the surface of endosomes and lysosomes and only recognise nucleic acid of different viruses, including IAVs (Kawai & Akira, 2011; Takeuchi & Akira, 2010). During virus replication, TLR3, TLR7, and TLR8 participate in the recognition of the IAV PAMPs in the cytoplasmic endosomes. It is known that TLR3 senses dsRNA in endosomes (Goubau *et al*., 2014). Recently, it was shown that TLR3 may sense unidentified RNA structures within the phagocytosed cells infected with IAVs (Schulz *et al*., 2005). In plasmacytoid dendritic cells (pDCs), TLR7 recognises the ssRNA of the IAV virions present in the endosomes (Crozat & Beutler, 2004). The downstream signalling of TLR7 is then activated via the adaptor protein myeloid differentiation factor 88 (MyD88) in pDCs. This action activates either NF-κB or IRF7 to induce the expression of pro-inflammatory cytokines and type I IFNs, respectively (Lund *et al*., 2004).

In macrophages and DCs, TLR3 binds to TIR-domain-containing adapter-inducing interferon-β. This interaction activates the serine-threonine kinases IκKε (IKKε) and TBK1 that phosphorylate IRF3 to regulate the production of IFN-β (Le Goffic *et al*., 2007). In monocytes and macrophages, TLR8 is induced by its ligand ssRNA, resulting in the expression of IL-12. However, the relationship between TLR8 and IAV infection is not known (Ablasser *et al*., 2009).

1.5.1 Antiviral molecules engaged in innate immunity against IAV infection

During IAV infection, specific transcription factors including NF-κB, IRF3, and IRF7 are activated, causing these factors to be displaced into the nucleus (Figure 1. 10). Upon entering the nucleus, they initiate the transcription of genes encoding IFNs and pro-inflammatory cytokines such as TNF, IL6, IL1β, etc. In both virus-infected and uninfected cells, it is well known that type I IFNs, such as IFN-α and IFN-β, and type III IFNs also known as interferon lambdas (IFN-λ1, IFN-λ2, IFN-λ3, IFN-λ4) play crucial roles in the antiviral response (Chen *et al*., 2016). Infection with IAV leads to strong expression of type I and type III IFN genes (Chauhan *et al*., 2009). After the expression, IFN-α and IFN-β bind to IFN-α/β receptors (IFNAR), while IFN-λs binds to IFNL receptors (IFNLR) in an autocrine or paracrine pattern, resulting in the activation of Janus kinase signal transducer and activator of transcription (JAK-STAT) signalling pathway. Phosphorylated STAT1 and STAT2 interact with IRF9 to form an ISG factor 3 complex (ISGF3). ISGF3 moves into the nucleus and interacts with IFN-stimulated response element. This factor triggers the transcription of multiple IFN-stimulated genes (ISGs) (Figure 1.10) (De Veer *et al*., 2001). These ISGs target different steps of the IAV replication cycle. Recently, a study showed that MxA, an ISG antiviral could retain incoming viral genome in the cytoplasm of a human cell (Frieman *et al*., 2009). Interferons-induced transmembrane protein family (IFITMs) is another antiviral ISG that limit the replication of IAVs by interfering with the fusion of viral and endosomal membranes following viral attachment and endocytosis (Brass *et al*., 2009).

1.6 Complement system pathways

The innate immune response is a first line in controlling virus replication in infected hosts. The complement system is considered as an essential element in this response. Complement

components are present in human serum in high concentration (more than 1mg/ml) and consist of a group of more than 40 soluble and membrane-associated proteins (Cserhalmi *et al*., 2019), which are activated to respond to pathogen invasion and eliminate infection. The complement system not only contributes to inflammation but also stimulates the adaptive immune responses. Complement activation (Figure 1. 11) takes place through three major pathways: classical, lectin, and alternative, resulting in the formation of the central protein of the complement system, C3-convertase, an unstable protease complex, which is called C4bC2a in both the classical and lectin pathway, whereas in the alternative pathway is named C3bBb (Reid *et al*., 1981; Carroll, 2004; de Córdoba *et al*., 2004).

The classical pathway (CP) is activated by the binding of C1q with antibody - antigen complex, giving rise to activation of C1r and C1s that cleaves C4 into C4b and C4a, whereas C2 is cleaved into C2b and C2a, creating C3 convertase (C4bC2a). The lectin pathway (LP) is triggered by the interaction of mannose-binding lectin (MBL) with pathogenic carbohydrate motifs, that activates the MBL-associated serine proteases (MASPs), cleaving C4 and C2 to create the classical and lectin pathway C3 convertase. C4bC2a cleaves C3 into C3b and C3a. The C3b binds to C4bC2a, forming the C5 convertase (C4bC2aC3b) of the classical and lectin pathways. The alternative pathway (AP) is activated by spontaneous hydrolysis of C3 (C3-H_2O) into C3b. Factor D cleaves Factor B into Bb and Ba, creating the initial AP C3 convertase (C3bBb). The C3 convertase binds to C3b making C5 convertase (C3bBbC3b), which cleaves C5 into C5a and C5b. C5b then binds to C6, C7, C8, and multiple copies of C9 to form the membrane-attack complex (MAC) that leads to cell perturbation. C3a and C5a bind to the G protein that associated with cellular receptors C3aR and C5aR1, respectively, resulting in chemotaxis, vasodilation, phagocytosis, and immunomodulation effects (Figure 1.6, A) (Dunkelberger & Song, 2010; Parente *et al*, 2016, Kulkarni *et al*., 2018).

The complement system is regulated by membrane-bound and plasma proteins to avoid excessive damage by inflammation. The cofactor protein (CD46) and the decay-accelerating factor (CD55) are known as membrane regulators. Factor H, Factor I, and the C4-binding protein (C4BP) act as soluble regulators. CD55 and irreversibly dissociates C2a from C4b, as well as Bb from C3b, to inactivate C3. FH also degrades the C3b convertases (C3bBb) by dissociating Bb from C3b, whereas C4BP protein dissociates the C4b convertases (C4bC2a) into C4b and C2a (Figure 1. 6, B-1). The factor I degrades C3b or C4b, only in the presence of

the cofactors such as FH, CD46, and C4BP. (Kulkarni *et al*., 2018) (Figure 1. 11, B-2). CD59 is a membrane regulator that inhibits the MAC by preventing insertion of C8 and C9 into the membrane (Figure 1. 11, B-3). The membrane-associated receptor complement receptor 1 (CR1; CD35) is another regulator expressed on hematopoietic cells, which shows both decay-accelerating and cofactor activity.

Complement activation occurred mainly in the blood because its components are produced primarily by hepatocytes (Barnum, 2017). However, complement proteins are also known to be released locally in tissues by different cell types (Killick *et al*., 2018). Several pathogens have developed different molecular mechanisms by which pathogens evade complement attack. A common evasion strategy used by many pathogens is the recruiting of soluble complement regulators to their surfaces to provide protection from complement activation. One of these regulators is the negative regulator, the FH protein (Kennedy *et al*., 2016).

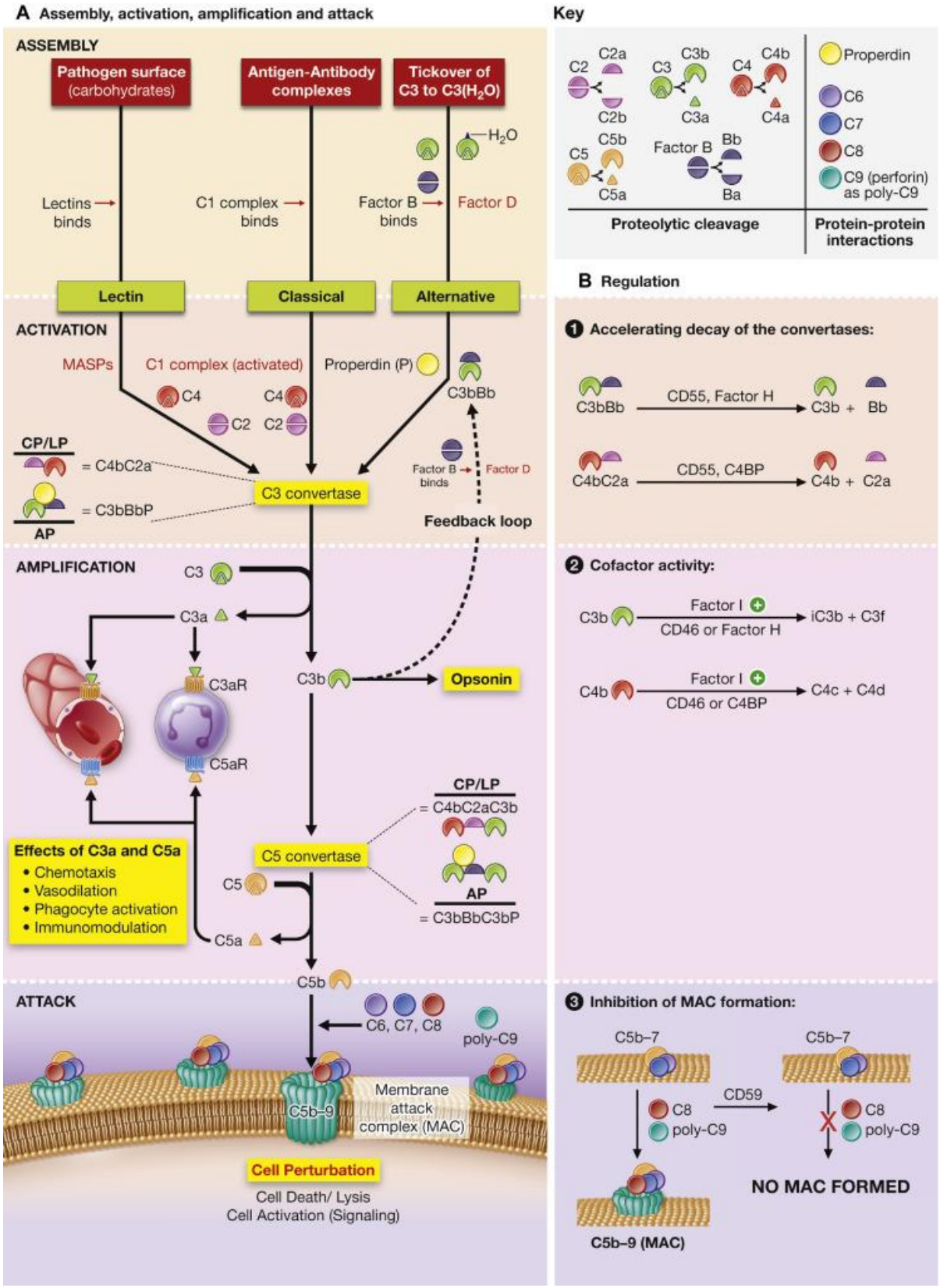

Figure 1. 11: Activation of complement system pathways. (A) Activation, amplification, and termination. complement activation can take place by three different pathways: classical (CP), lectin (LP), and alternative (AP). **(B)** Complement regulation. The complement system is regulated by membrane-bound and plasma proteins. The cofactor protein (CD46), the decay-accelerating factor (CD55), Factor H, Factor I, and the C4-binding protein (C4BP) (Kulkarni *et al*., 2018).

1.7 FH, FH-Like protein 1 and Factor H-related proteins

The first identification of FH was by Nilsson and Müeller-Eberhard (1965) as β1H globulin. FH is a monomer polypeptide plasma glycoprotein of 155 kDa. It is encoded by the single gene, located on human chromosome 1q32 in the regulators of complement activation (RCA) gene cluster (Makou *et al*., 2013). FH is mainly produced in the liver and presents in plasma at a concentration of about 200–800 μg/ml (Brandstätter *et al*., 2012). Although FH is mainly expressed in the liver, it can be also synthesised by a variety of cells including fetal tubuli, keratinocytes, skin fibroblasts, eyes, adipocytes, brain, lungs, heart, spleen, pancreas, kidney, muscle, placenta, and nerve cells (Mandal & Ayyagari, 2006). Human FH comprises of 20 repetitive units each containing 60 amino acids (Figure 1. 12), which are designated short consensus repeats (SCR) or called complement control protein (CCP) modules. CCPs 1 – 4 are identified as major binding sites for C3b or C3d as well as CCP 12 – 14 and CCP 19–20 (Pouw *et al*, 2015; Parente *et al*., 2017). The N-terminus binding site of the FH (CCPs 1 – 4) is responsible for the negative regulation of the AP. The complement FH affects the formation of the C3bBb convertase in two mechanisms. One such strategy is that FH inhibits C3bBb convertase formation by competing with factor B for binding to C3b. The second is that FH accelerates the decay of this convertase once it is already configured (decay-accelerating activity). Moreover, FH acts as a cofactor site for a serine protease factor I (cofactor activity), that inactivates C3b by cleavage of C3b to iC3b (inactivated C3b) (Figure 1. 13) (Cserhalmi *et al*., 2019). Thus, FH protects host cells that are in contact with complement. FH performs this function by discrimination between self and non-self surfaces. This ability is mostly driven by the C-terminal part (CCPs 19 – 20) of FH. These CCPs contain binding sites for C3b/C3d that is deposited on a surface, as well as for negative charge polyanionic molecules on host cells, such as sialic acids, glycosaminoglycans (GAG), heparin, and laminin. The domains 7 and 13 harbour further binding site for host markers. These CCPs can also interact with ligands such as pentraxins e.g. C-reactive protein (CRP) and PTX3, extracellular matrix (ECM) proteins, Malondialdehyde (MDA) epitopes and annexin II (Figure 1. 12). It is thought that binding of FH to these ligands direct the inhibitory activity of FH to sites of continuing complement activation and inflammation (Józsi *et al*., 2019; Cserhalmi *et al*., 2019).

FHL-1 is expressed by the complement FH gene by alternative splicing. It includes the N-terminal seven CCPs plus a unique four amino acids at the C-terminal end (Ser-Phe-Thr-Leu [SFTL]) (Misasi *et al*., 1989) (Figure 1. 12). Therefore, FHL-1 can also interact with C3b,

inhibiting complement activation. The C-terminal four amino acids have been reported to impact the interaction with CRP and PTX3 (Swinkels *et al*., 2018). Recent research suggests that retinal pigment epithelial cells in the eye can produce FHL-1 and pass the Bruch's membrane into the eye, whereas FH, due to its large size, cannot go through this membrane (Clark *et al*., 2014).

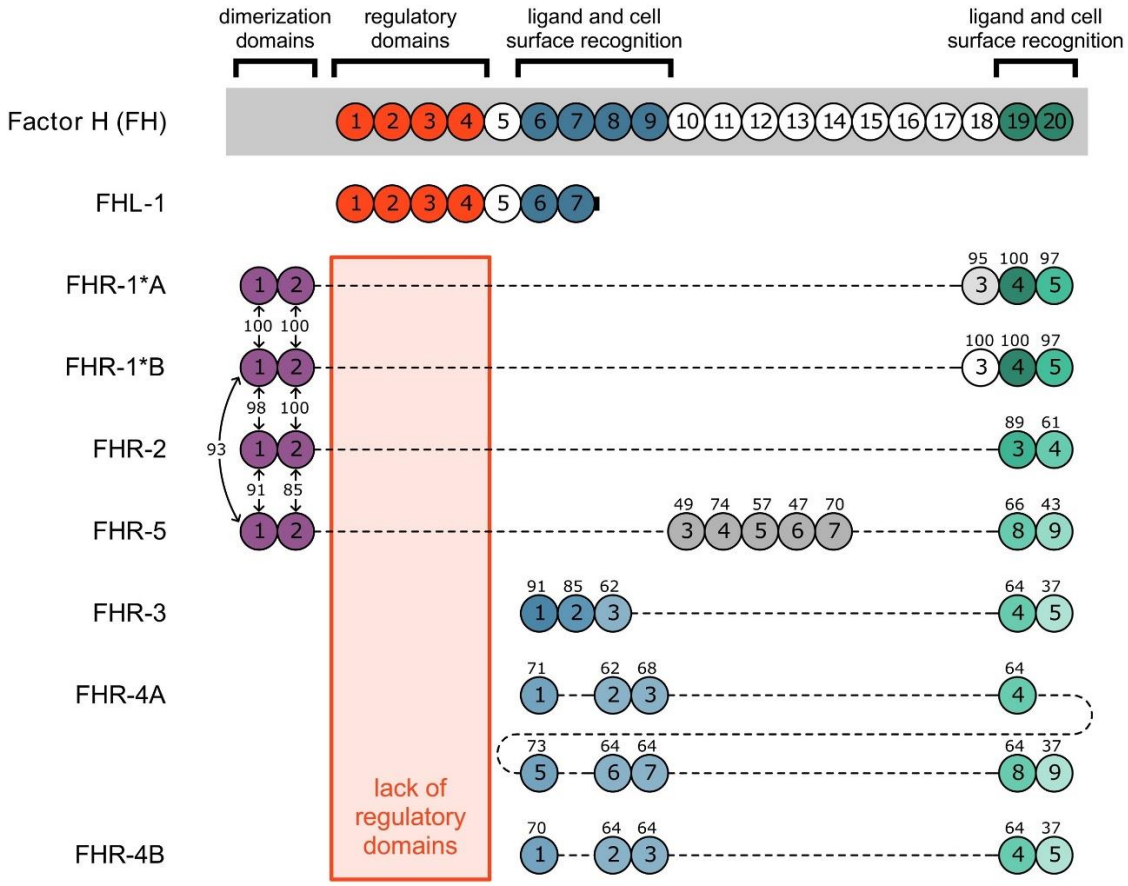

Figure 1. 12: Structure of human FH, FHL-1, and FHR proteins family. Factor H (FH), Factor H Like-1 protein (FHL-1), and Factor H related proteins (FHRs). Schematic illustration indicating complement control protein (CCP) domain structure of FH, FHL-1, and the FHR proteins is shown. Each CCP is represented by a circle, the N-terminal CCPs 1 – 4 of FH and FHL-1 perform the complement regulatory functions (shown in red). The main ligand- and host surface-recognition sites are located in CCPs 6 to 9 in FH, CCPs 6-7 in FHL-1 (shown in blue), and CCPs 19 – 20 of FH (shown in green). FHR proteins lack regulatory domains (CCPs 1 – 4). However, they contain domains that display a varying degree of amino acid sequence similarity to the ligand- and self-recognition domains of FH. FHR-1, FHR-2, and FHR-5 include unique N-terminal domains (CCPs 1 – 2 shown in purple) are closely related to each other and have the potential to mediate dimerization of these FHRs. The CCPs of each molecule are vertically aligned based on the highest similarity in sequence to one other. The numbers denote the percentage of amino acid sequence identity to the corresponding FH domains or dimerization domains between FHRs. The identical/similar colours of the CCPs of FHRs indicate the high similarity in amino acid sequence with the FH domains (Cserhalmi *et al*., 2019).

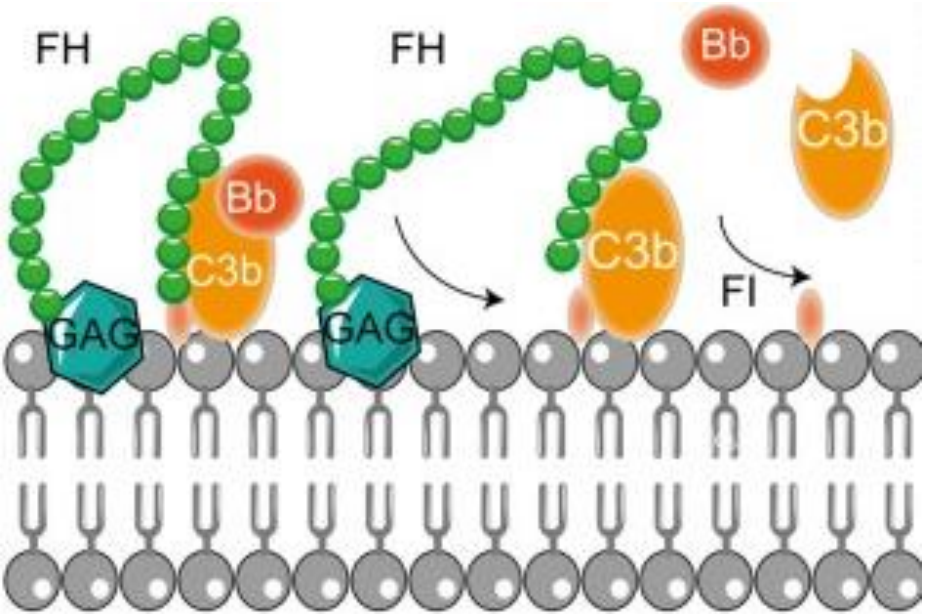

Figure 1. 13: Soluble regulator FH function. The major fluid phase regulator for AP, FH binds to GAG on the cellular membrane to discriminate between self and non- self surfaces. FH mediates the dissociation of the AP C3 convertases (C3b Bb) through binding to C3b leading to dissociation of Bb from the C3b. Additionally, FI is recruited to inactivate C3b by cleavage of C3b to iC3b (Hovingh *et al*., 2016).

FH related proteins (FHR) are five proteins encoded by the FHR genes located downstream of the FH gene. The first four CCP domains of FH are not involved in the FHR protein family. These proteins contain three regions that can show a high FH identity. The N-terminal domains of FHR proteins include a high amino acid sequence identity to CCPs 6 – 9 of FH. The second region includes identity to CCPs 10 – 14 of FH (Figure 1.12). The C-terminal domains of FHR proteins show sequence homologies to the C-terminal domains of FH CCPs 18 – 20 (Skerka *et al,* 2013). Due to these homologies, the FHRs may have the binding capacity to some of the FH ligands. FHR-5 can competitively inhibit FH binding to pentraxins and ECM. Thus FHR-5 indirectly enhances complement activation (Csincsi *et al*., 2015). It has been reported that FHR-1, FHR-4, and FHR-5 can bind to C3b by their C-terminal CCPs domains and lead to the formation of the AP C3 convertase (C3bBb). Thus, these FHR proteins can up-regulate AP similarly to properdin, the positive regulator of AP (Csincsi *et al*., 2017).

1.8 Complement and viral pathogenesis

To acquire the capability for causing disease and continue to survive in their hosts, pathogens need to avoid recognition and targeting by the host defence systems. Both innate and adaptive immune systems collaborate to effectively detect, curb, and clear the invading pathogens (Ricklin *et al*., 2010). The first reactions of the host defence against invading pathogens are mediated by a major humoral arm of innate immunity, the complement system. The complement pathway acts as an immune surveillance system by ensuring a rapid immune response. Activation of the complement system by the recognition molecules of the complement pathways launches a protease cascade on the surface of pathogens, generating active complement components that play a vital role in the elimination of pathogens and enhancing inflammatory and adaptive immune responses. When complement functions are manipulated by internal or external agents, they can become devastating and the complement system may function as a cause of several diseases including the microbial infections (Stoermer & Morrison, 2011; Muñoz Carrillo *et al*, 2017).

The complement system plays a crucial role in determining the outcome of viral pathogenesis, which has been demonstrated by identifying the specific mechanisms that the virus has developed to evade the complement system. One of the strategies employed by the virus to mitigate the complement pathway is the encoding of homologs that have structural and functional homology to host regulators of complement activation. The regulator of complement activation (RCA), γHV68 is homologous to the amino acid sequence of human decay-accelerating factor (DAF) (Liszewski *et al*., 1996; Kapadia *et al*., 1999). It is expressed as membrane-associated and soluble forms by the DNA Gammaherpesviruses, like Kaposi's sarcoma-associated herpesvirus, herpesvirus saimiri, and murine γ-herpesvirus 68 (γHV68) (Albrecht & Fleckenstein, 1992; Virgin *et al*., 1997; Kapadia *et al*., 1999; Mullick *et al*., 2003a; Spiller *et al.*, 2003). It was shown that γHV68 blocked the deposition of C3 on the infected cells by both the classical and alternative pathways (Kapadia *et al*., 1999).

Poxviruses also have been shown to encode RCAs such as the variola virus inhibitor of complement enzymes (SPICE), the vaccinia virus complement control protein (VCP), the monkeypox virus inhibitor of complement enzymes (MOPICE), and the ectromelia virus inhibitor of complement enzymes (EMICE) that all bind to C3b and C4b, which act as cofactors

of factor I for cleavage of C3b into iC3b (Sahu *et al*., 1998; Mullick *et al*., 2003b; Rosengard *et al*., 2002; Liszewski *et al*., 2006; Moulton *et al*., 2010).

A different mechanism of viral evasion of complement in which the virus encodes proteins that bind and prohibit complement components. The coat protein (CP) of human astrovirus type 1 (HAstV-1) binds to mannose-binding lectin (MBL) and C1q, suppressing the activation of both the lectin and classical pathways (Bonaparte et al., 2008; Hair *et al*., 2010). Flavivirus non-structural protein 1 (NS1) of dengue virus (DENV), West Nile virus (WNV), and yellow fever virus (YFV) binds to the soluble inhibitors C4b-binding protein (C4BP) and C1 (C1-INH) and inhibits the activation of classical and lectin pathways. (Avirutnan *et al*., 2010).

IAVs have been shown to evade complement activation by recruiting CD59, the membrane attack complex inhibitory protein (MAC-IP) on their envelopes. Thus, IAV can be protected from lysis by MAC (Shaw *et al*., 2008, Agrawal *et al*., 2017). IAVs have developed another evasion mechanism by binding of viral protein matrix 1 (M1) to C1q and obstructing the interaction between C1q and IgG antibodies, thereby inhibiting C1q mediated recognition of IAV and preventing the classical pathway-mediated neutralization of IAV by M1 protein (Zhang *et al*., 2009, Agrawal *et al*., 2020).

The alternative pathway (AP) is constitutively active at a low rate to survey continuously for the presence of the pathogens and is non-discriminative of pathogens and host cells. For that reason, the AP of complement is tightly controlled by the plasma glycoprotein FH (Pangburn, 2000; Zipfel & Skerka, 2009; Hovingh *et al*., 2016). Therefore, pathogens have also developed mechanisms to escape this pathway. Since FH is a major regulator of complement activation, many pathogens encode surface proteins that bind to FH preventing complement activation and thereby increase their pathogenicity (Zipfel & Skerka, 2009; Parente *et al*., 2017).

1.9 FH and immune evasion strategy by pathogens

FH is recruited by several pathogens for protection against complement activation. Interaction with FH eliminates opsonization and prevents the formation of cytolytic MAC. Thus, the binding of the pathogens to FH is important for the survival of pathogens in the host. Two major binding sites were identified on FH for pathogen binding. One is within the N-terminal domains 6 – 7 of FH and FHL-1. The other interaction site on FH is in the C-terminal domains

19 – 20 (Figure 1. 9) (Meri et al., 2016). Many microbes use CCPs 6 – 7 of FH to evade AP activation, such as the M protein, the main virulence factor of group A streptococci (Blackmore et al., 1998; Haapasalo et al., 2008; Clark at al., 2010), the Neisserial surface protein A (NspA) of Neisseria meningitidis (Lewis et al., 2010), the outer membrane protein, Ail from Yersinia enterocolitica (Biedzka-Sarek et al., 2008), and the lipoprotein factor H binding protein (fHbp) of N. meningitidis (Seib et al., 2015). Microbial proteins that interact with FH via CCPs 6 – 7 can also bind FHL-1 due to the first 7 conserved CCPs domains of FH (Kühn et al., 1995). Thus, allowing pathogens to inactivate both complements regulators (Meri et al., 2013).

It has been suggested that most pathogens bind to both sites, for instance, the outer surface protein H of *Haemophilus influenzae* has been shown to be involved in FH binding via CCPs 7 and CCPs 18 – 20 (Hallström *et al*., 2008) The association of FH with *H. influenzae* has been shown to decrease by deleting the H protein (Fleury *et al*., 2014). *Borrelia burgdorferi*, the bacteria that causes Lyme disease transmits from arthropod vector to the human via blood, therefore this bacterial pathogen expresses several proteins that mediate binding of FH to the bacterial surface to efficiently evade the AP attack. *B. burgdorferi* attaches to FH via both binding sites of FH, CCPs 5 – 7 and CCPs 19 – 20. It binds to CCPs 5 – 7 of FH by protein CspA, CspZ, and OspE, while the surface proteins ErpA and ErpP are capable of binding with the CCPs 19 – 20 (Figure 1. 14). This dual-binding capability provides effective protection against the AP attack. (Kenedy *et al*., 2009; Hallström *et al*., 2013; Bhattacharjee *et al*., 2013; Caesar *et al*., 2013; Brangulis *et al*., 2015).

An additional binding site has been identified in the CCPs 8 – 14 of FH, which is recruited by two surface proteins of *Streptococcus pneumoniae*. The first protein is called FH binding inhibitor of complement (Hic) that binds to CCPs 8 – 14 of FH (Kohler *et al*., 2014). A second FH binding protein of *S. pneumoniae* is PspC, which recruits FH via CCPs 8 – 11 (Dave *et al*., 2004; Herbert *et al*., 2015). A novel type of FH-binding was shown by the outer membrane protein YadA of *Y. enterocolitica*, which appears to bind with the whole FH molecule (Biedzka-Sarek *et al.*, 2008). Thus, microbial pathogens can recruit FH to their surface via different CCPs or throughout the entire FH (Figure 1. 15).

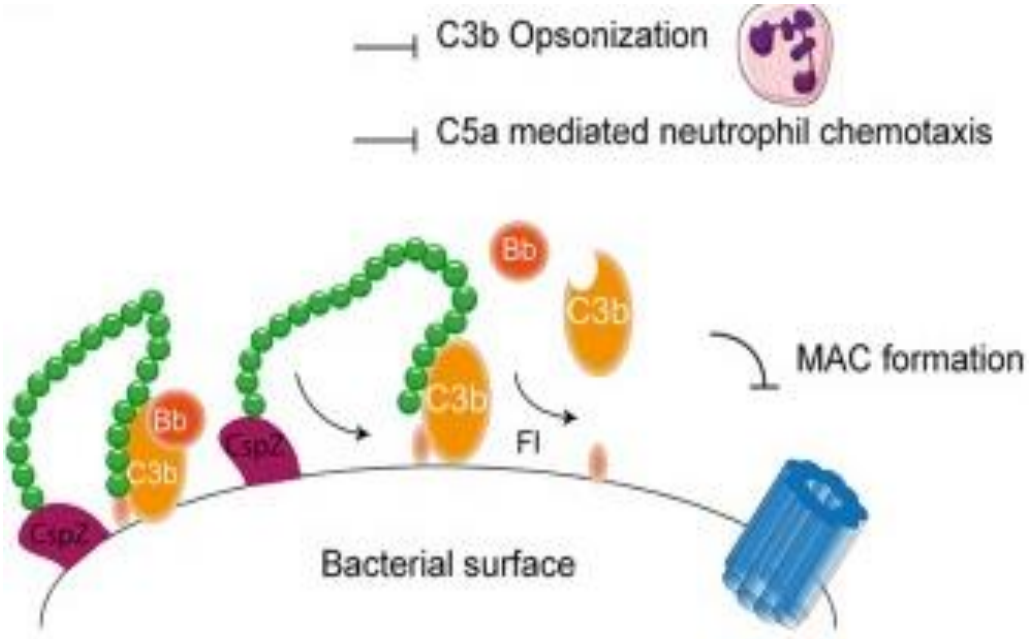

Figure 1. 14: Interaction of bacterial pathogens with FH. Binding of the surface protein CspZ of *B. burgdorferi* to FH is one example of a bacterial protein binding to CCP 20 of FH. Through this binding, bacteria recruit FH to their surfaces leading to the decay of the AP C3 convertase (C3bBb) and degradation of C3b into iC3b and C3d. This prevents MAC formation and decreases phagocytic uptake of the bacteria due to inhibition of C3b deposition and C5a production (Hovingh *et al*., 2016).

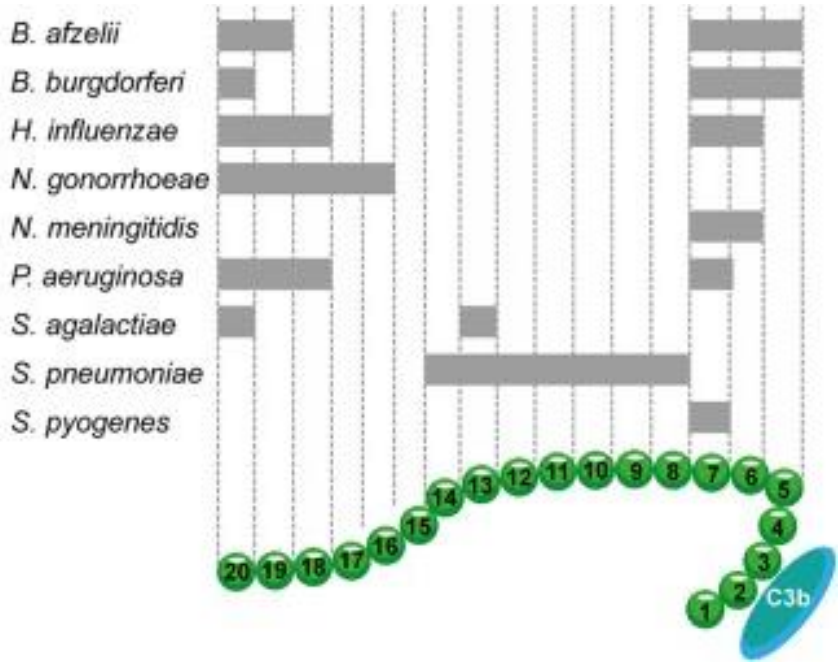

Figure 1. 15: Bacterial pathogens bind to different common binding sites on FH. Several bacteria can interact with FH at different binding sites as indicated by the grey rectangles. Domains 1 – 4 interact with C3b, whereas domains 19 – 20 discriminate self from non-self (Hovingh *et al*., 2016).

FH is recruited by various microbial pathogens to inactivate AP in the host using different strategies. One of these mechanisms is to mimic the glycosaminoglycans such as sialic acid on host cells. This action allows pathogens to attract FH on their surfaces and bind to a common binding site in CCPs 20 of FH. Through this binding, the FH-ligands expressed by pathogens overlaps but is not identical to the cellular binding sites (Meri *et al*., 2013; Hovingh *et al*., 2016). *S. pneumoniae* has evolved different strategy in which FH recruitment in CCPs 19 – 20 by the surface protein CbpA does not affect the binding of glycosaminoglycans on the surface of host cells to CCP 19 – 20. (Duthy *et al*., 2002; Agarwal *et al*., 2010). The ability of FH to bind on the outer membrane pneumococcal protein CbpA and glycosaminoglycans on the surface of human cells simultaneously enables pneumococci to attach to human cells via FH. Therefore, recruitment of FH not only protects *S. pneumoniae* from complement tagging for phagocytosis but also contributes to the pneumococcal attachment to and uptake of *S. pneumoniae* by host cells (Agarwal *et al*., 2010, Achila *et al.*, 2015).

Khatua *et al* (2010) showed that culture of *pseudomonas aeruginosa* in the presence of sialic acid results in sialoglycosylated of *p. aeruginosa*. Therefore, sialic acid may be taken up by *P. aeruginosa* in the host. Acquired sialic acid enables *P. aeruginosa* to mimic glycans on the host cell surface, attracting FH, thereby reducing C3b deposition on the bacterial wall and escaping AP mediated killing (Khatua *et al*.,2010). Some pathogens like *Staphylococcus aureus* mimic plasma HDL particles in their binding to CCPs 5 – 7 of FH, allowing their survival in blood (Haapasalo *et al*, 2015). It has been shown that CCPs 5 – 7 of FH binds with apolipoprotein (apoE) on the plasma anti-inflammatory HDL particles dose-dependently, resulting in excessive complement activation and phagocytosis of the microbes. Through this binding, HDL inhibits the regulatory action of FH at C3b level, thereby reducing iC3b formation of FH and enhancing neutrophils phagocytosis. Binding of FH to apoE on HDL particles via domains 5 – 7 protects plasma HDL against complement system attack, increasing the level of plasma C3a. The interaction between FH and HDL via CCPs 5 – 7 explains why microbes bind to these domains of FH, where this binding may enable pathogens to mimic the plasma HDL, allowing their survival in the blood (Haapasalo *et al.*, 2015).

The pathogenic yeast *Candida albicans* employs a different mechanism to evade the human complement system by secreting the proteolytic enzymes aspartic protease 2 (Sap2) which inactivate FH, FHR-1, and the macrophage FH-receptors CR3 and CR4, ensuring their survival in the human body. In the presence of *C. albicans*, FH is able to enhance the antifungal activity

of human macrophages. It was shown that FH binds to its cellular receptors CR3 and CR4 on the human neutrophils, enhancing the production of proinflammatory cytokines in macrophages and increasing their activation. However, *C. albicans* Sap2 cleaves FH, decreasing its complement regulatory activity and diminishing fungal recognition by macrophages (Svoboda *et al*., 2015).

The cellular and hyphal forms of *Candida* spp. have evolved an immune evasion strategy by recruiting FH from the host and utilising specific FH binding molecules on their surfaces to downregulate complement action by mimicking the host cells (Meri *et al*., 2004; Kraiczy & Wurzner, 2006; Vogl *et al*., 2008). Recent studies have shown that *C. albicans* hijack FH by utilising FH binding molecule, the transmembrane protein "High-affinity glucose transporter 1" (Hgt1p), to downregulate complement activation on its surface (Lesiak-Markowicz *et al*., 2011; Kenno *et al*., 2019). The glucose transporters (HGTs) are a large family of surface proteins (Hgt1p to Hgt20p) in *C. albicans* and play a vital role in glucose metabolism (Fan *et al*., 2002). The interaction between FH and Hgt1p protein on the surface of *C. albicans* was confirmed by blocking FH binding site on the Hgt1p protein and this was achieved with the anti-Hgt1p antibody that blocked FH binding to the Hgt1p protein. (Kenno *et al*., 2019). For this interaction, a chimeric molecule was created from a combination of human FH domains 6 and 7 and human IgG Fc receptor (FH6.7/Fc) (Shaughnessy *et al*., 2014). Thus, FH displacement increases the deposition of C3b on the surface of *C. albicans* and enhances phagocytosis by neutrophils. Blocking of Hgt1p-FH interactions by FH6.7/Fc can be used as a therapeutic agent against *C. albicans* (Kenno *et al*., 2019).

It has been shown that not only yeasts but also moulds, such as *Aspergillus fumigatus* and *Aspergillus terreus* bind FH by two different binding sites located within CCPs 6 – 7 and 19 – 20 (Vogl *et al*., 2008; Behnsen *et al*., 2008; Heinekamp *et al*., 2015) as shown for *Candida* (Meri *et al*., 2002). However, the molecular characterisation for fungal ligands have not yet been determined (Heinekamp *et al*., 2015).

Complex evasion strategies have been developed by malaria parasites *Plasmodium falciparum* at three points in its developmental cycle to maintain their vitality during the asexual life cycle in the human host and sexual life cycle in hematophagous vectors, *Anopheles* mosquito (Simon *et al*., 2013; Rosa *et al*., 2016; Kennedy *et al*., 2016). *P. falciparum* parasites are taken up with human blood meal by the mosquitos in the form of the intraerythrocytic immature sexual

gametes. Following the emerging of gametocytes, the ripening of the fertile gametes occurs about 20 min after absorbing a blood meal. After 1 hr post-feeding, the fertilization completed, forming the zygote, which subsequently produces the sporozoites, the infectious stage for human (Pradel, 2007). During this period, the human complement within the blood meal remains active in the mosquito midgut for approximately 1 hr, representing a severe threat to the survival of emerging gametes. To protect the emerging gametes of *P. falciparum* from complement-mediated lysis, gametes rapidly bind to CCPs 5 – 7 of FH and FHL-1 from the blood meal via plasmodial transmembrane gliding-associated protein 50 (PfGAP50) inactivating of surface-bound C3b via factor I and ensure their survival during the sexual replication in the mosquito midgut (Figure 1. 16) (Simon *et al*., 2013; Belachew, 2018). It has been shown that FH with blood meal not only protects the extracellular gametes in the midgut of *Anopheles* mosquito but also the luminal surface epithelium of mosquito's midgut and prevents the human complement activation on the epithelial cells (Khattab *et al*., 2016).

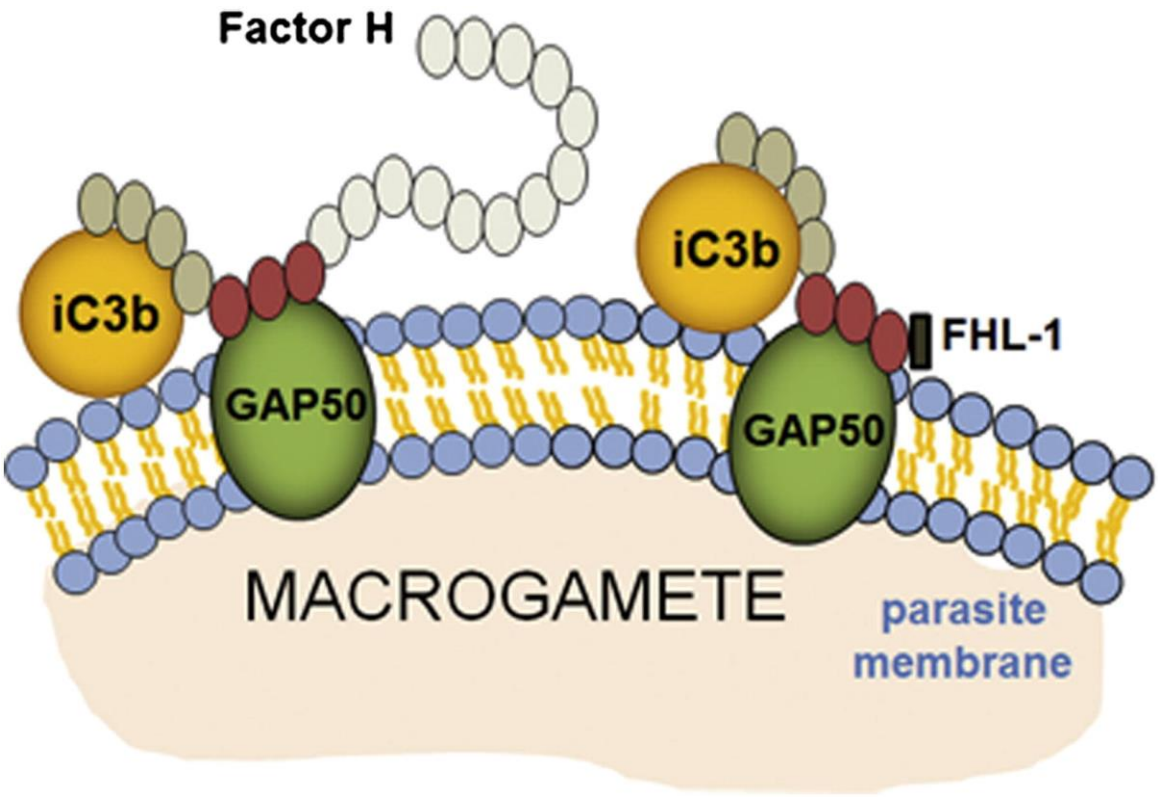

Figure 1. 16: Interaction between Malaria gametes and FH to evade human complement attack. The surface protein PfGAP50 binds to FH, leading to inactivating of the complement protein C3b (iC3b). Inhibition of FH or PfGAP50 function reduces parasite transmission to the insect vector (mosquito) (Simon *et al*., 2013).

In the human host, the blood-stage merozoites of *P. falciparum* need to evade the destruction of the complement system. To inactivate C3b on their surfaces, the free merozoites bind to FH and its alternative splicing form FHL-1 on their CCPs 5 – 6 by the surface coat protein pf92, the abundant protein on the merozoite surface (Kennedy *et al*., 2016). While the intraerythrocytic schizonts (merozoites that re-invaded the RBCs) recruit FH and FHL-1 by two binding sites, CCP 5 and CCP 20 to inactivate complement system, thereby ensuring their survival during the asexual replication in erythrocytes (Rosa *et al*., 2016).

A similar mechanism has been evolved by a protozoan parasite *Trypanosoma brucei*, the causal agent of human and animal trypanosomiasis (sleeping sickness) that is transmitted by the insect vector, tsetse flies (Ponte-Sucre, 2016; Kennedy & Rodgers, 2019). It has been identified the surface glycoprotein Tb927.5.4020 (protein name is indicated as its gene ID) of *T. brucei* as mammalian FH receptors. The structural mechanism studies reveal that FH receptor bind to CCP 5 of FH, leaving the inhibitory site CCPs 1 – 4 of FH functional to inactivate bound complement C3b to the trypanosome surface (Macleod *et al*., 2020). It was shown that the expression of FH receptor increases in the developmental forms of the parasite exposed to blood meals in the tsetse midgut as well as the differentiated blood forms of *T. brucei* which represent the infective stage for tsetse vectors. The deletion of the FH receptor gene reduces tsetse infection, identifying the importance of these receptors as a virulence factor to increase the transmission of *T. brucei* into the insect by recruitment of FH (Macleod *et al*., 2020).

Toxoplasma gondii is another protozoan parasite that recruits FH to downregulate complement activation on its surface (Sikorski *et al*., 2020). The surface of *T. gondii* is coated with glycosylphosphatidylinositol-linked proteins structurally related to the highly immunogenic surface antigen SAG1. This superfamily of surface proteins is known as the SRS (SAG1-related sequences) (Jung *et al*., 2004). As mentioned previously *P. falciparum* binds FH via surface protein Pf92 (Kennedy *et al*., 2016), a member of 6-CYS superfamily including 14 proteins encoded by Plasmodium which reveal a tertiary structural homology with the surface proteins SRS of Toxoplasma (He *et al*., 2002; Gerloff *et al*., 2005; Arredondo *et al*., 2012). This evidence indicates that Toxoplasma may utilise a similar mechanism to inactivate complement. However, the mechanism by which FH is recruited by the plasmodial Pf92 protein is unknown yet (Sikorski *et al*., 2020).

It is well-established that FH recognises self-cell surfaces by binding to the host polyanion molecules like sialic acid or heparan sulphated proteoglycans (SPGs) by two binding sites located on CCPs 7 and 20 (Hessing *et al*., 1990; Blaum, 2017). Some Pathogens utilise this interaction by either acquiring sialic acid to cover their surfaces or producing their own to bind FH and thereby protecting their surface from complement-mediated lysis (Guerry *et al*., 2000; Severi *et al*., 2007). Several studies have shown that *T. gondii* presents the ability to interact with host SPGs (Ortega-Barria & Boothroyd, 1999; Carruthers *et al*., 2000; He *et al*., 2002) and sialic acid (Monteiro *et al*., 1998; Friedrich *et al*., 2010). Thus, *T. gondii* may enlist its ability to bind glycosaminoglycans structures as a mechanism for FH recruitment (Sikorski *et al.*, 2020).

The larva of the parasitic worm *Echinococcus granulosus* (hydatid cyst) that causes cystic echinococcosis in humans is protected by the acellular laminated layer. This massive layer of the extracellular matrix expresses a protein that recruits FH to hydatid cyst wall, thereby inhibiting the deposition of complement C3b by converting C3b convertase into iC3b and C3d (Diaz *et al*., 1997; Breijo *et al*., 2008). Further research identified that the binding molecule was the myo-inositol hexakisphosphate (InsP6), the main component of the laminated layer of the hydatid cyst wall (Irigoin *et al*., 2008; Shao *et al*., 2019).

West Nile virus (WNV) is an example of a viral evasion from the complement activation by encoding non-structural protein NS1 which enables WNV to evade complement-mediated lysis (Chung *et al*., 2006). WNV NS1 is a glycoprotein secreted in infected cells and attaches back to cell surfaces and it was detected in high levels in the serum. The mechanism by which NS1 contribute to WNV pathogenesis remains uncertain. However, it was shown that flavivirus NS1 has a co-factor function for viral RNA replication (Youn *et al*., 2013). It was defined that WNV NS1 binds to and recruits FH resulting in enhancing factor I activity to cleave C3bBb (C3b convertase) to iC3b, attenuating the deposition of C3b and decreasing number of membranes (Chung *et al*., 2006).

1.10 Thesis aims and objectives

The hypothesis of this thesis is that **FH binds to IAV and this influences virus replication.**

To verify this hypothesis the following aims and objectives were set:

Aim 1: Investigate the interactions between FH and IAVs.

Objective 1: Determine if a direct interaction between live strains of human and avian IAVs and purified human FH occurs.

Objective 2: Identify which of the viral proteins of purified IAVs are responsible for the binding of IAV to FH.

Objective 3: Mapping the interacting footprints on FH and viral proteins that involved in the interaction between IAV and FH.

Aim 2: Investigate the potential effect of the interaction between IAV.

and FH on viral replication in the target cells.

Objective 1: Identify if FH influences IAV replication.

Objective 2: Track the mechanism of IAV replication alteration by FH.

Chapter 2: Materials and methods

2.1 Cells

Madin-Darby canine kidney (MDCK) cell line (BEI resources, ATCC # NR-2628) and human lung carcinoma epithelial (A549) cell line (ATCC, Rockville, MD, USA) were passaged in complete growth medium, Dulbecco's modified Eagle's medium (DMEM) (Gibco) complete growth medium. Human leukemic monocyte (THP-1) cell line (ATCC # TIB-202), hybridoma cell lines OX23 (ECACC # 00010402) and OX24 (ECACC # 00010403) were cultured in RPMI-1640 (Gibco) growth medium. Complete growth media contained 10% fetal bovine serum (FBS) (Fisher Scientific) heat inactivated at 56°C for 30 min, 100 U/ml penicillin (Pen) and 100 mg/ml streptomycin (Strep) (Fisher Scientific) All cell cultures were maintained at 37°C in 5% CO_2 with high humidity atmosphere.

2.2 IAV manipulations

2.2.1 Virus strains

Table 2. 1: IAV strains used in this study.

IAV Strains	Subtype	Name Used in this study	Host	Origin
A/HK/1174/1999	H3N2	H3N2/99	Human	Prof. Leo Poon (University of Hong Kong)
A/HK/4801/2014	H3N2	H3N2/14	Human	Dr Mark Fife (The Pirbright Institute)
A/England/195/2009	H1N1	H1N1pdm09	Human	Prof. Wendy Barclay (Imperial College, London)
A/Michigan/45/2015	H1N1	H1N1/15	Human	Dr Mark Fife (The Pirbright Institute)
A/chicken/Pakistan/UDL-01/2008	H9N2	H9N2	Avian	Prof. Munir Iqbal (The Pirbright Institute)
A/Duck/Singapore/3/97	H5N3	H5N3	Avian	Prof. Munir Iqbal (The Pirbright Institute)

2.2.2 Human IAV amplification

150 cm^2 flasks (Fisher Scientific) were seeded with MDCK cells. When the cell monolayer reached 90% confluence, the cells were washed three times with 0.01 M phosphate buffered saline (PBS). Cells were then inoculated with human IAV at a multiplicity of infection (MOI) of 0.001 in 10 ml of serum-free DMEM per flask for 1 h to allow adsorption of the virus. Flasks were rocked every 15 mins to prevent cells drying out. Cells were then washed with PBS and 25 ml of 1x infection medium (DMEM, 1% penicillin/streptomycin (Pen/Strep), 1 µg/ml Trypsin TPCK from bovine pancreas (TPCK-Trypsin) (Sigma), 0.3% bovine serum albumin (BSA) (Sigma # A8412)) was added. Flasks were incubated at 37°C in 5% CO_2 for 4 days. Following harvest, the virus was clarified by low-speed centrifugation at 3000 rpm at 4°C for 20 min, aliquoted and stored at -80°C until use.

2.2.3 Avian IAV amplification

For growing large quantities of avian IAV, 10-day embryonated chicken eggs (VALO BioMedia, Germany), were inoculated with 100 µl of virus diluted in PBS into the allantoic cavity. Eggs were candled daily to monitor viability. Between 48 h and 72 h post-infection, chicken embryos were euthanised by cooling in the refrigerator for a minimum of six hours. Allantoic fluid was then harvested from the eggs and pooled. Following harvest, the virus was clarified by low-speed centrifugation at 3000 rpm at 4°C for 20 min, aliquoted and stored at -80°C until use.

2.2.4 Production of pseudotyped lentiviral particles

Influenza lentiviral pseudotypes, expressing luciferase reporter gene and bearing HA or HA with NA on the surface were generated (Table 2. 2). Human embryonic kidney (HEK) 293T cells (ATCC) were co-transfected with HIV gag/pol constructs, firefly luciferase construct, the green fluorescent protein (GFP) reporter constructs and glycoprotein expression plasmids (HA, NA, and Vesicular stomatitis virus envelope glycoprotein (VSV-G)). The supernatant was harvested with the pseudotyped Lentiviral Particles and added to HEK293T cells. The titre of the pseudotyped virus was calculated from the level of reporter gene expression. The relative luminescence units (RLU) per ml was measured using a GloMax 96 luminometer (Temperton *et al*., 2007; Scott *et al*., 2012). All lentivirus pseudotyped particles used in this study were kindly provided by Dr Nigel Temperton (University of Kent).

Table 2. 2: Influenza pseudotyped particles and controls used in this study.

Viral strain	Envelope
A/Udorn/307/1972 (H3N2)	HA
A/California/7/2004 (H3N2)	HA
A/Texas/1/1977 (H3N2)	HA
A/Solomon Island/3/2006 (H1N1)	HA
A/England/195/2009 (H1N1)	HA
A/Hong Kong/33982/2009 (H9N2)	HA
A/FPV/Rostock/1934 (H7N1)	HA
A/Shanghai/02/2013 (H7N9)	HA
A/Vietnam/1194/2004 (H5N8)	HA
A/Vietnam/1194/2004 (H5N8)	HA+NA
Δ-envelope	-
Vesicular stomatitis virus	VSV-G

2.2.5 Purification of IAV

Purification of viral particles was performed using a Beckman Coulter Ultracentrifuge and a sucrose cushion. Virus was placed in an ultra-clear centrifuge tube (Beckman Coulter # 344058) and centrifuged for 30 min at 10,000 rpm at 4ºC in the chilled SW32Ti rotor to further clear supernatant from cell debris. 26 ml of the supernatant was transferred carefully into new ultra-clear centrifuge tubes containing a cushion of 8 ml of cold 30% sucrose and centrifuged at 25000 rpm at 4°C for 90 min. Viral particles have a density > 30% sucrose and thus precipitate at the bottom of the ultra-clear centrifuge tube. The medium in the upper phase and the sucrose in the lower phase were carefully removed. A white pellet containing viral particles was found at the bottom of the tubes that were serially resuspended in 100 µl of cold PBS and collected in a screw-capped tube. Finally, the virus was briefly centrifuged, and the supernatant was removed. The virus resuspended in 50 µl of PBS, aliquoted and stored at -80°C.

2.2.6 Tissue culture infectious dose $_{50}$ $TCID_{50}$ assay

$TCID_{50}$ assay was performed to assess virus titre. The amount of 100 µl of DMEM was added to all wells of 96-well microtiter plates (Sigma-Aldrich # 3599), except column 1, which was used to add 146 µl of the virus starting dilution. From column 1, 46 µl was serially transferred until column 11 of which, 46 µl was discarded. This results in a serial dilution of ½ log10 of the virus, column 12 was a negative control. The plates were incubated at 37°C in 5% CO_2 for 1 h. After the incubation period, MDCK cells were diluted in 2x infectious medium (2% Pen/Strep, 2 µg/ml Trypsin-TPCK, 0.6% BSA) and 5×10^4 cells/100 µl were added into each well and incubated at 37°C for 3 – 4 days until the cytopathic effects (CPE) were observed. Cells were fixed with ice cold methanol: acetone 1:1 (50% methanol, 50% acetone) for 20 min and stained with 0.1% crystal violet for 30 min (40 ml 1% crystal violet in water (Sigma-Aldrich), 80 ml methanol, 300 ml water). The numbers of positive and negative wells were recorded for each dilution and $TCID_{50}$ was calculated by the Reed Muench method (Klimov *et al*., 2012). In this method, the plate area in which the transition from all positive wells at one dilution to all negative wells was chosen. The cumulative numbers of positive wells in the specified area were calculated at each dilution, starting from the bottom, where the number of positive wells from each lower dilution was sequentially added. Likewise, the cumulative numbers of negative wells at each dilution were obtained by adding the number of negative wells from each higher dilution sequentially, starting at the top. The ratio was determined in each dilution and converted into a percentage of positive wells as follow:

$$Ratio = \frac{\text{Sum of cumulative positive}}{\text{Sum of cumulative positive} + \text{Sum of cumulative negative}}$$

The proportional distance between the dilution showing >50% positive and the dilution showing <50% positive was calculated as follows:

$$\text{Proportional distance} = \frac{\%\ \text{positive value above } 50\%}{\%\ \text{positive value above } 50\% - \text{positive value below } 50\%} \times (0.5) *$$

$* =$ Correction factor for log dilutions

$TCID_{50}$ was calculated by adding proportional distance to the dilution showing >50% positive.

2.2.7 Plaque assay

Plaque assay was performed to determine virus titre. MDCK cells were seeded in 6-well plates (5×10^5 MDCK cells/well). When the cell monolayer reached approximately 80 – 90% confluence, cells were washed three times with PBS and inoculated with serial dilutions of 10-

fold virus stock. After a 1 h incubation period at 37°C, cells were washed with PBS and overlaid with plaque assay overlay media (Table 2. 3) containing 1 µg/ml TPCK trypsin, 0.6% agar. The plates were then incubated for 2 – 3 days depending on the type of virus used. After incubation, the solid overlay was removed, and cells were stained with 0.1% crystal violet for 30 min. Plaques were counted and plaque-forming units (PFU)/ml were determined.

Table 2. 3: Components of plaque assay overlay media.

10× Eagle's Minimum Essential Medium (Sigma)	100 ml
7.5% w/v BSA	28 ml
L-Glutamine (Sigma)	10
7.5% w/v $NAHCO_2$	20 ml
1M Hepes (Sigma)	10 ml
1% w/v Dextran hydrochloride (Sigma)	5 ml
10×Pen/Strep	10 ml
H_2O	517 ml

2.2.8 Haemagglutination (HA) assay

This assay was performed to quantify virus based on the ability of the IAV HA protein to bind to sialic acid on the surface of red blood cells. Turkey red blood cells (TRBC) (Envigo) were washed twice with PBS at 800 rpm for 10 min. PBS was added to make 10% v/v stock solution of TRBC and the final working solution used was 1% v/v RBCs. A serial dilution of each virus was dispensed in wells of 96-well V-bottom microtiter plate (Fisher Scientific). 50 µl of PBS were added to each well. To the first column, 50µl of each virus were added and diluted serially until column 11, where it was discarded. 50 µl of the 1% TRBC solution were added to each well and mixed gently. As a control, 50 µl of PBS was added to the last column. The plate was left at RT for 30 min or at 4°C for 1 h and then photographed. Haemagglutination of RBCs leads to the formation of a lattice structure, in which the agglutinated RBCs are retained in a reddish suspension in the wells. The wells lacking haemagglutination show a red dot of RBCs settling at the bottom. HA titration (unit) is the highest dilution of the virus that causes complete haemagglutination. The standard solution should contain an HA titre of 8 HAU/50 µl (= 4

HAU/25 µl). This titre was used in haemagglutination Inhibition (HI) assay and was confirmed by back titration in which the working solution haemagglutinate the first four wells of the plate.

2.3 Purification of mouse monoclonal anti-FH antibodies OX23 and OX24

Mouse hybridoma cell lines OX23 or OX24 were cultured in 100 ml of complete RPMI-1640 medium in 75 cm^2 flask (Fisher Scientific) and incubated at 37°C in 5% CO_2 for 3 days to obtain a high density of cells. For optimal production of the monoclonal antibodies, each 25 ml of cell culture medium were transferred into a new 75 cm^2 flask with 75 ml of complete RPMI-1640 medium with a limited concentration of FBS (2%) and incubated in 5% CO_2 at 37°C. When the medium converted into a yellowish colour and 50% of the cells died, the media containing antibodies was then collected and spun down at 2500 rpm at 4°C for 5 min. The clarified supernatants were filtered with 0.22 µm filter top (Fisher scientific) and kept at 4°C until antibody purification. Confirmation of the presence of purified anti-FH antibodies in the supernatant of hybridoma cells culture was performed by dot blot assay.

2.3.1. Packing of protein G-Sepharose

Protein G-Sepharose 4 Fast Flow (GE Healthcare Life Sciences, # 71-7083-00) was packed in Polyethylene Filter Column (10 x1.5 cm diameter) (Thermo Fisher Scientific, # 29924) to purify anti-FH OX23 and OX24 antibodies. Protein G Sepharose was supplied pre-swollen in 20% ethanol. The slurry was prepared by replacing the 20% ethanol with binding buffer (PBS pH 7.4). An empty column was degassed by flushing the polyethylene disc in the bottom of the column with PBS. The column outlet was then closed with 2 ml of PBS remaining in the column. The slurry was mixed well and poured into the column. After the slurry was packed, the bottom cap was opened to start the flow of the buffer through the column until the resin bed was settled. The column was then equilibrated with PBS and stored in PBS containing 0.05 – 0.1% (w/v) sodium azide (Sigma) at 4ºC.

2.3.2 Purification of anti-FH OX23 and OX24 antibodies

The amount of 700 ml of supernatant from hybridoma cell culture OX23 or OX24 was applied to protein G-Sepharose column at 1 ml/min. The column was then washed with 50 ml of PBS. The antibodies were eluted with 10 ml of 100 mM glycine pH 2.5 (Fisher Scientific). Fractions of 1 ml were collected into tubes containing 60 µl of 1 M Tris-base (Fisher scientific) pH 9.5.

The tubes were gently mixed to neutralise the pH, immediately after the elution was completed (Figure 2. 1). The columns were then washed with 3 – 5 column volumes of elution buffer and immediately re-equilibrated by washing with 3 – 5 column volumes of PBS. All buffers which were applied to the column were cold and filtered, using 0.22 µm filter top. The eluted fractions were assessed by the measuring of absorbance at 562 nm, using NanoDrop (NanoDrop 2000, Thermo Scientific). sodium dodecyl sulphate polyacrylamide gel electrophoresis (SDS-PAGE) was performed to test the purity of purified antibodies. The fractions containing a high concentration of antibody were collected and dialysed against 2 L of PBS overnight, using dialysis tubing cellulose membrane (Sigma # D9652). The total concentration of purified antibody was determined by bicinchoninic acid (BCA) protein kit assay (Thermo Scientific Pierce # 23227) and read on NanoDrop.

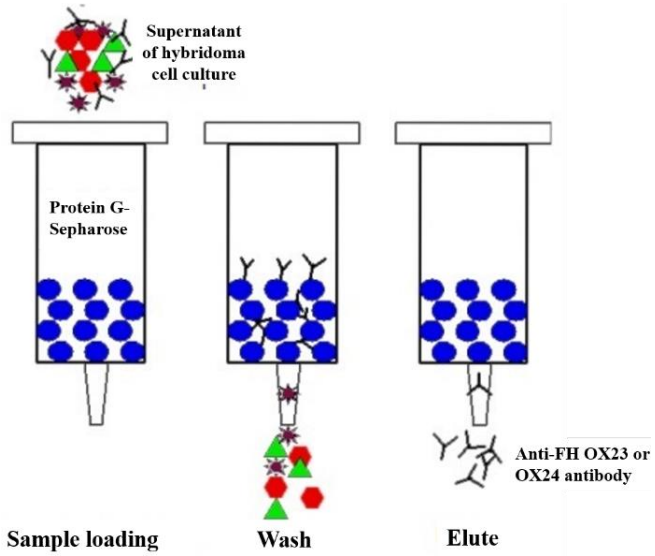

Figure 2. 1: Purification of anti-FH OX23 or OX24 antibodies by affinity chromatography. The supernatant of hybridoma cell culture was loaded on protein G-Sepharose column. The antibody bound to protein G. To remove undesired proteins, the column was then washed using pH 7.4 buffer. The antibody was eluted by changing the pH using glycine pH 2.5 buffer to break the bonds between protein G and antibody (http://www.meizhenggroupen.com/life_c/i=8&comContentId=8.html).

2.4 Purification of FH

Human FH was purified by applying human plasma mixed pool (TCS Biosciences LTD # TCS001P) to three-step affinity chromatography. The plasma was centrifuged at 4ºC, 10,000 rpm for 10 min. It was first passed through a column of lysine-Sepharose to eliminate plasmin/plasminogen. The flow-through plasma was then passed through immunoglobulin G (IgG)-Sepharose column to eliminate IgG-Sepharose binding proteins. Finally, the plasma was

then loaded on anti-FH OX23 immobilized on Sepharose. The buffers that were passed through the columns were cold and filtered (Yu *et al*., 2014).

2.4.1 Lysine-Sepharose column preparation and plasminogen depletion

Lysine-Sepharose column was prepared to remove the plasmin/plasminogen from the plasma. The weight of 1 g of cyanogen bromide-activated Sepharose 4B (Sigma # C9142) was added to 15 ml of 100 mM $NaHCO_3$ (Sigma) buffer, pH 8.9 with 2 g of L- lysine monohydrochloride (Fisher Scientific). The pH was then adjusted to 8.9 in 5 ml of H_2O. The slurry was stirred overnight at 5ºC (Deutsch and Mertz, 1970). The column (10 x1.5 cm diameter) was degassed by washing with 50 ml of binding buffer (100 mM sodium phosphate (Sigma-Aldrich), 150 mM NaCl (Sigma-Aldrich), 15 mM EDTA (Sigma), pH 7.4). The slurry was then loaded into a column. The column was immediately equilibrated with 50 ml of the binding buffer. The pooled human plasma (50 ml) was passed through the column at a rate of 1 ml/min. The column was then washed with 100 ml of the binding buffer. The plasmin/plasminogen was eluted by washing the column with 50 ml elution buffer (100 mM sodium phosphate, 150 mM NaCl, 0.5 M 6-aminocaproic acid (Sigma-Aldrich), 15 mM EDTA, pH 7.4). The column was then washed with 200 ml elution buffer and re-equilibrated with 100 ml of binding buffer. Serum depleted of plasmin/ plasminogen was dialysed overnight against 2 L of running buffer of the next column (25 mM Tris–HCL (Sigma-Aldrich), 140 mM NaC1, 0.5 mM EDTA, pH 7.4). Following the dialysis, the serum was then passed through the IgG-Sepharose column.

2.4.2 IgG purification

Human IgG was purified from human plasma to set up IgG-Sepharose column. This column was used to eliminate plasma proteins that could bind to anti-FH OX23 Sepharose used for FH purification. Human serum (20 ml) was centrifuged at 4ºC and 10,000 rpm for 10 min and dialysed against PBS overnight. The serum was then diluted to 40 ml with PBS. Protein G-Sepharose column was equilibrated with 50 ml of PBS. After running the serum through the column, it was then washed with 100 ml of PBS. Human IgG was eluted from the column in 25 ml of 100 mM Glycine, pH 2.5 and neutralized with 1.5 ml of Tris-base, pH 9.5. Following the dialysis with 2 L of PBS, the serum was then passed through the IgG-Sepharose column. The concentration of IgG was measured by absorption at 280 nm. IgG purity was tested by SDS-PAGE. The column was washed and stored as described in section 2.3.2.

2.4.3 IgG-Sepharose column

Purified IgG were immobilised to CNBr-activated Sepharose to remove proteins which could bind to IgG such as C1q, fibronectin and rheumatoid factors. CNBr-activated Sepharose (1g) was hydrated by adding 150 ml of 1mM HCl (0.25 g of dry resin for each 1 ml hydrated resin was needed) and left at room temperature for 15 min. The suspension was centrifuged at 1,000 rpm for 1 min. The supernatant was decanted, and the resin was transferred into a small, sintered glass funnel with Whatman filter paper and kept wet. The resin was then transferred immediately by using a clean spatula into a tube containing 20 mg of IgG antibody solution (10 mg of IgG/ ml of packed Sepharose) and mixed on a slow rotary stirrer for at least 2 h at 20ºC. A high pH (greater than 7.2 – 7.5) increases the coupling efficiency of the antibody with the resin. However, the antigen-binding capacity of the immobilised antibody is often greatly diminished at a higher pH. Therefore, the coupling pH should be not higher than pH 7.5. The slurry was then centrifuged at 1,000 rpm for 1 min and filtered in a sintered glass funnel. The supernatant was kept measuring optical density at OD280, which was 150-fold lower than its concentration before the coupling with the resin. The resin was then washed twice with 10 volumes of 2 M NaCl. Finally, the resin was mixed with about 20 times its volume of 100 mM ethanolamine hydrochloride Sigma-Aldrich) or 100 mM Tris-HCl, 150 mM NaCl, pH8.5 to block reactive sites, and was stirred for 2 h, at room temperature. The resin was vigorously mixed by using 1,000 µl pipette and poured in degassed column (10 x1.5 cm diameters). The column was then equilibrated with 50 ml of running buffer (25 mM Tris–HC1, 140 mM NaC1, 0.5 mM EDTA, pH 7.4) The serum depleted of plasmin/plasminogen was run through at 1 ml/min and kept for subsequent FH purification. The column was then washed with 100 ml of running buffer. Bound proteins were eluted with 10 ml of the chaotropic buffer, 3M $MgCl_2$, adjusted to pH 6.8 – 7.0 by adding Tris-base. Following regeneration with 50 ml of elution buffer, the column was re-equilibrated with 50 ml of running buffer. EDTA was added as a preservative by adding 200 mM sodium EDTA, pH 7.4 to the column to a final concentration of 5 mM prior to storage at 4°C.

2.4.4 Binding of anti-FH OX23 Antibody to Sepharose and FH purification

Purified anti-FH OX23 antibody was coupled to CNBr-activated Sepharose as described in section 2.3.3 and packed in a column to purify FH. Approximately 8 mg of antibody was bound with 1 g dry resin (2 mg of antibody immobilised to 1 ml of swollen resin). The concentration

of OX23 was 30-fold lower than its concentration before the binding with the Sepharose. The same procedure that used in section 2.4.3 was carried out to purify FH. The plasma depleted of plasmin and other proteins was passed through an anti-FH OX23-Sepharose column. Bound proteins were eluted by 3 M $MgCl_2$ and dialysed twice for 8 h against 2 L of water, then twice against PBS and stored at -20ºC, which can be stable for more than one year without degradation. The total quantification of purified FH was assessed by BCA protein kit assay. The purity of FH was confirmed by 10% SDS-PAGE. The reactivity with anti-FH OX23 and OX24 antibodies was verified by dot blot and the identity was confirmed by western blot.

2.5 Protein characterization techniques

2.5.1 SDS-PAGE

SDS-PAGE was performed to determine the presence of desired protein from the mixture after protein purification. The molecular weight of purified protein can be estimated by comparison with a Standard pre-stained protein marker (Thermo Sientific # 26619). Purified anti-FH antibodies, purified FH, recombinant IAV proteins, purified IAVs and deglycosylated IAVs were characterized by using 10% SDS-PAGE gel which consists of a resolving gel (Table 2. 4) and stacking gel (Table 2. 5) on which the sample was loaded. Samples were mixed with 2×Laemmli sample buffer (BIO-RAD # 161-0737) in 1:1 v/v ratio and either heated at 95ºC for 10 min in loading buffer with 5 % β-mercaptoethanol (denaturing and reducing condition or were left without heating and β-mercaptoethanol (non-reducing condition). Samples were loaded into a gel cassette immersed in 1×Tris/Glycine/SDS buffer (Bio Rad). Standard pre-stained protein markers were loaded to assess the size of the purified proteins. Electrophoresis was run at 110 V for 1 – 2 h. Subsequentially the gel was stained with Coomassie Blue staining solution (50 % Methanol, 10 % acetic acid with 0.1 % Coomassie Brilliant Blue R250) for 2 h with shaking. Following the staining, the gel was soaked in destaining solution (50 % methanol with 10 % acetic acid) with shaking for 2 h. Destaining solution was changed 3 times and then replaced with a diluted destaining solution (7 % methanol with 10 % acetic acid) for 1 h with shaking until bands were seen without background staining. The gel was then equilibrated in the storage solution (5 % acetic acid) with shaking for at least 1 h to return it to its original shape. Gel image was taken using Bio-Rad molecular imager or ODYSSEY CLX (LI-COR Biosciences).

Table 2. 4: Components of resolving gel.

Components	Volume
H2O	3.3 ml
30% Acrylamide/Bis Solution (biorad)	04 ml
1.5 M Tris-HCL, pH8.8	2.5 ml
10% sodium dodecyl sulphate (SDS)	50 µl
10% Ammonium persulfate (APS)	50 µl
TEMED	10 µl

Table 2. 5: Components of stacking gel.

Components	Volume
H2O	3.4 ml
30% Acrylamide/Bis Solution (Bio-Rad)	830 µl
1.5 M Tris-HCL, pH6.8	630 µl
10% sodium dodecyl sulphate (SDS)	50 µl
10% Ammonium persulfate (APS)	50 µl
TEMED	05 µl

2.5.2 Dot blot

Dot blot assay was performed to confirm the presence of anti-FH OX23 and OX24 antibodies in the supernatant of hybridoma cell culture. The assay was also used to verify the reactivity between purified FH and purified anti-FH antibodies. Increasing concentrations of FH (0.5 µg, 1 µg, and 2 µg) were blotted on Immobilon-FL Polyvinylidene Difluoride (PVDF) filter type transfer membrane (Sigma-Aldrich # IPF00010) and left to dry at room temperature. The membrane was blocked with 5% skimmed milk in PBS/0.1% Tween 20 (PBSTM) overnight on a rotary shaker at 4°C. The membrane was then incubated overnight with the supernatant diluted in PBS (1:1) on a rotary shaker at 4°C. It was then washed 3 times with PBST (10 min each) on a horizontal shaker. The binding of FH to anti-FH antibodies was detected by incubating the membrane with anti-mouse IgG-horseradish peroxidase (HRP) secondary antibody (Sigma) diluted 1:1000 in PBSTM with shaking for 1 h at room temperature. It was

then washed three times with PBST and a once with PBS. To visualise the binding, the membrane was placed into a chromogenic visualization solution, ECL Western Blotting Substrate (Thermo Scientific Pierce, # 32209) for 1 min. The blotted membrane was placed against the Amersham Hyperfilm ECL (Fisher Scientific) in a light-proof cassette. After the exposure to various periods, the film is developed using X-ray film developers (Abnova) in a darkroom.

The dot blot assay was also used to confirm the solubility of biotinylated HA peptides (Alta Bioscience) and that all HA peptides were in the same concentration range. IRDye 800CW streptavidin conjugated to horseradish peroxidase (LI-COR Bioscience) was used at a dilution of 1:500 to detect the presence of the peptides. The LI-COR® Odyssey® Infrared Imaging System (LI-COR Bioscience) was used to show the interaction between the HA peptide and the HRP-conjugated streptavidin.

2.5.3 Western blot

Western blot analysis was used to identify purified human FH and various recombinant CCPs of FH. After separating protein sample by electrophoresis (SDS-PAGE) as in section 2.5.1, they were transferred to an iBlot™ 2 Transfer Stacks PVDF (Invitrogen # IB24002) at 23 V for 6 min using Invitrogen iBlot 2 Dry Blot System (life Technology). The membrane was blocked for 1 h in Immobilon Signal Enhancer (Mereck # WBSH0500) that works as signal amplification and blocking buffer. The membrane was washed thrice with PBST and hybridised with the primary antibody, mouse monoclonal anti-FH OX23 or OX24 (purified in this study) or goat Anti-Human Factor H (Complement Technology # A237) diluted in immobilon buffer for 2 h at room temperature (RT) or overnight at 4°C under constant rotation. After washing three times in PBST, the membrane was blotted with secondary antibodies FH/CCPs were detected with IRDye 800CW goat anti-mouse (LI-COR Bioscience) or RDye 800CW donkey anti-goat secondary antibody (LI-COR Bioscience) and scanned by the Odyssey Imaging System. Complement factor H from human plasma (Sigma Aldrich # SIG001P) was as control to identify purified human FH in this study.

2.6 Enzyme-linked immunosorbent assay (ELISA)

ELISA was used to test IAV-FH interaction. Maxisorp 96-well microtitre plates (Fisher Scientific) were coated in triplicate with 10^4 PFU/well of purified live IAV in a carbonate-

bicarbonate buffer (CBC), pH 9.6, (Sigma-Aldrich # C3041-50CAP). Each capsule of CBC was dissolved in 100 ml distilled water. The plate was incubated overnight at 4°C and then washed 4 times with PBST. The ELISA plate was blocked for 1 h with blocking buffer (PBS with 5% BSA). After 4 times washing, FH was added in increasing concentrations and incubated for 2 h at RT. The plate was washed 4 times and incubated with the primary antibody, anti-FH OX24 diluted in blocking buffer (1:1000) for 1 h. A virus without FH was used as a positive control to indicate the presence of the virus. The positive control was incubated with monoclonal mouse anti-NP antibody (Prof. Munir Iqbal, Pirbright Institute) diluted 1:2000. After washing, the plate was incubated with polyclonal rabbit anti-mouse HRP (Dako # P0260) diluted 1:2000 in blocking buffer for 1 h. The plate was washed 4 times and the colour was developed using 3,3′,5,5′-Tetramethylbenzidine (TMB) substrate (Sigma-Aldrich) and the reaction was stopped using 2 N H_2SO_4 (Sigma-Aldrich). The experiment was carried out in Class II Biosafety Cabinet. The absorbance was read at 450 nm using Absorbance microplate Reader ELX 808 (Bio-Tek).

2.7 Far western blot

Far western blot is a protein-to-protein interaction assay. It was performed to identify potential viral proteins responsible for virus binding to FH. In these experiments, a purified virus preparation was loaded in triplicate for viral protein separation by electrophoresis on a 10% reducing or non-reducing SDS-PAGE gel. After electroblotting on PVDF membrane, the membrane was blocked and cut into 3 parts. As a control, half of the blotted membrane was hybridised with anti-HA antibody (Table 2. 5). The overlay was performed by incubating the second half of the membrane with 20 µg/ml of purified FH. FH binding was detected using anti-FH OX24. As a negative control, the third membrane was incubated with the anti-FH antibody. For detection of viral proteins, each membrane was incubated with either HRP-conjugated secondary antibody and visualised by AEC Substrate Chromogen (Dako # K3464) or Odyssey secondary antibody and scanned by the Odyssey Imaging System. Table 2. 6 shows primary and secondary antibodies used in far western blot.

Table 2. 6: Primary and secondary antibodies used in western blot and far western blot.

Protein desired	Primary antibody	Secondary antibody
FH	Mouse monoclonal anti-FH OX23 (This study)	IRDye 800CW goat anti-mouse
FH	Mouse monoclonal anti-FH OX24 (This study)	IRDye 800CW goat anti-mouse
FH	Goat anti-FH (Complement Technology # A237)	Rabbit anti goat conjugate (abcam)
H1 HA	Ferret polyclonal anti-HA California/7/09 (H1N1) (NIBSC)	goat anti-ferret HRP conjugate (abcam)
H3 HA	Ferret polyclonal anti-HA Hong Kong/99 (H3N2) (NIBSC)	goat anti-ferret HRP conjugate (abcam)
H5 HA	Mouse monoclonal anti-H5 (H5N3) (Prof. Munir Iqbal)	IRDye 800CW goat anti-mouse
H9 HA	Mouse monoclonal anti-H9 (H9N2) (Prof. Munir Iqbal)	IRDye 800CW goat anti-mouse
M1	Mouse monoclonal anti-M1 (Bio-Rad)	IRDye 800CW goat anti-mouse
N1 NA	Monoclonal anti-NA, (BEI Resources, ATCC # NR-50239)	IRDye 800CW goat anti-mouse

2.7 Immunoprecipitation assay

The direct interaction between IAV HA protein and FH was assessed by immunoprecipitation (IP) assay. According to the manufacturer's instructions, biotin anti-C-tag conjugate antibody (Life Technologies # 7103252100) (which recognises the 4-amino-acid "C-tag" peptide tag glutamic acid (E), proline (P), glutamic acid (E), alanine (A)) was immunoprecipitated with NHS (N-Hydroxysuccinimide) FlexiBind beads (Millipore # LSKMAGN01). The beads then were incubated with C-tag HA recombinant protein of H3N2. After washing with PBS, the beads were incubated with 20% human serum or purified FH. The beads were washed and subjected to SDS PAGE and Western blot analysis. Beads with or without HA protein and beads without anti-C-tag antibody were used as a negative control.

2.10 Haemagglutination inhibition (HI)

In this technique, Haemagglutination assay was modified to investigate whether FH can block IAV-HA adsorption to RBC. PBS (25 µl) was added to each well starting in column 2 of a 96-well V-bottom microtitre plate. To the first column, 50 µl of starting concentration of purified FH (40 µg/well) were added and serially diluted to 40, 20, 10, 5, 2.5, 1.25, 0 µg/well by transferring 25 µl to the next columns. Working dilution (25 µl) of the virus (4 HAU/25 µl) were added to each well except the control. FH at the highest concentration (40 µg/well) was

as a negative control. The plate was gently mixed and left at RT for 1 h. After the incubation period, 50 µl of TRBCs were added and incubated for 30 – 60 min at RT or 4°C. Inhibition of Haemagglutination shows red dots in the centre of the well.

2.11 IAV entry assay

Virus entry assays were performed to investigate whether interaction of FH with IAV alters the entry stage of IAV replication in the target cells. H1N1pdm09 at MOI 1 or H3N2/99 at MOI 0.1 pre-incubated in the presence or absence of 100 µg/ml FH were inoculated on A549 cells (5×10^5) in 6-well plate for 1 h at 37°C. Uninfected and FH-untreated cells were used as a negative control. Following incubation, cells were washed three times with PBS to remove unattached viruses. The cells then were incubated with an infectious medium for 4 h or 8 h. Following extensive washing in cold PBS, cell lysates were prepared by adding the lysis buffer (1% Triton X 100, 20 mM Tris-HCl, 150 mM NaCl, 1mM EDTA, 1% anti-proteases cocktail (Fisher Scientific)). The cells were scraped then centrifuged at 10,000rpm for 10 min at 4°C. The addition of anti-proteases cocktail and prepare the lysates on ice or at 4°C prevent the degradation of the proteins by protease enzymes. Cell lysates were then analysed for M1 protein levels by western blot using an antibody directed against M1.

2.12 IAV infection assays

To assess if the interaction of IAV and FH perturbs IAV viral replication in A549 and THP-1 cells, two sequential assays were performed. The initial assay determined the titre of the virus that causes 50% CPE (a marker in this assay of infection) of A549 and THP-1 cells following 24 h of infection. This was important to allow the correct amount of virus to visualise positive or negative impacts of FH interaction on IAV replication. This IAV titre was then used to infect cells in a second assay which measured the effect of FH interaction on the replication cycle of IAV.

2.12.1 The optimal MOI of IAV infection

This assay was performed to determine the titre of IAV causing 50% cell death. The wells of two columns of a 96-well microtitre plate were coated with 50 µl of 2.5% collagen type 1 (Sigma-Aldrich). Two other columns were coated with 50 µl of 0.01% poly-L-lysine (Sigma-Aldrich). The plate was incubated at RT for 1 – 2 h. The wells were then washed twice with PBS and seeded with 7.5×10^4 A549 or THP-1 cells in 100 µl of 1x infectious medium. The

plate was incubated at 37°C in for 3 – 4 h to allow the cells to adhere to the surface of the wells. Serial dilutions of IAV in MOIs of 0, 0.001, 0.01, 0.1, and 1 were prepared. After the incubation period, the cells in each column inoculated with different MOI of IAV in triplicate and incubated for 24 h. The supernatant (146 µl) of the cell culture from each well was then transferred into the first column of a new plate as a starting dilution and serially transferred into all wells containing 100 µl pure DMEM as in section 2.2.5. The number of wells that showed positive for CPE was then determined for each MOI. Using a GraphPad Prism, the mean CPE percentages for each MOI were plotted on linear Y-axis against the logarithmic value of the MOI in X-axis. The MOI that led to the CPE in 50% of wells with infected cells (optimal MOI) was then calculated through interpolation of the best fit line determined by non-linear regression.

2.12.2 Evaluation of the effect of FH on IAV replication

To examine the impact of FH binding on IAV infectivity, an experiment was designed that consisted of two steps: 1/ infection of target cells for 24 h at a pre-defined MOI in presence or absence of FH; 2/ measure the cytopathic effect (CPE) on MDCK cells to assess virus titres using serially diluted cell supernatant from step 1.

The first 4 columns of a 96-well microtitre plate (1, 2, 3 and 4) were seeded with A549 cells. Four other columns (9, 10, 11 and 12) were seeded with THP-1 cells in 100 µl of 1x infectious medium (without TPCK-Trypsin) as in section 2.12.1 (Figure 2. 2). The plate was incubated at 37°C for 3h. After the incubation period, FH was added (5 µg/ml) to each well of column 2 and 10 and incubated at 37°C for 1 h (cells pre-treated with FH). The optimal MOI of each virus was diluted in 1x infectious medium (without TPCK-Trypsin) without or with 5µg/ml of FH at 37°C 1 h (virus pre-treated with FH). After 1 h of the incubation period, 2X TPCK-Trypsin was added to the incubated viruses. A virus without FH was added into cells with FH in columns 2 and 10 (FH+cells) and columns 3 and 11 (control). A virus pre-treated with FH (FH+ virus) was added into cells without FH in columns 1 and 9. The cells in columns 4 and 12 left uninfected and untreated with FH as a negative control. The plate was incubated for 24 h at 37°C. After the incubation period, 146 µl of the supernatant from each column was transferred into the first column in a new plate and $TCID_{50}$ was performed to evaluate the impact of FH on viral replication.

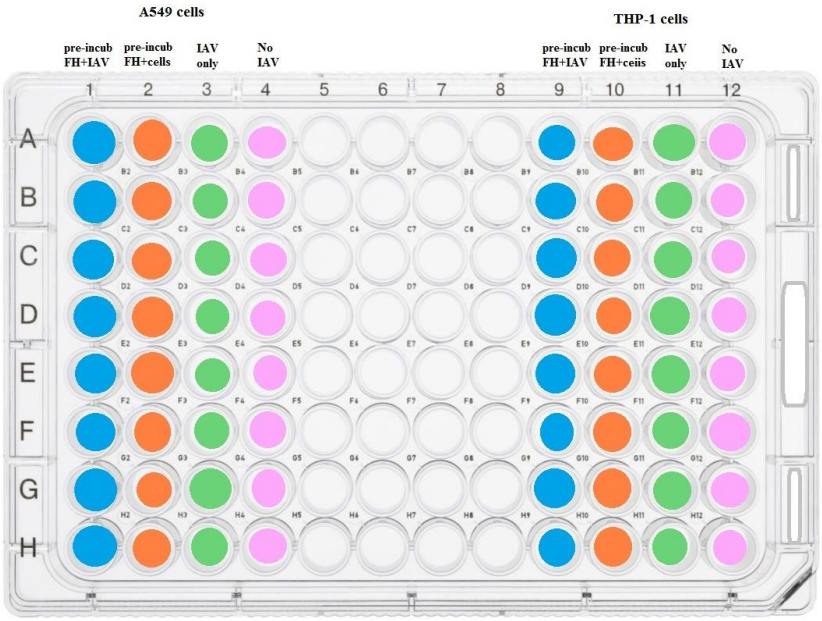

Figure 2. 2: Experimental design to assess the effect of FH on IAV replication in infected A549 and THP-1 cells. Columns 1, 2, 3 and 4 were used for seeding A549 cells. Columns 9, 10, 11 and 12 were used for seeding THP-1 cells. In columns 1 and 9 (blue), the cells were infected with a virus that had been pre-incubated with FH. In columns 2 and 10 (orange), cells were pre-incubated with FH before the addition of the virus. In columns 3 and 11 (green), cells were infected with the virus, in the absence of FH (control). Finally, untreated, and uninfected cells were incubated in columns 4 and 12 (pink) as a negative control.

2.13 Immunohistochemistry assay

Immunohistochemistry assay was performed to analyse the role of FH at the entry stage of IAV infection in A549 cells. A549 cells ($2.5x10^4$ ells/well in 24-well plate) were cultured on the sterilised coverslips (Appleton # MS311) and incubated for 24 h. The cells were then inoculated with H1N1pdm09 at MOI 1 or H3N2/99 at MOI 0.1 pre-incubated in the absence or presence of 100 µg/ml of FH in pure DMEM media and incubated for 1 h. Uninfected and untreated cells with FH used as a negative control (C). After the incubation period, cells were washed with PBS and infectious media was added. The plates were then incubated for different time points at 4, 8,18, 24 h. The cells were washed and fixed by methanol/acetone 50:50% (v/v) for 5 min at RT. After excessive washing with PBS, the cells were blocked with 5% FBS overnight at 4°C. The cells were incubated with monoclonal mouse anti-NP antibody (Prof Munir Iqbal, Pirbright institute) (1:1000) at 4°C overnight. After washing, the cells then were incubated with anti-mouse secondary antibody HRP (1:1000). Following a final wash, the cells were stained with Dako substrate. The effect of FH on virus entry and replication was observed under the Invitrogen EVOS XL Core Cell Imaging System (transmitted light microscope).

2.14 Immunofluorescence assay

Immunofluorescence assay to track the effect of FH binding on H1N1pdm09 entry into A549 cells. A549 cells (2.5 x 10^5 cells/well) were cultured on the sterilised coverslips in 24-well plate and incubated for 24 h. After washing the cells with PBS, pre-incubated H1N1 (MOI=1) without or with FH at 100 µg/ml in pure DMEM media for 1 h was added into the cells and incubated for I h. The cells were then washed and incubated with infectious media at different time points (attachment, 15 min, 30 min, 1 h, 2, 6, 8 and 24 h). The cells were washed and fixed using methanol/acetone 50/50% (v/v) for 5 min at RT. After washing, the cells were blocked with 0.5% BSA overnight at 4°C. The cells were subsequently stained with anti-NP antibody (1:1000) at 4°C overnight. After washing with PBS, the cells were stained with Alexa Fluor 488-conjugated goat anti-mouse secondary antibody (Invitrogen # A32723) (1:1000) for 1 h. After a final wash, the cells were then completely covered with vectashield Mounting Medium with DAPI (Vector # H-1200) for nuclear staining and sealed with a coverslip and nail varnish the fluorescence was visualised under a TCS SP5 Confocal microscope (Leica**)** and the analysis was performed using Leica Application Suite X (Leica).

2.15 De-glycosylation of IAV and FH

To understand the effect of glycans on the interaction between FH and IAV, purified IAV and FH were de-glycosylated using PNGase F (New England BioLabs # P0704S). According to the manufacturer's instructions for PNGase F, about 10 µg of purified virus or FH protein was denatured by adding 10 X glycoprotein denaturing buffer (5% SDS, 0.4 M DTT) with H_2O to obtain a total reaction volume of 10 µl. The glycoprotein was heated at 100°C for 10 minutes. 2 µl of 10 X GlycoBuffer 2 (0.5 M Sodium Phosphate, pH 7.5), 2 µl 10% NP-40 and 6 µl H_2O were added to obtain a 20 µl reaction volume. 1 µl PNGase F, was added and mixed gently. The reaction mixture was incubated at 37°C for 24 h. After the incubation period, the de-glycosylated protein was mixed with protein loading buffer and β-mercaptoethanol. After heating to 95°C for 5 min, SDS-PAGE and western blot were performed.

2.9 Statistical Analysis

Data were analysed statistically with GraphPad Prism version 8.3.0 (538) software. Statistical significance was determined by using one-way ANOVA and Dunnett’s test for multiple comparisons was performed to compare each mean to a control mean.

Chapter 3- Purification and characterization of human FH

3.1 Introduction

Complement FH is predominantly produced by the liver and circulates in the bloodstream (Pouw *et al*., 2016; Olivar *et al*., 2016) at a large concentration variance of 63.5–847.6 µg/mL (van der Maten *et al*., 2016). This variation is due to the combined influence of environmental factors (such as smoking and age) and genetic component (van der Maten *et al*., 2016). Human plasma is a rich source of FH. Therefore, it is a suitable starting material for FH purification (Wang *et al*., 2013).

Recombinant full-length FH has been produced in the yeast cells, *Pichia pastoris*, the moss *Physcomitrella patents* and a baculovirus-insect cell system which are able to apply post-translational protein modification to recombinant proteins close to human N-glycans (Büttner-Mainik *et al*., 2011; Brandstätter *et al*., 2012). However, recombinant FH glycosylation does not occur in the same manner as native FH, and this may have consequences for interaction with partner proteins. (Wang and Zhao, 2013; Büttner-Mainik *et al*., 2011). Failure to give full glycosylation is because of the plant-specific sugar residue, a xylose not included within human glycans. In addition to that, the structure of fucose associated with the core glycan differs from its human analogue in plants. Therefore, in this project human plasma was used as a source to purify full-length FH (Büttner-Mainik *et al*., 2011; Wang *et al*., 2013).

Affinity chromatography using inexpensive natural ligands or synthetic ligands such as anionic phospholipid, cardiolipin or trinitrophenyl groups has been used to purify FH from human plasma (Yu *et al*., 2014). However, these methods are suitable only for purifying FH from a relatively small scale of plasma (50 ml or less). This is due to the low binding capacity of these ligands to FH (Yu *et al*., 2014). Since this project required a large amount of purified FH protein, we chose to use affinity chromatography that incorporated anti-human FH monoclonal antibody as the ligand immobilised on Sepharose. In this method, each single FH molecule will bind to one molecule of the monoclonal antibody. Where each monoclonal antibody has one paratope comprised of 15 amino acids and only 5 of these amino acids contribute to binding energy for the epitope (binding area of an antibody on the antigen) (Frank, 2002). Therefore, 1 mg of the monoclonal antibody will yield about 1 mg of FH (Yu *et al*., 2014). In addition, use of monoclonal antibodies allows the discrimination between FH, FHL-1 and other FHR proteins, where these antibodies specifically bind to FH and FHL-1 without detecting the other FH family proteins (Yu *et al*., 2014; Berra & Clivio, 2016). OX23, OX24, 35H9, and 5H5 are

all human monoclonal antibodies that have been used to purify FH from human plasma using affinity chromatography (Sim *et al*., 1993; Schneider *et al*., 2006; Hakobyan *et al*., 2008; Okemefuna *et al*., 2010; Yu *et al*., 2014; Berra & Clivio, 2016). Purification of FH using immunoaffinity is a reproducible method, giving a high yield of FH approximately 80% with high purity about 98% (Sim *et al*., 1993).

Previous studies were shown that OX24 inhibits the binding of FH and FHL-1 to surface-bound C3b. On the other hand, OX23 which binds to a different epitope from OX24 has no effect on the binding of FH and FHL-1 to surface-bound C3b (Sim *et al*., 1983). OX23 is only convenient for purification of FH from human and primates such as rhesus, cynomolgus, and African green monkey plasma since they have a conserved OX23 epitope (Yu *et al*., 2014).

The objective of this chapter was to obtain high yield and purity FH from human plasma. In this study, purification of FH from human plasma is schematised in Figure 3. 1 and comprised three three-step affinity chromatography, including the elimination of plasmin through a L-lysine Sepharose column because FH can be degraded by plasmin, removal of other proteins that can bind to IgG (such as C1q, fibronectin, some IgG and IgM) and subsequently may contaminate the final product of purified human FH by applying to IgG-Sepharose column and finally, the serum will be processed through anti-FH antibody OX23 Sepharose column. Characterisation and identification of purified FH will be performed using Coomassie-stained SDS-PAGE, western blot, and dot blot assays.

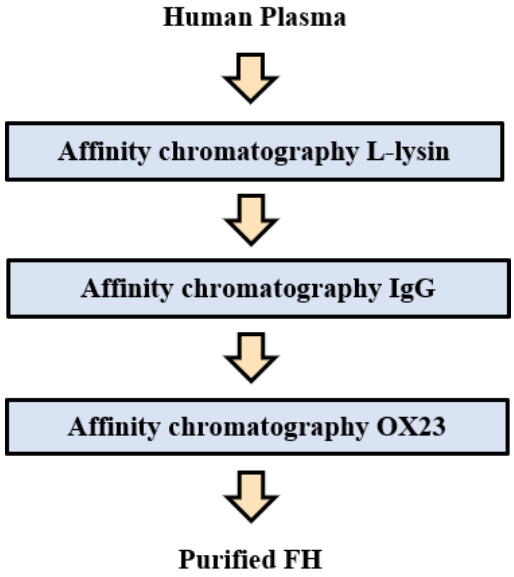

Figure 3. 1: **Human FH purification scheme.** Three-affinity chromatographies including plasminogen/plasmin elimination using L-lysin Sepharose column, removal plasma proteins that can bind to OX23 column using IgGs Sepharose column and isolation of FH from OX23 column.

3.2 Results

3.2.1 Purification of anti-FH antibodies, OX23 and OX24

Purification of anti-human FH antibodies, OX23 and OX24 from hybridoma cell lines OX23 and OX24 was essential since they were required for the purification of human FH by affinity chromatography from human plasma.

3.2.2 Confirmation of the presence of anti-FH antibodies OX23 and OX24 in the supernatant of hybridoma cell culture

To detect the presence of anti-FH antibodies, OX23 and OX24 in the supernatant of the hybridoma cell culture a dot blot assay was performed. Increasing concentrations of commercial FH (0.5 µg, 1 µg, and 2 µg) were dotted on PVDF membrane and this was then incubated with the supernatant of hybridoma cell culture. Bound antibodies to human FH were detected using an HRP-conjugated anti-mouse (IgG) secondary antibody. As Figure 3. 1 shows it was confirmed that the monoclonal antibodies, OX23 and OX24 were successfully produced by hybridoma cells and recognised specifically human FH. These antibodies did not recognise a control protein maltose binding protein (MBP) as is shown in Figure 3.6.

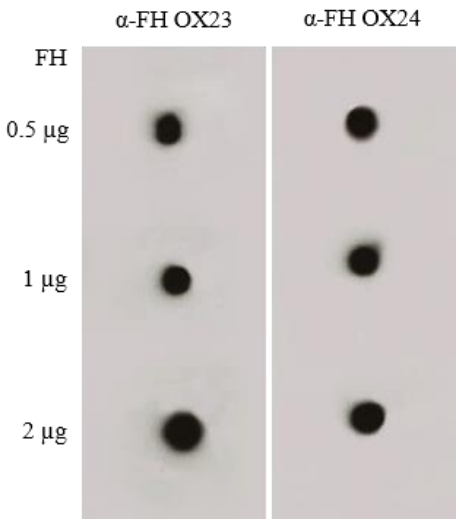

Figure 3. 2: Dot blot assay confirming the specificity of anti-FH antibodies OX23 and OX24 in the supernatant of hybridoma cells culture. The dots of different concentrations of FH were incubated with the supernatant in PBSTM diluted 1:1. The presence of anti-FH antibodies OX23 (α-FH OX23) and OX24 (α-FH OX24) was identified by incubating the membranes with HRP- conjugated anti-mouse IgG secondary antibody diluted at 1:1000. The binding was detected using ECL western blot substrate. The image was then developed by exposure to x-ray film.

3.2.3 SDS-PAGE analysis of purified anti-FH antibodies OX23 and OX24

Anti-FH antibodies, OX23 and OX24 in hybridoma cells culture supernatant were purified using protein-G Sepharose affinity chromatography. The eluted fractions from each antibody were collected with the total amount of 11.8 mg and 9.9 mg respectively which were extracted from 700 ml of the supernatant. The purity of purified antibodies was characterised by a Coomassie-stained SDS-PAGE under non-reducing and reducing conditions. Figure 3.2 shows that under non-reducing conditions, the presence of one band of purified OX23 or OX24 antibody at 150 kDa, which is the predicted size of the antibodies, corresponding to the immunoglobulin tetramers of two heavy chains and two light chains. This 150 kDa band was also observed for commercial mouse anti-FH monoclonal antibody OX23 (Com OX23) used as control (Figure 3. 2, A). The β-mercaptoethanol, reduced gel of both antibodies revealed heavy chain bands at 50 kDa and light chain bands at 25 kDa which was in line with the observation of the monoclonal mouse ascites anti-H1(Anti-H1) antibody used as a control (Figure 3. 2, B). The flow through (Flowt) of the supernatant of the hybridoma cell culture OX24 showed a clear band for albumin at 66 kDa. The bands with high molecular weight at the top of each gel may be due to either the accumulation of tested antibodies or an IgG dimer (300 kDa). These results confirm the purity of purified anti-FH antibodies, OX23 and OX24 by one-step affinity purification using protein G-Sepharose.

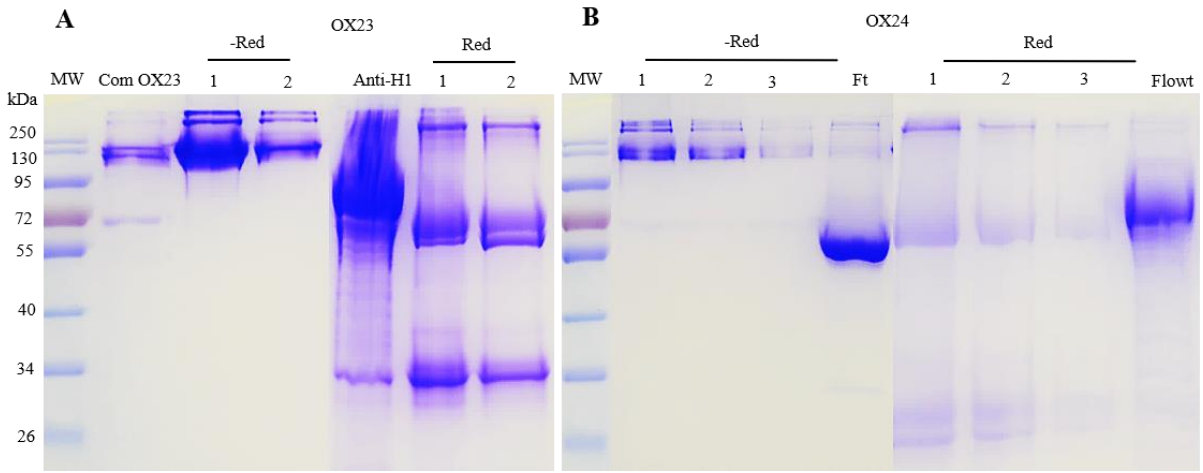

Figure 3. 3: Analysis of purified anti-FH antibodies, OX23 and OX24 by Coomassie-stained 10% SDS-PAGE. (A) Two fractions of purified OX23 (1 and 2 with concentrations >2.5 and 0.7 mg/ml), and **(B)** three fractions of OX24 (1,2, and 3 with concentrations > 2.5, 1.4 and 0.3 mg/ml respectively) were subjected to non-reducing (-Red) and reducing (Red) conditions. The flow-through (Flowt) of the supernatant of hybridoma cell culture OX24 was run into the gel to confirm the binding of a purified antibody to protein G Sepharose. Commercial anti-FH OX23 (Com OX23) antibody, and mouse ascites anti-H1(Anti-H1) antibody were used as controls. The mobility of size markers is indicated to the left of the gel.

3.2.2 Purification of IgGs from human serum

Human IgGs were purified from human plasma by one-step affinity chromatography on protein G-Sepharose column. This column was used to eliminate plasma proteins that could bind to anti-FH OX23 Sepharose used for FH purification. The total amount of purified IgGs was 25 mg eluted from 20 ml of human plasma. IgGs purity was tested by Coomassie-stained 10% SDS-PAGE under non-reducing and reducing conditions. IgGs under non-reducing condition were detected as a single band around 150 kDa, whereas under reducing condition presented heavy chain (H-chain) band around 50 kDa and light chain (L-chain) band around 25 kDa (Figure 3. 4). In addition, three faint bands at 70, 100, and 150 kDa were observed in reducing SDS-PAGE. These multiple bands are noticeable when IgG was exposed to a low concentration of β-mercaptoethanol that reduce the inter-heavy chain disulphides, resulting in formation of half molecules of antibody, heavy-heavy, and heavy-heavy-light chains, respectively. The current results emphasised the purity of eluted IgGs and enabled it to be used in preparation of IgGs Sepharose column which was an essential preparation step for FH purification from human plasma. This column was used to remove other proteins in plasma, such as C1q, and some IgG and IgM that may contaminate the final product of purified human FH.

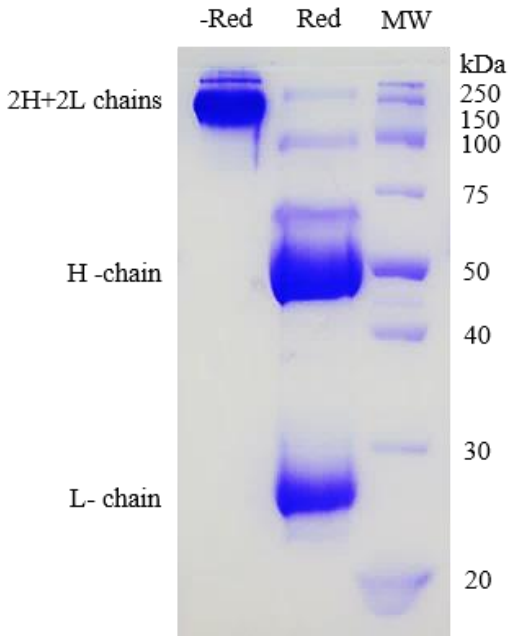

Figure 3. 4: Coomassie stained SDS-PAGE analysis of purified human IgG. After the processing of human serum through protein G-Sepharose column, purified IgGs were loaded on a 10% gel under non-reducing (lane 1) and reducing (lane 2) conditions and subjected to SDS-PAGE. The mobility of the size marker is indicated in lane 3.

3.2.3 Purification of human FH

FH was purified from human plasma by three-step affinity chromatography. The serum was first passed through the L-lysine Sepharose column to remove plasmin/plasminogen. Plasmin depleted human plasma was then applied to the IgG-Sepharose column to remove the proteins that bind to IgG or modified Sepharose. Finally, the plasma was passed through the OX23 Sepharose column. Quantities of FH yield were ranged from 1.6 to 2.4 mg eluted from 50 ml of human plasma as quantified by bicinchoninic acid (BCA) protein kit assay and read on NanoDrop at 562 nm absorbance.

3.2.3.1 Confirmation of human FH purity

Contamination of purified human FH with FHL-1 and FHR proteins could be observed in the final preparation of FH. The successful purification of FH was confirmed and evaluated by non- reducing and reducing Coomassie stained 10% SDS–PAGE (Figure 3. 5) and was compared with commercially available purified FH (Com. FH). OX23 affinity-purified FH demonstrates two bands around 155 and 37 kDa in both conditions non-reducing and reducing, corresponding to the molecular weight of full-length human FH and FHL-1, respectively.

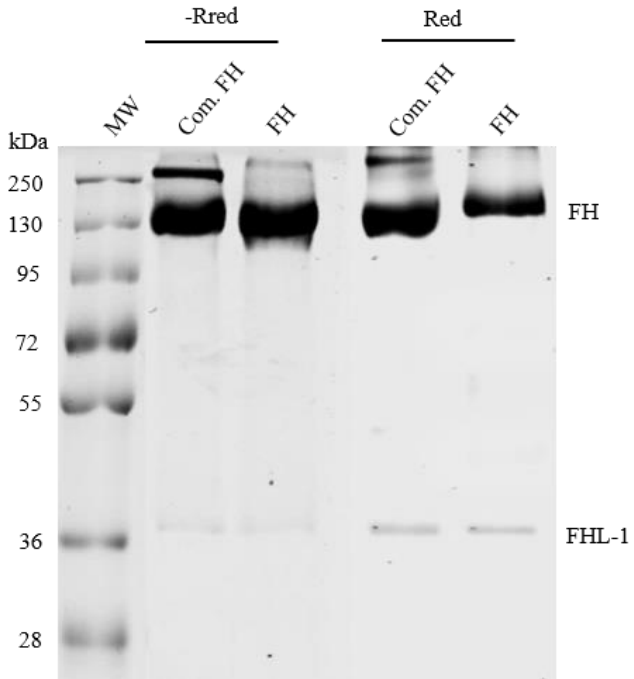

Figure 3. 5: Identification of purified FH by Coomassie stained 10% SDS–PAGE. Purified FH was subjected to non-reducing (-Red) and reducing (Red) condition gel electrophoresis, Commercial purified FH (Com. FH) used as a control. The mobility of the size marker is indicated in lane 1.

3.2.3.2 Verification of reactivity of FH and anti-FH antibodies by dot blot

To confirm the reactivity of purified FH with OX23 and OX24 anti-FH antibodies, dot blot assay was performed. Ascending concentrations (0.5 µg, 1 µg, and 2 µg) of purified FH were blotted on the PVDF membrane. Maltose binding protein (MBP) was used as a control at similar concentrations. The blotted proteins were probed with purified anti-FH antibody OX23 or OX24. After incubation with an HRP-conjugated goat anti-mouse secondary antibody, the reactivity between FH and anti-FH was detected using a chromogenic solution of the ECL substrate. Figure 3. 6 shows that all concentrations of FH are recognised by both anti-FH antibodies OX23 and OX24 in a dose-dependent manner, whereas no recognition of the MBP protein was observed. These results confirm the identity of the purified human FH.

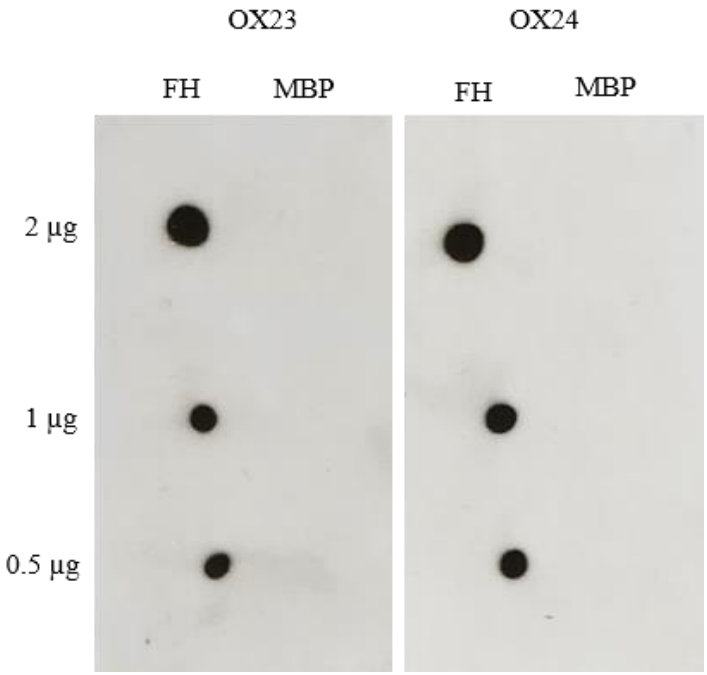

Figure 3. 6: Characterisation of FH by dot blot using purified anti-FH antibodies OX-23 and OX-24. Various concentrations of FH (0.5 µg, 1 µg, and 2 µg) were dotted on the PVDF membrane. The membrane was hybridised with OX23 or with OX24 diluted at 1:1000. Binding of anti-FH antibodies to purified FH was detected by probing the membranes with HRP-conjugated anti-mouse secondary antibody diluted 1: 1000. To visualise the interaction, the membranes were placed into a chromogenic solution of ECL western blot substrate and then revealed by exposure to x-ray film. As a control, MBP protein was used at similar concentrations.

3.2.3.3 Identification of purified human FH by western blot

To confirm the identity of FH, 5 µg of purified FH was electrophoretically separated on 10% SDS-PAGE gels under reducing and non-reducing conditions. Commercial purified human FH was used as a control at similar concentration. The purified FH was then blotted onto PVDF membrane. The membrane was probed with purified mouse anti-FH OX24 at 1:1000 dilution. Binding OX24 to the purified FH was detected by HRP-conjugated anti-mouse secondary antibody diluted 1: 1000. Western blot analysis for both condition, non-reducing and reducing highlighted two bands of FH at 155 kDa and FHL-1 at 37 kDa compared to the commercial FH (Com. FH) (Figure 3. 7). These results characterised the identity of purified FH which was eluted with FHL-1.

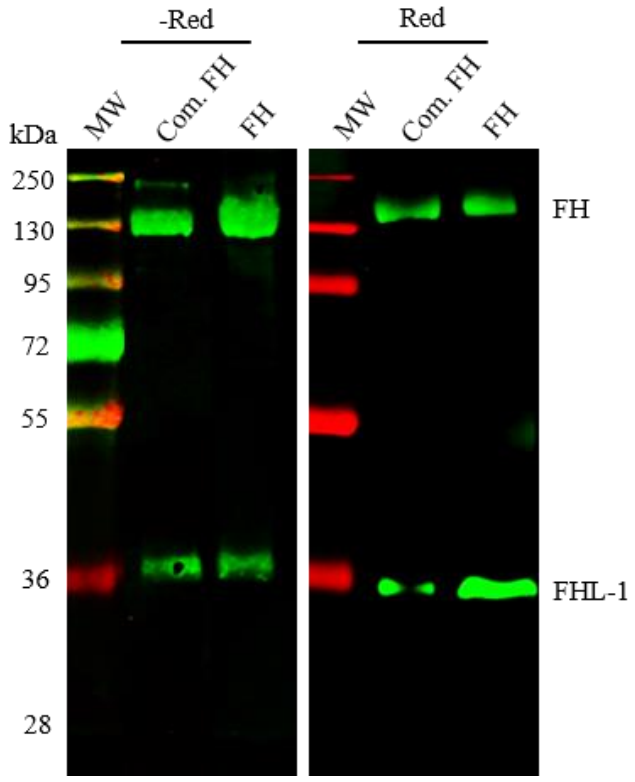

Figure 3. 7: Confirmation of FH identity by western blot. FH was purified from human plasma and subjected to non-reducing and reducing condition gel electrophoresis, followed by western blot with anti-FH OX24 antibody. Commercial purified FH (Com. FH) used as a control. The mobility of the size marker is indicated in lane 1.

3.3 Discussion

Various methods of conventional chromatography were applied to isolate FH from human plasma. (Sim & DiScipio, 1982; Ripoche *et al*., 1984; Oppermann *et al* et al., 2006; Carron *et al.*, 1996; Griffiths *et al*, 2009; Okemefuna *et al*., 2010; Yu *et al*., 2014). One of the downsides of these methods is that they involve multiple and complicated steps, combining immunoadsorption, protein precipitation, affinity chromatography, gel filtration, or addition of protease inhibitors which is not recommended for the multiple purifications due to the high cost of these chemicals. Another limitation of these methods is the low yield of the eluted protein (Sim *et al*., 1993; Brandstätter *et al*., 2012; Wang *et al*., 2013). Maintaining the integrity of purified FH using the fractionation methods is challenging. This is due to the fact that these purification techniques are based on changes in pH, temperature, and addition of chemicals (Brandstätter *et al*., 2012). Therefore, it is preferred to reduce the steps that affect the integrity of FH. In this study, FH was purified by immunoaffinity with high yield and purity compared to the previous methods, with some effective modifications.

In the current study, fresh frozen plasma was used to purify FH. It has been shown that FH is not stable when stored in plasma with multiple freeze-thaw cycles or plasma which has not been stored in good conditions, Therefore, outdated plasma should not be used in FH purification. A single 155 kDa polypeptide FH undergoes gradual cleavage into two chains linked by a disulfide bond of 38 and 120 kDa within the sixth CCP domain. This cleavage is most likely caused by plasmin action, resulting in a slight modification in FH activity (Sim *et al*., 1993; Yu *et al*., 2014: Amara *et al*., 2008; Barthe *et al*., 2012). Thus, removal of plasmin can maintain FH stability in subsequent processes (Sim *et al*., 1993; Wang *et al*., 2013). In addition, plasmin plays a vital role in enhancing the replication of some influenza A virus strains by cleavage of the viral haemagglutinin (Longping et al., 2015; Longping et al., 2013). In this study, plasma was passed through the lysine Sepharose column to remove the serine-protease protein, plasminogen/plasmin. Previous studies have been shown that the plasminogen binds albeitto the anti-FH antibody immobilised to the Sepharose, and subsequently contaminates the final product of FH (Sim *et al*., 1993; Yu *et al*., 2014). Plasminogen binds to complement proteins via lysine amino acid residues (Barthe *et al*., 2012). Thus, the high-affinity lysine binding sites on plasmin were utilised in plasminogen purification using L-lysine Seahorse (Winn *et al*., 1980).

In our study, all buffers used in the FH purification contained EDTA, except for the elution buffer. EDTA is a chelating agent binds tightly to metal ions such as calcium and magnesium. This ability inhibits metal-dependent enzymatic reactions, preventing enzymatic activity. Thus, adding protease inhibitors is not required (Wang *et al*., 2013). In the present study, protease inhibitors were not added, since FH was robust and stable in the final product according to recent studies (Licht *et al*., 2005; Brandstätter *et al*., 2012; Wang *et al*., 2013).

In this modified process, plasmin depleted plasma was passed through IgG Sepharose column to eliminate plasma proteins that could bind to anti-FH OX23 Sepharose. Previous studies recorded that it is important to remove plasma proteins such as fibronectin, C1q, and the antibodies which have cross-reactivity with OX23 and can eventually contaminate the final product of eluted FH (Sim *et al*., 1993; Yu *et al*., 2014). As the isoelectric point (pI, is the point at which a protein has no net electrical charge) of FH is approximately 6 – 6.2 (Pío *et al.,* 2002; Wang *et al*., 2013), the pH value of the elution buffer (3M $MgCl_2$) used was 6.8 to exclude IgG or albumin contamination through the elution process (Sim *et al*, 1982; Wang *et al*., 2013; Yu *et al*., 2014). Another reason to adjust pH of the elution solvent below 7.0 is to prevent formation and precipitation of magnesium hydroxide during the purification process because magnesium hydroxide is insoluble in water at neutral and higher pH values (Sim *et al*, 1993). In previous studies, acid or alkaline elution were frequently used with antibody columns. However, these elution techniques affect OX23 and OX24 activity because acid elution can cause rapid destruction of the antigen-binding capacity. While the alkaline elution is not effective and inhibits the antigen-antibody reaction, resulting in FH precipitation at pH >11. The OX23 antibody column can stay stable for 5 years and can be used several times if stored at 4°C in physiological buffer containing 5 mM EDTA to inhibit microbial growth. Thus, elution of bound FH using chaotropic 3M $MgCl_2$ preserves the binding efficiency of the antibody column for much longer period than do the acid or alkaline elution (Sim *et al*., 1993; Yu *et al*., 2014).

It has been known that chaotropic agents can decrease the stability of proteins by either disrupting the hydrogen bond networks between water molecules or by binding to the proteins resulting in a weakening of the hydrophobic effect between nonpolar amino acids that are essential for the stability of the native state of proteins (Kauzmann, 1959; Frank & Franks, 1968; Bennion & Daggett, 2003; Salvi *et al*., 2005). Eluted FH with 3M $MgCl_2$ was dialysed against water before it was stored in PBS. Exposure of $MgCl_2$ to phosphate or alkaline buffers

leads to precipitation of magnesium phosphates or hydroxide. Moreover, it is incompatible with SDS-PAGE analysis. Thus, it is essential to remove it by dialysis against water followed by dialysis against PBS (Sim *et al*., 1993; Yu *et al*., 2014).

In this immunoaffinity purification, OX23 was purified from hybridoma cell culture and bound to CNBr-activated Sepharose at pH 7.2-7.5. This pH value for coupling of the antibody to the Sepharose gives a high antigen-binding capacity (95–98%) for the immobilised OX23. Although the high pH (greater than 7.2) increases the coupling efficiency of the antibody to the resin, the antigen-binding capacity of the immobilised antibody is often greatly diminished at higher pH. Therefore, it is particularly important that the coupling pH is not higher than pH 7.5 (Sim *et al*., 1993; Yu *et al*., 2014).

To confirm the presence of FH in the purified FH fraction, dot blot was performed using two purified monoclonal antibodies OX23 and OX24 compared with the negative control MBP (Figure 3.4). The results showed that FH was recognised by both antibodies. Cross-reactive with the negative control tested was not observed. The purity and characterisation of the final preparation of purified FH were evaluated by Coomassie stained SDS–PAGE and western blot, respectively, compared with commercial purified human FH. The results revealed that the final fraction of FH purification contains FH and FHL- 1 were visualised at approximately 150 and 37 kDa, respectively (Figure 3.5 A & B). The monoclonal antibodies OX23 and OX24 not only detect FH but also FHL-1, an alternative splicing product of FH consisting of CCPs 1–7 (Alsenz *et al*., 1985; Martinez *et al*., 2003; Ajona *et al*., 2004; Schneider *et al*., 2006; Clark *et al*., 2014). This protein binds to OX23 and is eluted with FH. FHL-1 protein can only be detected in preparations made from fresh plasma, as it is not stable in the outdated plasma due to plasmin action (Sim *et al*., 1993). In FH fraction eluted from OX23 column, FHL-1 shows as a faint band because FHL-1 circulate in the plasma at level 10–50 µg/mL which is less abundant FH (Friese *et al*., 1999; Sánchez-Corral *et al*., 2018).

In conclusion, a feasible process for purifying intact FH protein from human plasma has been developed. This purification technique isolates specifically FH and FH-L 1 from FH-related proteins. Purified human FH produced in this study is similar to the quality of commercially available FH in its purity.

Chapter 4- Characterising the interaction between IAV and human FH.

4.1 Introduction

In this chapter, the direct binding of IAV to human FH was determined and the molecular footprint on both partners characterised. In the present study, ELISA was used to test the direct interaction between human and avian subtypes and strains of purified live IAV and purified human FH. Unlike bacterial pathogens, little is known about the direct interaction of viruses with the complement FH protein and whether virus evasion of complement pathways could be achieved by such interactions. The complement system is a main humoral arm of innate immunity that mediates the first reactions of the host defence against invasive pathogens, ensuring a rapid immune response (Stoermer & Morrison, 2011; Muñoz Carrillo *et al*., 2017). The alternative pathway (AP) of the complement system is constitutively active without a specific signal at a low rate to survey continuously for the presence of the pathogens. It is non-discriminatory between pathogens and host cells. For that reason, the AP activation on self-cells is tightly controlled by FH (Pangburn, 2000; Hovingh *et al*., 2016). As FH is a major regulator of AP, many pathogens hijack FH to their surfaces and recruit it for self-defence like *Streptococcus pneumoniae* (Jarva *et al*., 2002), *Aspergillus fumigatus* (Vogl *et al*., 2008), the malaria parasite *Plasmodium falciparum* (Rosa *et al*., 2016) and West Nile virus (WNV) (Chung *et al*., 2006).

In this study, the number of virus particles in the purified IAV preparation was estimated by various methods such as HA, $TCID_{50}$ and plaque assays. Specific properties like the ability to agglutinate red blood cells (RBCs) and induce cytopathic effects (CPE) in cell monolayers are used to quantify the viral particles. However, these techniques are not sensitive methods for virus quantification. Consequently, they have been partially replaced by faster, high-sensitive methods that rely on the quantification of viral genomes, such as the quantitative real-time reverse transcription PCR (RT-qPCR) (Karakus *et al*., 2018). However, PCR methods cannot determine virus infectivity, which conventionally investigated using techniques such as the plaque assay and TCID50 (Nakaya *et al*., 2020).

In this chapter, the far-western blot was also used to characterise which viral proteins were involved in the FH interaction. Since pathogens bind to FH by presenting FH binding proteins on their surfaces (Andre *et al*., 2007) and HA and NA are surface proteins of IAV (Kosik & Yewdell, 2019), they are attractive targets for the FH binding. In this study, several experimental approaches were used to confirm these interactions like lentiviral pseudotype

particles that display HA protein from different human and avian IAVs, recombinant NA, M1 proteins, and HA viral protein of various IAV subtypes and immunoprecipitation assay.

FH comprises of 20 complement control protein (CCP) domains. CCPs 1 – 4 modules are responsible for the regulatory properties. The first four domains and CCP 19 bind to C3b, whereas CCPs 6, 7 and 20 are self-surface recognition sites (Malou *et al*., 2013; Parente et al., 2017). Pathogens recruit FH using two main interaction sites: the first one is within N-terminal domains 6 – 7 of FH and FHL-1. This site is utilised by several pathogens, for example, the outer membrane protein, Ail, from *Yersinia enterocolitica* (Biedzka-Sarek *et al*., 2008), and the lipoprotein factor H binding protein (fHbp) of *Neisseria meningitidis*, bind to FH by this site (Seib *et al*., 2015). The second binding site is located on the C-terminal domains 19 – 20. It has been shown that most pathogens use both interaction sites, for instance, *Borrelia burgdorferi* which causes Lyme disease attaches to FH via CCPs 5 – 7 using protein CspA, CspZ, and OspE and via CCPs 19 – 20 using the surface proteins ErpA and ErpP (Kenedy *et al*., 2009; Hallström *et al*., 2013; Bhattacharjee *et al*., 2013; Caesar *et al*., 2013; Brangulis *et al*., 2015). In the present chapter, we mapped the CCPs involved in the interaction with the whole IAV. To determine where on the FH molecule, the IAV bound, FH CCPs domains 1 – 4, 1 – 7, 8-11, 8 – 20, 11 – 15, 15 – 18, and 19 – 20 with live purified human and avian IAVs used in ELISA. We also mapped the HA peptides involved in the interaction with full-length FH molecule using two HA peptide libraries (H1N1pdm09 and H3N2/99) which comprised of 20mers, overlapping by 10 amino acids, with N-terminal biotin and C-terminal amides.

Protein glycosylation is the mechanism by which carbohydrates attach to proteins after translation which occurs in either the endoplasmic reticulum (ER) lumen or Golgi cisterns. The glycans link to protein by either the amide nitrogen of asparagine (Asn) (N-linked glycans) or the hydroxyl group of serine (Ser) or threonine (Thr) (O-linked glycans) (Lin *et al*., 2020; Lee *et al*., 2015). Glycosylation plays a critical role in determining the three-dimensional configuration of proteins that is important in protein – protein interactions such as host-secreted protein and pathogen surface protein interactions. The best example of this interaction is the interaction between pathogens and the FH protein (Arey, 2012; Lin *et al*., 2020). Numerous pathogens have been reported to interact with FH in the same domains (CCPs 19 – 20 and CCPs 6 – 8) that were described to bind to several glycans on the host cell surface such as sialic acid (CCP 20) and glycosaminoglycans (CCPs 6 – 8 and 19 – 20) (Ferreira et al., 2010; Schmidt et al., 2018). FH contains nine potential glycosylation sites. These sites are distributed in the

amino acid sequences 199, 511, 700, 784, 804, 864, 893, 1011 and 1077 (Ripoche *et al*. 1988; Malhotra *et al*. 1999). Of these glycosylation sites, only eight were identified as N-glycosylation sites, while the first glycosylation site (199) could be due to mannose or hybrid glycans (Fenaille *et al*., 2007).

HA and NA are both include N-glycans. N-linked glycosylation sites on the globular head of the HA protein display large variability both in number and location across different virus strains. This variation can block or modify antigenic sites (Tate *et al*., 2014). It was demonstrated that the addition of the glycosylation site in residue 63 of HA1 inhibited the binding of the monoclonal antibody to H3 HA, indicating that glycans mediate the modification of HA antigenicity (Skehel *et al*., 1984). N-linked glycosylation sequence on the stalk region tends to be conserved. N-glycosylation of the stalk region plays a critical role in folding and conformation of the HA protein and removal of glycans from the stalk impaired trimerization, folding and transport of HA to the cell membrane, and modified the HA sensitivity to changes in pH (Tate *et al*., 2014). As both HA protein and FH are glycoproteins that bind to sialic acid residues, thereby FH may interact with HA of IAV by binding to glycans on the surface of HA protein. In this study, ELISA and far-western blot were performed to investigate whether removal of glycans from the surface of HA or FH could alter the interaction between IAV and FH.

Understanding of virus-specific protein interactions is critical study to investigate whether these interactions can facilitate or inhibit virus capabilities to exploit the host molecular machinery to support its replication in the infected cells (Zhao *et al*., 2017; Nathan & Lal, 2020). Therefore, the main aim of this chapter was to show the binding capability of IAV to human FH and to map the binding molecular determinants in both the FH protein and IAV viral proteins.

The main objectives of this chapter were to:

1. Investigate the direct interaction between live strains of human and avian IAVs and purified human FH.

2. Analyse which of the viral proteins of purified IAVs are responsible for the binding of the virus to FH.

3. Investigate whether removing glycans from HA IAV or FH would affect their interaction.

4. Determine the region on FH and HA protein that involved in the interaction between IAV and FH.

4.2 Results

4.2.1 Purification and characterisation of IAVs

To study the interaction between IAVs and purified human FH required purified virus particles. In this study, six strains of IAVs were selected including two human H1N1strains, the wild type A/England/195/09 (H1N1pdm09) and vaccine strain A/Michigan/45/15, (H1N1/15), two human strains of H3N2, the wild type, H3N2 A/HK/1174/99, (H3N2/99), and vaccine strain A/HK/4801/14, (H3N2/14), and two avian IAV strains, A/duck/Singapore/3/97 (H5N3), and A/chicken/Pakistan/UDL-01/08 (H9N2). Since in this study different strains of human and avian IAVs were used, the choice of host cell used to amplify the virus was an important consideration. Mammalian MDCK cells were used to propagate human IAVs in order to prevent the adapting mutations in HA that occur when the human IAVs are amplified in embryonated hens' eggs. Whereas avian IAVs were amplified in embryonated hens' eggs as these are avian in origin. Amplified IAV stocks were clarified by differential centrifugation to remove the contamination of cell debris. After the presence of IAV was detected by HA assay, the virus was concentrated and purified through 30% sucrose gradient centrifugation.

Coomassie-stained 10% reducing SDS-PAGE analysis (Figure 4. 1) was performed to verify the purity of the viral strains and characterise viral proteins by size identification. The results show that the viral protein migration varies between IAVs strains tested. However, all major viral proteins of subjected viruses were observed in the gel and their identitis were prescribed on their average predicted molecular weights (Shaw *et al*., 2008). The three polymerase subunits (PB1/PB2, PA) are determined as two bands 90 and 95 kDa, respectively. HA0 represents the un-cleaved HA at 72 kDa, HA1 and HA2 (cleaved HA subunits) at 50 and 25 kDa, respectively. NP at 60 kDa, NA at 57 kDA, and M1 at 29 kDa and NS2 at 13 kDa. Thus, SDS-PAGE analysis confirmed the purity of IAV subtypes migrating at the expected molecular weight for viral proteins.

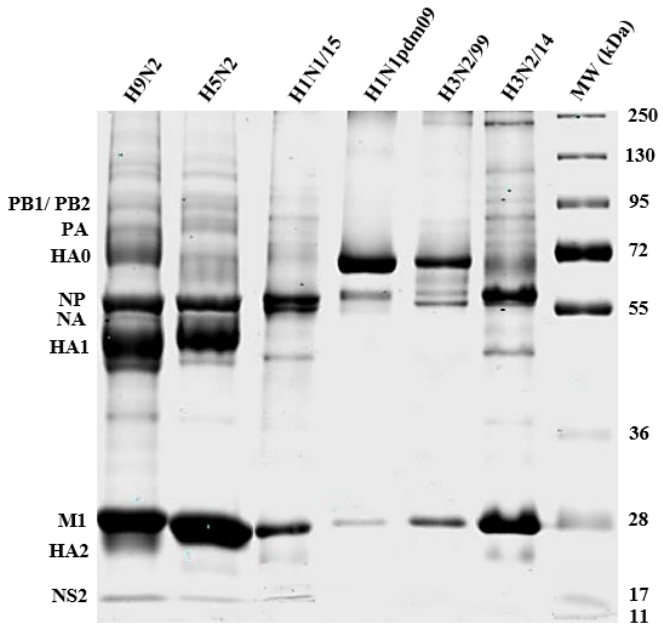

Figure 4. 1: Coomassie-stained SDS-PAGE analysis of purified IAV preparations. The six strains of avian and human viruses in the panel were purified by sucrose gradient centrifugation and subjected to a 10% reducing SDS PAGE and stained with Coomassie blue. Lane 1: A/England/195/09 (H1N1pdm09), Lane 2: Vaccine strain, A/Michigan/45/15, (H1N1/15), Lane 3: the wild, H3N2 A/HK/1174/99, (H3N2/99), Lane 4: Vaccine strains A/HK/4801/14, (H3N2/14), Lane 5: Avian H5N3 A/Duck/Singapore/3/97, Lane 6: Avian H9N2 A/chicken/Pakistan/UDL-01/08, and Lane 7: the molecular size marker (MW). The locations of the viral proteins are characterised by their expected molecular weights.

4.2.2 Validation of the direct interaction between IAVs and FH by ELISA

4.2.2.1 Assay optimization

To evaluate the direct interaction between purified IAVs and purified human FH, ELISA was carried out. The results obtained by ELISA may be affected by several parameters, including target protein concentration, virus titre, antibody quality and concentrations, incubation times, and the optimal temperature for incubation. Therefore, the optimisation of an ELISA is essential to obtain reproducible results. In these experiments we looked at varying FH concentrations, virus titres, primary antibody dilutions and temperatures in order to optimise the ELISA experiments.

4.2.2.1.1 Binding of the range of FH concentrations to IAV

This experiment showed the trend of FH binding to IAV, the minimum concentration of FH that reveals a notable binding and the dilution that demonstrates the best binding to IAV using ELISA. The results show that binding of human H3N2/99 (Figure 4. 2, A) and avian H5N3

(Figure 4. 2, B) IAV to FH increases in a dose-dependent manner compared with negative control, virus without FH (0) and the low dilution of FH that showed a notable binding capacity to both IAVs tested (3-fold increase in binding compared with negative control) was estimated around 4 µg/well, whereas the best binding of FH to both IAVs tested was observed at 32 µg/well. However, all FH dilutions were used in future experiments to investigate whether all IAVs used in this study have a similar trend in binding to FH.

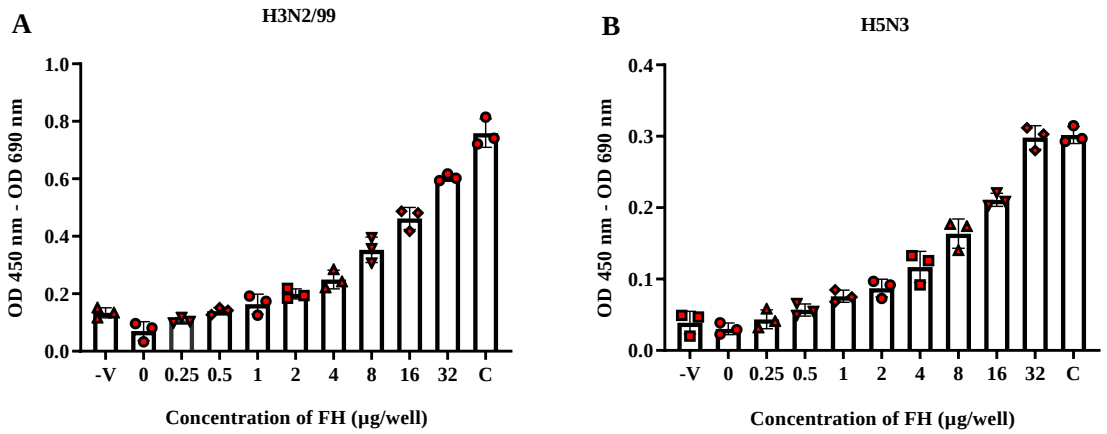

Figure 4. 2: ELISA to estimate the optimum concentration of FH for binding to IAVs. Microtitre plate wells were coated with 10^4 PFU/well (Jegaskanda *et al*., 2013) of **(A)** purified human H3N2/99 or **(B)** avian H5N3 in coating buffer overnight. After washing and blocking, serial dilutions of purified FH (0, 0.25, 0.5 1, 2, 4, 8, 16, and 32 µg/well) were added. Two negative controls were used in this assay, the highest dilution of FH (32 µg/well) without virus (-V), and virus without FH (0). Bound FH to IAV was detected with a mouse monoclonal anti-FH OX24 antibody, while a positive control (C) for the virus alone was incubated with mouse monoclonal anti-NP antibody. Polyclonal rabbit anti-mouse (HRP) was used as a secondary antibody to detect the mouse antibodies bound and the colour was developed using TMB substrate. Microplate Reader was used to measuring the change in the colour at ΔOD = 450 – 690 nm. The data are representative for one independent experiment performed in triplicate (mean ±standard deviation (SD).

4.2.2.1.2 Binding of FH to different titres of IAVs by ELISA

To evaluate how binding of FH to IAV may change with different titres of IAVs, ELISA was performed using various titres (0, 10^2, 10^3, and 10^4 PFU/well) of human IAVs (H1N1pdm09 and H3N2/99) or avian IAVs (H5N3 and H9N2). As shown in figure 4. 3, A-D, binding of FH (at 5 µg/well) was noticeably observed with all titres of all IAV subtypes tested compared to the negative control, virus at a titre of 10^4 PFU/well without FH (V-FH). The results also showed that there was no tangible difference in FH binding to IAV between the different titres of IAVs tested. However, these assays did show that using of a high titre of IAV to coat the microtitre well plate reduced the FH attachment to the plastic surface of the well, thereby

decreasing the background of nonspecific binding with anti-FH antibody. Altogether these results suggest that the 10^4 PFU/well is the best titre to use in future ELISA experiments to minimise the background staining.

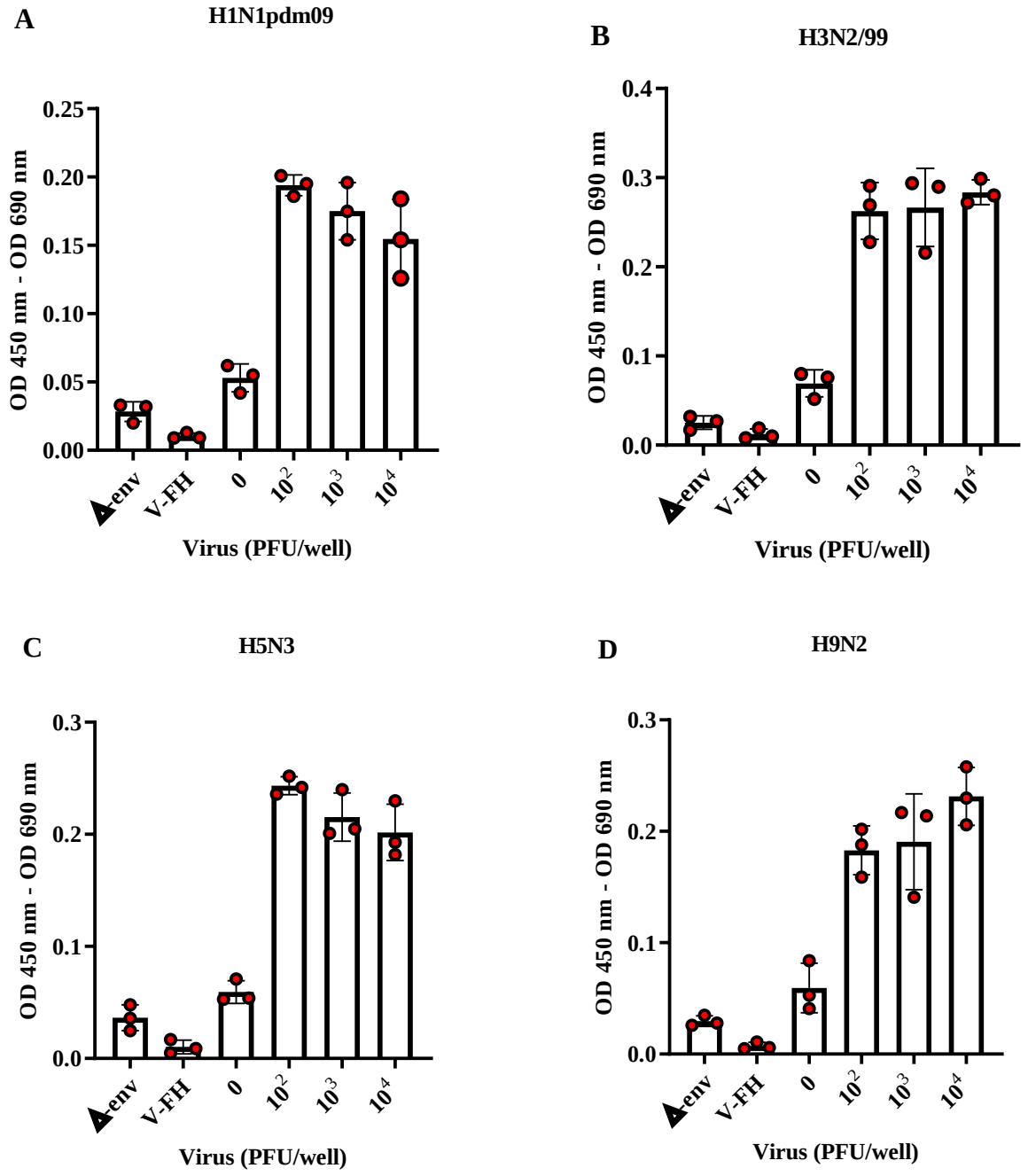

Figure 4. 3: Binding of purified FH to solid phase of different titres of purified human and avian IAV subtypes. Microtitre plate wells were coated with various titres (0, 10^2, 10^3, and 10^4 PFU/well) of **(A)** H1N1 pdm09, **(B)** H3N2/99 **(C)** H5N3, and **(D)** H9N2 in coating buffer overnight. After washing and blocking, FH was added (5 µg/well). After 2 h incubation period, the bound FH was detected with anti-FH OX 24 antibody. Three negative controls were used, the highest titre of the virus (10^4 PFU/well) without FH (V-FH), lentivirus particles that contained no envelope protein on the surface Δ-envelop (Δ-env) and FH without virus (0). The data are representative for one independent experiment was performed in triplicate (means ±SD).

4.2.2.1.3 Checkerboard titration assay

To optimise the optimal working dilution of primary and secondary antibodies for ELISA assay, a checkerboard titration assay was performed (Figure 4. 4, A). As shown in Figure 4. 4, A the shaded area represents the optimal combination of primary and secondary antibodies which gave the highest signal using the higher dilution of antibody and with the lowest background compared to the negative control (-) was 1:1000 for the primary antibody and 1:2000 for the secondary antibody This experiment was performed in duplicate to evaluate the impact of temperature on binding of IAVs to FH in ELISA. One plate was incubated at room temperature (RT) (Figure 4. 4, B). and the second at 37°C (Figure 4. 4, C). The results demonstrate that the temperature changes did not have a noticeable effect on the results obtained. Therefore, all ELISA experiments were performed at ambient temperature.

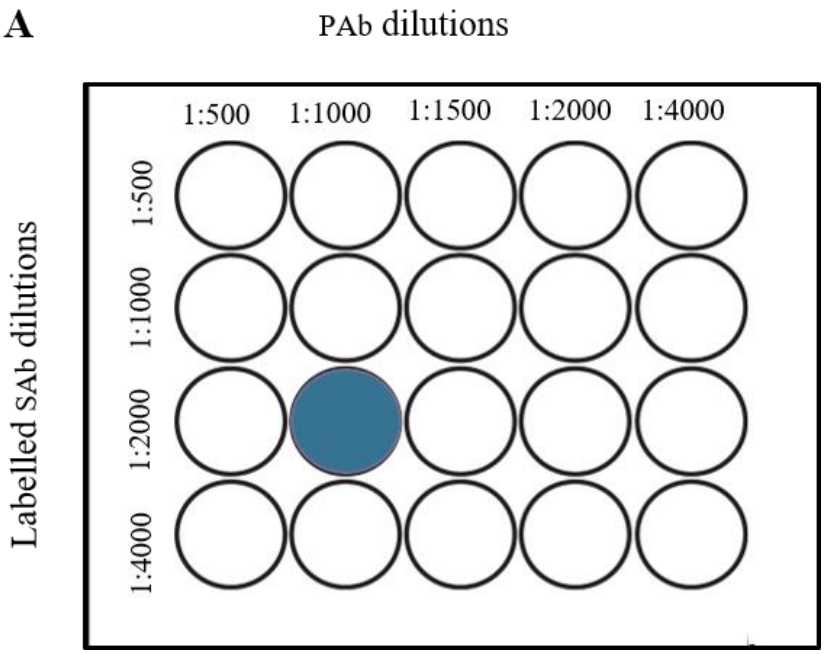

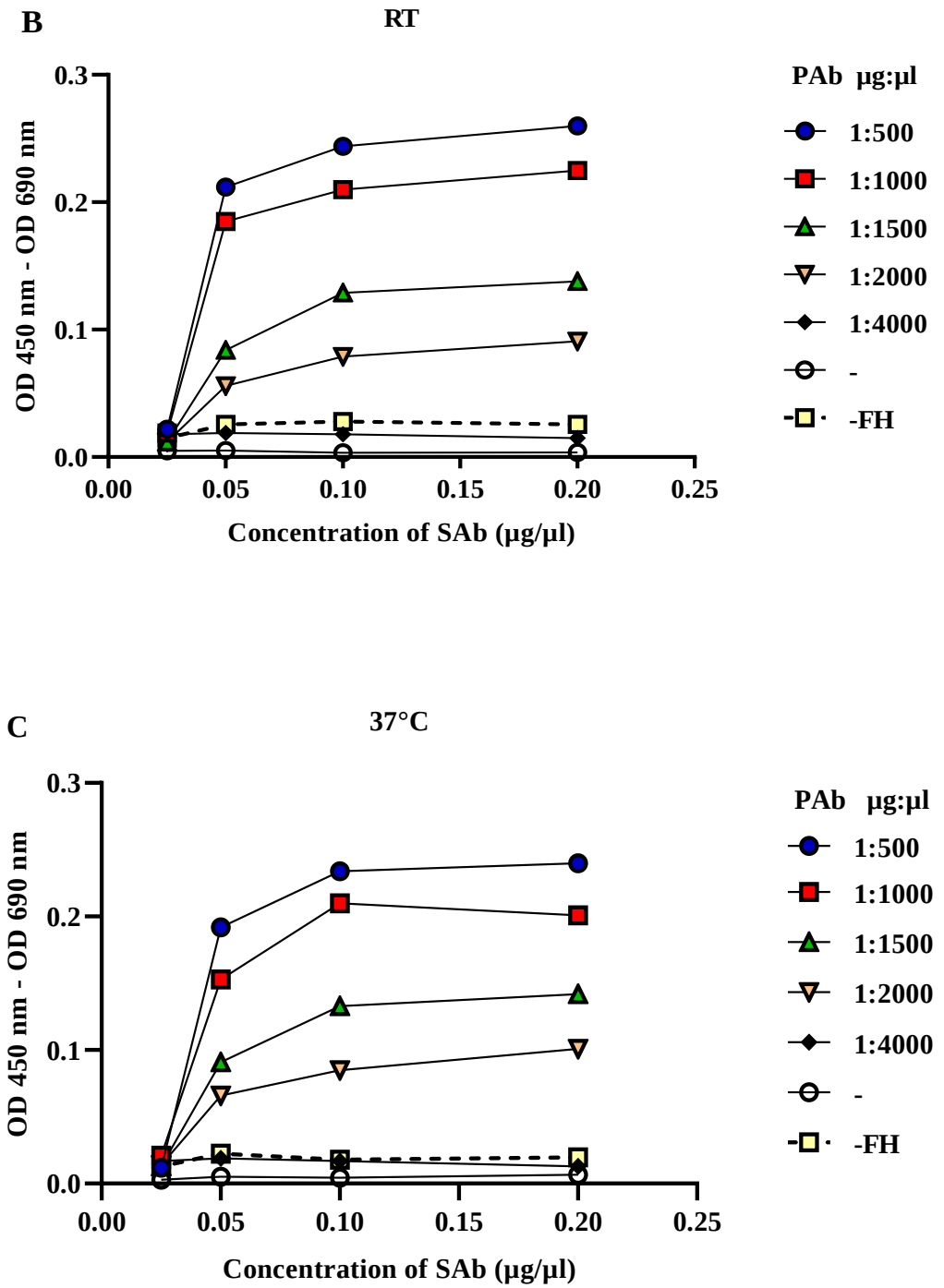

Figure 4. 4: Checkerboard titration to optimise primary and secondary antibody and incubation temperature. (A) Schematic representation demonstrates a checkerboard titration for the optimal combination of primary and secondary antibodies. The columns of Microtitre plate wells were coated with five different dilutions (1: 500, 1: 1000, 1: 1500, 1: 2000, 1: 4000 µg: µl) of primary antibody (PAb), anti-FH OX24, whereas the rows were coated with four different dilutions (1: 500, 1: 1000, 1: 2000, and 1: 4000) of the secondary antibody, HRP polyclonal rabbit anti-mouse. No detection antibody (-) and the absence of FH (-FH) were used as negative controls. One dilution for each purified FH (5 µg/well) and purified IAV (10^4 PFU/well) was used. **(B)** a checkerboard titration at room temperature (RT). **(C)** a checkerboard titration at 37°C.

4.2.3. Direct interaction between human and avian IAVs and FH by ELISA

To verify whether a direct interaction between IAV and FH protein can occur, ELISA was carried out (Figure 4. 5, A – J). In these experiments, different subtypes of human IAVs (H1N1pdm09, H1N1/15, H3N2/99, and H3N2/14) and avian IAVs (H5N3 and H9N2) at 10^4 PFU/well were coated on the Microtiter plate wells. After blocking, purified FH was added in increasing concentrations (0, 1, 5, 20, 40, and 80 µg/well) and bound FH was detected with anti-FH, OX24. Significant and dose-dependent manner binding of FH was observed with all six IAV strains tested, compared with negative control, 0 µg of FH (figure 4. 5, G – H).

The ELISA was also performed in reciprocal format to confirm the results, whereby the wells were coated with purified FH at 20 µg/well and then the wells were probed with purified human IAVs (H1N1 pdm09 and H3N2/99) or avian IAVs (H5N3 and H9N2) (figure 4. 5, G – H). The negative control used for this assay was the unrelated protein BSA coated on the ELISA wells with a similar concentration of FH with presence of the virus (BSA+V). With this assay, notably, significant binding of FH to all IAVs strains tested compared to the BSA control.

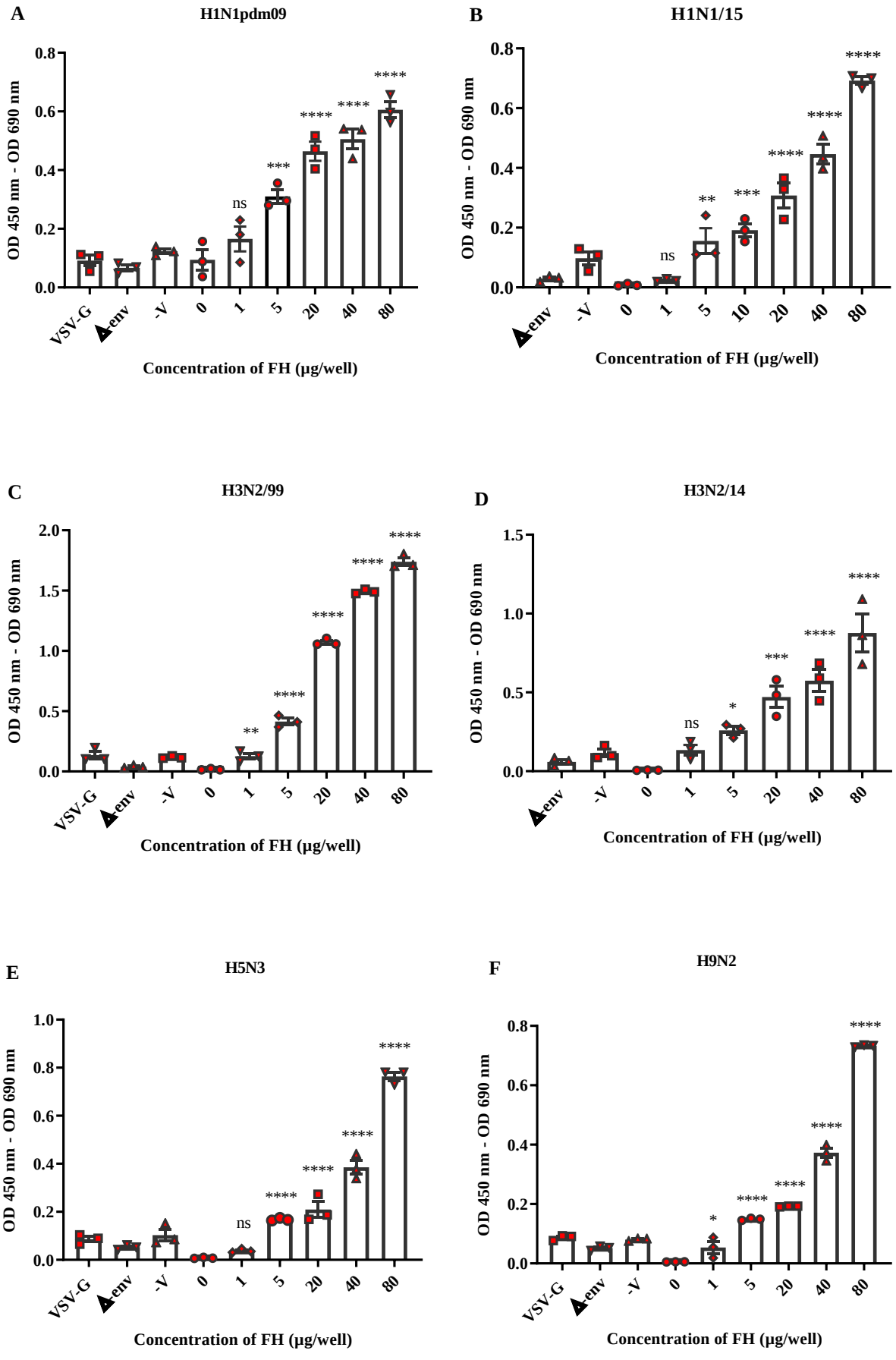
A
H1N1pdm09
OD 450 nm - OD 690 nm
Concentration of FH (µg/well)
VSV-G
env
-V
0
1
5
20
40
80
ns
***
****
B
H1N1/15
10
**
C
H3N2/99
D
H3N2/14
*
E
H5N3
F
H9N2

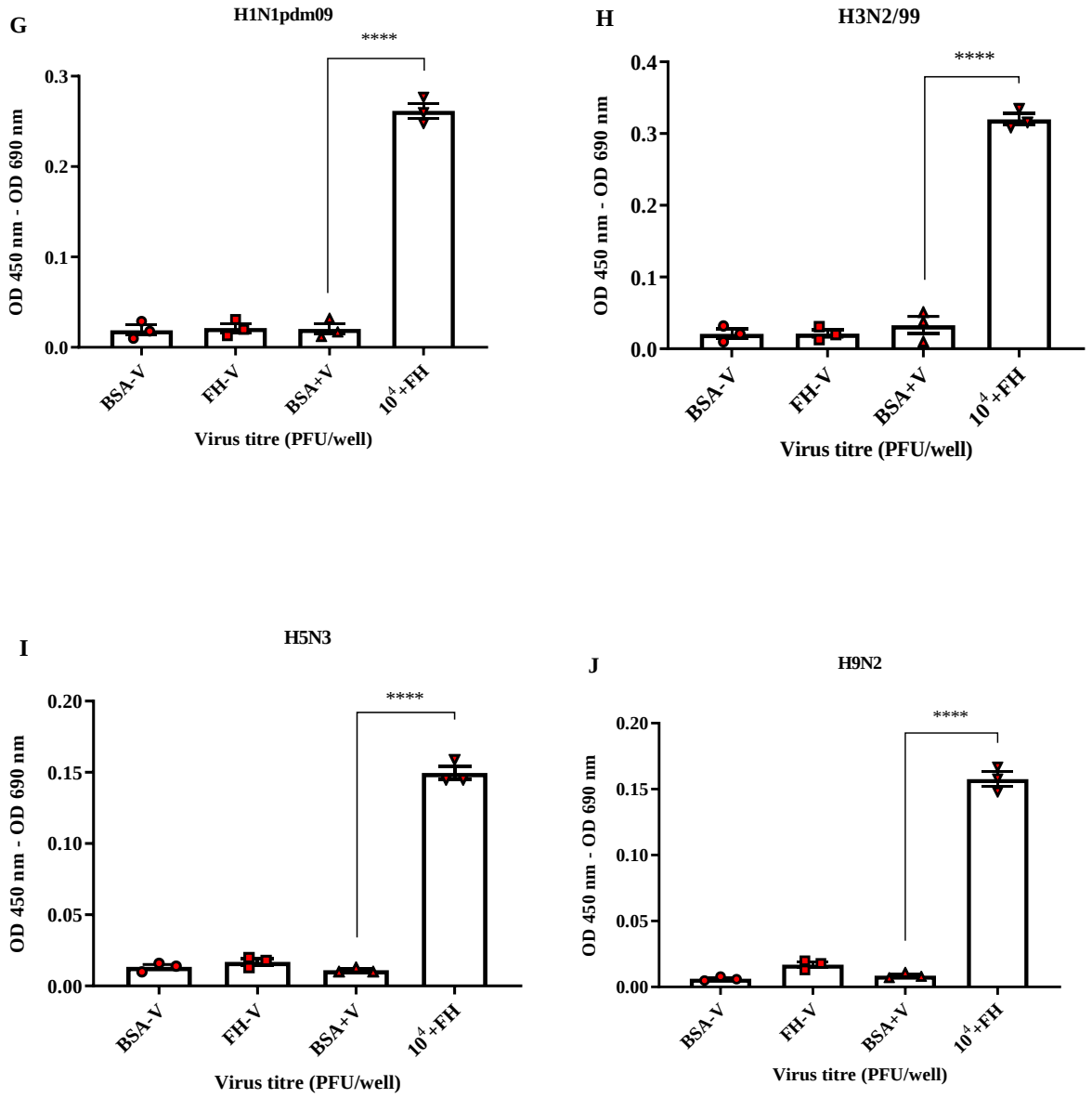

Figure 4. 5: Purified IAVs and purified FH binding by ELISA. The direct interaction between six different strains of human IAVs **(A)**: H1N1pdm09, **(B)**: H1N1/15, **(C)**: H3N2/99, (**D)**: H3N2/14 and avian IAVs (E): H5N3 and (F): H9N2 with various concentrations of purified human FH (0, 1, 5, 20, 40, and 80 µg/well) was performed. IAV at 10^4 PFU/well without FH (0 µg) was used as a negative control. In addition, absence of IAV (-V) with the presence of FH, Δ-envelope pseudotyped particles (Δ-env) or lentivirus particles VSV-G with FH were also used as negative controls. The results were confirmed by doing the experiment in the reverse order: Microtitre plate wells were coated with 20 µg/well of FH, and IAV (G): H1N1pdm09, (H): H3N2/99, (I): H5N3, (J): H9N2 was added. The bound virus was detected with anti-NP antibody. In this assay BSA at 20 µg/well with 10^4 PFU/well of virus was used as a negative control. In addition to other two negative controls were used, BSA, and FH at 20 µg/well with absence of virus. Error bars represent the ±SEM of three experiments performed in triplicate. P value was calculated by the multiple comparisons, Dennett's test (*$p \leq 0.05$, **$p \leq 0.01$, ***$p \leq 0.001$, and ****$p \leq 0.0001$).

4.2.4 Interaction of IAV proteins with FH

4.2.4.1 Analysis binding of IAV to FH by far western blot

To investigate which of the viral proteins of purified IAV subtypes tested (H1N1pdm09, H3N2/99, H9N2, and H5N3) is responsible for the binding of the virus to FH, the technique of far western blot was used. The separated viral proteins overlaid with FH and detected with anti-FH OX24 antibody showed a band around 72 – 82 kDa for a full-length HA0, the bands of 50, and 23 kDa for subunits HA1 and HA2, respectively. The bands detected on the overlaid membranes correspond to expected molecular weights of HA protein of IAV in the positive control (C) treated with anti HA antibodies. No band of HA was detected on the negative membrane. These results confirmed that the proteins that showed interaction with FH were indeed HA (Figure 4. 6, A – D).

In the overlaid H9N2 membrane with FH (Figure 4. 6, D), the 23 kDa band of HA2 and the 25 kDa band of matrix 1 protein were seen bound to FH compared to expected molecular weights for HA2 and M1 proteins in the positive control, suggesting that M1 protein may bind to FH. However, the 25 kDa band of M1 protein was also detected (faint band) in the negative control (-C) of both H5N3 (Figure 4.6, C) and H9N2 (Figure 4. 6, D), suggesting a non-specific binding between M1 viral protein and anti-FH antibody may occur. Therefore, further investigation is required to confirm whether M1 protein binds to FH by far-western blot using recombinant M1 protein. In conclusion, the current results establish binding of IAV to human FH due to HA protein.

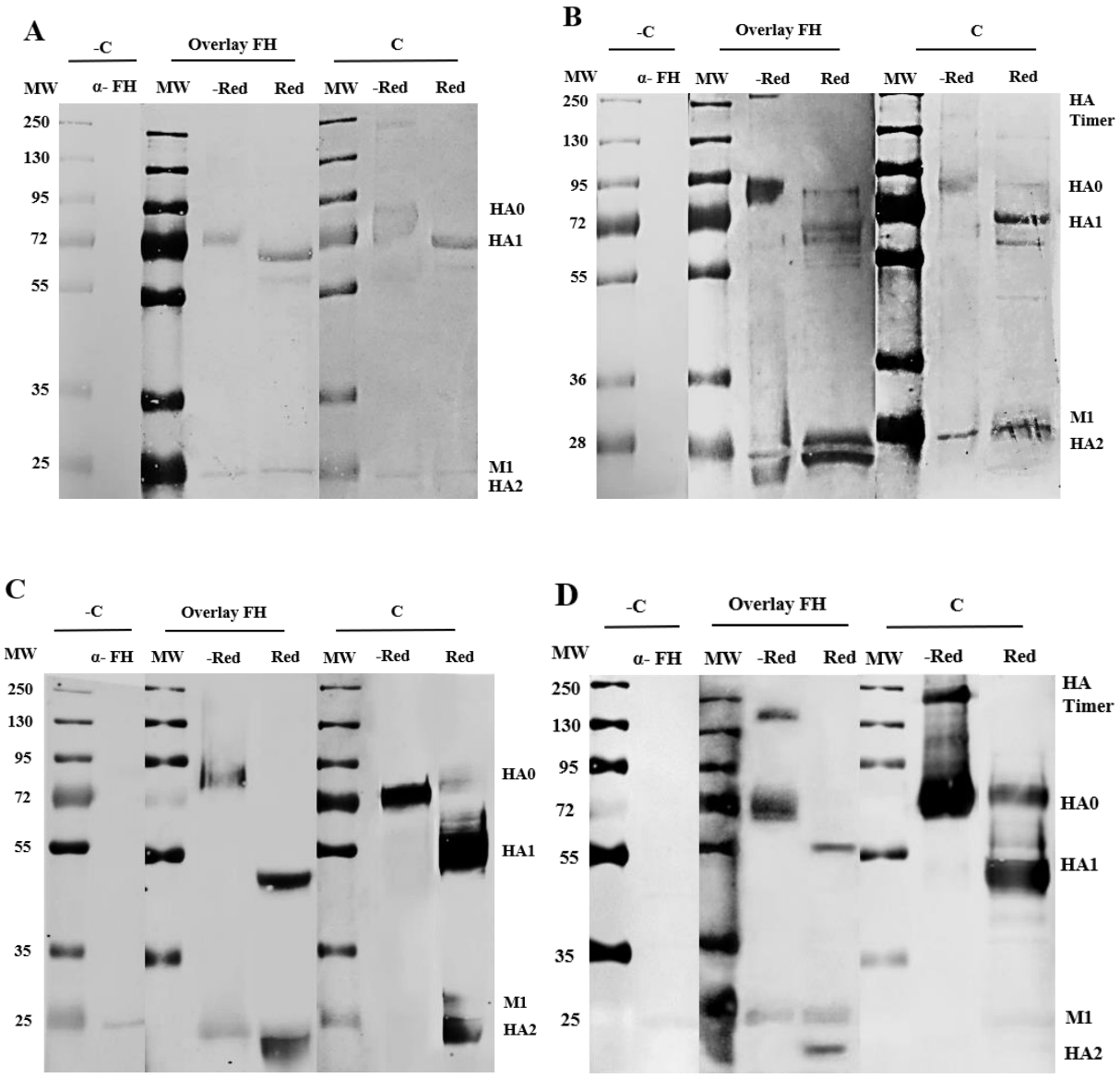

Figure 4. 6: Analysis of binding of purified IAV subtypes to FH by far western blot. Purified IAV (5 µg) subtypes of **(A)** H1N1pdm09, **(B)** H3N2/99, **(C)** H5N3, and **(D)** H9N2 was subjected to electrophoresis in triplicate under reducing (Red) and non-reducing (-Red) 10% SDS-PAGE. After viral proteins were transferred into a PVDF membrane, the membrane was cut into three parts. To detect the interaction between HA protein and FH, one of the membranes was overlaid with 20 µg/ml of purified human FH, which then was immunoblotted with the anti-FH OX24. To detect the HA protein on the positive control membrane (C), anti-HA antibodies (Table 2. 6) against HA protein of four IAVs tested were used, ferret anti-HA H1N1, anti-HA H3N2 (1:500), mAb anti-H9 and mAb anti H5 antibody (1:1000). To visualise the binding of HA protein to FH, the membrane was hybridised either with goat anti-ferret secondary antibody HRP conjugate (1:1000) for H1N1 and H3N2 viruses or with IRDye 800CW anti-mouse secondary antibody (1:1000) for H9N2 and H5N3 viruses. Followed by the colour development with DAKO as a substrate for the membranes with HRP secondary antibody or the Odyssey Imaging System was used to visualise the binding in the membranes with IRDye secondary antibodies. As a negative control (-C), a virus probed with mAb anti-FH OX24 was used. The viral proteins, trimer HA, a full-length HA protein (HA0), cleaved HA (HA1 and HA2), and matrix 1 (M1) were detected by their expected molecular weights. The mobility of size markers (in kDa) is indicated to the left of each gel. Data shown are representative of three independent experiments.

4.2.4.2 FH binds to HA protein displayed on influenza pseudotyped particles

To confirm the interaction of FH with the HA protein of influenza viruses, ELISA was performed (Figure 4. 7) similar to Figure 4. 5 but using lentiviral pseudotype particles that contained either the HA of IAV alone or together with NA (Table 2. 2). As negative controls, purified FH without pseudotyped particles (-), Δ-envelope (Δ-env) and VSV-G pseudotyped particles (10^4 RLU/well) with FH were used. Notably, significant binding was observed between FH and all displayed HA proteins on the surface of influenza pseudotyped particles tested compared to the negative control, VSV-G lentivirus particles (VSV-G). No significant differences (ns) between the different pseudotyped particles in their binding to FH were detected. Pseudotyped particles H5N8 that displayed viral proteins HA and NA (Table 2. 1) did not show a significant difference in their binding to FH compared with the similar pseudotyped particles that lack NA protein. These results confirm that HA protein mediates the binding of IAVs to human FH.

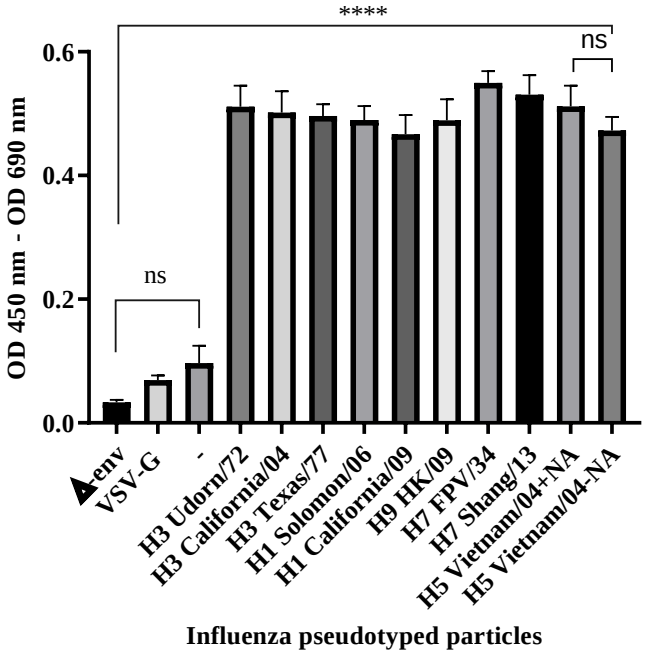

Figure 4. 7: Binding of FH to solid phase influenza pseudotyped lentiviral particles by ELISA. Microtitre plate wells were coated with 10^4 RLU/well of different influenza pseudotyped lentiviral particles (Table 4.1) overnight. After washing and blocking, purified human FH (20 µg/well) was added. Bound FH to the particles was detected using anti-FH OX24. As a negative control, VSV-G lentivirus particles (VSV-G) with FH was used. Moreover, other negative controls were used in these experiments, Δ-envelope pseudotyped (Δ-env) with the presence of FH and purified FH with the absence of pseudotyped particles (-). One-way ANOVA test was used for statistical analysis. Error bars represent the ±SEM of three experiments performed in triplicate. P-value (****$p \leq 0.0001$) was calculated by multiple comparisons, Dunnett's test.

4.2.4.3 Interaction between recombinant IAV proteins and FH

In order to confirm that HA viral protein of IAV interacts with FH and investigate whether other viral proteins such as neuraminidase (NA), and M1 proteins bind to FH, recombinant viral proteins of NA, M1 protein, and HA proteins of different strains of IAV were used in ELISA or far western blot.

4.2.4.3.1 Characterisation of recombinant IAV proteins by SDS-PAGE

To characterise recombinant viral proteins used in this study, Coomassie-stained 10% SDS-PAGE analysis was performed (Figure 4. 8). Recombinant NA protein derived from H1N1pdm09 was obtained from BEI Resources, ATCC. Insect cell generated (Drosophila S2 cells) M1 protein and HAs protein of different strains of human IAVs, H1N1pdm09, H3N3, and avian IAVs A/Ty/Turkey/1/05 (H5N1), H9N2, and A/Ty/Italy/984/00 (H7N1) were kindly provided by Professor Munir Iqbal (The Pirbright Institute). The recombinant proteins were subjected to 10% SDS-PAGE analysis under reduced conditions at concentration of 2 µg for NA, M1 and 10 µg for HAs proteins. Protein bands then visualized with Coomassie blue staining. The recombinant M1 protein of IAV has an expected molecular weight of 28 kDa. In this study, the visible molecular weight of the protein was approximately 36 kDa. Recombinant NA showed the predicted molecular mass of 55 kDa. HA recombinant full-length protein and HA subunits (HA1 and HA2) appeared different molecular mass levels depending on glycosylation form for each HA protein.

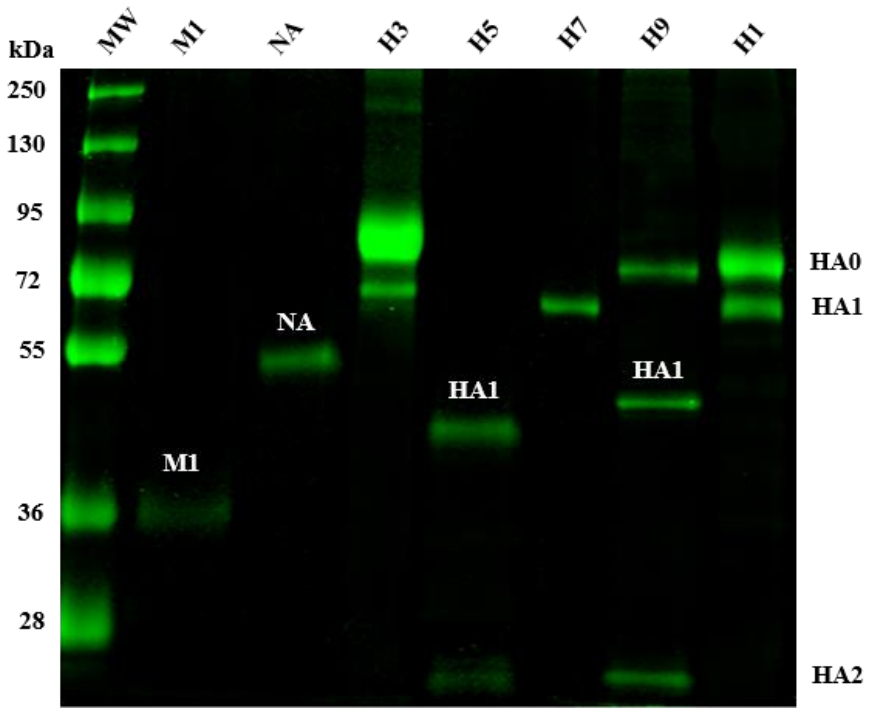

Figure 4. 8: Coomassie-stained SDS-PAGE analysis of recombinant IAV proteins used in the study. The reduced 10% SDS-PAGE shows the recombinant viral protein, M1, NA from H1N1, HA subunits (HA1 and HA2) or full-length HA (HA0) from H3N2 (H3), H5N1 (H5), H7N1 (H7), H9N2 (H9), and H1N1pdm09 (H1). Size markers (MW) are indicated on the left side ranging from 250 – 28 kDa. The expected molecular weight of the recombinant protein tested are indicated on the right of the gel.

4.2.4.3.2 Recombinant HA viral protein binds to FH by ELISA

To confirm the direct interaction between HA viral protein and human FH, ELISA (Figure 4. 9) was assessed using recombinant C-tag HA proteins of human and avian IAVs (Figure 4. 8). The HA proteins were absorbed to Microtiter plate at concentration 10 µg/well. A similar concentration of BSA was incubated in parallel as a negative control. The second negative control was the absence of HA protein (0) with presence of FH. Subsequently, nonspecific binding sites were blocked, and 20 µg/well FH was added. Bound FH (20 µg/well) was detected by anti-FH OX24 antibody. Significant binding of FH was observed with all HA proteins tested compared to the control, BSA. The binding of H3 HA protein to FH was significantly high compared with other HA proteins tested H1 ($P<0.001$), H5, H7, and H9, ($P<0.0001$). HA protein from H1N1 appeared to have significantly higher binding compared to H5 ($P<0.02$), but not H7 and H9. The direct interaction was performed in reverse order to confirm the results obtained (Figure 4. 9) . FH at 20 µg/well was attached to plastic surface and HAs were added at 10 µg/well. Bound HAs were detected with biotin anti-C-tag conjugated antibody. The

interaction was visualised by HRP-Conjugated streptavidin. With this experiment, significant binding was observed between FH and all HA proteins tested compared with BSA control. HA proteins from H3N2 showed high significant of binding with FH compared with other HAs proteins tested H1 ($P<0.001$), H5, H7, and H9, ($P<0.0001$). While HA protein from H1N1 appeared a significant difference in its binding to FH compared with H5 ($P<0.02$), but not H7 and H9. Importantly, these experiments confirm the interaction between HA protein from different strains of avian and human IAVs with FH.

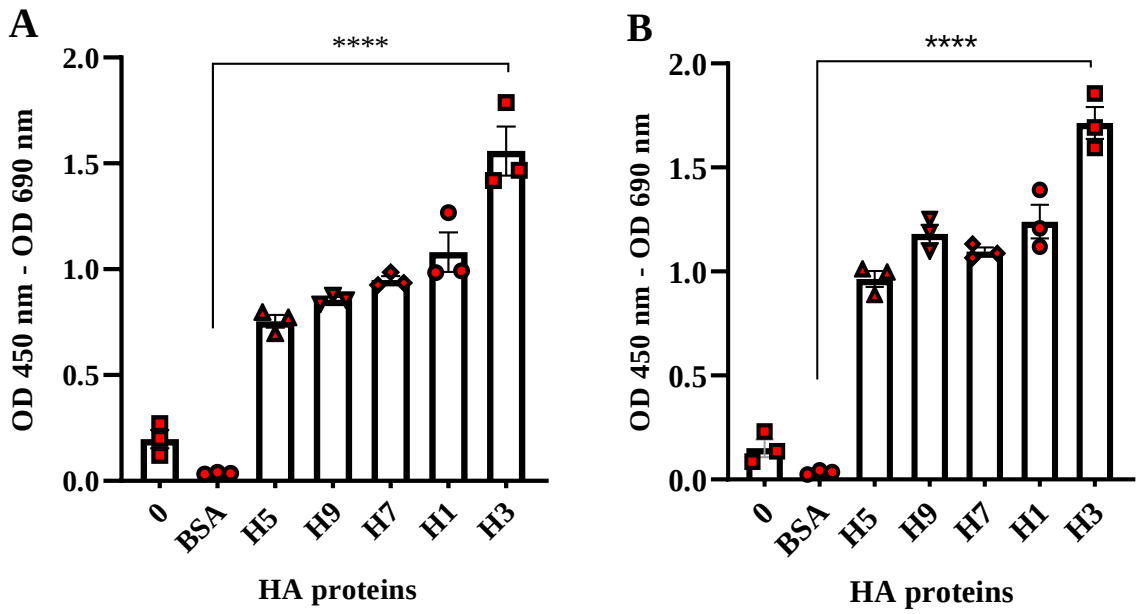

Figure 4 9: HA viral proteins and human FH binding by ELISA. (A) FH binds to solid phase HA proteins. Microtiter plate wells were coated with 10 µg/well of HA viral proteins overnight. After washing and blocking, 20 µg/well of purified FH was added. The binding was detected with anti-FH OX24 antibody. BAS was used as a negative control **(B)** HA protein binds to solid phase purified FH. The Microtiter plate wells were coated with 20 µg/well of purified FH or BSA as control. After blocking, HA proteins were added. Bound HAs were detected with Biotin Anti-C-tag conjugated antibody. The data for each panel is reprehensive of three independent experiment performed in triplicate. The error bars indicate the ±SEM. Statistical differences compared to the BSA control were calculated by Dennett's test for the multiple comparisons (****$p < 0.0001$).

4.2.4.3.3 Evaluation of the interaction between recombinant NA and M1 proteins with FH by far western blot

To assess whether the IAV binding to FH is only due to viral HA protein or other viral proteins such as NA and M1, far western blot was performed (Figure 4.10). Recombinant M1 or N1 NA proteins (Figure 4. 8) were subjected in triplicate to reducing 10% gel electrophoresis, followed

by immunoblotting with mAb anti-M1 or anti-NA for the positive control membrane (C). The second membrane (T) was overlaid with 20 µg/ml of FH. The negative control membrane (-C) was incubated with anti-FH OX24 antibody. As shown in Figure 4. 10 (A), a strong 36 kDa band of M1 is observed in the positive control, but not in overlaid membrane with FH and in the negative control, suggesting that no binding occurs between M1 protein and FH. Interestingly, these experiments reveal binding of human FH to NA protein (Figure 4.10- B). The band of N1 NA at MW of 55 kDa was observed in both the positive and overlaid membrane (T), but it was not shown in negative control. Collectively, these results confirm that human FH interacts with a viral N1 NA protein, but no interaction is observed with M1 protein.

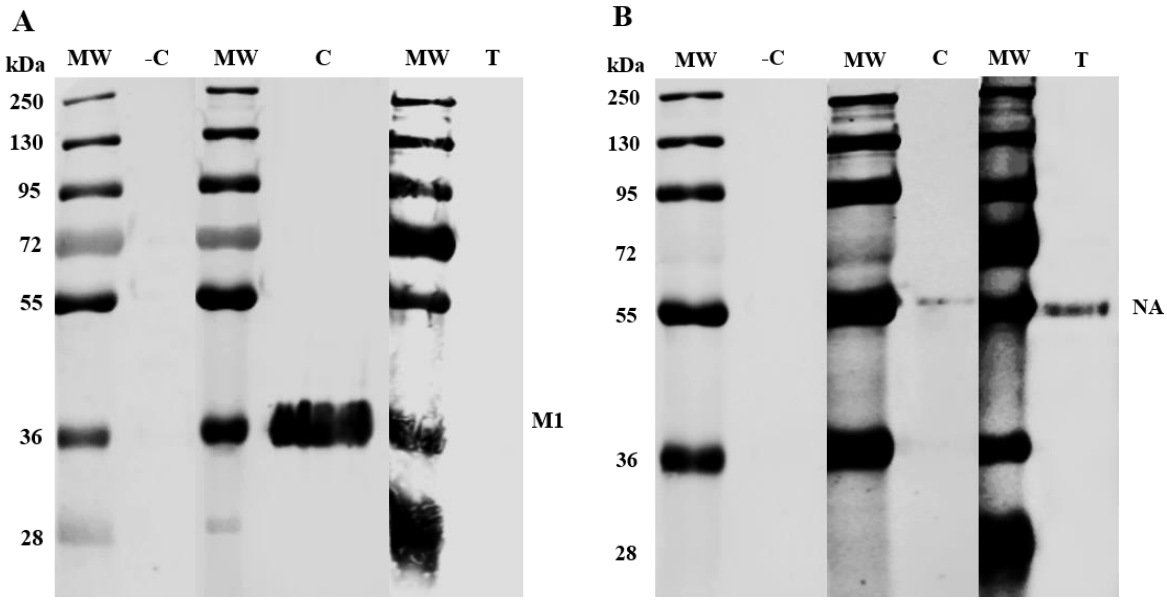

Figure 4. 10: Recombinant M1 and NA viral protein interaction with human FH by far western blot. (A) Recombinant M1 and **(B)** NA proteins were subjected to 10% reducing gel electrophoresis. Following the separation, the proteins were transferred to a PVDF membrane and incubated either with mAb against M1or NA for the positive control (C) or with mAb anti-FH OX24 for the overlaid membrane (T) and negative membrane (-C). Data shown are representative of three independent experiments.

4.2.4.4 HA protein directly binds FH by immunoprecipitation assay

Immunoprecipitation assay was designed to confirm a direct interaction between HA protein of IAV and FH. Western blot with a mAb anti-FH OX24 was used to evaluate the presence of FH in immunoprecipitates (IP) (Figure 4. 11). The result showed that only biotin anti-C-tag antibody bead that was incubated with C-tag HA protein coprecipitated a 150 kDa band of FH and a broad band (37 – 49 kDa) of FHL-1 protein, corresponding to the FH and FHL-1

respectively in the positive control (FH or HA in starting material (Input) without immunoprecipitation) which were indicated with a red colour. Bound HA protein to biotin anti-C-tag antibody bead was visualised by biotin anti-C-tag antibody (green). A broad band (78-95 kDa) of HA0 with HA dimer and trimer was observed. The two HA subunits (HA1 and HA2) were detected by their predicted molecular weights at 50 kDa for HA1. HA2 reveals a broad band at 28-34 kDa. Taken together, these findings indicate the direct interaction between HA protein and human FH.

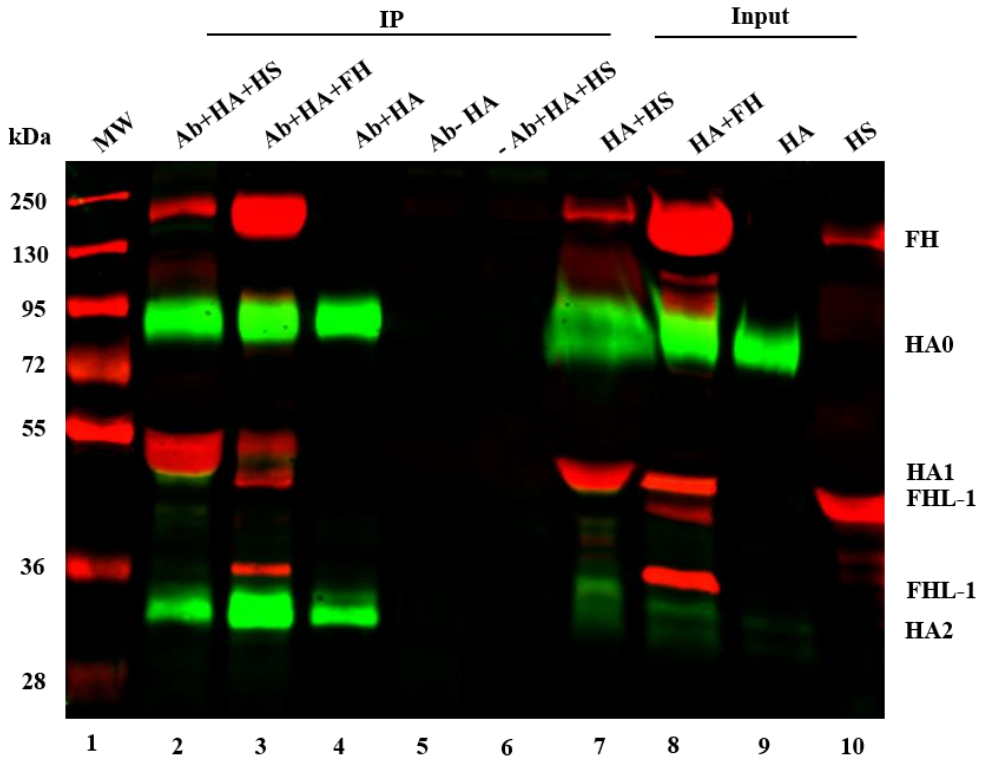

Figure 4. 11: Immunoprecipitation of viral HA protein and human FH. Western blot with a mAb anti-FH OX24 after immunoprecipitation with biotin anti-C-tag antibody-HA protein. According to the manufacturer's instructions, 100 µg of biotin anti-C-tag conjugated antibody was immunoprecipitated with 120 µl of N-Hydroxysuccinimide (NHS) FlexiBind bead. bead-conjugated biotin anti-C-tag antibody (biotin anti-C-tag bead) was incubated with 1 – 2 mg of recombinant C-tag HA protein from H3N2 (HA). After washing with PBS, biotin anti-C-tag bead was incubated with 20% human serum (HS) or purified FH (FH). The bead was washed and subjected to SDS-PAGE and western blot analysis. Three negative controls were used in this study, biotin anti-C-tag bead with the presence of HA (Ab+HA) or absence of HA protein (Ab-HA) and bead without biotin anti-C-tag antibody was incubated with the presence of HA and HS (-Ab+HA+HS). FH is shown in red colour, whereas HA protein is shown in green. Lane 1: molecular size marker (MW), lane 2 – 6: starting material with immunoprecipitation (IP), lane 7 – 10 starting material (Input) without immunoprecipitation. Experiments were repeated three times with similar results.

4.2.5 Molecular determinants of the interaction between IAV and FH

To gain more insight into the molecular determinants of IAV and FH interaction, ELISA was performed with recombinant FH fragments (see Figure 4.15) to determine where on the large 150 kDa FH molecule, the IAV bound. FH CCP domains 1 – 4, 1 – 7, 8 – 11, 8 – 20, 11 – 15, 15 – 18, and 19 – 20 (Figure 4. 12) were expressed in the baculovirus or in *Pichia pastoris* and they were kindly provided by Professor Christine Skerka (Leibniz Institute for Natural Product Research and Infection Biology – Hans Knöll Institute, Jena, Germany). To localise the region in HA viral protein that are involved in the interaction with FH, ELISA was performed, using the whole length of two HA peptide libraries (H1N1pdm09 and H3N2/99) which comprised of 20 mers, overlapping by 10 amino acids, with N-terminal biotin and C-terminal amides (Appendix A and B, respectively).

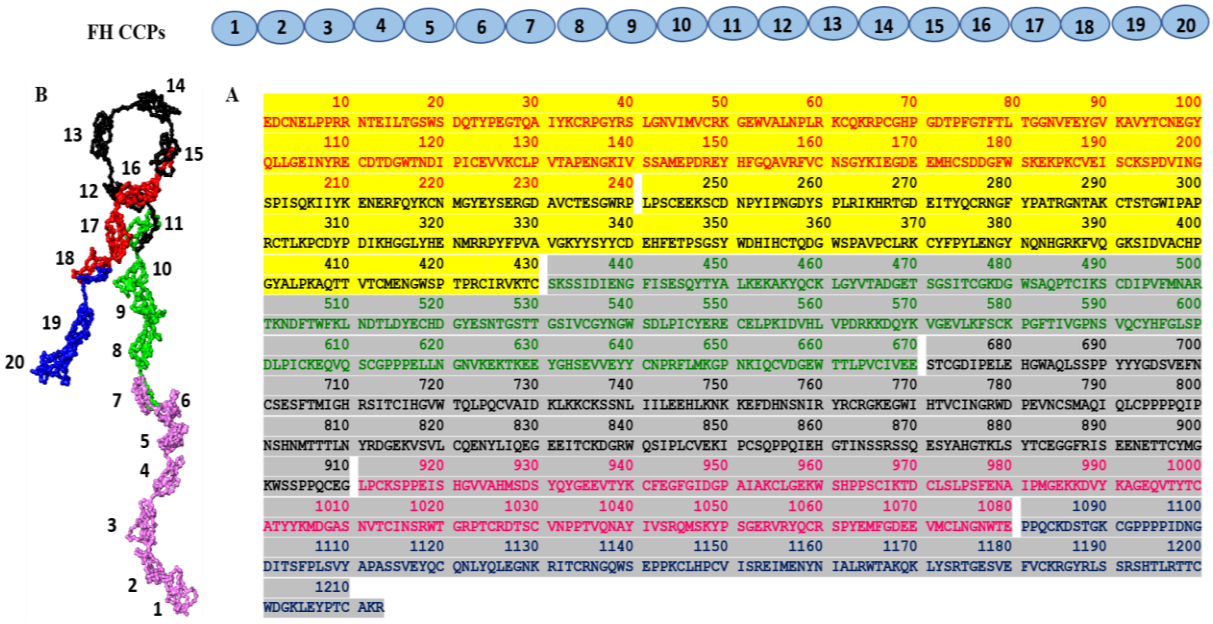

Figure 4. 12: The 20 CCP domains of human FH. (A) Amino acids sequences of recombinant FH fragments shown within FH molecule. CCPs 1 – 4 (1 – 240 residues) are shown in red letters within CCPs 1 – 7 (241 – 430 residues) highlighted in yellow, CCPs 8 – 11 (431 – 670 residues) are presented in green, CCPs 11 – 15 (671 – 910 residues) are displayed in black letters, CCPs 15 – 18 (911 – 1080 residues) are shown pink letters, CCPs 8 – 20 (1080 – 1213 residues) are displayed in black letters and CCPs (430 – 2213) are shown in light grey. **(B)** structure three-dimensional modelling of FH (PDB code 3GAW, Perkins & Bonner, 2009) showing FH fragments used in the molecular determinants of IAV-FH interaction. CCPs 1 – 7 are shown in violet, CCPs 8 – 11 are shown in green, CCPs 11 – 15 are displayed in black, CCPs 15 – 18 are presented in red, CCPs 19 – 20 are shown in blue. The image was generated with PyMOL (Schrödinger, LLC).

4.2.5.1 Characterisation of the reactivity of purified mAbs anti-FH OX23 and OX24 with different recombinant CCPs of FH by western blot

To investigate whether mouse mAb anti-human FH OX23 and OX24 antibodies can interact with different fragments of FH (CCPs 1 – 4, 1 – 7, 8 – 11, 8 – 20, 11 – 15, 15 – 18, and 19 – 20), western blot analysis was performed (Figure 4. 13). Purified full-length FH (5 µg) was used as a positive control, while BSA was used as a negative control at a concentration of 5 µg. Notably, strong binding of antibodies tested with CCPs 1 – 4 at 32 kDa, CCPs 1 – 7 at 43 kDa and whole FH at 155 kDa were detected, but no binding with other CCPs of FH and the BSA control was observed. These results suggest that anti-human FH OX23 and OX24 antibodies bind to the N-terminal of the FH molecule, thereby cannot be used to detect different recombinant fragments of CCPs 1 – 20 of FH.

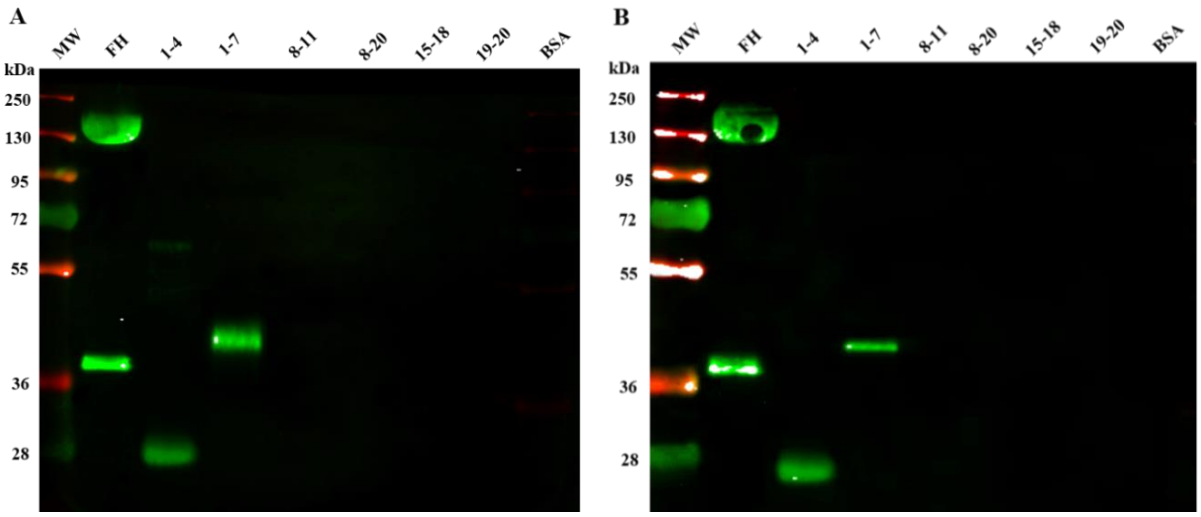

Figure 4. 13: Western blot analysis of the interaction between mAb anti FH OX23 and OX24 with CCPs 1 – 20 of FH. Different recombinant of FH CCPs (1 – 4, 1 – 7, 8 – 11, 8 – 20, 15 – 18, and 19 – 20) were subjected at 5 µg to reducing SDS-PAGE electrophoresis. Separated CCPs were then transferred into a PVDF membrane using the iBlot 2 Dry Blotting System. Followed by western blot, the membrane was blocked with commercial blocking buffer, Immobilon Signal Enhancer. The membrane was then hybridised with mouse mAb anti-human FH **(A)** OX23 and **(B)** OX24 diluted 1:1000 in blocking buffer. The binding was detected using IRDye 800CW goat anti-mouse IgG secondary antibody (1:10000). The LI-COR® Odyssey® Infrared Imaging System was used to visualise the interaction between the CCPs of FH and the antibodies tested. The mobility of size markers is indicated to the left of each gel.

4.2.5.2 Characterisation of different CCPs of FH by polyclonal anti-human FH antibody

In this experiment, western blot was performed to investigate whether polyclonal goat anti-human FH can bind to various CCP modules of FH, thereby it can be used to detect binding of IAV to CCPs of FH in ELISA assay. Different CCPs (1 – 4, 1 – 7, 8 – 11, 11 – 15, 15 – 18, 8 – 20) of FH were subjected to reducing SDS-PAGE. As a positive control, the full-length FH was used, whereas BSA was used as a negative control. As shown in Figure 4. 14, this experiment demonstrates that polyclonal goat anti-human FH can interact with all CCPs of FH tested and the full-length FH. The band of each CCP domain is corresponding to its expected molecular weight that indicated in the marker as following: CCPs 1 – 4 at 32 kDa, CCPs 8 – 11 at 35 kDa, CCPs 11 – 15 at, 42 kDa, CCPs 15 – 18 at kDa 38, CCPs 8 – 20 at 92 kDa, and CCPs 1 – 7 at 43 kDa, but no binding was observed with BSA control. These results indicate that polyclonal anti-human FH binds to all FH fragments tested of the C and N-terminal of FH. Thus, this antibody can be used in ELISA to detect binding of FH fragments to IAV.

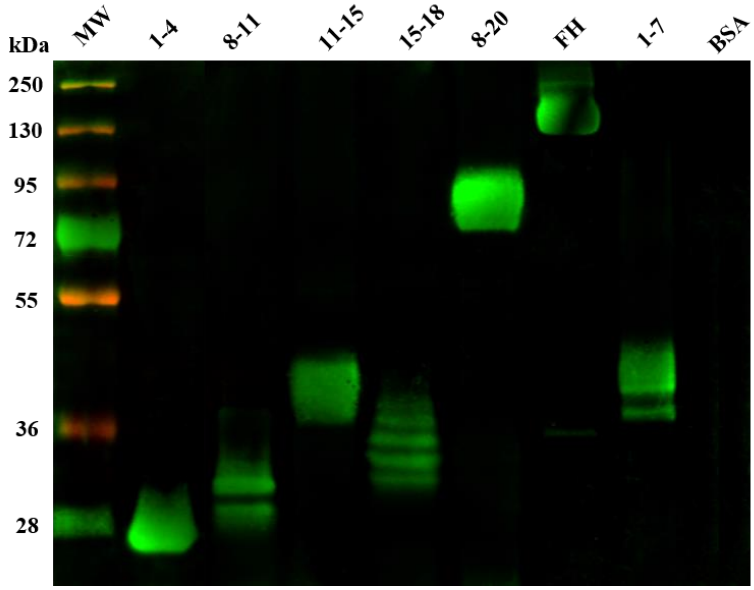

Figure 4. 14: Identification of FH fragments using anti-human FH antisera by western blot. 5 µg of each recombinant peptides CCPs 1 – 4, CCPs 8 – 11, CCPs 11 – 15, CCPs 15 – 18, CCPs 8 – 20, and CCPs 1 – 7 were subjected to 10% reducing SDS-PAGE electrophoresis followed by immunoblotting with polyclonal anti-human FH antiserum. Full-length FH was used as a positive control, whilst BSA was used as a negative control at similar concentrations of FH and FH fragments (5 µg). The mobility of size markers is indicated to the left of the gel.

4.2.5.3 Interaction of Human and avian IAVs with FH via specific sites

Characterisation of the molecular binding site of the FH protein that is involved in the interaction with IAV can provide an insight into the design of novel antiviral therapeutic agents from FH aimed at stopping viral infection by inhibition of virus attachment to the host cells. To determine the CCPs within FH that interact with IAV, the ELISA was used (Figure 4. 15, A – D). Four different human (H1N1pdm09 and H3N2/99) and avian (H5N3 and H9N2) IAV subtypes at 10^3 PFU/well and seven different recombinant fragments of FH domains (CCPs 1 – 4, 1 – 7, 8 – 11, 8 – 20, 11 – 15, 15 – 18, and 19 – 20) at 5 µg/well were used in these experiments. As a negative control (C) each individual fragment of FH domains without virus was used. To confirm the presence of the virus, IAV was used in the absence of FH as a positive control and was detected with anti-NP antibody. Moreover, three negative controls were used in these assays, absence of IAV (-V) in the presence of FH, absence of virus and FH (0), and lentivirus particles that contained no envelope protein on the surface (Δ-env).

The CCPs 1 – 7, 15 – 18, and 8 – 20, as well as 19 – 20, were directly involved in binding to four IAVs tested compared to the control (C) for each fragment of FH. Only the latter fragment was tested with H3N2 (Figure 15, B) due to the limited amount available from this fragment. No binding was observed between CCPs 1 – 4, 8-11 – 15 and IAVs tested. The largest signal in the ELISA assay was observed for all four IAV strains with the 8 – 20 CCP fragment (Figure 4. 15, A – D). In conclusion, these results establish that CCPs 5 – 7 and 15 – 20 were involved in FH binding to IAV, leaving the functional CCPs of FH (CCPs 1 – 4) free for inhibitory activity. These results were similar to what was described in previous research that many pathogens bind to FH through two common binding sites, CCPs 5 – 7 and 18 – 20. (Hovingh *et al*., 2016)

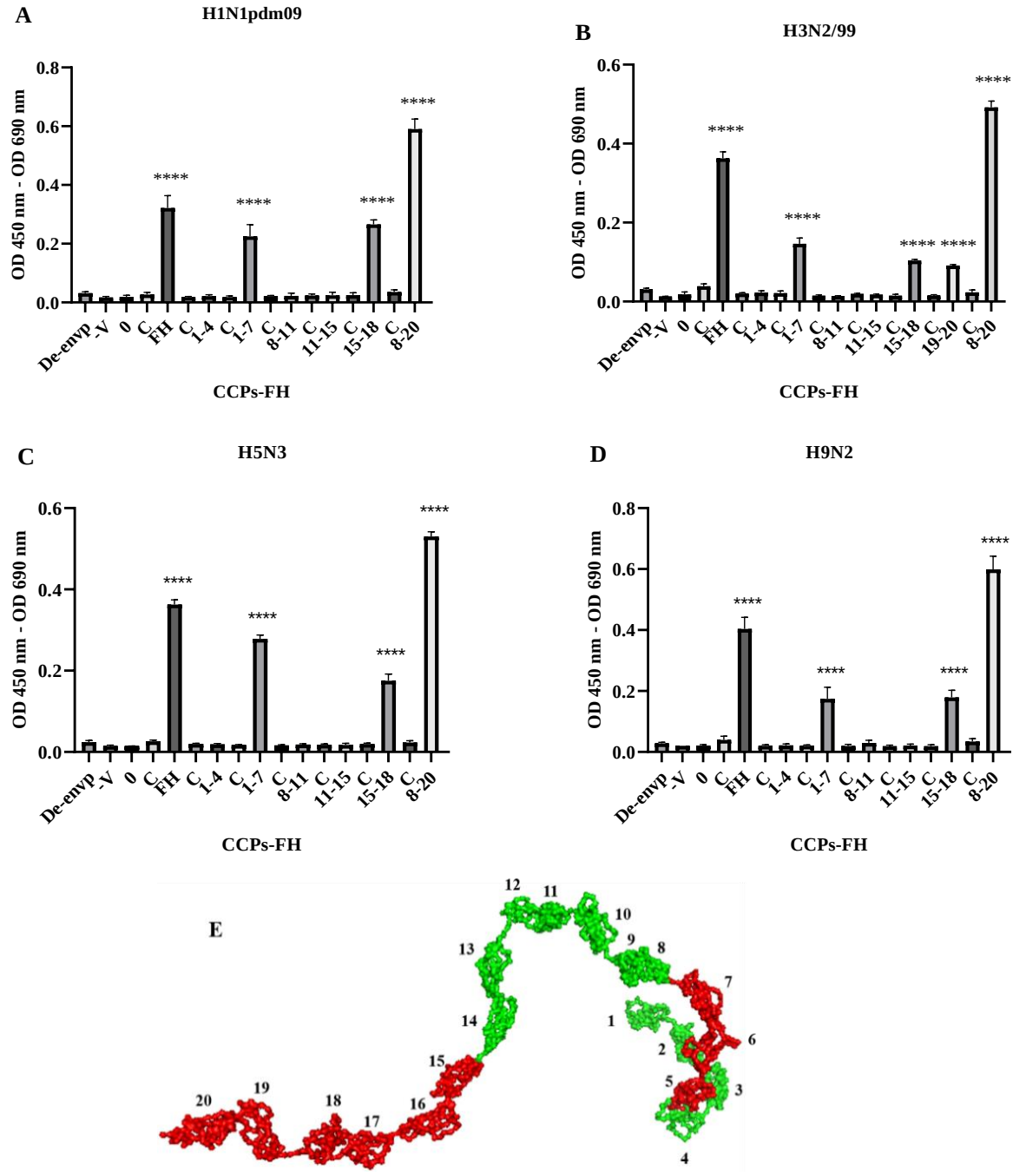

Figure 4. 15: Determination of binding sites of human and avian IAVs on FH surface by ELISA. Microtitre plate wells were coated with 10^3 PFU/well of purified IAV **(A)** H1N1pdm09, **(B)** H3N2/99, **(C)** H5N3, **(D)** H9N2 in blocking buffer overnight at 4°C. Excess virus was removed by washing. The plate was then blocked and incubated with full-length FH or various recombinant fragments of FH domains (CCPs 1 – 4, 1 – 7, 8 – 11, 11 – 15, 15 – 18, 8 – 20, and 19 – 20 (with H3N2/99) at 5 µg/well for 2 h at RT. After incubation with goat anti human FH antibody (1:28000), the interaction was detected by polyclonal anti-goat /HRP. With each individual fragment of FH, negative control without virus (C) was used to compare the results. In addition, three negative controls were used, wells without FH and virus (0), Δ-envelope pseudotyped particles (Δ-env) with FH, and control with FH, but without virus (-v). One-way ANOVA test was used for statistical analysis. Error bars represent the ±SEM of three experiments performed in triplicate. P value (****$p < 0.001$) was calculated by multiple comparisons, Dunnett's test. (E) The localisation of the binding sites of human and avian IAVs on the surface of the 3-D model structure of human FH 1-20 (PDB code 1 HAQ, Aslam & Perkins, 2001). The involved CCPs are shown in red. The image was made by PyMOL (Schrödinger, LLC).

4.2.5.4 Determination of the molecular binding site of the viral HA protein that is involved in the interaction with FH

Since HA protein is exposed on the surface of the virus, it is an attractive target for the development of anti-viral drugs and vaccines. Characterisation of FH binding sites on HA protein can enable us to understand the impact of FH on viral replication. HA is responsible for virus attachment and entry into target cells, and it is the main target of neutralising antibodies. Therefore, this detailed knowledge of the molecular determinants of FH interaction with HA protein will provide more information about whether FH could inhibit any of these vital functions of HA. A panel of biotinylated HA peptides from H1N1pdm09 and H3N2/99 subtypes (appendices A & B) was used in ELISA (Figure 4. 17 – 18) to determine binding sites of FH on the surface of HA protein.

4.2.5.5 Confirmation of the solubility of HA Peptides by dot blot

Synthetic biotinylated peptides were obtained from Alta Bioscience and derived from HA protein either from IAV H1N1pdm09 or H3N2/99 were used to localise FH binding sites in HA by ELISA. Each individual peptide is comprised of 20mers, overlapping by 10 amino acids, with N-terminal biotin and C-terminal amides was dissolved in 50% (v/v) DMSO in water as stock solution. To confirm the solubility of 56 biotinylated HA peptides and that all HA peptides were in the same concentration range, a dot blot assay was performed (Figure 4. 16). The amount of 2.5 µg of each peptide was blotted on PVDF membrane. The membrane was then probed with IRDye 800CW HRP-conjugated Streptavidin. BSA was used as a negative control. The results demonstrated that all HA peptides tested appeared to show dots of similar density, where their surface area showed no dramatic differences. No binding with BSA control was observed. These results suggest that the concentration of HA peptides was roughly equivalent.

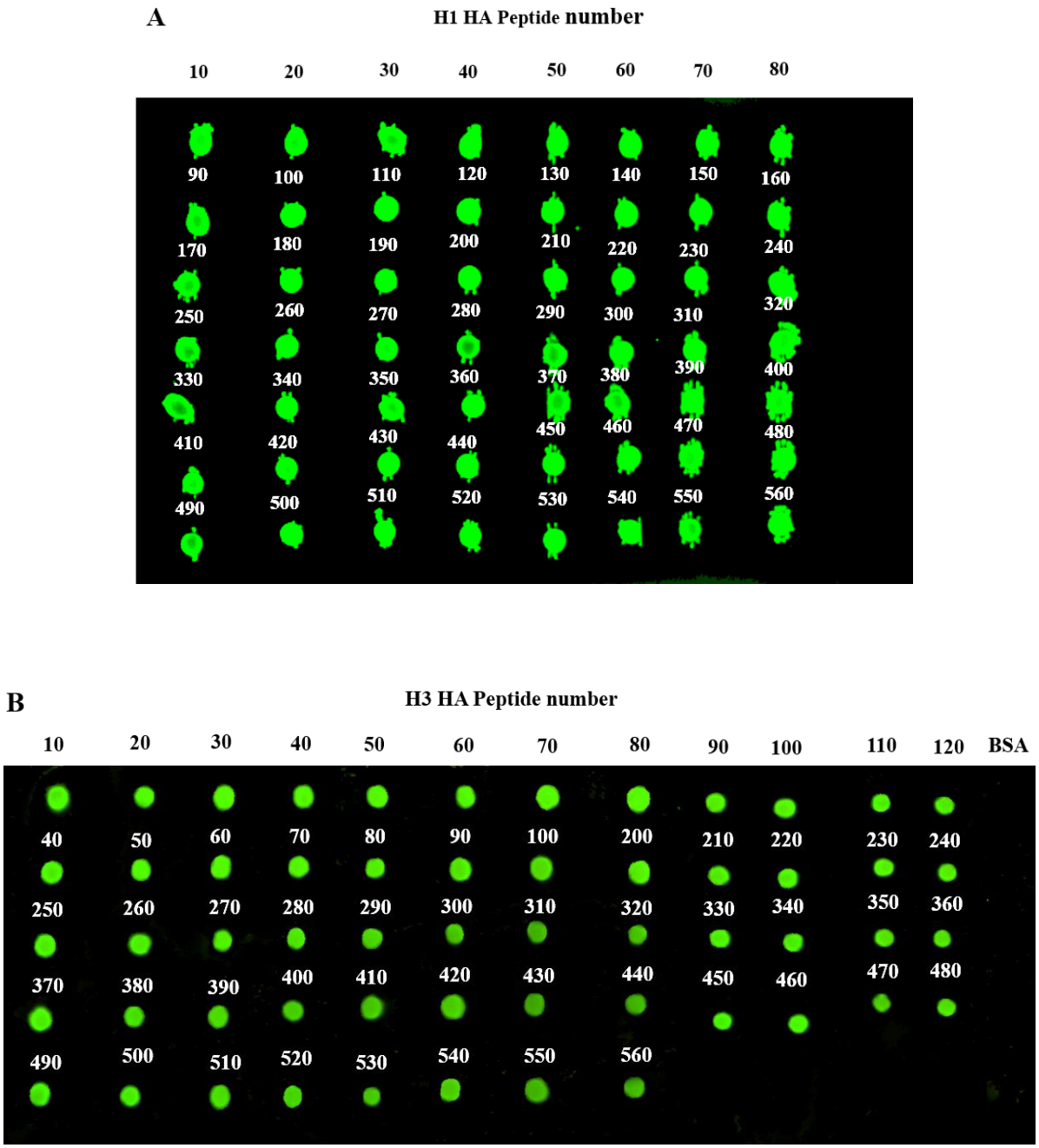

Figure 4. 16: Dot blot assay to confirm the solubility of synthetic HA peptides from (A) H1N1pdm09 and (B) H3N2/99. Each individual peptide (10 amino acids) was blotted on PVDF membrane with concentration of 2.5 µg. The membrane was then probed with with IRDye 800CW HRP-conjugated Streptavidin at 1:500. As a negative control, BAS was used at the same dilution of HA peptide. The Odyssey Imaging System was used to visualise the interaction between the HA peptide and the HRP-conjugated streptavidin.

4.2.5.6 Localisation analysis of FH binding sites in HA protein by ELISA

To determine the region on the HA protein which interacts with FH, the ELISA assay was used, in which a panel of biotinylated HA peptides from H1N1pdm09 or H3N2/99 were assessed for

interaction with a full-length, purified FH protein. As negative controls, biotinylated -GH loop peptide with amino acid sequence, CRYNRNAVPNLRGDLQVLAQKVARTKKKKKK from foot and mouth disease virus (FMDV), FH in DMSO, and FH in PBS (FH) were used in this assay. Purified FH was adsorbed at 5 µg /well onto a 96-well plate. The HA peptide (2.5 µg/well) of H1 or H3 subtypes was added, and bound HA peptides were detected by HRP-conjugated streptavidin (Figure 4. 17, A). The assay was also performed in the reverse order to confirm the results, whereby the wells of streptavidin 96-well coated plate were coated with 2.5 µg/well of H1 or H3 HA peptides. FH was then added at the concentration of 5 µg/well. Bound FH was detected by anti-FH OX24. Both versions of the assays (Figure 4. 17, A – B) demonstrated that 12 peptides H1 HA protein showed significant binding above the negative control, FH only in DMSO (FH). These peptides clustered into five groups of one or more peptides adjacent to each other and thus sharing 10 amino acid sequence overlap (see Figure 4. 17, A – B and Table 4. 1).

The current results have shown that FH binds to the region (PNHDSNKGVTAAC-PHAGAKS) that includes the 130-loop (DSNKGVTAAC) shown in yellow (Figure 4. 17, C – E), which is one of the four structural elements of the receptor-binding site (RBS) pocket in HA1. As shown in the left panel (-FH) of figure 4. 17, D, the RBS pocket that binds to the cell surface receptor sialic acid consists of four structure elements are located at the apex of the HA1 globular head subdomain of the viral HA protein, the 130-loop shown in yellow, 150-loop (LIWLVKKGNS) labelled in purple, 190-helix (DQQSLYQNAD) shown in green, and 220-loop shown in brown (IRPKVRDQEG). The heart of the RBS pocket consists of highly conserved amino acid residues Tyr98, Trp153, His183, and Tyr195 which represent the base of binding site with cellular receptor sialic acid (Skehel & Wiley, 2000; Sriwilaijaroen, & Suzuki, 2012).

The results also showed that FH binds to the fusion domain, F′ in the N-terminal region of HA1 which includes residues 34 – 63, residues 111 – 120, residues 199 – 219 and the residues 287 – 306 in C-terminal of HA1. No interaction was observed between FH and the fusion peptide in the stalk region (HA2 subdomain) or the cleavage site (residues 324 – 29) in HA1 (Figure 4. 17, C – F). In the stalk of the HA protein before the transmembrane domain, there is a fusion peptide that includes a pocket in which the peptide sits prior to activation by low PH. The fusion peptide pocket comprises from the interface between loop B in HA2 and the subdomains

R, E′ and F′ of the HA1 with the contribution of residues 85 – 90, 104 – 115 and 265 – 270 of HA1 and 64 – 72 of HA2 (Mair *et al*., 2014).

The H1 HA antigenic sites localise on the residues 79 – 84, 140 – 145, 156 – 160, 162 – 166, 169 – 173, 187 – 198, 206 – 208, 224 – 225 and 238 – 24 in the HA1 (Xu *et al*., 2010; Sriwilaijaroen & Suzuki, 2012). The results showed that FH bound to the residues 79 – 84, 127 – 128, 140 – 145 and 206 – 225 of antigenic epitopes (Figure 4. 17, G). Thus, these results suggest that FH may impact IAV antigenicity. The GH loop peptide of FMDV used in this study as negative control is a surface loop contains antigenic site and responsible for attachment and cell entry of the virus by binding to integrin receptors of the host cell (Ruiz-Sáenz *et al*., 2009). Notably, significant binding of FH was observed with FMDV control (Figure 4. 17, A – B), suggesting a possible novel interaction between FMDV and FH.

Table 4. 1: Amino acid sequence of HA peptides from H1N1pdm09 that interact with FH.

Peptide number	Amino acid sequence
41 – 50	VTVTHSVNIL
51 – 60	EDKHNGKLCK
61 – 70	LRGVAPLHLG
121 – 130	QLSSVSSFER
141 – 150	FEIFPKTSSW
151 – 160	AACPHAGAKS
211 – 220	NADAYVFVGS
221 – 230	SRYSKKFKPE
231 – 240	IAIRPKVRDQ
301 – 310	GAINTSLPFQ
311 – 320	NIHPITIGKC
551 – 560	SFWMCSNGSL QCRICI

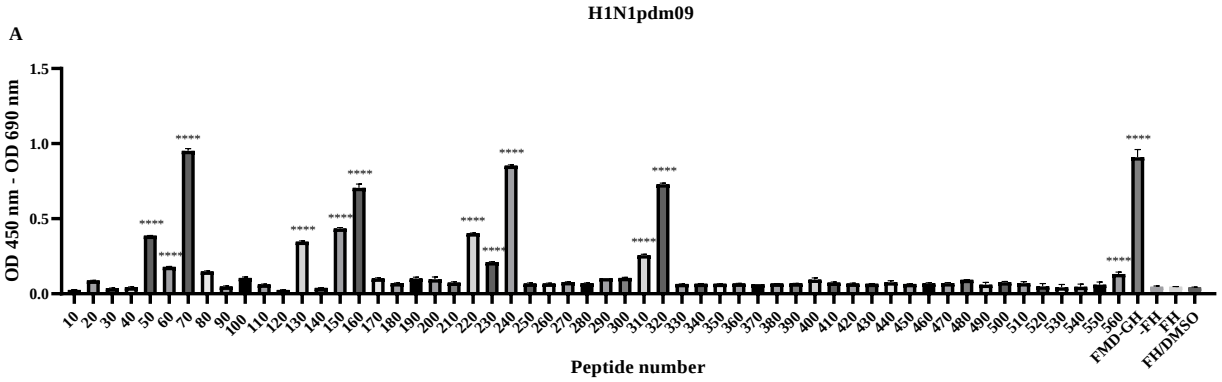
H1N1pdm09
A
OD 450 nm - OD 690 nm
Peptide number
FMD-GH
FH
FH/DMSO

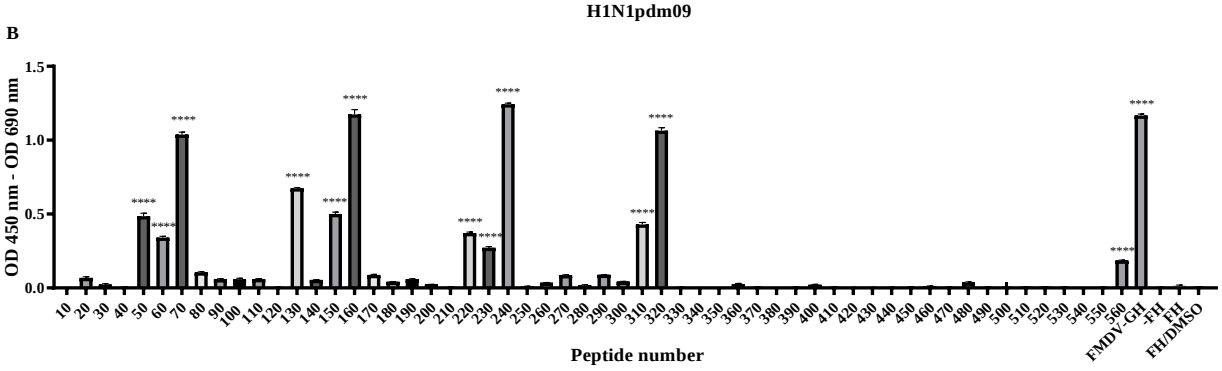
H1N1pdm09
B
OD 450 nm - OD 690 nm
Peptide number
FMDV-GH
FH
FH/DMSO

C

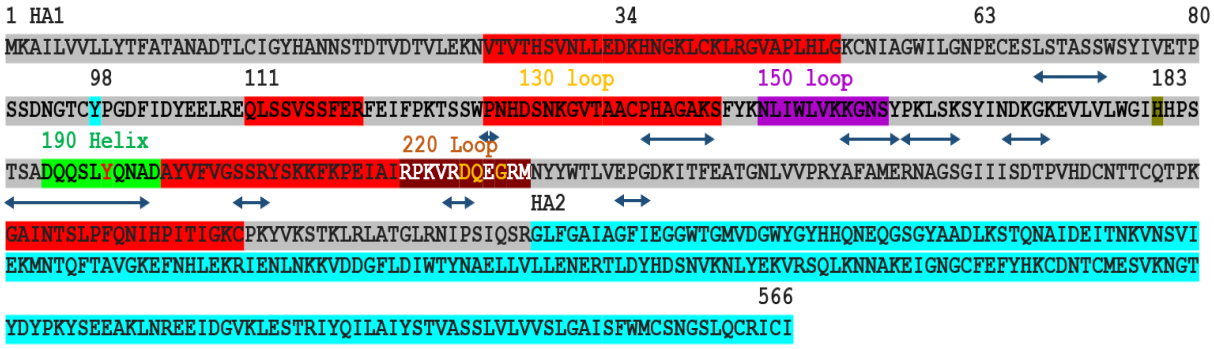
1 HA1
34
63
80
MKAILVVLLYTFATANADTLCIGYHANNSTDTVDTVLEKNVTVTHSVNLLEDKHNGKLCKLRGVAPLHLGKCNIAGWILGNPECESLSTASSWSYIVETP
98
111
130 loop
150 loop
183
SSDNGTCYPGDFIDYEELREQLSSVSSFERFEIFPKTSSWPNHDSNKGVTAACPHAGAKSFYKNLIWLVKKGNSYPKLSKSYINDKGKEVLVLWGIHHPS
190 Helix
220 Loop
TSADQQSLYQNADAYVFVGSSRYSKKFKPEIAIRPKVRDQEGRMNYYWTLVEPGDKITFEATGNLVVPRYAFAMERNAGSGIIISDTPVHDCNTTCQTPK
HA2
GAINTSLPFQNIHPITIGKCPKYVKSTKLRLATGLRNIPSIQSRGLFGAIAGFIEGGWTGMVDGWYGYHHQNEQGSGYAADLKSTQNAIDEITNKVNSVI
EKMNTQFTAVGKEFNHLEKRIENLNKKVDDGFLDIWTYNAELLVLLENERTLDYHDSNVKNLYEKVRSQLKNNAKEIGNGCFEFYHKCDNTCMESVKNGT
566
YDYPKYSEEAKLNREEIDGVKLESTRIYQILAIYSTVASSLVLVVSLGAISFWMCSNGSLQCRICI

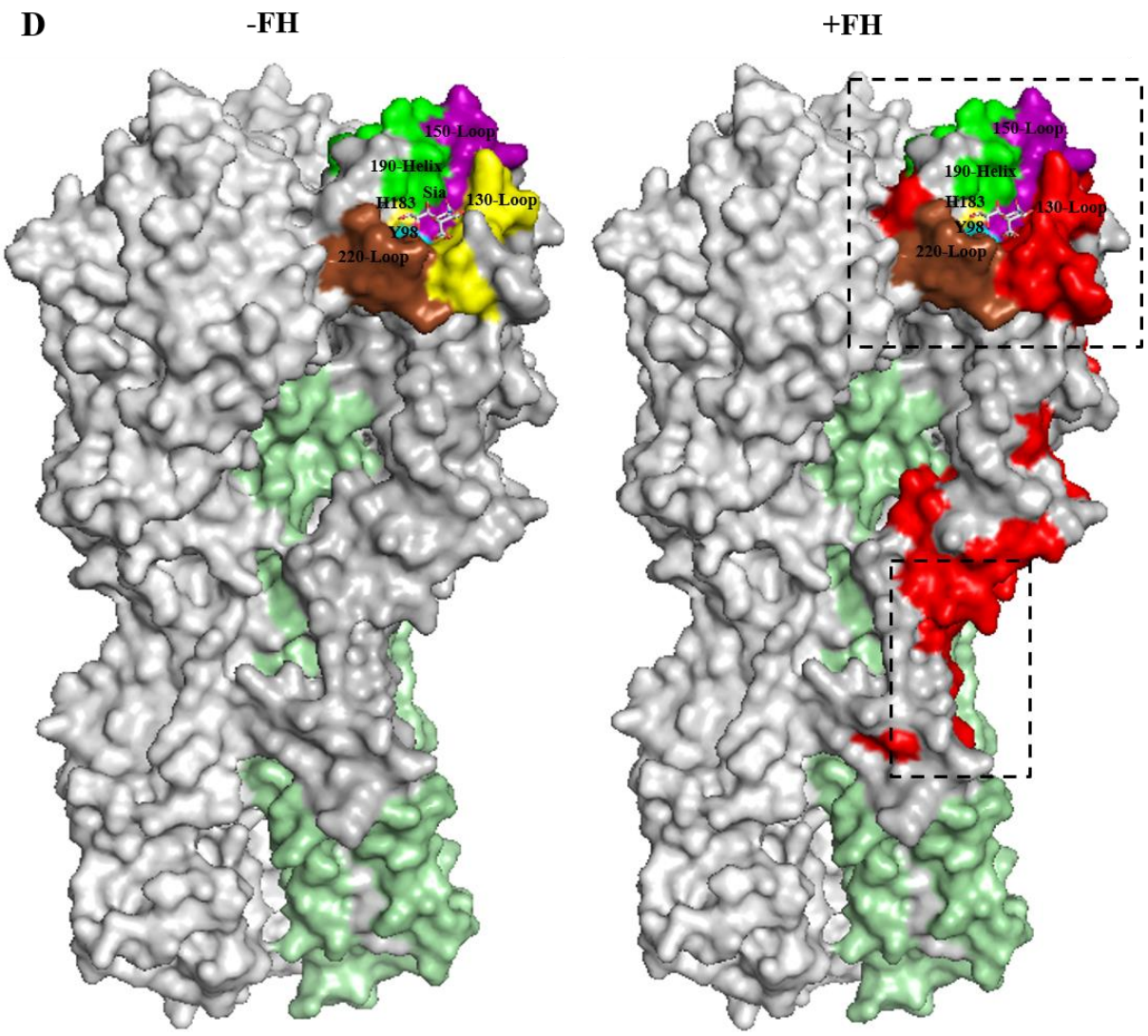
D
-FH
+FH
150-Loop
190-Helix
H183
Sia
130-Loop
Y98
220-Loop
150-Loop
190-Helix
H183
130-Loop
Y98
220-Loop

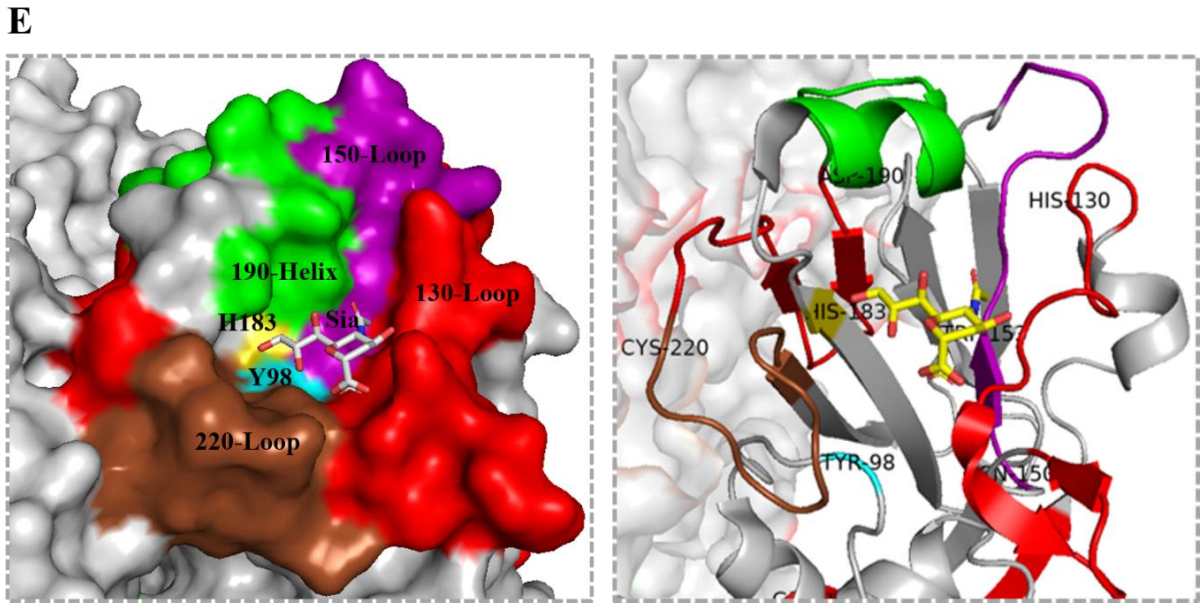
E
150-Loop
190-Helix
130-Loop
H183
Sia
Y98
220-Loop
HIS-130
CYS-220
TYR-98

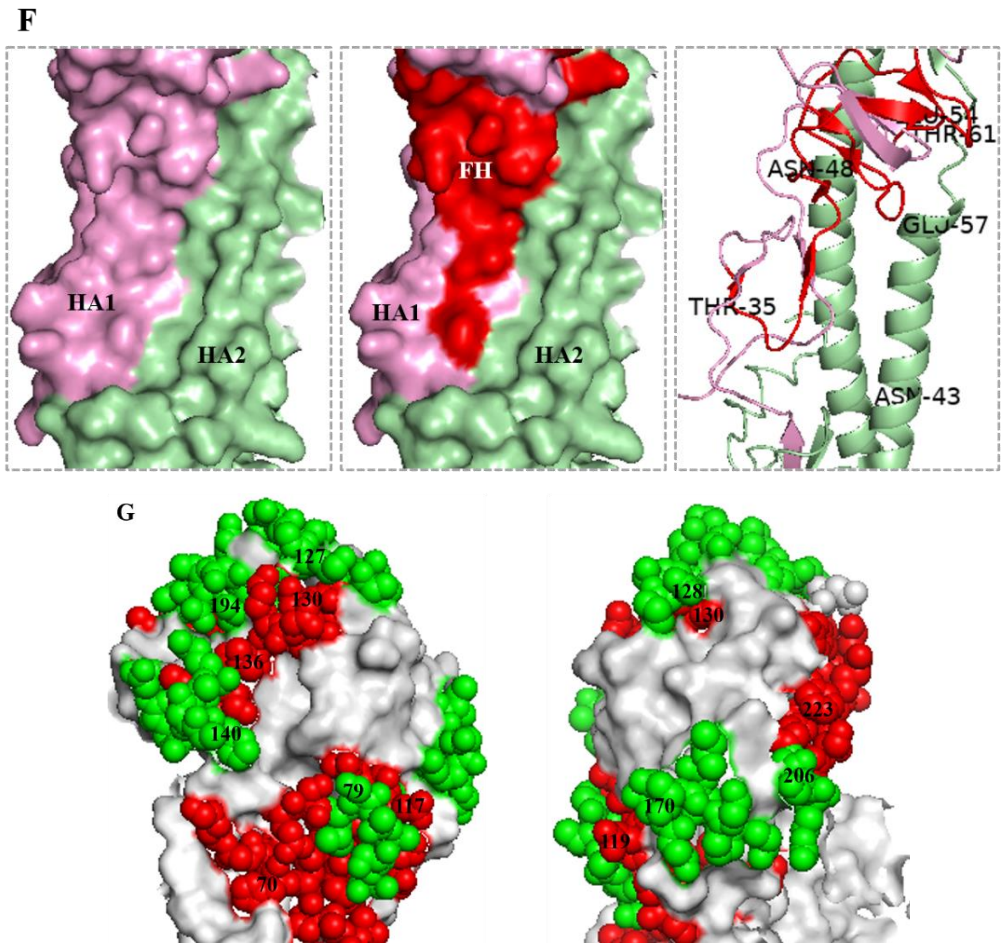

Figure 4. 17: ELISA to localise FH binding sites on the surface of HA from H1N1pdm09. (A) biotinylated -HA peptides bind to solid-phase FH. **(B)** purified FH binds to solid-phase biotinylated -HA peptides. As negative controls, biotinylated -GH loop peptide from FMDV, the absence of FH (-FH), FH in DMSO (FH/DMSO), and FH in PBS (FH) were used. The data for each panel is representative of three independent experiments performed in triplicate. The error bars indicate the ±SEM. Statistical differences compared to the control (FH in DMSO) were calculated by Dennett's test for the multiple comparisons (****$p < 0.0001$). **(C)** amino acid sequence of HA IAV (A/England/195/2009 (H1N1)) showing the residues that are involved in the binding to FH labelled in red. The subunits HA1and HA2 were displayed in grey and turquoise, respectively. The receptor-binding site (RBS) is made up of four structural elements highlighted: 130-loop in yellow, 150-loop in purple, 190-helix in green, 220-loop in brown. The heart of the RBS is composed of the conserved residues displayed: Tyr 98 in cyan, Trp153 in purple, His183 in olive, and Tyr195 in green. Antigenic sites are represented by arrows under the sequence. **(D)** The crystal structure of two molecules of H1 HA trimer (PDB: 3UBE, Xu *et al*., 2012) is shown in surface representation (grey). In the left panel, one of the monomers with globular head HA1 is shown in grey and the HA2 subunit labelled in pale green. The RBS pocket at the apex of HA1 subdomain with the structural elements labelled with the same colour code as shown in panel C. Sialic acid (Sia) is shown in stick representation in grey or yellow. The right panel shows the location of the binding sites of FH on the surface of H1 HA protein is shown in red. **(E)** The magnification of RBS region at the apex of HA1 subunits. The left panel shows a surface presentation of RBS pocket with the location of amino acids contributing to FH binding highlighted in red. The right panel is a cartoon representation of the RBS pocket representing FH binding site shown in red. All elements were labelled with the same colour code as shown in panel D. **(F)** The magnification of HA1–HA2 interface region at the stem domain of H1 HA. The left panel shows a surface presentation showing HA1 subdomain in salmon and HA2 in pale green. The middle panel demonstrates FH binding site on the HA1 region shown in red. The right panel shows a cartoon representation of FH binding sites is depicted in red. **(G)** Test whether the binding of FH shown in red spheres could interfere with the antigenic sites shown in green spheres. The globular head HA1 shown in grey. The images in the panel, D, E, and G were generated with PyMOL (Schrödinger, LLC).

ELISA results to analyse FH binding with HA peptides from H3N2/99 (Figure 4. 18, A – B) showed a larger number of significant peptides in the H3N2 screen than the H1N1 screen. Comparing to the negative control (FH in DMSO), significant binding was observed between FH and 25 HA peptides (Table 4. 2) grouped into 7 groups of one or more peptides adjacent to each other and thus sharing 10 amino acid sequence overlap. As shown in the Figure 4. 18, C – G, that FH bound to the 130-loop (TQNGGSNAC) labelled in yellow, and the first three residues (PWV) in 220-loop shown in blue, and with residue Tyr98 (lime green) (Figure 4. 18, C – E). Moreover, the results showed that FH binds to residues 85 – 90 (LFIER), 104 – 114 (EHASLRSLIAS), which are shown with yellow letters in the fusion peptide pocket of HA (Figure 4. 18, C). FH also binds to the major residues (1 – 25) of the fusion peptide in subdomain HA2 (Figure 4. 18, C and F). These findings suggest that FH binds to the major elements of RBS and fusion peptide pocket on H3 HA. In conclusion, the results established that human FH binds to 130-loop and the residues surrounding it, as well as with the amino acids between 190-helix and 220-loop in RBS pocket of both H1 HA and H3 HA. In addition to its interaction with several residues included in fusion peptide pocket in HA1 or HA2. Thus, HA-FH interaction may impact attachment, entry, and virus replication in the target cells.

Table 4. 2: Amino acid sequence of HA peptides from H3N2/99 that interact with FH.

Peptide chains	Amino acid sequence
21 – 30	GKGNNTATLC
51 – 60	EVTNATELVQ
61 – 70	NLSMGKICSN
71 – 80	PHRILDGANC
81 – 90	TLIDALLGDP
91 – 100	HCDGFQNEKW
101 – 110	DLFIERSKAF
111 – 120	SNCYPYDVPE
121 – 130	HASLRSLIAS

149 – 150	FNWTGVTQNG
151 – 160	GSNACKRGPD
221 – 230	STKRSQQTII
231 – 240	PNVGSRPWVR
261 – 270	RGYFKVHTGK
281 – 290	SSIMRSDAPI
291 – 30	ETCSSECITP
301 – 310	NGSIPNDKPF
311 – 320	QNVNKITYGA
321 – 330	CPKYVKQNTL
331 – 340	KLATGMRNIP
341 – 350	EKQTRGIFGA
351 – 360	GMVDGWYGFR
501 – 510	NSCIDSIRNG
511 – 520	TYDHNEYRDE
561 – 560	IMWACQKGNIRCNIC

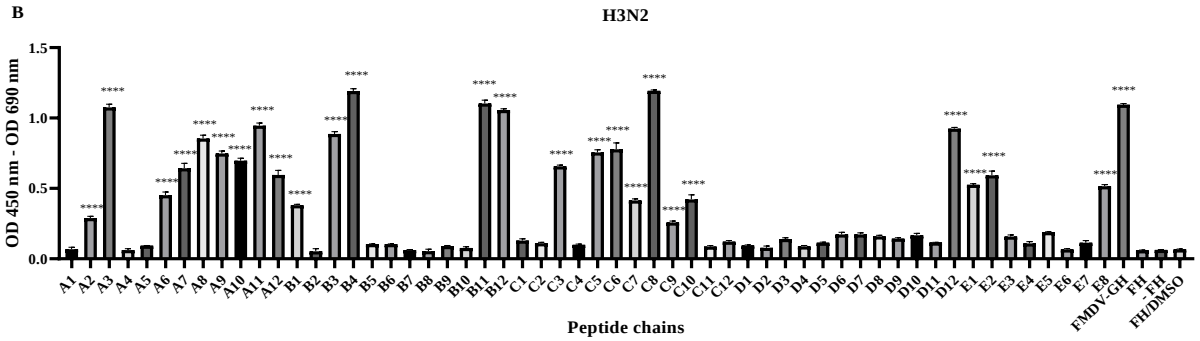

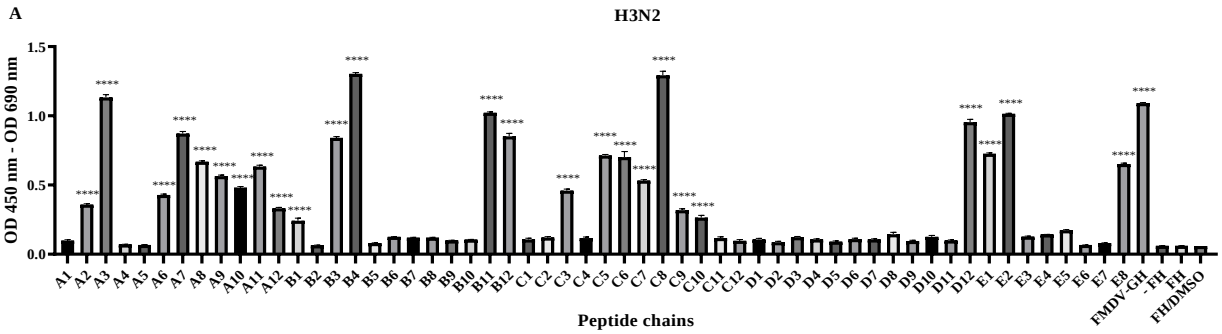

C

1 HA1

MKTIIALSYIFCMVLGQDLPGKGNNTATLCLGHHAVPNGTLVKTITDDQVEVTNATELVQNLSMGKICSNPHRILDGANCTLIDALLGDPHCDGFQNEKW

85 98 104 114 130 loop 150 loop 183

DLFIERSKAFSNCYPYDVPEHASLRSLIASSGTLEFVNESFNWTGVTQNGGSNACKRGPDSSFFSRLNWLYKSGNTYPMLNVTMPNSDGFDKLYIWGVHH

190 loop 220 loop

PSTDREQINLYVQASGKITVSTKRSQQTIIPNVGSRPWVRGLSSRISIYWTIVKPGDILIISSNGNLIAPRGYFKVHTGKSSIMRSDAPIETCSSECITP

1 Fusion peptide HA2 159

NGSIPNDKPFQNVNKITYGACPKYVKQNTLKLATGMRNIPEKQTRGIFGAIAGFIENGWEGMVDGWYGFRHQNSEGTGQAADLKSTQAAINQINGKLNRV

IEKTNEKFHQIEKEFSEVEGRIQDLEKYVEDTKIDLWSYNAELLVALENQHTIDLTDSEMNKLFEKTRKQLRENAEDMGNGCLKIYHKCDNSCIDSIRNG

566

TYDHNEYRDEALNNRFQIKSVELKTGYKDWILWISFAISCFLLCVVWLGFIMWACQKGNIRCNIC

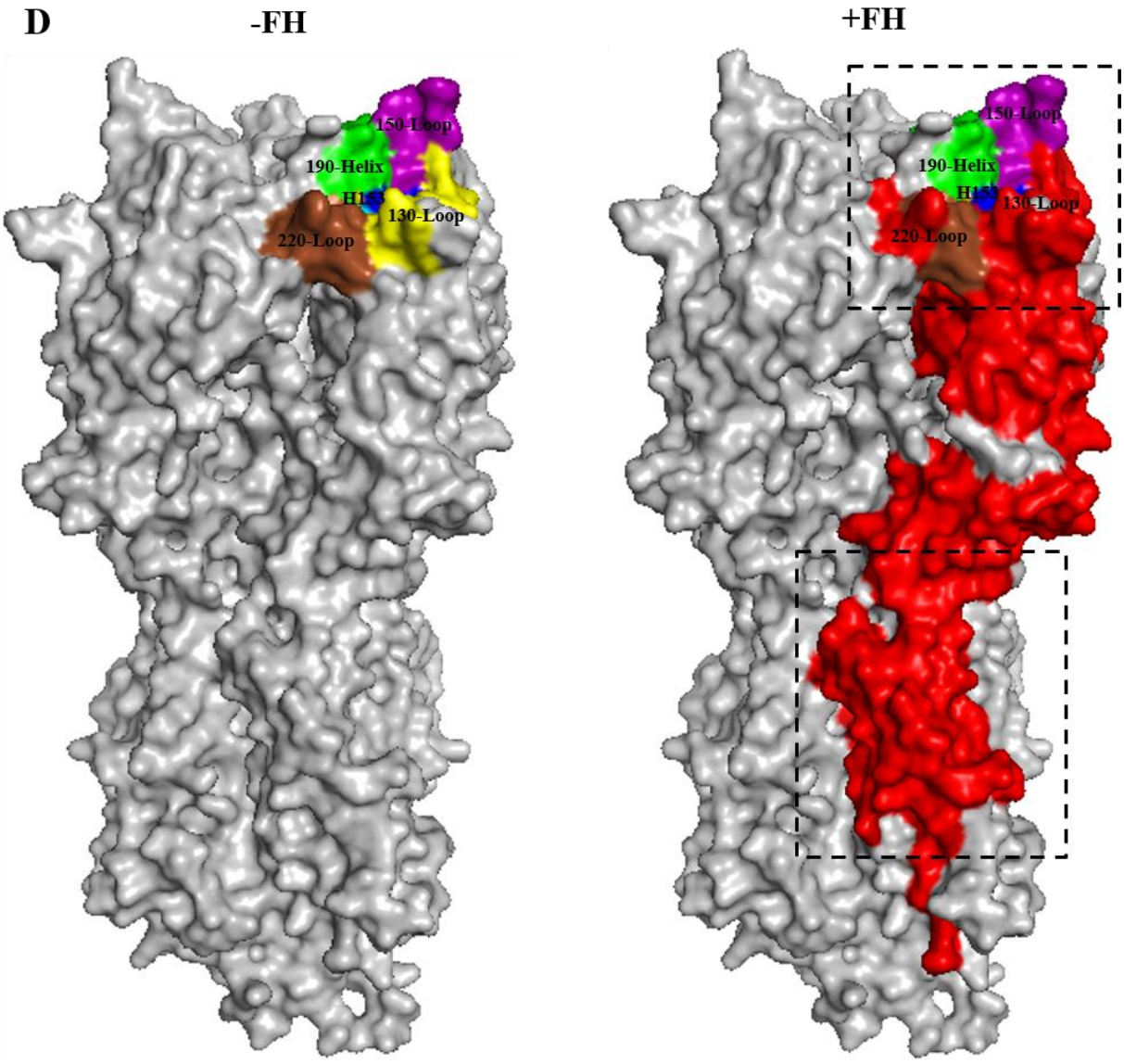
D
-FH
+FH
150-Loop
190-Helix
H153
130-Loop
220-Loop
150-Loop
190-Helix
H153
130-Loop
220-Loop

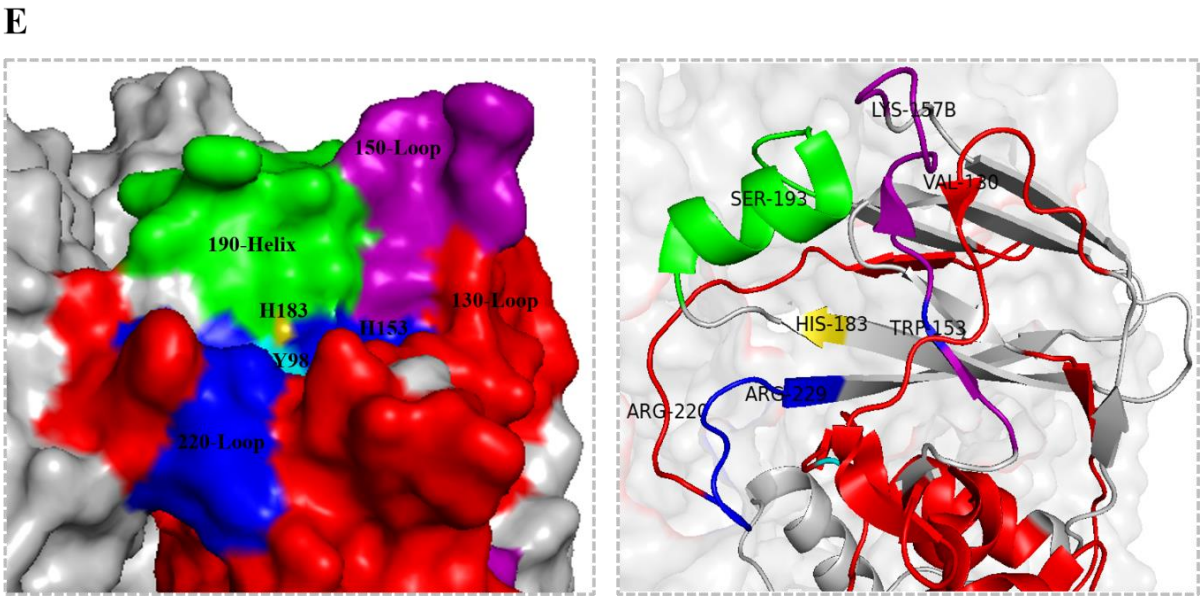
E
150-Loop
190-Helix
H183
H153
130-Loop
Y98
220-Loop
LYS-157B
VAL-130
SER-193
HIS-183
TRP-153
ARG-229
ARG-220

F

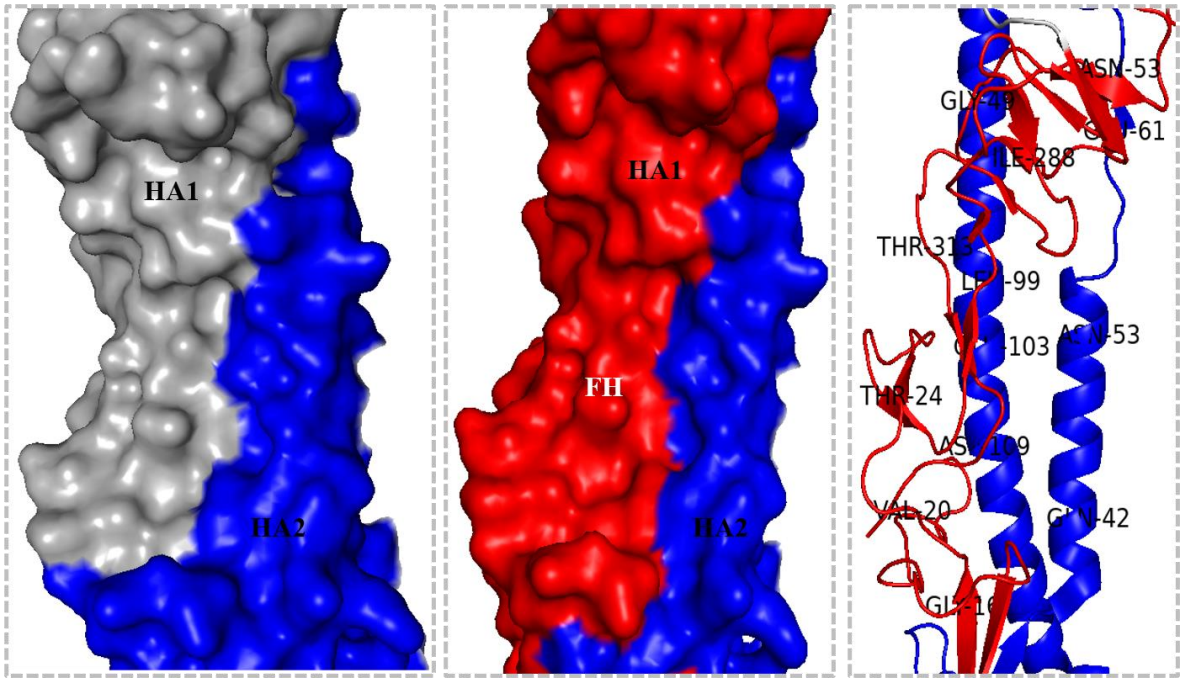

Figure 4. 18: Localisation analysis of FH binding sites in HA protein H3N2/99 by ELISA. (A) biotinylated-HA peptides bind to solid-phase FH. **(B)** purified human FH binds to solid-phase biotinylated-HA peptides. As negative controls, biotinylated -GH loop peptide from FMDV, the absence of FH (-FH), FH in DMSO (FH/DMSO), and FH in PBS (FH) were used. The data for each panel is representative of three independent experiments performed in triplicate. The error bars indicate the ±SEM. Statistical differences compared to the control (FH in DMSO) were calculated by Dennett's test for the multiple comparisons (****$p < 0.0001$). **(C)** The alignment of residues 1 to 566 of the HA3 HA sequence from IAV (A/Hong Kong/1774/99(H3N2). Amino acids that are involved in the binding to FH labelled in red. The subunits HA1 and HA2 were displayed in grey and turquoise, respectively. The RBS structural elements highlighted: 130-loop in yellow, 150-loop in purple, 190-helix in green, 220-loop in blue. The conserved residues Tyr 98 and His183 are shown in cyan and olive, respectively. **(D)** Surface representation of two molecules of H3 HA trimer (PDB: 2YPG, Lin *et al*., 2012) are shown in grey. The left panel shows the RBS in one of the monomers with the structural elements are colour-coded as in the panel (C). The right panel shows the location of the binding sites of FH on the surface of the H3 HA protein is shown in red. **(E)** The magnification of RBS region at the apex of HA1 subunits. The left panel shows a surface presentation of RBS pocket with the location of amino acids contributing to FH binding are highlighted in red. The right panel is a cartoon representation of the RBS pocket representing FH binding site is shown in red. All elements are labelled with the same colour coded in panel D. **(F)** Magnification of HA1–HA2 interface region at the stem domain of H1 HA (Fusion peptide pocket). The left panel shows a surface presentation showing HA1 subdomain in grey and HA2 in blue. The middle panel demonstrates FH binding site on the HA1 region is shown in red. The right panel shows a cartoon representation of FH binding sites depicted in red. The images in the panel, D, E, and G were generated with PyMOL (Schrödinger, LLC).

4.2.6 Is anti-HA antibody able to inhibit HA-FH interaction?

To assess whether anti-HA antibody can inhibit or decrease HA-FH binding, ELISA was performed in the absence or presence of serial dilutions (0, 10^{-2}, 10^{-3}, 10^{-4}, and 10^{-5}) of antiserum to H9N2. Four negative controls were used in this assay, a highest dilution (10^{-2}) of antiserum without virus (-V), antiserum without FH (-FH), FH without virus and antiserum (-V/0), virus and FH without antiserum (0). As shown in figure 4. 19, pronounced binding of human FH to purified H9N2 IAV in the presence and absence of antiserum (the negative control (0)). FH binding to H9N2 at low concentration of antiserum increased from $p<0.01$ at 10^{-2} to $p<0.000$ at 10^{-5} of antiserum. No significant difference was observed in FH binding to antiserum treated H9N2 compared to the negative control (0). These results suggest that antiserum to H9N2 does not inhibit binding of FH to purified H9N2 virus. However, the presence of a high concentration of antibody may decrease, to some extent, FH binding to IAV.

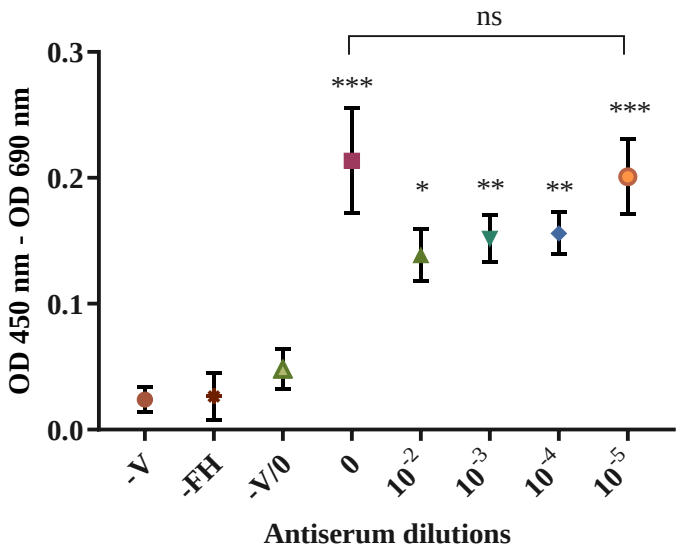

Figure 4. 19: Investigation of the interference of anti-HA antibody binding site in HA with FH binding site by ELISA. Microtiter plate wells were coated with purified H9N2 at 10^4 PFU/well overnight at 4°C. After blocking and washing, increasing dilutions of antiserum to H9N2 were added. purified FH was added at 20 µg/well and detected with anti-FH OX24. Four negative controls were used in this assay, a highest dilution (10^{-2}) of antiserum without virus (-V), antiserum without FH (-FH), FH without virus and antiserum (-V/0), virus and FH without antiserum (0). The data represent three individual experiments. Each experiment was performed in triplicate (mean ±SEM). statistical analysis was performed using unpaired one-way ANOVA test. P values (*p<0.01, **p<0.001, and ***p<0.0001) were indicated and calculated using a multiple comparison, Dennett's test.

4.2.7 The role of deglycosylation of IAV in binding to FH

Glycosylation plays a crucial role in determining the three-dimensional structure of proteins, affecting their structures, functions, and stability. It has particular importance in protein-to-protein interaction. FH binds to carbohydrates including sialic acid on host self-cells to protect them from the complement activation. HA is a glycoprotein with both N-linked and O-linked glycans on its surface, which terminate in sialic acid residues. Therefore, one hypothesis is that FH interacts with HA of IAV by binding to glycans on the surface of HA. Thus, an investigation was carried out to determine whether removing glycans from the surface of HA could alter the interaction with FH. Various subtypes of IAV were deglycosylated by the amidase, Peptide -N-Glycosidase F (PNGase F) and tested in ELISA and far-western blot.

4.2.7.1 Analysis of N-deglycosylated IAVs by SDS-PAGE and western blot

To identify the efficiency of N-deglycosylation of H9N2 and H5N3 IAV subtypes, a 10% Coomassie-stained SDS-PAGE analysis was performed. The results showed that both the H5N3 and H9N2 virus proteins migrated with similar mobilities on the 10% SDS-PAGE (Figure 4. 20, A). Consistent with observations from Harvey *et al* 2008, in reduced conditions the HA1 and HA2 subunits for both viruses migrated with a molecular weight of 55 and 28 kDa, respectively. PNGase F was observed as a separated band from viral proteins with the MW of 38 kDa. Following treatment of the viruses with PNGase F to deglycosylate the viral proteins, both bands shifted toward a lower molecular mass of 38 and 23 kDa, respectively. To confirm whether these bands were the HA subunits (HA1 and HA2), western blot analysis was performed with monoclonal antibodies against the H9 and H5 HA proteins. Immunoblot analysis of N-deglycosylated H5N3 and H9N2 IAVs showed a strong HA1 band with MW of 38 kDa in which the epitopes for these monoclonal antibodies were located. Whereas the HA2 subunit was observed as a faint band with MW of 23 kDa (Figure 4. 20, B). These results suggest that the N-deglycosylation of the virus was efficient.

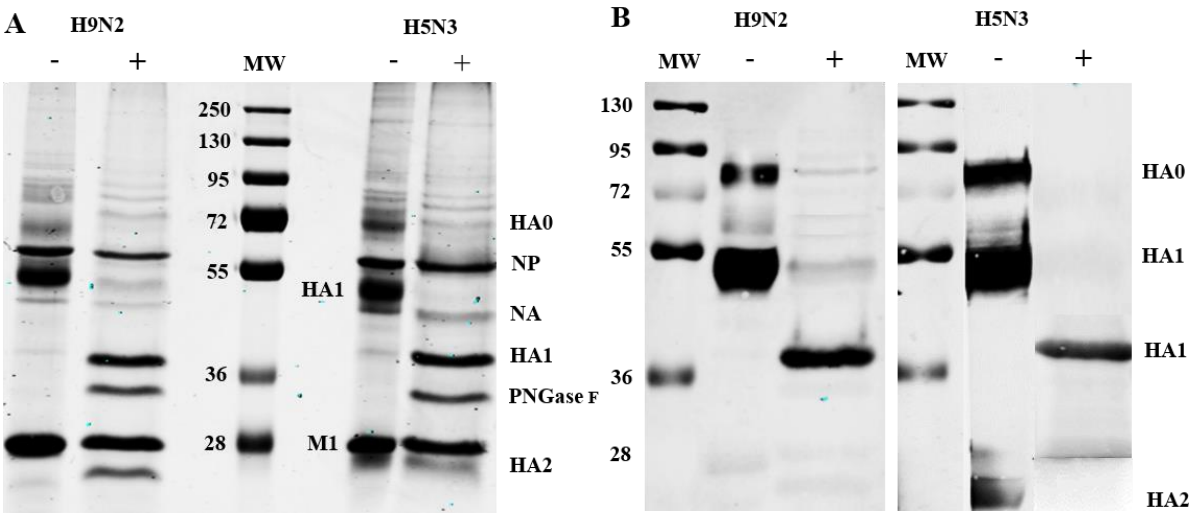

Figure 4. 20: Analysis of N-deglycosylated purified H9N2 and H5N3 IAVs by SDS-PAGE and western blot. (A) Coomassie-stained 10% SDS-PAGE of untreated (-) and treated (+) H9N2 and H5N3 with PNGase F. **(B)**: Western blot analysis to confirm N-de-glycosylation of HA proteins of untreated (-) and treated (+) H9N2 and H5N3 with PNGase F. HA protein for both viruses were detected using mouse monoclonal anti-H9 and H5 antibodies, respectively. The mobility of size markers (kDa) is indicated.

4.2.7.2 ELISA to assess the effect of deglycosylation of IAV on FH binding

To investigate whether removal of glycans from IAV affects the binding interaction between the viruses and FH protein, ELISA was performed using PNGase F treated (+) and untreated (-) H5N3 or H9N2. The negative controls used in these experiments were the presence of FH with the absence of IAV (FH-V), virus without FH (V-FH) and the lentivirus particles that contained no envelope protein on the surface (Δ-env). In this assay, binding of FH to deglycosylated H9N2 and H5N3 viruses was statistically significant compared to virus untreated with PNGase F (Figure 4. 21, A – B). The experiments were repeated in reverse order; virus binding to solid-phase FH. The MBP protein was used as a negative control with untreated (- PNGase F) or treated (+PNGase F) viruses with PNGase F. FH without virus was also used as a negative control. As shown in Figure 4. 21, C – D, binding of de-glycosylated viruses to FH and the negative control, MBP protein was significantly increased compared to the untreated virus with PNGase F. Interestingly, these results suggest that the lack of the carbohydrates from HA protein of IAV not only increases the ability of IAV to bind to FH but also increases the binding of IAV to the MBP control protein.

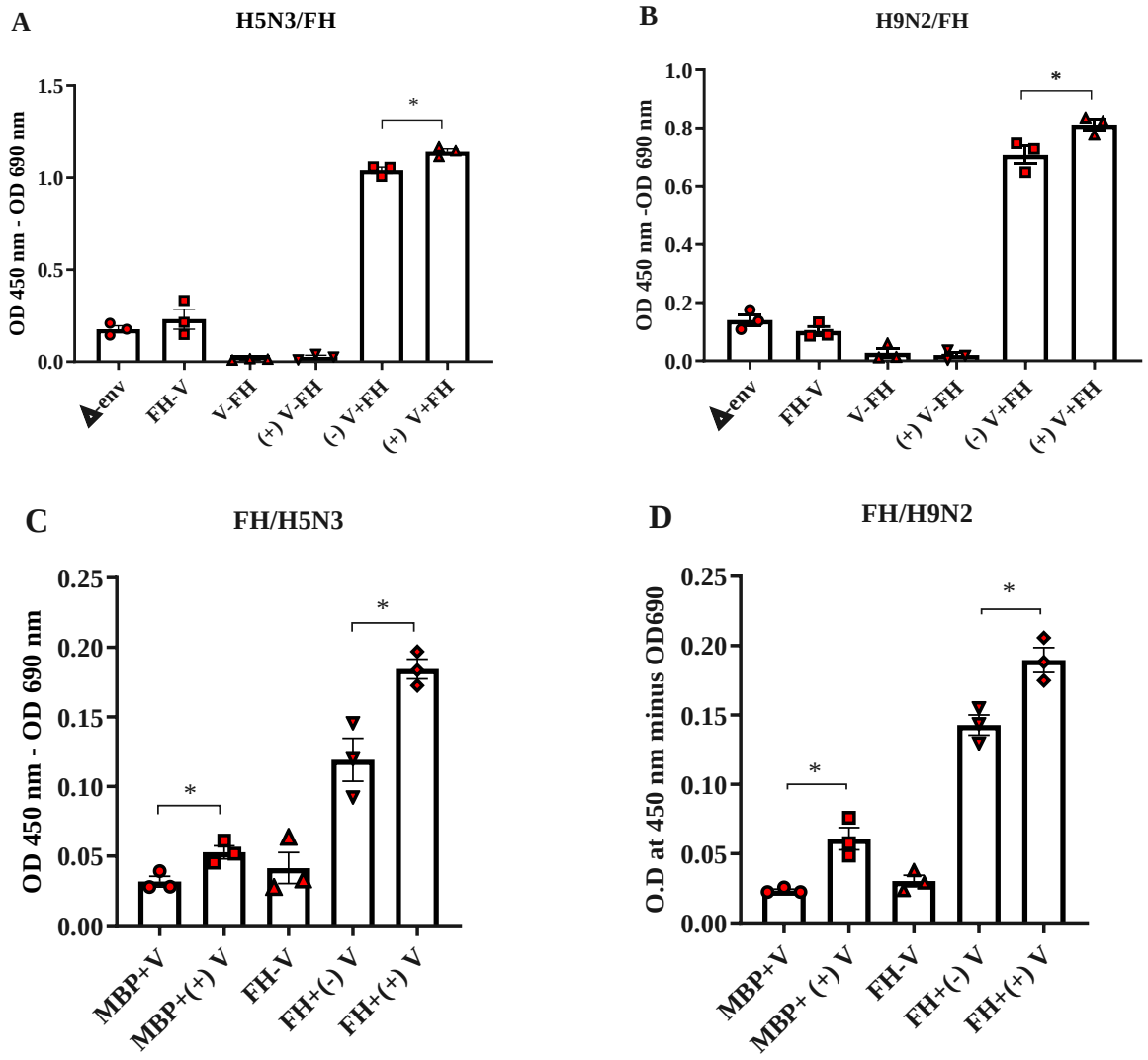

Figure 4. 21: Deglycosylated H5N3, H9N2 IAVs and FH binding by ELISA. (A) and **(B)** FH binds to solid-phase de-glycosylated H9N2 and H5N3, respectively. Untreated (-) and treated (+) virus with PNGase F were absorbed to the surface of Microtitre plate wells at 10^4 PFU/well overnight. After blocking, purified FH was added at a concentration of 20 µg/well. mAb anti-FH OX24 was used to detect bound FH. The negative controls used in these assays were, lentivirus particle without envelope protein on the surface (Δ-env), a virus without FH (V-FH), and FH without virus FH-V). **(C)** Deglycosylated H5N3 and **(D)** H9N2 interact with the solid phase FH. FH (20 µg/well) was incubated in coating buffer overnight. After blocking, an untreated and treated virus with PNGase F were added. The bound virus was detected by mAb anti-NP. MBP was used as a negative control protein. The data of each graph are the average of three independent experiments were performed in triplicate. The error bars indicate the ±SEM. Significant difference value (*$p < 0.01$) was calculated compared to the untreated virus using t-test.

4.2.7.3 Far western blot to analyse the effect of deglycosylation of IAV on FH binding

Far western blot was performed to confirm the effect of HA deglycosylation on its binding to human FH (Figure 4. 22, A – D). The PNGase F-treated (+) IAVs (H5N3, H9N2, H1N1 pdm09, H3N2/99) that were overlaid with FH indicated binding of the FH to 38, and 23 kDa bands.

These are the bands that correspond to expected molecular weights of HA1 and HA2 subunits, respectively in IAV control (C) treated with PNGase F (+) and probed with anti-HA antibodies. De-glycosylated HA proteins of IAVs tested appeared to indicate increased binding to FH, most noticeable for H5N3, H9N2 and H1N1 pdm09 (Figure 4. 22, A – C) compared to PNGase F-untreated IAVs (Red) in the overlaid membrane. No band of HA protein was observed on the negative control (-C), suggesting that there is no cross-reactivity between viral proteins and anti-FH OX24. These findings suggest that removal of glycans from HA protein may increase the ability of HA protein to bind to human FH.

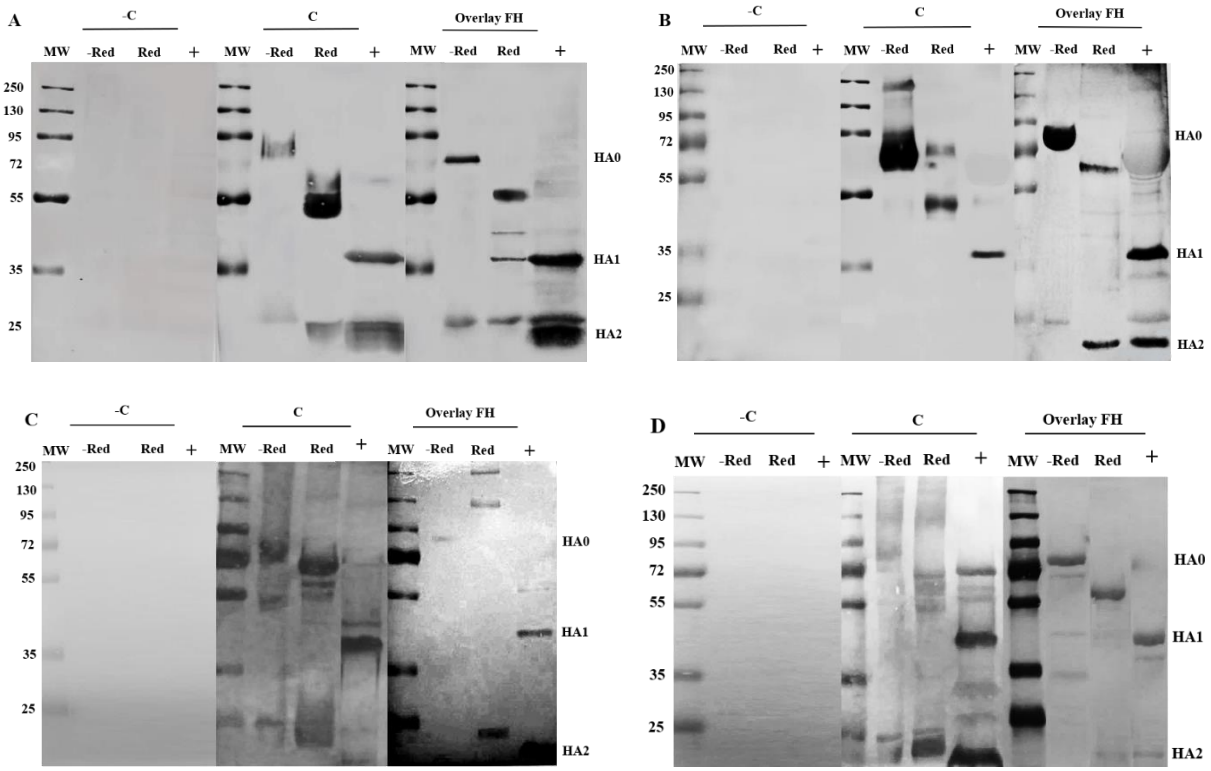

Figure 4. 22: Far western blot to assess the effect of deglycosylation of IAV on FH binding. Purified **(A)** H5N3, **(B)** H9N2, **(C)** H1N1pdm09, and **(D)** H3N2/99 IAVs were subjected to 10% non-reduced (-Red), reduced (Red) and treated with PNGase F (+) gel electrophoresis in triplicate. After electroblotting on PVDF membrane, each membrane was sectioned into three parts, negative, positive control and overlaid. To assess the interaction between HA protein and FH, the overlaid membrane (Overlay FH) was incubated with 20 µg/ml of purified human FH. Bound FH to HA protein was detected by mAb anti-FH OX24. The HA protein in the positive control (C) was detected by HA antibody against HA protein of four IAVs tested. These antibodies include mouse mAb anti-H9 or H5 for H9N2 and H5N3, respectively and ferret anti-H1and anti- H3 HA (1:500). In the negative control (-C), the separated IAV proteins were probed with mAb anti-FH OX24. To visualise viral proteins bands of H9N2 and H5N3, the membranes were hybridised with anti-mouse secondary antibody IRDye 800CW (1:1000) and displayed by Odyssey Infrared Imaging System. Whereas, to show separated viral proteins of H1N1pdm09 and H3N2/99, anti-ferret secondary antibody HRP conjugate (1:1000) was used and followed by the colour development with DAKO substrate. The viral proteins, uncleaved HA protein (HA0), cleaved HA (HA1 and HA2), were detected by their expected molecular weights. The mobility of size markers (kDa) is indicated to the left of each gel. Data shown are representative of four independent experiments.

Mapping of the FH binding sites on the H1 HA protein (Figure 4. 17, D) showed that FH interferes with the glycosylation sites at amino acid positions N40, N289, N293 and N304 in HA sequence (Figure 4. 23). The glycosylation sites have been identified on the HA molecule of H1N1pm09 virus, including N28, N40, N104, N278, N293, N304, N498 and N557 (Sriwilaijaroen &Suzuki, 2012; Sun *et al*., 2011; Al Khatib *et al*., 2019). In this study, increase binding of FH to IAV after PNGase F treatment suggest that the interaction between IAV and FH is a protein-protein interaction and not via glycans. Thus, removal of HA glycans increased amino acids exposure to the FH surface, resulting in elevated IAV-FH interaction signals in ELISA and far-western blot.

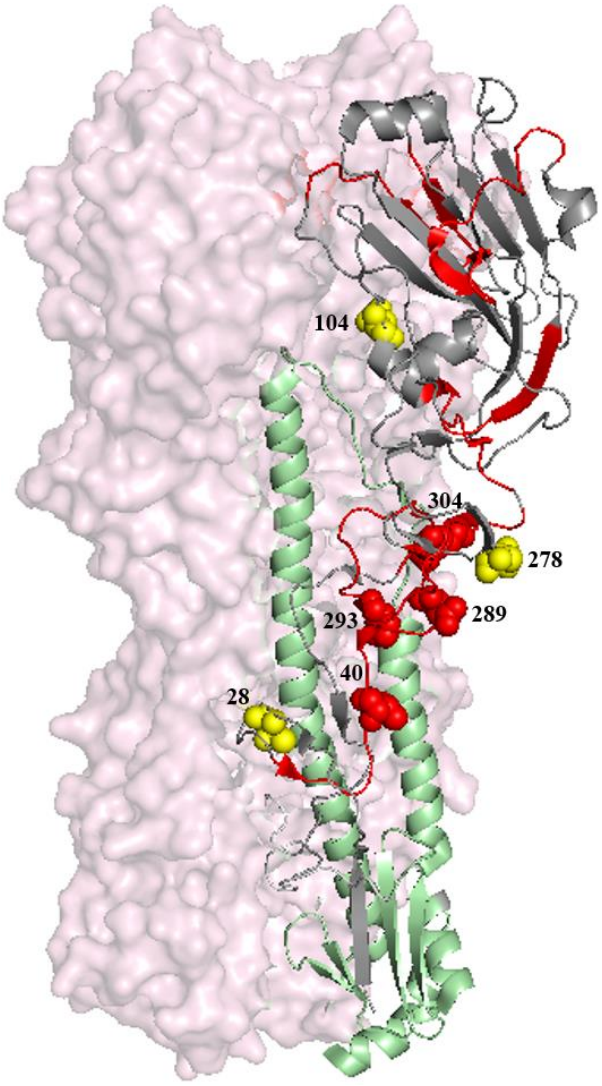

Figure 4. 23: Structural overlap of FH with glycosylation sites on H1 HA of H1N1pdm09. A trimeric HA molecule of IAV (PDB: 3UBE, Xu *et al*., 2012) is shown in surface representation (light pink). One of the monomers is shown in cartoon representation with HA1 subdomain shown in grey and the HA2 subunit in pale green. On this monomer, the locations of glycosylation sites are highlighted with yellow spheres. The Binding sites of FH on the surface of H1 HA protein is shown in red. Overlap of FH with amino acids at glycosylation sites is displayed in red spheres. The image was generated with PyMOL (Schrödinger, LLC).

4.2.8 The role of deglycosylation of FH in IAV binding to FH

The IAV HA protein binds to the cellular receptor sialic acid to facilitate entry to host cells. The sialic acid binding site is located in the HA1 globular head of the HA protein (Lazniewski *et al*., 2018). FH is a glycoprotein with nine potential N-glycosylation sites (Fenaille *et al*., 2007). Therefore, the interaction between FH and IAV also has the potential to occur through the IAV HA interaction with terminal sialic acid on the FH glycans. Thus, to understand the effect of FH glycans on the interaction with IAV, purified human FH was N-deglycosylated by PNGase F and tested in ELISA.

4.2.8.1 Analysis of deglycosylation of FH by SDS-PAGE

To confirm the efficiency of deglycosylation of FH, SDS-PAGE analysis was performed (Figure 4. 24). FH was compared under denaturing conditions deglycosylated (+) or untreated (-) to untreated FH under non-reducing conditions (-Red). The results showed that non-reduced FH protein with no PNGase F treatment (-Red) elucidated the two expected bands of 150 kDa band representing the full-length FH and the second band of 36 kDa corresponding to FHL-1. The denatured FH exhibited multiple bands due to the highly glycosylated pattern of this protein which exists in multiple glycosylated forms. FH treated with PNGase F showed decreased mobility compared to that of non-reducing FH. A clear band at the lowest molecular weight seen in the treated sample (MW ~ 55). This suggests that the glycosylation has efficiently been removed from the FH. FHL-1 does not change between treated and untreated. The lack of size change may be due to the fact that of the nine known FH glycosylation sites, only one is located in the overlap with FHL-1 coding region (Fenaille *et al.*, 2007).

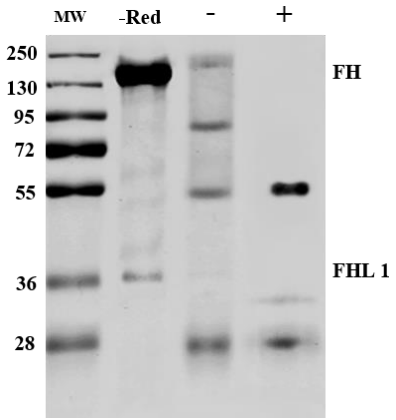

Figure 4. 24: Analysis of N-deglycosylated purified FH by SDA-PAGE. Coomassie-stained 10% SDS-PAGE of PNGase F-treated FH (+) and denature FH (-) in which FH denatured according to the PNGase F manufacturer's instructions without incubation with PNGase F. Deglycosylated and denatured FH were compared with non-reducing FH (-Red). The mobility of size markers (in kDa) was indicated in the left of the gel.

4.2.8.2 ELISA to analyse the binding of deglycosylated FH to IAV

To examine whether the binding of IAV to FH could be affected by deglycosylation or denaturation of FH, an ELISA was performed (Figure 4. 25, A – B). The results showed that the binding of H5N3 and H9N2 IAVs to deglycosylated (+) and denatured (-) FH notably decreased compared to the control PNGase-untreated FH (FH). No significant difference (ns) was observed between deglycosylated and denatured FH in their binding to both viruses tested. Thus, these results suggest that the reduced binding between IAV and FH was due to denaturation of FH during the deglycosylation process and not due to glycans removal. Altogether, these results demonstrate that deglycosylation of FH does not affect the binding of IAV to FH.

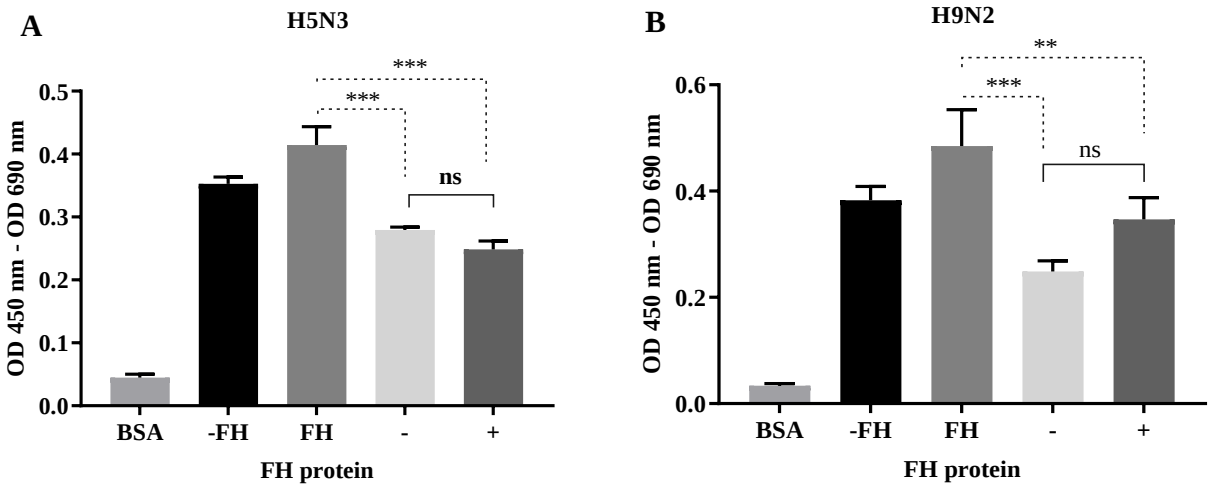

Figure 4. 25: Binding of IAV to Deglycosylated FH by ELISA. PNGase F-treated FH (+), denatured FH (-) in which it was denatured according to the PNGase F manufacturer's instructions without incubation with PNGase F were absorbed to the plastic surface of Microtiter plate wells at a concentration of 20 ug/well. A purified IAV, **(A)** H5N3 or **(B)** H9N2 was added at a titre of 10^4 PFU/well. The binding of IAV to FH was detected by mAb anti-NP and compared to the positive control, PNGase F-untreated FH (FH) with virus presence. A virus without FH (-FH) was also used as a positive control to indicate the presence of the virus. BSA was used as a negative control protein. The data of each graph are the average of three independent experiments were performed in triplicate. The error bars indicate the ±SEM. Significant differences values were calculated by Dennett's test for multiple comparisons.

4.3 Discussion

The virulence of pathogens is determined by their ability to invade the host, cause infection, and evade immune surveillance. The complement system is one of the earliest responses to invasive pathogens, especially the alternative pathway which is spontaneously activated on unprotected surfaces. To ensure their survival in the host body, pathogens may recruit host complement regulators from plasma or host body fluids. Some pathogens bind to FH to inhibit alternative pathway activation or bind with C4b protein for protection against classical and lectin pathways (Meri *et al*., 2013). Since alternative pathway activation occurs spontaneously to survey the presence of pathogens in the host body, FH regulates complement proteins cascade to prevent self-surface damage. Complement FH acts as a cofactor for factor I to degrade the central protein in complement system C3b. This inactivation prevents the deposition of C3b proteins on pathogen surfaces, protecting them from opsonisation for phagocytosis and lysis by the membrane attack complexes. Therefore, pathogens bind to and recruit FH to minimise complement recognition of pathogen surfaces, thus ensuring their survival within a host (Chung *et al*., 2006; Meri *et al*., 2013; Rosa *et al*., 2016).

While the FH recruitment to evade recognition and destruction of AP is well known for bacterial pathogens like *Haemophilus influenzae* (Hallström *et al*., 2008), *Streptococcus pneumoniae, Staphylococcus aureus, Neisseria meningitides, Borrelia burgdorferi* (Zipfel *et al*., 2007, 2008, 2013; Józsi and Zipfel, 2008; Blom *et al*, 2009; Sharp *et al*., 2012; Hyams *et al*., 2013; Zipfel and Skerka, 2014; Seib *et al*., 2015; Zhang *et al*., 2017), *Yersinia enterocolitica,* (Biedzka-Sarek *et al*., 2008) fungal pathogens, such as *Candida albicans* (Meri *et al*., 2002; Kenno *et al*., 2019) and *Aspergillus fumigatus* (Behnsen *et al*., 2008), or parasites like malaria parasite *Plasmodium falciparum* (Simon *et al*., 2013; Kennedy *et al*., 2016; Rosa *et al*., 2016; van Beek *et al*., 2018), African sleeping sickness parasite *Trypanosoma brucei* (Macleodand *et al*., 2020) and *Toxoplasma gondii* (Sikorski *et al.*, 2020). The interaction of FH with viruses has only been investigated with West Nile virus (Chung *et al*., 2006).

In this study, ELISA was performed to investigate the direct interaction between FH and six live strains of purified IAVs including four different subtypes, two strains of human H1N1 subtypes, the wild type, A/England/195/09 H1N1and vaccine strain A/Michigan/45/15 H1N1, two strains of human H3N2 subtypes, the wild type, H3N2 A/HK/1174/99, and vaccine strain A/HK/4801/14, and two avian IAV subtypes, A/Duck/Singapore/3/97 H5N3, and

A/chicken/Pakistan/UDL-01/08 H9N2. The results established significant binding of all purified IAVs tested with human FH.

Far western blot analysis for the interaction of four IAV subtypes, human H1N1pdm09, H3N2/99, and avian H5N3, H9N2 with FH suggests that the IAV-FH interaction is mediated by HA surface protein which has a key role in the attachment, entry mediated by membrane fusion, antigenicity, pathogenicity, and host specificity. FH binds to viral proteins with molecular weights of 80 – 50, and 25 kDa which represent the different versions of HA; full-length HA0, and the subunits HA1 and HA2, respectively as demonstrated by antibody reactivity with anti-HA antibodies used in this study. In these experiments, the HA band showed different intensities, and this may be due to many factors. One of these factors could be the concentration of the virus. The propagation of IAVs used in these experiments was performed in different methods depending on the source of the isolated virus. Avian IAVs (H5N3 and H9N2) were propagated in hens' eggs, which commonly yields high titre viral stocks (Brauer & Chen, 2015), while human IAVs (H1N1 and H3N2) were cultured in MDCK cells. Although amplification of IAV in hens' eggs produces high titre viruses in large quantities, various studies have reported that the growth of the virus in this method can alter the structure of HA protein, making it different from the wild-type virus. IAV that is propagated in mammalian cell-derived tissue culture resembles the natural virus (Oxford *et al*., 1987; Oxford *et al*., 1991; Robertson *et al*., 1987). Therefore, H1N1 and H2N3 showed faint bands of H1 and H3 HA compared to the strong bands of H5 and H9 HA. Variation in virus concentrations can be avoided by measuring the concentration of the denatured virus with NanoDrop. The difference in band intensity may be due to another reason such as the specificity of primary antibodies to detect the HA protein and the validation of antibodies for western blot. The methods used to develop the band may be another reason for dark or faint bands appearance. In these experiments, separate viral proteins for H1N1 and H3N2 were developed by chromogenic substrates which is a medium-sensitivity technique, while H5N3 and H9N2 membranes were scanned on the LI-COR Bioscience Odyssey CLx imaging system using infrared detection with a sensitive, robust signal. This may explain why the H1, and H3 HA bands were faint, while the H5 and H9 HA showed dark bands.

In the present study, several experimental approaches were carried out to confirm the interaction between the HA protein of IAV and FH. In addition to whole virion binding of FH, HA protein from nine strains of IAVs that belong to five human and avian subtypes H3, H1,

H9, H7, H5 were displayed without or with NA viral protein on the surface of pseudotyped lentiviral particles. They are all human immunodeficiency virus (HIV) core - Luciferase with HAs from H7 FPV, H1 Solomon, H3 Udorn, H3 California, H5 1194 (with and without NA), H9 HK and pH1. The IAV pseudotyped particles efficiently bound human FH in ELISA compared to the negative control, VSV-G lentivirus particles (VSV-G). These results suggest that IAV binding to FH via the HA protein is conserved over multiple subtypes. In these experiments, no significant difference was shown between HAs of different subtypes in their binding to FH. Moreover, the comparison between HA-pseudotyped particles with HA and NA containing particles did not appear statistically different, suggesting that HA protein holds the major responsibility for binding to FH. These results were confirmed using different recombinant HAs proteins H3, H1, H9, H7, and H5 (expressed in *Drosophila* S2 cells) in ELISA (Figure 4.8) that revealed a significant binding to purified human FH. The HA proteins from H3N2 showed the highest level of FH binding compared to other HAs proteins tested H1, H5, H7, and H9, whereas HA protein of H1N1 revealed a statistical difference in FH binding compared to H5, but not with H7 and H9. The great variations in HA protein sequences of different subtypes and strains of IAV (Air, 1981) may contribute to these differences in the amount of FH binding. This is consistent with what was shown that the amino acid variation within the surface membrane P5 of non-typeable *Haemophilus influenzae* (NTHi) influences the amount of FH binding between different strains (Langereis *et al*., 2014). Seib *et al* (2011) have shown that FH binding protein (FHbp) for 12 strains of *Neisseria meningitidis* revealed different levels in their expression for the surface protein FHbp and each strain bound different amounts of FH. However, the differences in FH binding not only related to the level of FHbp expression but also to differences in sequence between variant strains that influence the stability of FHbp-FH complex. The kinetics analysis of binding affinity, association, and dissociation of FHbp from different strains of *N. meningitidis* revealed that some strains include amino acid residues with low affinity for FH, leading to higher dissociation rates, while other strains contain residues with higher affinity for FH, increasing the stability of binding. This may explain why the ability of HA protein to bind to FH is different between various strains of IAV.

Recombinant HA protein from human IAV H3N2 showed the highest FH binding, while the HA protein from human IAV H1N1 bound FH to a lesser extent compared to HA (H5, H7, H9) of avian IAVs and this may be due to the host specificity determinants. Binding of FH to various bacterial pathogens has been shown to be a host-specific interaction. These bacteria are

Neisseria gonorrhoea, N. meningitides and NTHi that bind human FH but no FH from primates, rodents, or lagomorphs such as chimpanzee, baboon, rhesus, rat, and rabbit (Ngampasutadol *et al*., 2008; Granoff *et al*., 2009, Langereis *et al*., 2014). In an immunoprecipitation experiment using recombinant H3, 20% of human plasma and purified human FH as a positive control confirmed that HA binds to FH in human serum and to purified FH.

This study has demonstrated that NA protein also shows the ability to bind FH by far-western blot analysis using recombinant NA protein from H1N1pdm09. Binding of NA protein to FH was not observed in the far western blot performed with the whole virion to identify viral proteins which contribute to FH binding, while binding of FH to viral protein HA showed a strong band. HA is a major envelope glycoprotein forms approximately 80% with 300 – 400 molecules per virion, while NA occupies 10 – 20% of the total envelope glycoproteins with roughly 40 – 50 spikes (Sami, 2009; McAuley *et al*., 2019). The low number of NA may explain why NA protein band was not visible within the viral proteins on the membrane overlayed with FH.

Far western blot using the whole virion revealed a faint 25 – 28 kDa band that may be due to subunit HA2 of HA or M1 protein. The M1 is the most abundant protein component of the virion particles with about 3000 molecules per virion and composes a rigid matrix layer under the viral membrane derived from host cells (Sato *et al*., 2003; Heldt *et al*., 2012). Thus, if FH is bound to M1 protein, it might be hypothesised a strong band should be observed at approximately 28 kDa. To identify whether M1 protein was involved in direct interaction between IAV and FH, far western blot with recombinant M1 protein was used. The results established that no interaction was observed between M1 protein and FH because there was no visible band at 25 kDa in the membrane overlayed with FH compared to the positive control membrane that showed the M1 protein band at the expected molecular weight of 25 kDa. These results suggest that the faint band observed at the molecular weight of 25 kDa in far western blot analysis for the interaction between IAVs and FH due to the HA2 subunit and not due to M1 viral protein.

In this study, the binding of IAV HA and NA proteins to FH was not surprising given these are the surface glycoproteins of the virus and interaction between FH and pathogen surface proteins is common among pathogens. The important function of FH in the regulation of AP

activation and its high concentration in the plasma makes it a target for surface binding by microbial pathogens that mimic normal host cells to evade the elimination by the complement system (Zhang *et al*., 2017).

FH is composed of 20 CCP domains, and it was shown that diverse pathogens recruit FH to their surfaces by binding to different regions of the FH molecule (Hovingh *et al*., 2016). To identify which region of FH was involved in the IAV-FH interaction, seven recombinant proteins spanning the FH molecule were used to analyse the binding to various human and avian IAV subtypes H1N1pdm09, H3N2/99, H5N3, and H9N2 in ELISA. Significant and reproducible binding of IAVs tested was observed with CCPs 1 – 7, 15 – 18, 19 – 20, and 8 – 20 of FH. No interaction was observed between IAVs tested and CCPs 1 – 4. Thus, these results suggest that CCPs 5 – 7 and 15 – 20 are involved in FH binding to IAV. A stronger signal was observed for all four IAV strains with the 8 – 20 CCP fragment. The possible reason for the strong signal could be that the dual binding site may form a particular residue distribution, making the interaction platform more accessible to accommodate the largest number of viral particles.

The results of this study are consistent with previous research findings that several pathogens bind to FH by two common binding sites. One of the binding sites is conserved in the FH and FHL-1 and is located in the N-terminal CCPs 6 – 7, whereas the second site is existing in the C-terminal CCP 19 – 20 (Meri *et al*., 2013). These binding sites leave the functional site of FH CCPs 1 – 4 available to negatively regulate the AP complement pathway. This regulator site is responsible for the regulatory activity of FH, the cofactor activity for protease factor I, which cleaves the central complement opsonin C3b to the inactive iC3b (Kühn *et al*., 1995; Tsiftsoglou *et al*., 2006). In addition, this active site presents decay acceleration activity, since it regulates AP activation by interfering with factor B in binding to C3b, resulting in accelerating the decay of AP convertase C3bBb (Weiler *et al*., 1976; Whaley & Ruddy, 1976). The lack of binding of IAV to the functional site for cofactor activity CCPs 1 – 4 suggests that FH may still retain the ability to negatively regulate the AP. Thus, the functionality of FH through its binding to IAV needs to be tested in future research. Further studies are needed to verify whether FH can maintain its function when pathogens recruit CCPs 5 – 7 of FH and FHL 1 because these domains are also involved in FHL1 protein, thereby allowing pathogens to inactivate both complements regulators (Meri *et al*., 2013). Many microbial proteins or whole microbes like *Haemophilus influenzae, Bordetella pertussis, Pseudomonas aeruginosa*,

Candida albicans (Meri *et al*., 2013), the outer surface protein E (Hellwage *et al*., 2001) and CspA (Kraiczy *et al*., 2004) of *Borrelia burgdorferi* (Meri *et al*., 2013), Sbi protein from *Staphylococcus aureus* (Haupt et al., 2008) and the surface protein C of *Streptococcus pneumonia* (Janulczyk *et al*., 2000; Melin *et al*., 2010; Meri *et al*., 2013; Herber *et al*., 2015) use CCPs 19 – 20 to the so-called "common microbial binding site" (Meri *et al*., 2013), which discriminates between host and non-host surfaces (Pangburn, 2002; Jokiranta *et al*, 2005). Binding of pathogens to this site overlaps but are not identical with heparin and cellular binding sites to allow glycosaminoglycans to bind to FH molecule (Meri *et al*., 2013).

It seems that a lot of pathogens bind to both FH binding sites; CCPs 6 – 7 and CCPs 19 – 20. This ability for dual binding provides efficient protection for pathogens against the AP attack. (Kenedy *et al*., 2009; Hallström *et al*., 2013; Bhattacharjee *et al*., 2013; Caesar *et al*., 2013; Brangulis *et al*., 2015). This study showed that IAVs tested have this ability. Thus, further studies are required to investigate the effect that this interaction may have on the capability of IAV to evade the complement system activation.

Despite the FH-binding proteins on pathogens being structurally different, they share one or two related binding sites on FH that are localised on CCP19 – 20 and 5 – 7. The survival of pathogens within the host is associated with the capability of these pathogens to bind FH enabling evasion of complement attack. Therefore, a detailed molecular understanding of the interactions between pathogen and FH offers opportunities to develop complement vaccines (Parente *et al*., 2017). Directing of antibodies against FH-ligands on the pathogen surfaces could block the interaction between pathogen proteins and FH. If this interaction is inhibited, complement activation would be increased on the microbial surfaces resulting in their phagocytosis or lysis by the membrane attack complex, thereby inhibiting AP evasion (Meri *et al*., 2008; Hovingh *et al*., 2016; Parente *et al*., 2017).

To characterise the molecular determinants of the IAV HA protein involved in the binding with human FH, an ELISA was designed using a panel of biotinylated HA peptides from H1N1pdm09 and H3N2/99 subtypes with a full-length, purified FH protein. The results defined that FH binding overlaps with 130-loop and the residues surrounding it, as well as with the region between 190-helix and 220-loop in RBS pocket. It is known that the surface glycoprotein HA of IAV plays a vital role during the attachment and virus entry into the respiratory epithelial cells (Webster *et al*., 1992). Attachment of IAV with the host cell occurs

through binding of HA protein to terminal sialic acid on the surface of the target cells (Rogers *et al*., 1983; Matrosovich *et al*., 1997; Matrosovich *et al*., 2009). RBS is a shallow pocket existing at the top of the globular head domain of HA and bordered by four structural elements the 130-loop (residues 134–138), 150-loop (188–195), 190-helix, and 220-loop (221–228). The heart of the RBS pocket consists of highly conserved amino acids in different subtypes of IAV which include Tyr98, Trp153, His183, and Tyr195 (Weis *et al*., 1988; Eisen *et al*., 1997; Skehel and Wiley, 2000; Ha *et al*., 2001). Therefore, blocking the interaction of HA with its receptor could prevent the attachment of IAV to the host cell surface.

The results also showed that FH binds to residues 34 – 63, 111 – 120, and 199 – 219 in the N-terminal region of HA1 subdomain. Moreover, FH interacted with residues 287 – 306 in the C-terminal of HA1. No interaction was observed between FH and the fusion peptide in HA2 subdomain. The globular domain HA1 is connected to the virion membrane by the stalk domain (HA1 and HA2). The stalk region contains a fusion pocket which made up by the interface between loop B in HA2 and the sub-domains R, E′ and F′ of the HA1 with the contribution of residues 85 – 90, 104 – 115 and 265 – 270 of HA1 and 64 – 72 of HA2. The fusion pocket plays a crucial role in fusion activity by mediating viral and cell membranes fusion process (Ha *et al*., 2002; Rachakonda et al., 2007; Mair *et al*., 2014). Thus, targeting the fusion peptide or its pocket could prevent the conformational change result from the low pH in the endosome, subsequently inhibiting the fusion process and release of ribonucleoprotein molecules from the endosomal membrane (Mair *et al*., 2014).

These results of this study suggest that FH may hinder virus attachment to a cellular receptor, sialic acid to a certain extent. However, it is unlikely to cause a complete blocking of the binding site because FH does not interact with all residues in RBS pocket that binds to sialic acid. In addition, the stability of the HA-FH complex should be considered. If the affinity binding level between HA protein and human FH is low, this may suffice for dissociation of the bound FH molecule from HA. Thus, additional experiments are needed to verify the strength of the affinity binding of full-length FH and FH fragments that showed a binding ability to HA protein. The potential effect of the HA-FH interaction on viral replication will be tested to investigate whether FH can block RBS of HA protein, thereby preventing virus attachment to the target cells by binding to sialic acid receptors and subsequently stopping viral replication.

In this study, characterisation of the molecular determinants of the FH-H1 HA interaction showed that FH binds to several residues (79 – 84, 127 – 128, 140 – 145 and 206 – 22) localised in the antigenic epitopes of H1 HA protein. The H1 HA antigenic sites were identified on the residues 79 – 84, 140 – 145, 156 – 160, 162 – 166, 169 – 173, 187 – 198, 206 – 208, 224 – 225 and 238 – 240 in the HA1 (Xu *et al*., 2010; Sriwilaijaroen & Suzu-ki, 2012). The interference of FH with H1 HA antigenic sites may have an influence on the antigenicity of the virus. Binding of FH to several residues of antigenic sites may minimise virus attachment to the antibodies, thereby reducing virus neutralization.

In this study, residues of HA protein from H3N2/99 that are involved in the direct interaction with FH were identified by ELISA. Interestingly, the number of significant peptides from H3N2/99 screen (25 peptides) was greater than H1N1screen (15 peptides). These results suggest that the number of FH molecules that bind to the HA protein from H3N2 is greater than that which bind to the HA1 HA. The amount of FH binding may correlate with binding stability which is a critical factor to increase assay sensitivity (Seib *et al*., 2011). Sequence variation between HA protein of IAV subtypes may be responsible for the increase or decrease the binding affinity for FH. Thus, the number of FH binding or strength of binding affinity may explain why a recombinant HA protein from H3N2 the highest FH binding in ELISA had compared with other recombinant proteins tested, H1, H5, H7, and H9. More studies are needed to analyse the amount and stability of FH binding to HA protein of various IAV subtypes. The result of this study identified that FH binds to 130-loop and the residues surrounding it. FH has also shown its interaction with residue Tyr98, the first three residues in 220-loop and the region between 190-helix and 220-loop. Moreover, the results showed that FH bound to residues in HA1 that involved in fusion peptide pocket structure, 85 – 90, 104 – 114 and it also bound to residues of the fusion peptide (1 – 25) in subdomain HA2. These findings suggest that FH binds with a broad range of amino acid residues in RBC and the fusion peptide. Thus, FH may block the binding site of the receptor sialic acid and virus entry into the host cells, inhibiting the virus infectivity.

In this study, HA proteins in purified IAV preparation of H5N3, H9N2, H1N1 pdm09, H3N2/99 subtypes were deglycosylated to investigate the impact of removing glycans on the binding of HA protein to FH. The ELISA test showed that when the carbohydrates were abolished from HA protein, the ability of IAV to bind to FH was increased. This may be due

to FH interfering with the glycosylation sites on HA protein. Removal of glycans from the surface of the HA protein where FH binds rendered them susceptible to FH binding.

Purified FH was N-deglycosylated by PNGase F or denatured without incubation with PNGase F and tested in ELISA to evaluate its capacity for binding to H5N3 and H9N2 IAVs after removal of glycans. The results showed that the binding of IAVs to deglycosylated and denatured FH significantly decreased compared to the control PNGase-untreated FH, but no significant difference was observed between deglycosylated and denatured FH in their binding to both viruses tested. These results indicate that the low association between IAV and FH is due to denaturation and not due to glycans removal. Denaturation due to the use of reducing agents and heating distorted the conformation and folding of the FH polypeptide chain to obtain a unique shape of three-dimensional structure. The disruption of FH structure can affect its biological, chemical, physical, and functional properties (Eckersall *et al*., 2008). This may explain the decreased sensitivity of FH to IAV. To avoid interference between the deglycosylation and denaturation in the experimental approach used, a native glycoprotein can also be subjected to PNGase F protocol with non-denaturing reaction conditions. The denatured reaction can then be compared to the non-denaturing reaction to determine the completeness of the reaction.

Various approaches are available to understand the functional roles of glycosylation sites in protein-protein interactions without the need for enzymatic or chemical deglycosylation. These approaches include preventing initial glycosylation, preventing elongation of the glycan chain, altering glycan processing, genetic elimination of glycosylation sites, the addition of abnormal monosaccharides, and mutation studies (Varki & Gagneux, 2017). In conclusion, these results suggest that glycosylation sites on HA protein may affect the interaction between IAV and FH. Understanding the functional roles of glycosylation sites can be exploited to predict specific glycosylation sites in protein design with beneficial properties.

The present study establishes that different subtypes and strains of IAV bind to human FH domains 5 – 7 and 15 – 20 by viral proteins HA and NA. This interaction may have an impact on viral replication since our results demonstrate that FH could compete with cellular receptor sialic acid in the binding to the RBS or fusion peptides on HA viral protein, thereby inhibiting attachment and viral entry into the host cells. This is investigated further in Chapter 5.

4.4 Conclusion

1. Different strains of human and avian IAVs have shown their ability to bind to human FH.

2. The HA and NA viral proteins have been identified as FH ligands.

3. The binding of IAV to FH occurs in two regions of the FH protein: CCP 5 – 7 and 15 – 20.

4. De-glycosylation of the IAV resulted in an increase the ability of HA protein to bind to FH.

5. Characterisation of the molecular binding sites on the surface of the H1 and H3 HA protein that are involved in the interaction with FH revealed that FH binds to 130-loop and the surrounding area, as well as with residues between 190-helix and 220-loop in RBS pocket. Moreover, it interacts with several residues involved in fusion peptide pocket in HA1 or HA2 in both H1 and H3 HA protein.

Chapter 5- Does FH modulate IAV replication.

in target cells?

5.1 Introduction

In Chapter 4, characterisation of the molecular determinants of the interaction between IAV and human FH showed that FH bound to some amino acid residues in the receptor binding site (RBS) or fusion peptide of the viral HA protein. These results suggest that human FH may modulate viral replication in cells through altering entry mechanisms either by viral attachment to sialic acid or the process of membrane fusion between the virus and endosome. In this chapter, the impact of human FH on human and avian IAV replication was investigated and the potential mechanisms by which FH affects IAV replication at the entry stage into the target cells characterised.

It is well-known that HA mediates attachment of IAV to the cellular sialic acid via the RBS, facilitating virus entry into the target cells, making viral attachment a target to blocking virus infection at the earliest step (Edinger *et al*., 2014). To investigate whether FH can hinder the interaction between HA protein and sialic acid on the surface of target cells, an Haemagglutination inhibition (HI) assay using human and avian IAVs preincubated with human FH was designed.

FH showed the ability to mediate pathogen-host cell interactions in which FH work as a linking molecule by binding to pathogen and complement receptor 3 (CR3; CD11b/CD18) on host cells. This non-canonical role of FH may facilitate either pathogen entry into epithelial cells or uptake of the pathogen by immune cells and modulate their function (Hammerschmidt *et al*., 2007; Svoboda *et al*., 2015; Schneider *et al*., 2016). Such interactions were characterised between FH and *Streptococcus pneumoniae*, *Neisseria gonorrhoeae*, and *Candida albicans* (Hammerschmidt *et al*., 2007; Losse *et al*., 2010). It was shown that FH bound on *C. albicans* facilitates the adhesion, phagocytosis, and antifungal responses by neutrophils, increasing of lactoferrin and reactive oxygen species production (Losse *et al*., 2010). FH is also able to enhance the antifungal activity of human macrophages, promoting the production of proinflammatory cytokines in macrophages, thereby increasing their uptake of the *C. albicans* (Svoboda *et al*.,2015).

In other cases, binding of FH to pathogens is beneficial for their survival. Well-known examples include the *Borrelia burgdorferi* (Hellwage *et al.*, 2001), malaria parasites *P. falciparum* (Rosa *et al*., 2016), a protozoan parasite *Trypanosoma brucei* (Macleodand *et al*.,

2020) and West Nile virus (Chung *et al*., 2006; Suthar *et al*., 2013). In the present study, to assess the impact of HA-FH interaction on IAV replication, an infectious assay was designed using increasing concentrations of FH to examine whether FH affects negatively or positively on the IAV replication in human target cells, the alveolar epithelial cell line A549 and the monocytic cell line THP-1. The selection of these cells is because respiratory epithelial cells are the initial target for IAV infection that release many viral particles to infect monocytes and alveolar macrophages (La Gruta *et al*., 2007).

To characterise the exact stage(s) of IAV replication cycle influenced by FH, immunohistochemistry and immunofluorescent assays were performed during a time-course of infection to identify the effect of FH particularly during the early stages of IAV replication cycle.

5.1.1 Chapter objectives

The main research objectives of the current chapter were:

1. Investigate the potential effect of FH on viral replication of different strains of human and avian IAVs that have potential zoonotic transmission from natural reservoirs.

2. Assess the role of FH at the entry stage of human IAVs replication in A549 and THP-1 cells.

3. Track the attachment, entry, and replication of IAV in A549 cells at different time points using fluorescent microscopy to understand if the interaction with FH altered these.

5.2 Results

5.2.1 Evaluation of the impact of HA-FH binding on the ability of IAV to bind to sialic acid measured by HI assay

To assess the effect of FH-HA interaction on the functionality of binding to sialic acid of viral HA protein, haemagglutination inhibition (HI) assay was performed. The hypothesis for this experiment is that FH binding to HA protein of IAV can prevent attachment of the virus to sialic acid on the surface of the red blood cells (RBCs), thereby inhibiting RBC agglutination by IAV. In this assay, the surface viral protein HA binds to sialic acid on the surface of the RBCs resulting in the formation of a lattice structure, in which the agglutinated RBCs are retained in a reddish suspension in the wells. Wells that lack haemagglutination show a red dot of RBCs settling at the bottom. Human IAVs have a preference for the cellular receptor, sialic acid, on the surface of red blood cells that is linked to galactose (Gal) residues through α2,6-Gal linkage, while avian IAVs have α2,3-Gal preference (Suzuki *et al*., 2000; Tan *et al*., 2018). In this study, Turkey RBCs (TRBC) were used due to the presence of a mixture of α2,3-Gal and α2,6-Gal linkages on their surfaces and thus both human and avian IAVs can hemagglutinate them (Pawar *et al*., 2012; Trombetta *et al*., 2018).

Four strains of human (H1N1pdm09, H1N1/15, H3N2/99, H3N2/14) and two strains avian (H5N3 and H9N2) IAVs, were titrated by haemagglutination (HA) assay and then all diluted to a standard 8 haemagglutinin units (HAU). As negative controls, PBS lacking virus (PBS) and FH with no virus (FH) were used. While as a positive control, the virus was used without FH (0). In HA assay, a 2-fold serial dilution of each virus was dispensed into individual wells of 96-well V-bottom microtitre plates. TRBCs (1%) were added to all wells. The plate was incubated at RT for 30 min or at 4°C for 1 h. Incubation the plate in cold conditions prevents the dropping out of suspension of the RBCs in the first wells of HA titration that can occur with IAVs with strong NA activity which cleaves the cellular receptor sialic acid of RBC (Mögling *et al*., 2017). In the panel of viral strain used here this was especially evident in the H5N3 and the vaccine strain H1N1 (Figure 5.1, A). HAU titre (8 HAU/50 µl or 4 HAU/25 µl) is the virus dilution of the last well (highest dilution of the virus) showing complete haemagglutination (Figure 5. 1, A). To verify the HAU calculation, a virus back titration of the working dilution (8 HAU/50 µl) was performed by a second HA test in which a 2-fold serial

dilution of the working solution of the virus was prepared. As shown in Figure 5. 1, B, this titre caused haemagglutination in the first four wells of the back-titration plate. In the HI assay, serial dilutions of purified human FH (40, 20, 10, 5, 2.5, 1.25, 0 µg/well) were incubated with the working dilution (8 HAU/50 µl) of the virus for 1 h at RT (Figure 5. 1, C) or 4°C (Figure 5. 1, D). After the incubation period, TRBCs were added. In the HI assay performed at RT, FH inhibited the haemagglutination of TRBCs by IAVs tested at all dilutions used except the lowest concentration of FH (1.25 µg/well). Haemagglutination of all IAVs was efficient in the positive control (the virus only without FH). It is possible that FH bound to IAV particles and prevented attachment of IAV virions to TRBCs, allowing them to precipitate to the bottom of the well (Figure 5. 1, C). Surprisingly, the inhibition of haemagglutination by FH was not observed in the HI assay performed at 4°C, where the red dots did not form except in PBS alone without virus (Figure 5. 1, D), suggesting that FH may cause agglutination of RBC at the cold condition. Taken together these results demonstrate that FH inhibits TRBC haemagglutination by IAV, suggesting that FH may hinder binding of HA protein of IAV to sialic acid on the target cell. Thus, this binding may modulate virus infectivity.

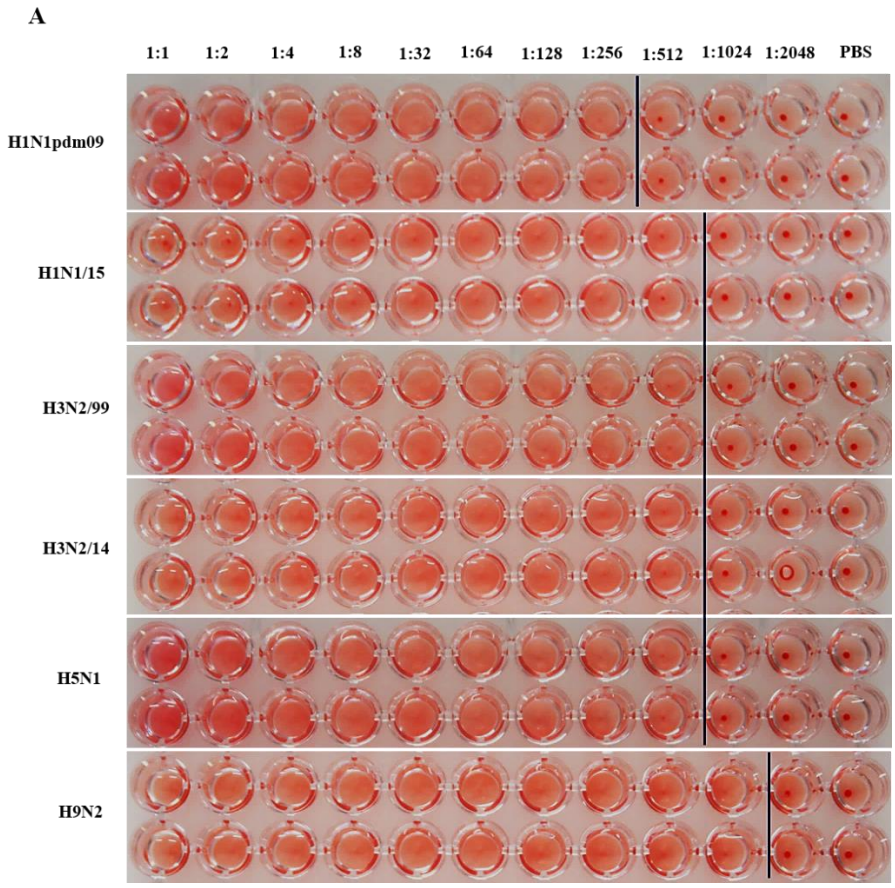

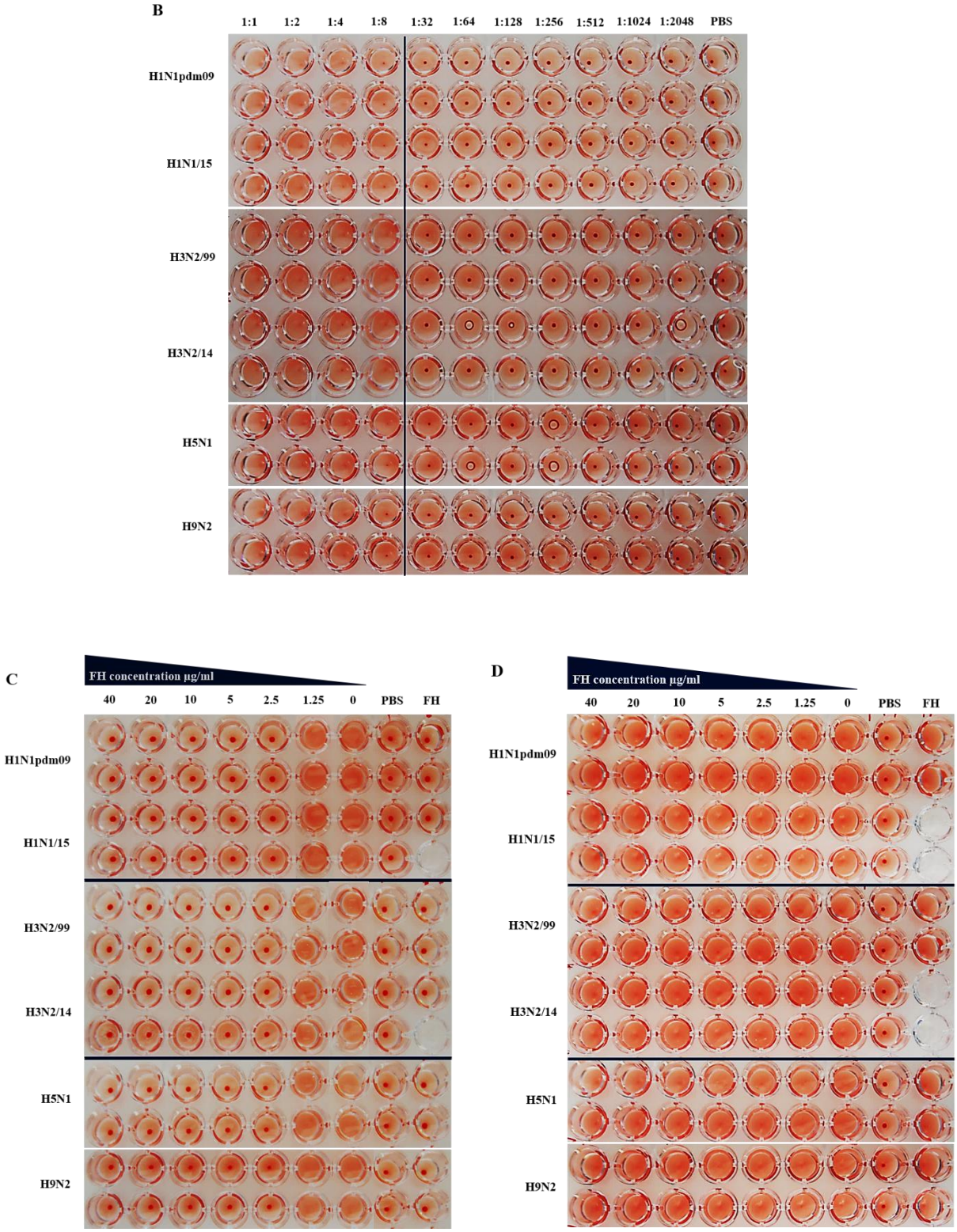

Figure 5. 1: Haemagglutination inhibition (HI) assay to evaluate the effect of FH on biological activity of HA protein of IAV. (A) Haemagglutination assay for HAU titration for various subtypes and strains of IAVs H1N1pdm09, H1N1/15, H3N2/99, H3N2/14, H5N3 and H9N2. **(B)** Back titration to verify if working dilution is equal to 4 HAU/25 µl. **(C)** to investigate whether FH can inhibit haemagglutination of TRBCs by IAV. Various concentrations of FH 40, 20, 10, 5, and 2.5, 1.25 µg/well were incubated with IAVs tested at RT or **(D)** at 4°C. PBS or FH without virus (FH) were used as negative controls. Virus without FH (0) was used as a positive control. Data represent one of three independent experiments.

5.2.2 Evaluation of the effect of FH on IAV replication

To examine the impact of FH binding on IAV infectivity, an experiment was designed that consisted of two steps: 1/ infection of target cells for 24 hours at a pre-defined MOI in the presence or absence of FH; 2/ measure the cytopathic effect (CPE) on MDCK cells to assess virus titres using serially diluted cell supernatant from step 1. Target cells used in this assay were the human alveolar epithelial cell line A549 and the human monocytic cell line THP-1.

5.2.2.1 Determination of the optimal MOI for infection

To look for the effect of human FH on the infection efficiency of various human (H1N1pdm09, H3N2/99) and avian (H5N3 and H9N2) IAV subtypes in the human cells A549 and THP-1, the optimal MOI of each virus that show CPE in 50% of infected cells was evaluated (Figure 5. 2, A – H). This optimal MOI allows for a difference (more or less CPE) when FH is added. The modified end point dilution assay (Chaurasiya & Hitt, 2016) was designed to estimate the optimal MOI for each virus tested. A549 or THP-1 cells were incubated without (C) or with the virus at MOI of 1, 0.1, 0.01, and 0.001 for 24 hours. The supernatant of infected cells was then serially diluted and incubated with MDCK cells to evaluate the CPE of each virus. The result has shown that to observe CPE in about half of the wells the following MOI can be used to infect A549 and THP-1 cells: MOI of 0.1 for H1N1pdm09 (Figure 5. 1, A – B), and 0.01 for H3N2/99 (Figure 5. 2, C – D). The optimal MOI for avian (H5N3 and H9N2) IAVs was 0.1 (Figure 5.2, E – H). These results demonstrate that different IAV strains exhibit different MOI values.

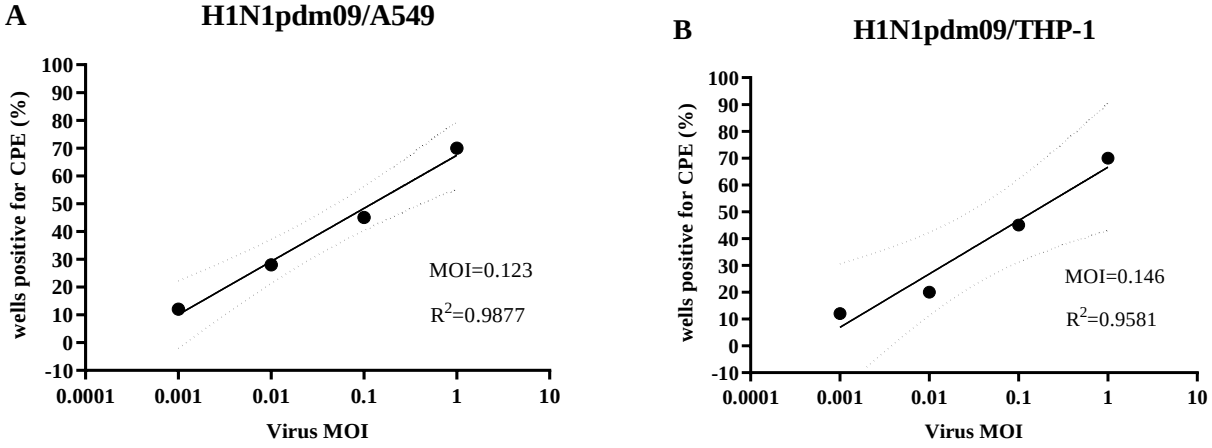

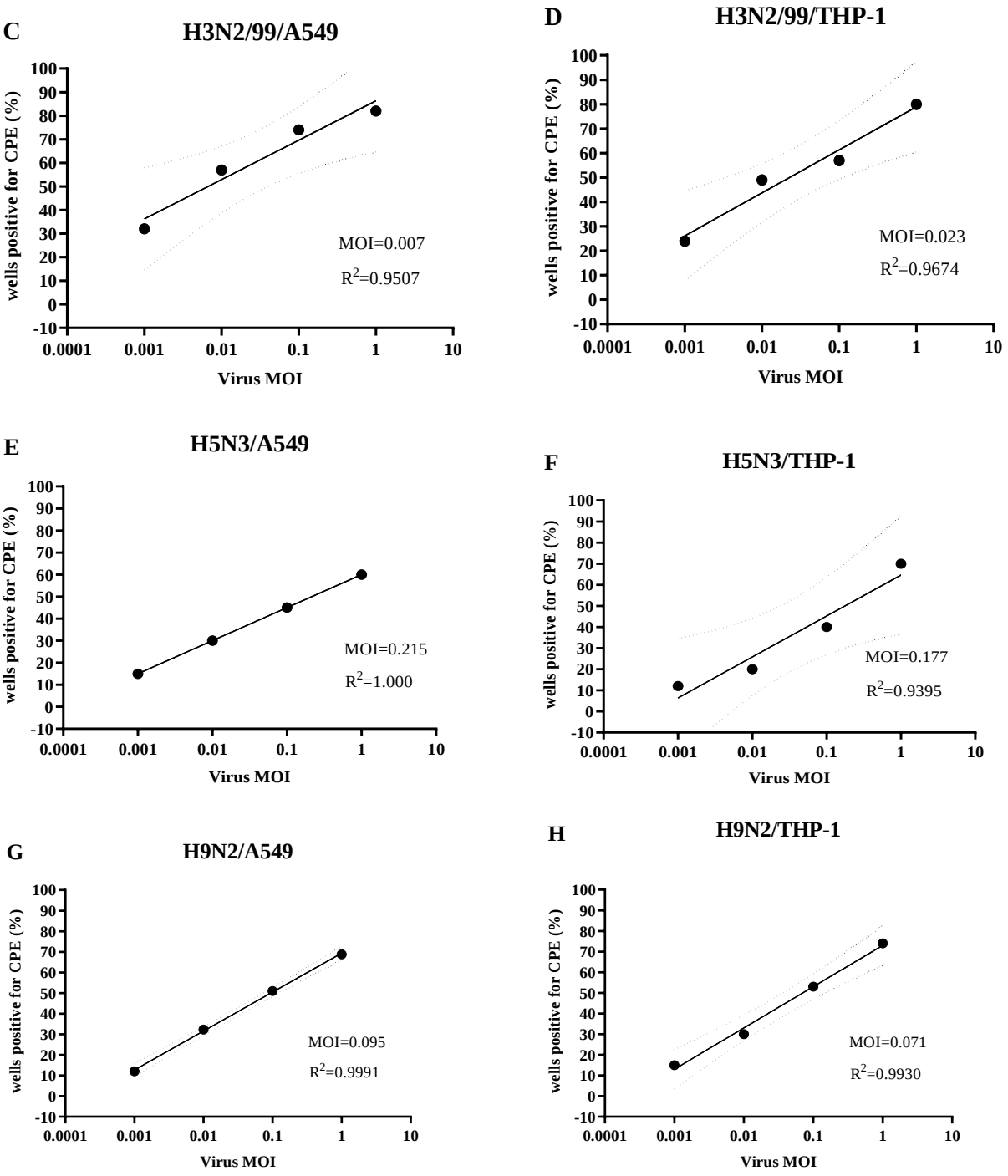

Figure 5. 2: Estimation of optimal MOI for different IAV subtypes. H1N1pdm09 infected **(A)** A549 and **(B)** THP-1 cells, H3N2/99 infected **(C)** A549 and **(D)** THP-1 cells, H5N3 infected **(E)** A549 and **(F)** THP-1 cells, and H9N2 infected **(G)** A549 and (H) THP-1 cells. As a negative control, uninfected cells were used. Increasing values of MOI (0.001, 0.01, 0.1, 1) of each virus were inoculated in triplicate onto cell cultures of A549 or THP-1 cells in a 96-well plate. After 24 h post-infection, a ½ tenfold serial dilution of the supernatant was then prepared for each MOI to infect 10 wells seeded with MDCK cells in a 96-well plate. Following 3-5 days incubation period, CPE of each virus was visualised using crystal violet staining. The number of wells that showed positive for CPE was then determined for each MOI. Each graph is non-linear regression produced by GraphPad Prism using a semi logarithmic line (the X-axis is logarithm, but the Y-axis is linear). The mean CPE percentages for each MOI were plotted against the logarithmic value of the MOI in X-axis. The R2 represents the proportion of the variance for Y explained by X. The MOI that led to the CPE in 50% of wells with infected cells was then estimated to be the optimal MOI for target cell infection.

5.2.2.2 The initial investigation of FH effect on IAV infection

A549 and THP-1 cells were either pre-incubated with FH (5 µg/ml) and infected with H1N1pdm09 or H3N2/99 (FH+Cells), or the IAVs were pre-incubated with FH (5 µg/ml) before infection of A549 and THP-1cells (FH+IAV). As a control (C), cells were infected with IAV in the absence of FH (Figure 5. 3). The results showed that the presence of FH slightly enhances H1N1pdm09 replication in both infected cells, A549 and THP-1 compared to the control. No difference was observed in the FH effect on H1N1pdm09 replication between FH+Cells and FH+IAV (Figure 5. 3, A – B).

In contrast, the result demonstrated that FH exhibited a suppression action against H3N2/99 replication in both target cells compared to the control (Figure 5. 3, C – D). Moreover, FH+IAV revealed antiviral activity in both A549 and THP-1 target cells (20-fold decrease in viral replication in A549 cells (Figure 5. 3, C) and a 10-fold decrease in THP-1 cells (Figure 5. 3, D). No difference was observed between FH+Cells and FH + IAV in its effects on H3N2/99 replication in A549 cells (Figure 5. 3, C). However, FH+IAV revealed an inhibitory effect on H3N2/99 replication in THP-1 cells (10-fold decrease greater than FH+Cells 5-fold reduction).

In conclusion, these results show that human FH (5 µg/ml) enhances H1N1 pdm09 replication to a slight extent in both cells types (A549 and THP-1), whereas it inhibits H3N2/99 replication in both target cells and these effects were evident with FH pre-incubated with the virus. Thus, in future experiments, FH pre-incubated with the virus was used to investigate the impact of FH at increasing doses (50 and 100 µg/ml) on H1N1pdm09 and H3N2/99 replication in A549 and THP-1 cells.

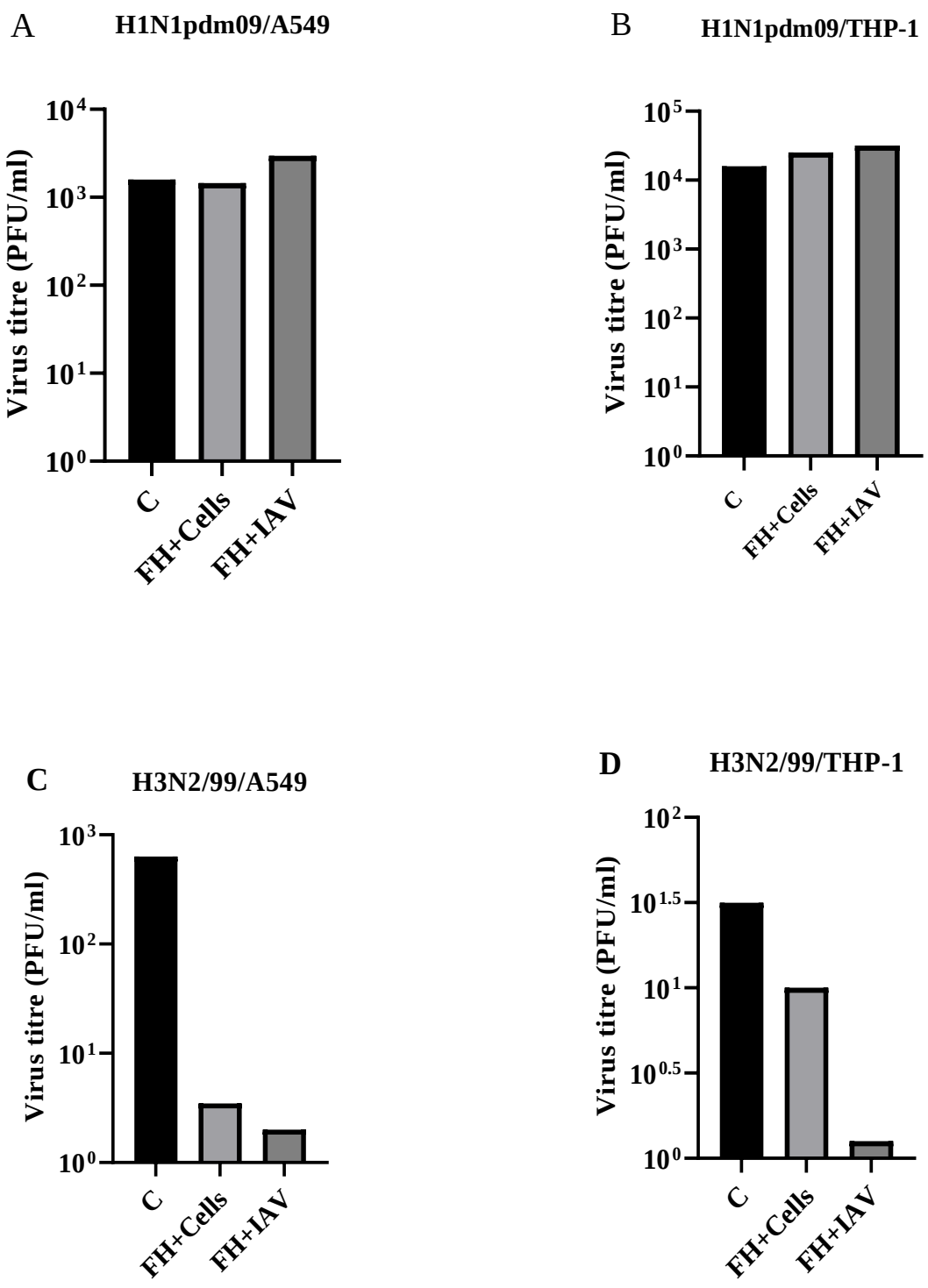

Figure 5. 3: Primary investigation of FH effect on viral replication of H1N1pdm09 (A) in A549, (B) in THP-1 and H3N2/99 (C) in A549 (D) in THP-1 cells. A549 and THP-1 cells pre-incubated without or with FH (5 µg/ml) were seeded in 96-well plates and incubated for 3 h. After the incubation period, the cells pre-incubated with FH were infected with H1N1pdm09 at optimal MOI of 0.1 or with H3N2/99 at MOI of 0.01, whereas the cells without FH were infected with H1N1pdm09 or H3N2/99 pre-incubated with FH and maintained in an infectious medium for 24 h. A ½ tenfold serial dilution was then prepared from the supernatant of the culture medium to infect MDCK cells in a 96-well plate. The cytopathic effect was estimated by the Reed–Muench method compared to the negative control, non-infected A549 and THP-1 cells with the absence of FH.

5.2.2.3 Investigating the role of increasing concentrations of FH in IAV replication

In view of the FH effect on viral replication, the infectious assay was repeated to assess whether the impact of FH is dose dependent. A549 and THP-1 cells were infected with H1N1pdm09 or H3N2/99 pre-incubated without or with FH at different concentrations (5, 50, and 100 µg/ml). Infected A549 and THP-1 cells with the absence of FH were used as a control (C). The viral titre was higher in a dose-response manner when H1N1 was pre-incubated with FH-treated in comparison to absence of FH (C). The titre of H1N1 virus significantly increased in the presence of 100 µg of FH from $10^{5.5}$ to 10^{7} for infected A549 cells and from $10^{5.5}$ to $10^{6.5}$ for THP-1 cells. The means of $TCID_{50}$ values of three experiments were summarised and shown in Figure 5. 4, A – B.

In contrast, dose-dependent inhibition of H3N2 replication by FH in both A549 and THP-1 cells compared to the control was demonstrated. The H3N2 viral replication was reduced from $10^{4.5}$ to 10^{3} in A549 cells and from $10^{5.5}$ to 10^{3} for THP-1 cells (Figure 5. 4, C – D). Given the binding of human FH to avian IAV subtypes, the effect of this interaction on H5N3 and H9N2 replication in the human cell lines A549s and THP-1s were also evaluated using MOI of 0.1 for both H5N3 and H9N2 IAVs preincubated with 100 µg/ml FH before infection of A549 and THP-1 cells. The choice of this concentration of FH is because it had given a significant effect on human viral replication and it is lower than the physiological concentration for FH in plasma. The results suggest that FH exhibited a slight suppressing action against H5N3 and H9N2 in both infected cells (A549 and THP-1) compared to the control, infected and untreated cells with FH (C). However, these results were not statistically significant.

Taken together, FH has divergent effects on the replication of the IAV subtypes, enhancing human H1N1pdm09 replication and restricting H3N2/99 replication in A549 and THP-1 cells, while having no impact on the replication of avian H5N3 and H9N2 viruses.

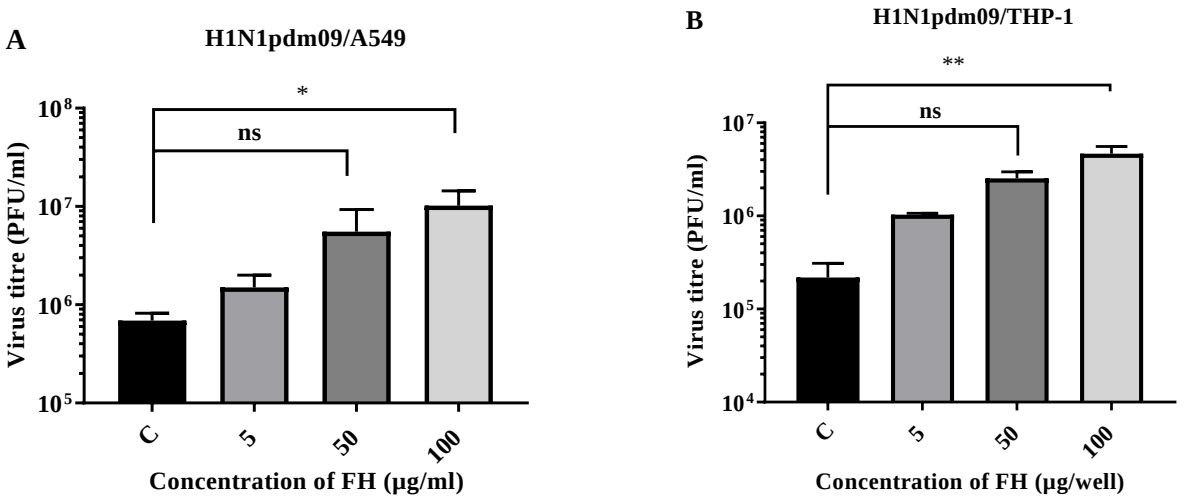
A
H1N1pdm09/A549
Virus titre (PFU/ml)
10^8
10^7
10^6
10^5
*
ns
C
5
50
100
Concentration of FH (µg/ml)
B
H1N1pdm09/THP-1
Virus titre (PFU/ml)
10^7
10^6
10^5
10^4
**
ns
C
5
50
100
Concentration of FH (µg/well)

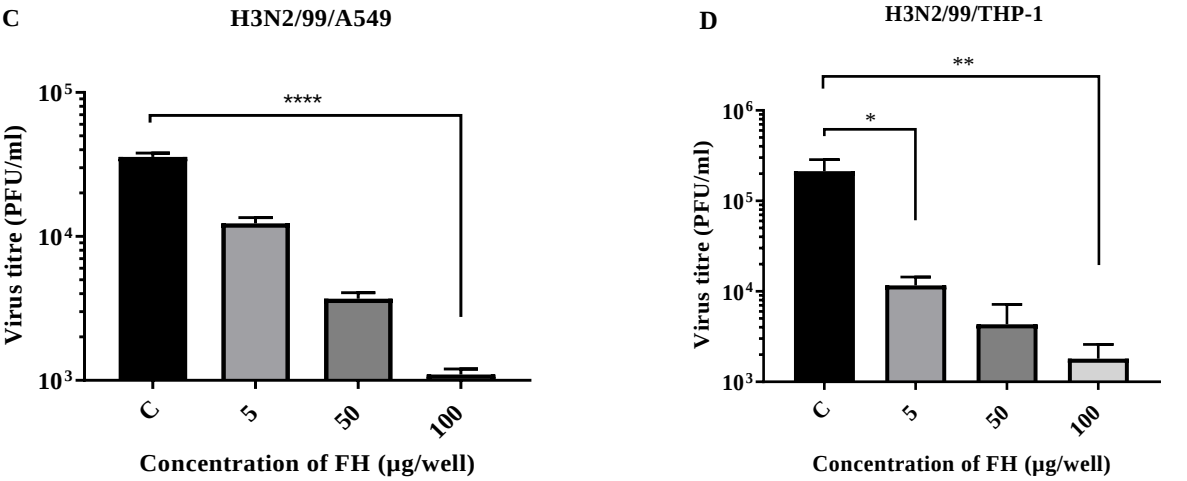
C
H3N2/99/A549
Virus titre (PFU/ml)
10^5
10^4
10^3
****
C
5
50
100
Concentration of FH (µg/well)
D
H3N2/99/THP-1
Virus titre (PFU/ml)
10^6
10^5
10^4
10^3
**
*
C
5
50
100
Concentration of FH (µg/well)

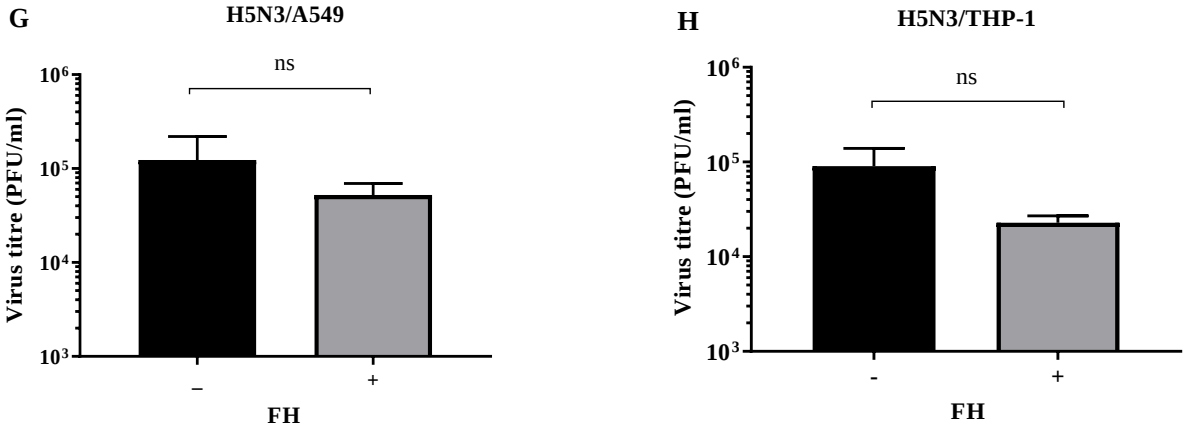
G
H5N3/A549
Virus titre (PFU/ml)
10^6
10^5
10^4
10^3
ns
–
+
FH
H
H5N3/THP-1
Virus titre (PFU/ml)
10^6
10^5
10^4
10^3
ns
-
+
FH

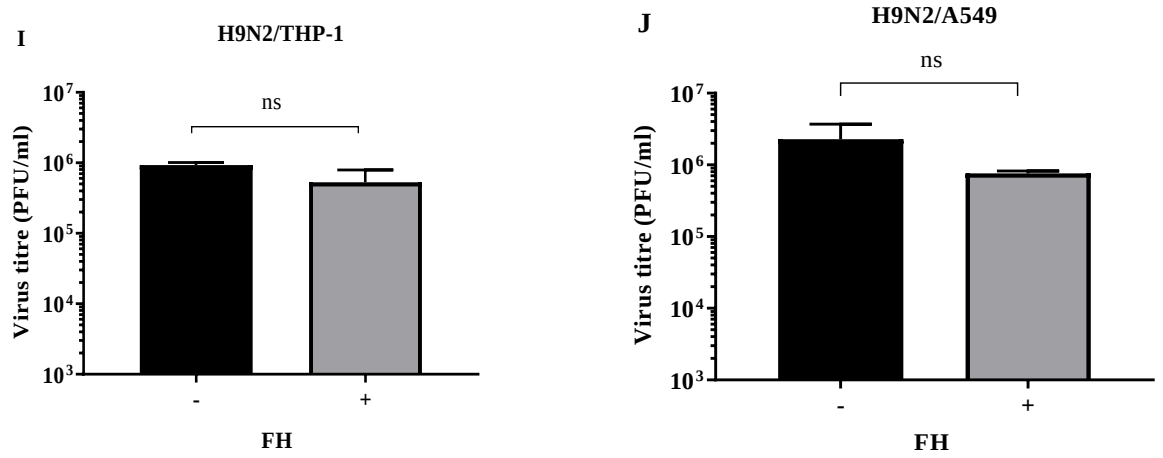

Figure 5. 4: Evaluation of FH effect on human and avian IAVs replication in A549 and THP-1cells. (A) A549 and **(B)** THP-T cells were infected with H1N1pdm09 pre-incubated with FH at different concentrations (5, 50, and 100 µg/ml). H3N2/99 pre-incubated with FH at similar concentrations of FH were used to infect **(C)** A549 cells or **(D)** THP-T. After 24 h incubation, CPE was estimated by infecting MDCK cells with the culture supernatant and $TCID_{50}$ was performed. Uninfected and untreated with FH cells were used as negative control. Antiviral activity of FH against H3N2 in **(E)** A549 and **(F)** THP-1 cells. H5N3 at MOI of 0.1 pre-incubated with FH at 100 µg/ml was used to infect **(G)** A549 and **(H)** THP-1 cells. Effect of FH on viral replication of H9N2 in **(I)** A549 and **(J)** in THP-1 cells. The data for each panel is reprehensive of three independent experiments performed in triplicate. The error bars indicate the ±SEM. Statistical differences were calculated by Dunnett's test for the multiple comparisons (****$p < 0.0001$, **$p < 0.01$, *$p < 0.05$, ns= non-significant).

5.2.3 Investigating the role of FH at the entry stage of IAV infection

The aim of these experiments was to investigate whether FH plays a role at the entry stage of IAV replication in the target cells. Since M1 protein is one of the most abundant proteins in the virus particles, using an antibody directed against M1 allows the detection of the virus even at early time points in the replication cycle. H1N1pdm09 at MOI 1 or H3N2/99 at MOI 0.1 pre-incubated in the presence or absence of 100 µg/ml FH were inoculated on A549 cells. Uninfected and untreated cells with FH were used as a negative control (C) (Figure 5. 5). At 4 h post-infection, western blot analysis to detect the presence of M1 protein in cell lysate showed a weak M1 protein band at the expected size of 28 kDa for FH pre-treated H1N1pdm09 (H1N1 + FH) compared to the strong M1 band from the positive control, untreated H1N1pdm09 (H1N1). These results suggest that FH may slow H1N1pdm09 entry into A549 cells, but the entry of the virus does still occur. On the other hand, no M1 protein band in the FH pre-treated H3N2/99 condition (H3N2 + FH) was observed compared to the strong M1 band of the control, untreated H3N2/99 (H3N2). The absence of M1 band may be due to the prevention of virus binding to sialic acid on the cell surface by FH. (Figure 5. 5, A).

Interestingly, at 8 h post-infection, when you would expect a complete life cycle of an influenza virion to have occurred and thus newly synthesised viral proteins in the cell should be observed, there was comparatively more viral M1 protein present in the FH pre-treated H1N1pdm09 (H1N1+FH) virus lysate compared to the corresponding untreated control. This suggests that following entry of the virus into cells, FH enhances viral replication. In comparison, no visible band was identified as M1 protein in the FH pre-treated H3N2/99 (H3N2 + FH) compared to the untreated control (H3N2), suggesting that the entry block seen at 4 hours post infection (Figure 5. 5) is not relieved over time. In conclusion, these results suggest that FH completely blocks the entry of H3N2 into the target cells whereas it only slows down the entry of H1N1pdm09, however once entry has occurred the presence of FH alters the internal cellular environment which may enhance viral replication. (Figure 5. 5, B).

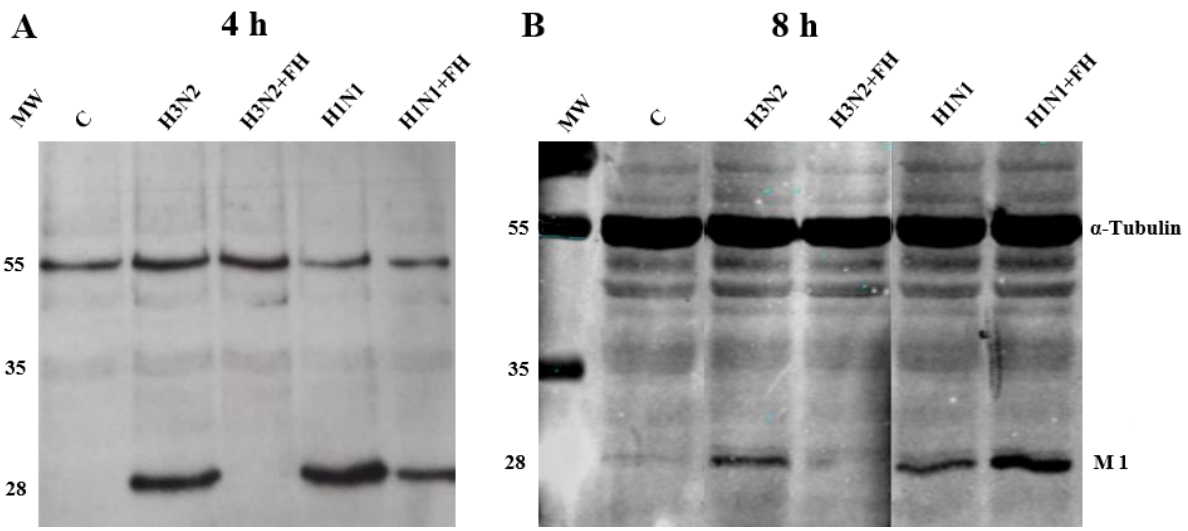

Figure 5. 5: Analysis of the role of FH in the entry stage of IAV infection by western blot. A549 cells were infected with H1N1pdm09 or H3N2/99 at MOI of 1 and 0.1, respectively without or with 100 µg/ml FH in the 6-well plate. After 1 h incubation, the cells were washed three times with cold PBS to remove unattached viruses. The cells then were incubated with the infectious medium for **(A)** 4 h and **(B)** 8 h. Cell lysates were subjected to reducing gel electrophoresis followed by western blotting with anti-M1 antibody, to detect M1 protein level. As a negative control, uninfected and untreated cells with FH were used. Alpha tubulin (α-Tubulin) was used as loading control. The mobility of size markers is indicated to the left of each membrane.

5.2.4 Immunohistochemistry to analyse the role of FH at the entry stage of IAV infection

To confirm the western blot results of FH altering the entry of H3N2/99 and H1N1pdm09 into the target cell, immunohistochemistry for the presence of the virus was performed at different time-points post-infection. A549 cells were inoculated with H1N1pdm09 or H3N2/99 pre-incubated without or with FH. The results showed that FH efficiently inhibited H3N2/99 entry into A549 target cell and this effect was stable and unchanged at any of the different time points post-infection analysed (4, 8, 18, and 24 h) (Figure 5. 6, A). The current results suggest that the inhibitory effect of FH is through direct binding to the HA protein of IAV. Interestingly, the results showed that FH slowed the entry of H1N1pdm09 during the first hours of infection (at 4 h) (Figure 5. 6, B). However, the entry has occurred resulting in promoting viral replication compared to FH-untreated control after at 8 h post-infection. Further investigation is needed to track the attachment, entry, and replication of H1N1pdm09 in target cells at different time points using fluorescent microscopy.

5.2.5 Immunofluorescence assay to analyse the role of FH at the entry stage of IAV infection

These experiments were performed to track the effect of FH on H1N1pmd09 entry and replication in A549 cells at different time points, attachment, 15, 30 min, 1, 2, 6, 8, 24 h (Figure 5. 7, B). The results showed that the virus attached to both FH-treated (+) and untreated cells (-). However, there was more virus presence in FH-untreated cells up 6 h post-infection. After 6 h, the replication of the virus increased in infected cells treated with FH compared to untreated cells. Moreover, in these experiments, the cells treated with antibodies against the virus (green) and FH (red) showed that the virus continued to attach to FH even after it entered the cells (Figure 5. 7, B). These results confirmed the results obtained in western blot and immunohistochemistry assays that FH slowed H1N1 entry into the target cell but enhances viral replication at a late stage of infection.

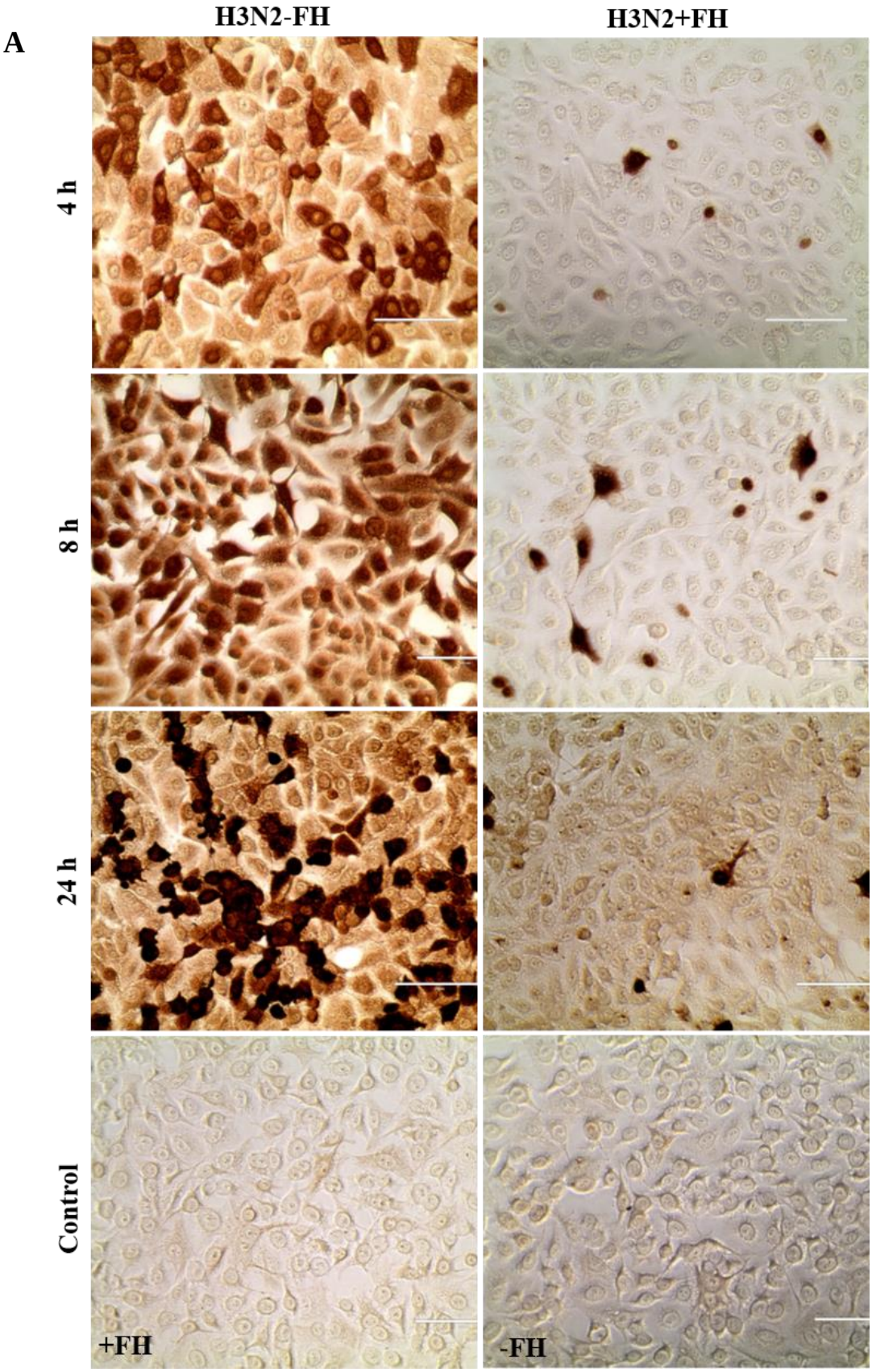
A
H3N2-FH
H3N2+FH
4 h
8 h
24 h
Control
+FH
-FH

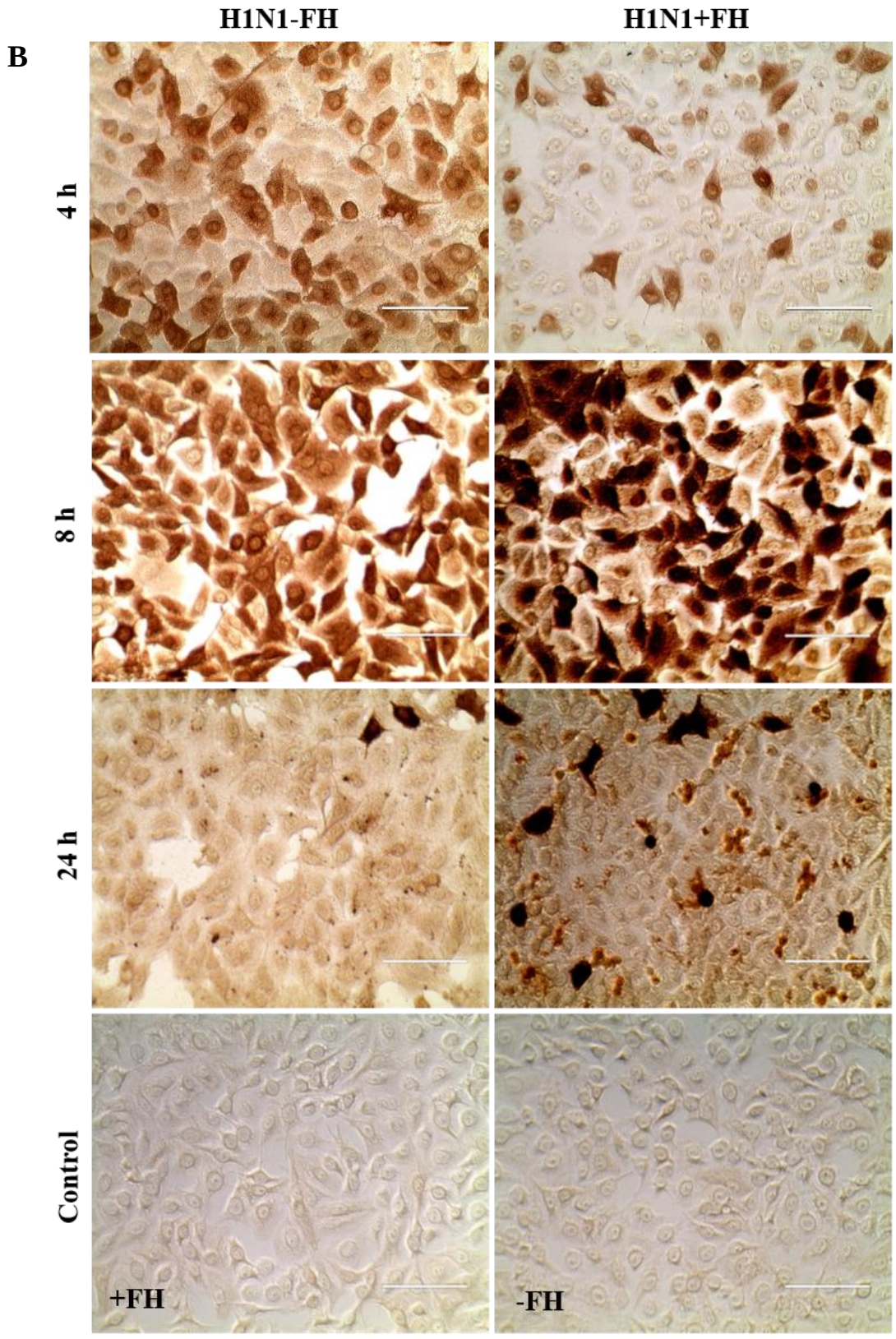

Figure 5. 6: Immunohistochemistry to analysis the role of FH at the entry stage of IAV virus infection. A549 cells were infected with (A) H1N1pdm09 at MOI of 1 or (B) H3N2/99 at MOI of 0.1 pre-incubated 1 h without or with FH at 100 µg/ml. After different time points post-infection (4, 8, and 18 h, and 24 h), the cells were fixed, and the infection was detected with mAb anti-NP. Scale- bar equals 10 µm. Images shown are representative of three independent experiments.

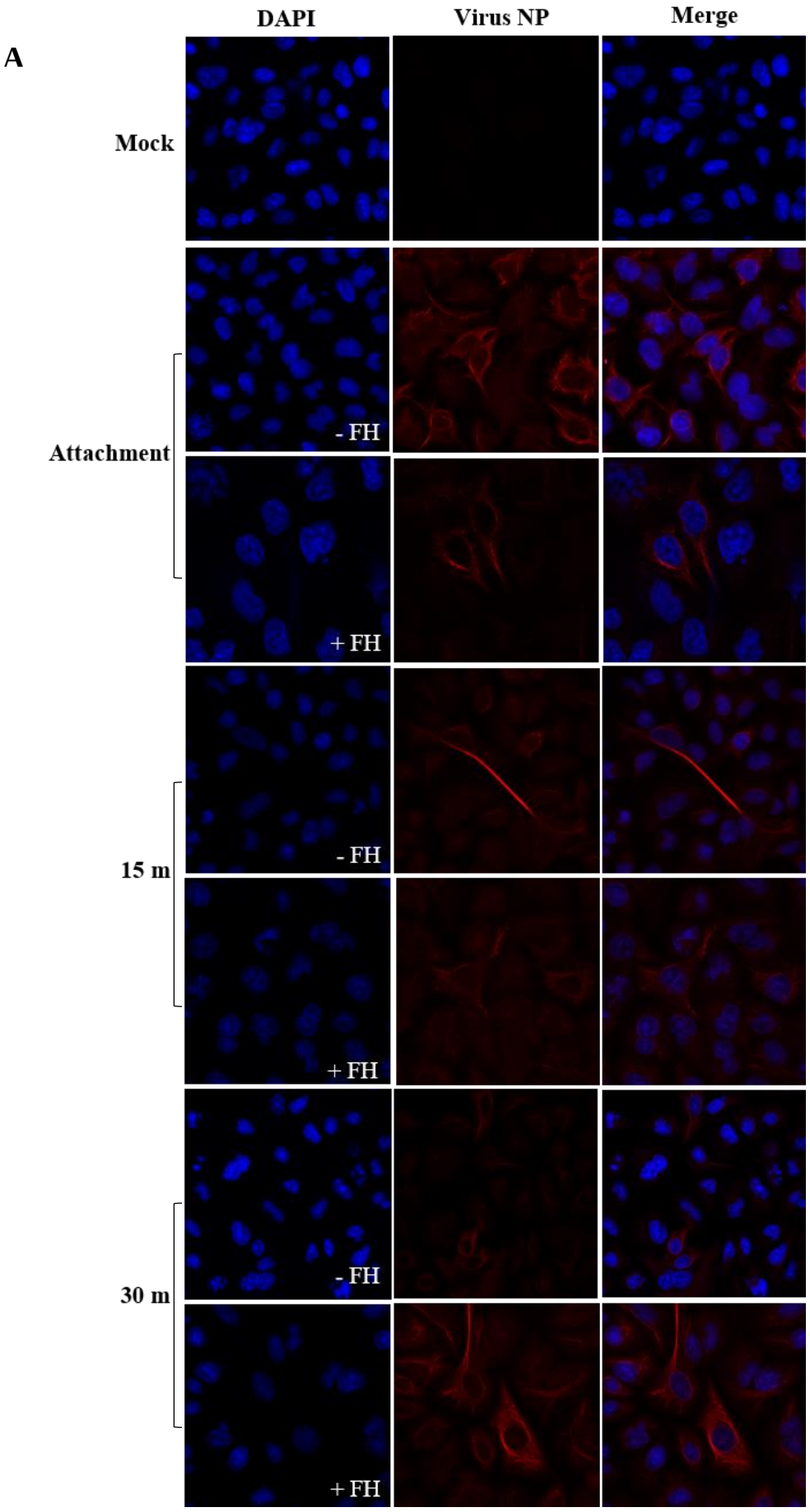
A
DAPI
Virus NP
Merge
Mock
Attachment
- FH
+ FH
15 m
- FH
+ FH
30 m
- FH
+ FH

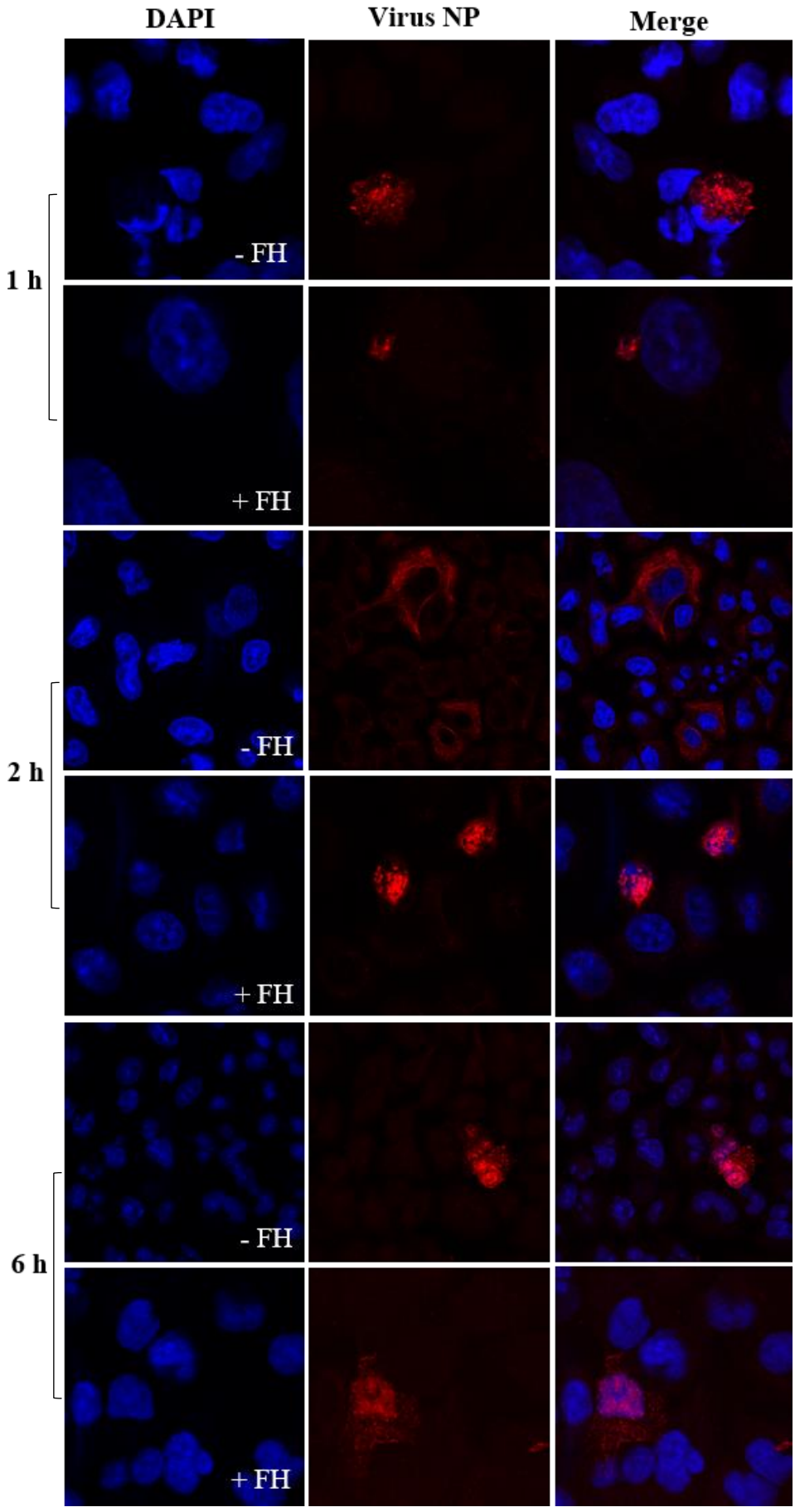
DAPI
Virus NP
Merge
1 h
- FH
+ FH
2 h
- FH
+ FH
6 h
- FH
+ FH

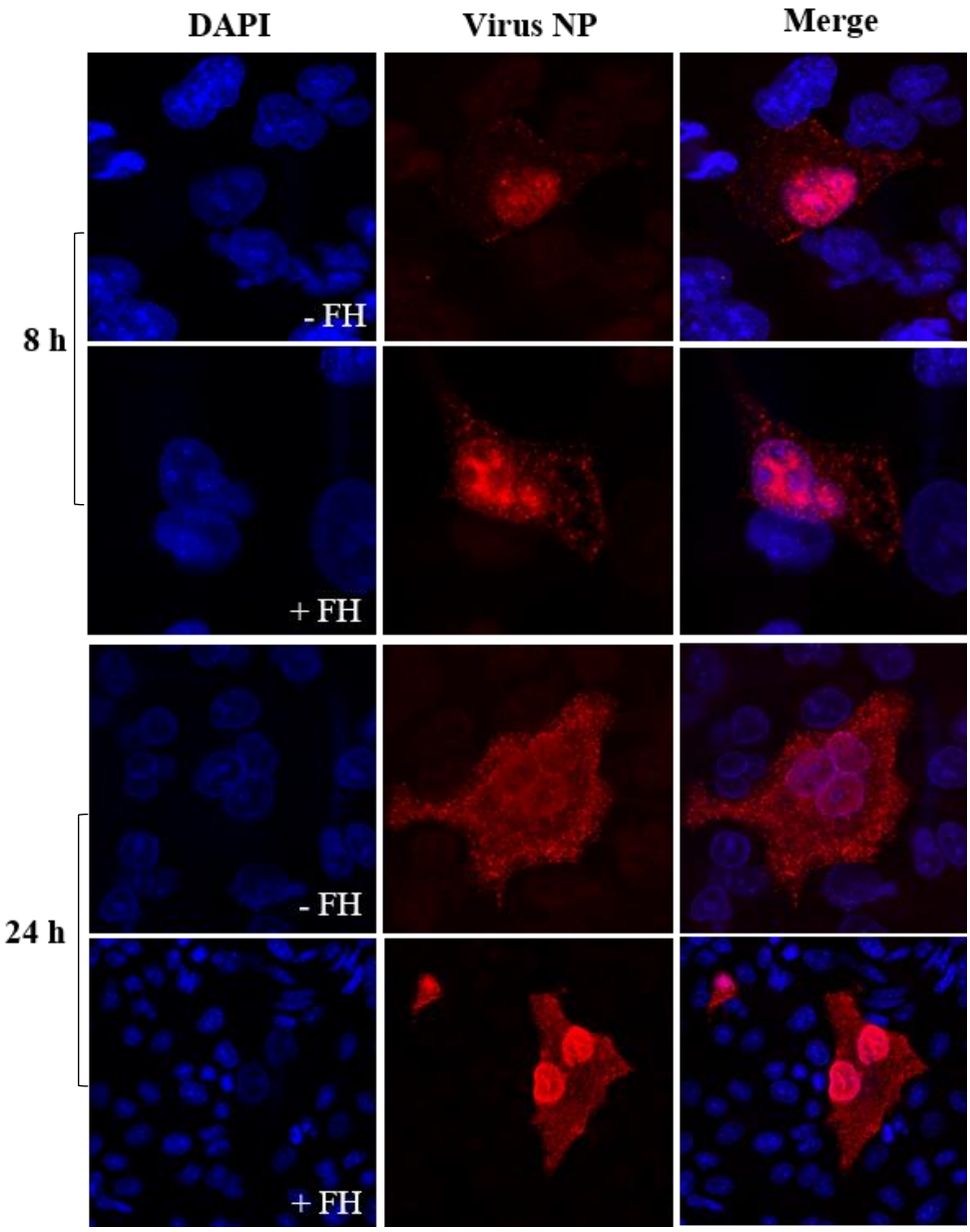

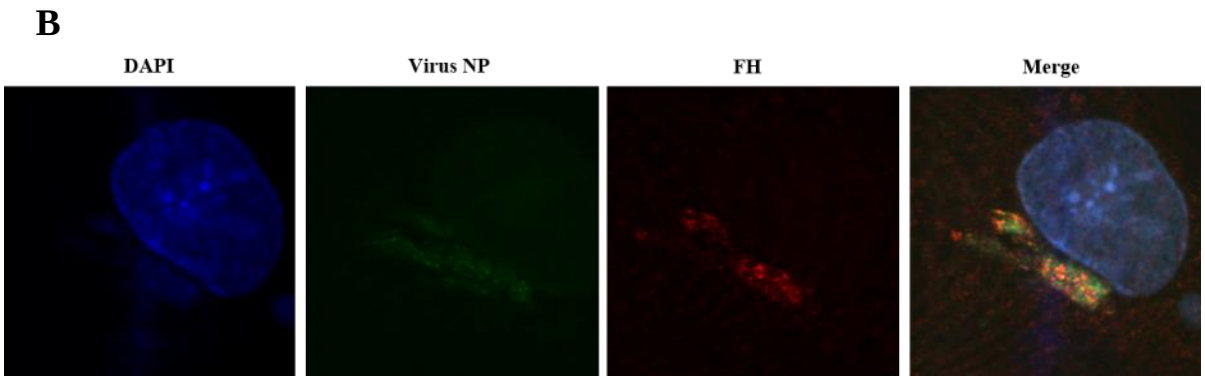

Figure 5. 7: Immunofluorescence assay to analyse the role of FH at the entry stage of IAV infection. **(A)** Immunofluorescence microscopy to track the role of FH in the attachment, entry, and replication of IAV HIN1pdm09 in A549 cells. A549 cells were infected without (-) or with (+) FH-preincubated H1N1. Mock cells were non infected and untreated with FH. The cells were immunostained with DAPI for the nucleus (blue), anti-NP antibody (red), **(B)** Binding of IAV (green) to FH (red).

5.3 Discussion

In this chapter, the primary aim was to identify any impact of the interaction between FH and IAV on viral infectivity. To investigate whether FH can block IAV-HA attachment to sialic acid the model assay of IAV adsorption to RBCs (HI) was adapted to measure FH inhibition of this interaction. HI is a serological test and was originally used to either titrate the antibody response to a virus or to detect an unknown virus (Payne, 2017). Interestingly, the results of HI assay obtained at RT showed that FH inhibited the haemagglutination by interfering with IAV-HA attachment to TRBC at concentrations <1.25 µg/well compared to the negative control, FH without virus (FH). These results suggest that FH might have an inhibitory effect at the earliest stage of the viral replication cycle. In contrast, the inhibition of haemagglutination by FH was not observed in HI assay performed at 4°C. However, agglutination of TRBCs was observed in the absence of the virus at 4°C, suggesting that FH may cause agglutination of RBCs in the cold condition. FH is known to bind to cell surface sialic acid (cell self-marker) to protect the host cells from complement attack (Cserhalmi *et al*., 2019). This interaction may be transitory at RT, but at 4°C, the interaction between FH and sialic acid may be more kinetically stable and thus the FH is maintaining the TRBC in suspension much like IAV can.

In this study, haemagglutination was inhibited by FH, suggesting that FH binds to H1 HA and inhibits its binding to sialic acid on the surface of TRBCs. However, this action did not prevent H1N1pdm09 replication in A549 and THP-1 cells. The results suggest that incubation of IAV with FH prior to application to cells enhanced H1N1pdm09 viral replication in a FH dose-dependent manner in both A549 and THP-1 cells. The enhancement effect of FH was significant at FH concentration of 100 µg/ml, but not at the lowest concentrations (5 and 50 µg /ml). This may indicate that the interaction between FH and HA could be of low affinity. The use of a large amount of FH could strengthen the interaction. Where multiple FH molecules can bind to H1 HA protein leading to increase avidity binding between FH and HA protein. This may explain why the effect of FH was significant at high concentration. It has been reported that the affinity of bacterial surface protein fHpb of *N. meningitidis* of diverse strains to human FH is different, affecting its association-dissociation rates and binding kinetics (Seib *et al*., 2011). Thus, further studies are needed to estimate the binding affinity of H1 HA protein to human FH.

To explain why FH inhibited the haemagglutination of TRBC in the presence of the virus and at the same time increased virus replication, a western blot was performed to characterise the role of FH in the H1N1pdm09 entry strategy. As M1 protein is one of the most abundant proteins in the virus particles with about 3000 molecules per virion (Shtykova *et al*., 2013), the high amount of this protein will increase the sensitivity of the assay to detect the virus in infected A549 cells without or with FH at two-time points: at 4 h (before the new progeny is produced and at 8 h (after one replication cycle to generate the new virions). It has been reported that one IAV replication cycle starting from virus attachment, internalisation, RNA replication and viral protein synthesis, assembly, budding and finally release the new progeny from the target cells occurs on average at 6 – 8 h, depending on the type of cell (Liao *et al*., 2013; Edinger *et al*., 2014). At 4 h post-infection, western blot analysis of M1 protein levels showed that H1N1pdm09 entry was observed represented by the weak band of M1 protein at approximately 28 kDa compared to the strong band of M1 protein obtained for non-FH treated control. To track the effect of FH on viral replication at different time points (4, 8, 18, and 24 h) in A549 cells, an immunohistochemistry assay was performed in which the NP viral protein was stained to detect the virus. These experiments showed results corresponding to those obtained from western blot analysis. FH has shown partial inhibition of H1N1pdm09 during the early stages of the replication cycle (4 h) and an increase in growth from 8 h post-infection. These results suggest that H1N1pdm09 entry was slowed but not completely inhibited and the virus entry has occurred. However, at 8 h post-infection the virus that has entered the cells has enhanced viral protein production compared to non-FH treated control.

This increase in viral growth may be due to the manipulation of the host immune response by FH. FH has been shown to inhibit the release of interleukin-12p70 (IL-12p70) and significantly reduce the production of tumour necrosis factor-α (TNFα), interferon-gamma (IFN-γ), IL-8, and IL-6 and in the early stages of monocytes differentiation into dendritic cells (MoDCs) compared to FH-untreated MoDCs. This immunomodulatory action of FH on human MoDCs requires the CCP19–CCP20 cell surface recognition binding domain of FH and thus FHL-1 lacks this activity (Olivar *et al*., 2016). Cytokines, such as IL-6, IL-8, TNF-a, have been shown to be released by epithelial cells at high rates to involve in reducing the spread of IAV infection (Eliopoulos *et al*., 1999; Kaiser *et al*, 2001). TNF-α exhibited robust antiviral activity against avian, swine, and human IAV, and its impact was more than that of IFN-γ or IFN-α (Seo & Webster, 2002). H5N1-infected mice treated with anti-TNF-α antibodies or deficient in TNF receptors showed no significant difference in survival rate compared to uninfected controls

(Peiris et al., 2009). Thus, TNF-α is believed to be the main cytokine that plays a crucial role in the initial host defence against IAV infection in lung epithelial cells. (Seo & Webster, 2002).

It was found that the secretion of cytokines and chemokines such as IL-12p40, TNF-R2, TNF-α, IL-6, IL-12p70, and IL-6R is significantly increased in the plasma and nasopharyngeal aspirate of the patients infected with H5N1 IAV (Phung *et al*., 2011). In addition to H5N1, other subtypes of IAV can produce INF-α, INF-γ, and IL-10 (De Jong *et al*., 2006; Kaiser *et al*., 2001; Hackney *et al*., 2003). In previous studies, the cytokines IFN-α, IFN-β, IL-28, and IL-29 were shown to be weakly produced by A549 cells infected with human H1N1. However, their concentrations significantly increased exclusively when A549 cells were pre-treated with IFN-α or TNF-α (Phung *et al*., 20011; Veckman *et al*., 2006). All these reported results indicate that TNF-α plays an essential role in enhancing innate immunity in response to IAV infection (Phung *et al*., 20011).

In this study, FH may downregulate cytokines such as IFNs or TNFs in A549 cells infected with H1N1/99, resulted in enhancing IAV replication. Therefore, more research is needed to investigate whether FH can alter host immune response to virus infection and track the impact of human FH on the attachment, entry, and replication of H1N1pdm09 in target cells at different time points during the infection cycle. In conclusion, these results suggest that FH slows down H1N1pdm09 entry but once entered it promotes its growth during the replication cycle.

In this study, the HI assay showed that FH inhibits the H3N2/99 virus-mediated agglutination of TRBC by interfering with H3 HA uptake to TRBC. These results raised the hypothesis that FH might hinder binding of H3 HA protein to sialic acid on the cell surface and thus inhibits the viral life cycle. To verify this hypothesis, the infectious assay was performed using increasing concentrations of FH. These results demonstrated that FH had significant dose-dependent inhibition against H3N2/99 in both A549 and THP-1 cells. Mapping of binding sites for the FH molecule on the surface of H3 HA protein showed that FH binds to the large region of the HA1 subdomain and to a lesser extent to HA2, in particular the RBS pocket, fusion peptide and fusion peptide pocket compared to H1 HA which showed a smaller FH binding region. Hence, this large interaction region with FH may cover H3 HA protein with FH and prevent the initial stages for IAV infection. These stages include cleavage of HA protein by the protease, attachment to the sialic acid on the cell surface, and fusion of viral and endosomal

membranes. Membrane fusion requires cleavage of HA which is induced by low pH in the endosome. Cleavage of HA triggers a conformational change that exposes the fusion peptide consisting of about 14 hydrophobic amino acids at the N-terminus of HA2 (Böttcher-Friebertshäuser *et al*., 2013; Straus & Whittaker, 2017; White & Whittaker, 2016). Cleavage of HA can occur in diverse cellular compartments and at various time points during the viral life cycle: during transport of HA to the plasma membrane, during assembly and budding of progeny virus or at a very late time point during attachment and entry into a new cell (Böttcher-Friebertshäuser *et al*., 2013). Avian influenza viruses are classified based on their pathogenicity in chickens into low or high pathogenic avian influenza viruses (LPAIV or HPAIV, respectively). LPAIVs cause mild or asymptomatic infections in birds, while HPAIVs cause severe systemic infections in poultry with mortality rates as high as 100%. (Luczo et al., 2018; Böttcher-Friebertshäuser *et al*., 2013). The HA of LPAIVs contains a monobasic cleavage site and requires the addition of exogenous trypsin to most tissue cultures for HA activation. In contrast, HPAIVs possess HA with a multibasic cleavage site that is cleaved by endogenous proteases such as furin and the proprotein convertase 5/6 (PC5/6) in the trans-Golgi network (TGN), which leads to the release of infectious progeny virus-containing cleaved HA from the cells. (Böttcher-Friebertshäuser *et al*., 2013; Izaguirre, 2019). Seasonal and pandemic IAVs belong to the H1and H3 subtypes possess monobasic cleavage site motifs I-Q-S-R, and K-Q-T-R, respectively. These cleavage sites are activated at a single arginine by trypsin-like proteases such as human airway trypsin-like protease (HAT); also identified as TMPRSS11D and transmembrane protease serine S1 member 2 (TMPRSS2); also called as epitheliasin on the plasma membrane in vitro. However, it remains unclear whether the HAT and TMPRSS2 play a role in vivo infection in the human airway ((Böttcher-Friebertshäuser *et al*., 2010; 2013). Further detailed knowledge of relevant proteases provides the basis for the development of specific protease inhibitors as a novel approach for influenza treatment (Böttcher-Friebertshäuser *et al*., 2013). In this study, ELISA results for analysing FH binding with HA peptides of H3N2/99 showed that FH binds to the cleavage site (K-Q-T-R) at the N-terminus of HA2. These results suggest that FH may inhibit the cleavage of non-activated HA.

Western blot analysis to investigate the antiviral effect of FH on H3N2/99 during early phases of viral infection has shown that FH block virus entry at 4 h post-infection. This inhibitory effect of FH was not alleviated at 8 h, where one life cycle is believed to have completed. These results suggest that the ability of FH to exhibit an inhibitory effect against H3N2/99 may be due to FH binding to RBS in the viral protein H3 HA1, preventing virus attachment to the sialic

acid on the surface of target cells. Immunohistochemistry assay showed that FH exhibited efficient inhibition to H3N2/99 entry. During the time course of viral infection, no virus was observed in FH-treated cells compared to FH-untreated cells. These results again suggest that FH exerts its inhibitory effect through the entry stage of IAV infection. Virus entry is the first important step of virus replication and is an ideal target to efficiently prevent virus infection (Edinger *et al*.,2014). Thus, the inhibitory effect of FH against H3N2/99 could herald development as an efficient anti-IAV drug.

On the other hand, FH did not show significant impact on H5N3 and H9N2 avian IAV replication in A549 and THP-1 cells compared to the control, FH-untreated cells. Since the HI assay results demonstrated that FH inhibited haemagglutination by interfering with H5 and H9 HA adsorption to RBC, these results raise the question of whether FH might have a weak binding with the receptor-binding domain of H5 and H9 HA, which needs further investigation. Moreover, the lack of influence of FH on H5N3 and H9N2 replication may be due to host specificity. The interaction of FH with diverse pathogenic bacteria was shown to be specific to human (Ngampasutadol *et al*., 2008; Granoff *et al*., 2009; Langereis *et al*., 2014). The fHbp surface protein of *N. meningitidis* was reported to specifically bind to human FH, but not to murine FH (Stevenson *et al*., 2002). Another piece of evidence on host specificity showed that the outer surface protein E (OspE) of *B. burgdorferi* strain N40 could specifically bind to human FH (Hellwage *et al*., 2001). The OspE protein is a member of a protein family known as OspEF-related proteins (Erp proteins) (Lam *et al*., 1994; Stevenson *et al*., 1997). These proteins showed different affinities for FH of different animal species (Stevenson *et al*., 2002). A comparison of FH among different animal species showed that amino acid sequences and glycosylation patterns vary from one animal to another (Alexander *et al*., 2001; Horstmann *et al*., 1985; Kristensen *et al*., 1986). This variation restricted the host range of a pathogen by which FH binds to its receptor. This could explain why the Lyme disease bacteria, *B. burgdorferi*, express different Erp proteins on the bacterial surface that enable them to bind to FH of the wide range of potential hosts (Stevenson *et al*., 2002). Low numbers of avian FH amino acid sequences are available. However, FH sequences of chickens and ducks are not yet available. Based on the comparison between primary amino acid sequences of human FH (P08603) and avian FH (A0A094KF68) from great crested grebe (*Podiceps cristatus*), the identity was 28.44%. Thus, more studies are needed using avian FH.

Further studies are needed to confirm the results obtained in a mice model of influenza infection. The study of IAV infection is routinely performed in several mammalian models such as the mouse, ferret, guinea pig, cotton rat, and swine. The ferret is best suited for studying IAV-host interactions, pathogenesis, transmission, and therapeutics (Belser *et al*., 2011). The ferrets demonstrate similar binding patterns to human and avian IAV sialic acid receptors in the respiratory tract (Maher & DeStefano, 2004; van Riel *et al*., 2007). Moreover, the analyses of ferret genome sequence demonstrate high similarity in protein-sequence and tissue-expression manners between human and ferret. This is an important addition to the advantage of using the ferret model to study respiratory disease (Peng *et al*., 2014). However, unlike mice, the advantage of using ferret models is unfavourable due to the relatively limited commercial availability, the breeding requirements are sophisticated and more expensive. Additionally, the rarity of ferret-specific reagents such as ferret-specific antibodies and recombinant ferret cytokines have limited IAV studies in ferrets. Hence it is preferred to use mice. However, a major drawback to using the mouse model is the need to use mouse-adapted viruses to produce productive infection and clinical systemic symptoms of the disease. Also, unlike the human, murine IAV infection is a lower respiratory tract infection that differs physiologically from IAV infection in human (Thangavel *et al*., 2014; Belser *et al*., 2016).

Infection of mice with IAV and treated with human FH may produce results similar to those of this study or demonstrate competition between other immune system molecules with FH for binding to the viral HA protein. Many studies have shown that *N. meningitidis* binds to human FH by the surface lipoprotein, factor H binding protein (fHbp). By this binding, FH molecules coat the bacterium and make it undetectable to C3. This action allows *N. meningitidis* to avoid complement-mediated lysis and maintain their survival in human blood (Schneider *et al*., 2006; Seib *et al*., 2015; Principato *et al*., 2020). Other studies have demonstrated that FH related protein-3 (FHR-3) interferes with FH to bind to fHbp of *N. meningitidis*, acting as a competitive inhibitor of FH and enhancing complement activation. FHR3 shows high sequence similarity to FH (Skerka *et al*., 1993). This means that the bacteria cannot efficiently discriminate between FH and FHR-3. Since the two complement factors, FH and FHR-3 have opposing effects, the susceptibility to meningococcal infection will be controlled by the relative levels of each of the complement factors in the serum. This is associated with genetic variation in individuals. In addition, many variants of *N. meningitidis* show the variation in the affinity of FH and FHR3 binding to fHbp, affecting the strength of the interaction (Caesar *et al*., 2014). Since FH binds to the anionic polysaccharides of the extracellular matrix such as heparin

(Kajander *et al*., 2011), these molecules may compete with FH ligands for binding to FH on heparin-binding sites CCP 7 and CCP 20 (Perkins *et al*., 2014; Meri *et al*., 2013). Thus, inhibition of the interaction between FH and the pathogens and promoting complement activation. Previous research has shown that heparin inhibited binding of the complement protein C4BP with the surface proteins LigA and LigB of the bacteria, *Leptospira interrogans* (Breda *et al*., 2015).

If the binding to FH promotes pathogen replication as demonstrated in this study with H1N1pdm09 pre-treated FH, then pathogen spread can be controlled by blocking its binding to FH, which is expected to direct the complement activation to the pathogen surface, leading to its phagocytosis and lysis. Recently, binding of FH to pathogens has been utilised as a functional target for an immunotherapeutic strategy to generate anti-infective chimeric proteins comprising of FH domains that most FH-binding pathogens use to interact with FH (CCPs 6 – 7 and 18 – 20) fused with the Fc domain of IgG1. The chimeric proteins FH/FC compete out the natural, full-length-FH from the pathogen surface. Upon complement activation, copious amount of anaphylatoxins such as C3a and C5a are released, attracting phagocytic cells which engulf pathogens bond to the C3 fragments. Moreover, the Fc portion of the chimeric protein attracts phagocytes by binding to Fc receptors (FcγR) on their surfaces, results in pathogen killing in phagocytosis (Shaughnessy *et al*., 2016; Wong *et al*., 2016; Blom e*t al* 2017).

However, because the CCPs 19 – 20 region of FH plays a crucial role in the regulation of complement activation by discrimination between self and nonself (Kajander *et al*., 2011; Blaum *et al*., 2015), recent research has proved that the non-mutated FH18 – 20/Fc molecule shows the ability to interfere with the endogenous FH to bind to the host cells and activate the complement (Shaughnessy *et al*., 2016; Wong *et al*., 2016). In the C-terminal region of FH, CCP 19 binds to C3b fragments, whereas CCP 20 interacts with glycosaminoglycans to eliminate the complement on the host cells. Binding of FH to sialic acid on the surface of the host cells increases FH affinity for C3b, enhancing the functional activity of N-terminal domains of FH, the cofactor, and decay-accelerating activities (Kajander *et al*., 2011; Blaum *et al*., 2015). Therefore, the use of FH/Fc molecules as therapeutics should not interfere with the physiologic functions of endogenous FH (Wong *et al*., 2016). In recent research, a mutation was incorporated into crucial amino acids in the CCPs 18 – 20 domains of a chimeric protein that abrogated its binding to the erythrocytes, while maintaining the interaction with *Neisseria gonorrhoeae* (Shaughnessy *et al*., 2016). Therapeutic use of FH/Fc molecules against

Haemophilus influenzae, *N. gonorrhoeae*, and *Streptococcus pyogenes* in a mouse model showed their ability to decrease bacterial survival in the host (Wong *et al*., 2016; Shaughnessy *et al*., 2016; Blaum *et al*., 2015). Hence, the integrity of the FH/Fc molecules should be demonstrated before they are used as anti-infectious agents in human (Blaum *et al*., 2015).

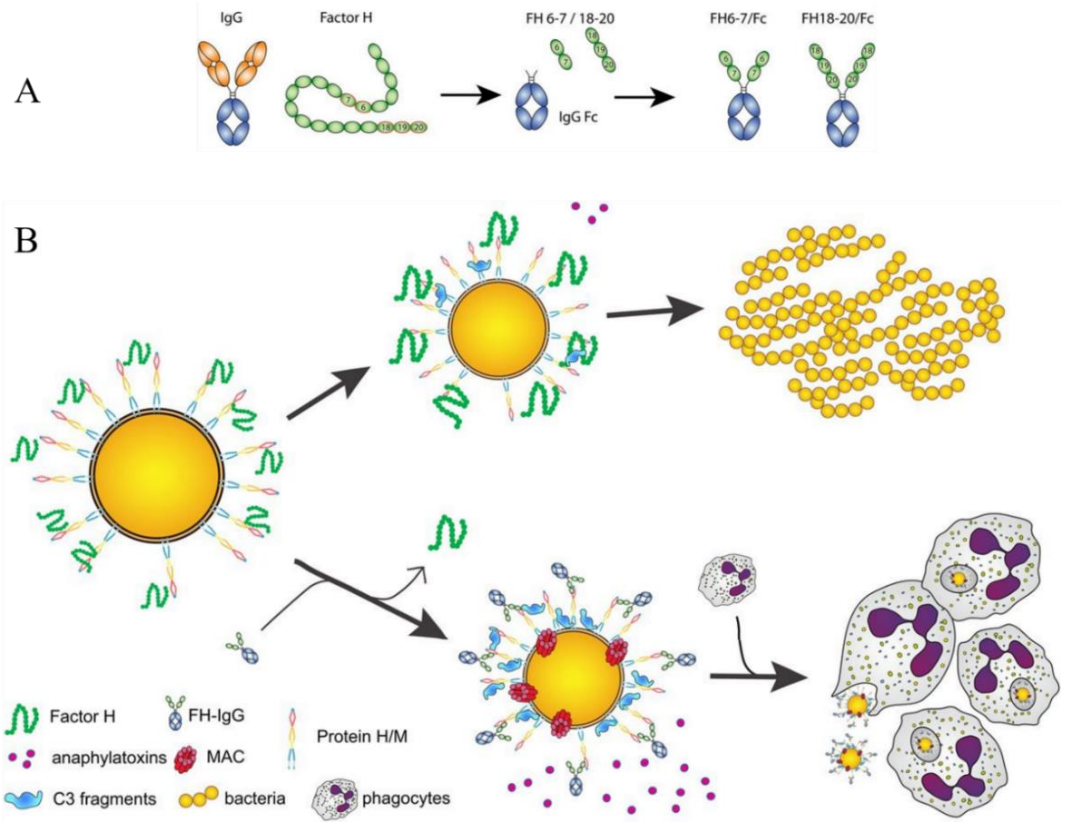

Figure 5. 8: Schematic representation of the structure and therapeutic mechanisms of FH/FC against the pathogen (*S. pyogenes*). (A) FH6 – 7/Fc or FH18 – 20/Fc is fused with the Fc region of IgG to form a chimeric protein (FH/FC) **(B)** The upper panel shows recruitment of FH by the bacterial surface protein, inhibiting complement activation. Moreover, the low quantities of anaphylatoxin released to bind to a few C3 fragments on the bacterial surface are not adequate to attract phagocytes, increasing bacterial survival. The lower panel demonstrates how FH/FC binds to FH-ligands, diverting the physiological FH from the bacterial surface and enhancing complement activation. As a result of the complement activation, high amount of anaphylatoxins attract phagocytic cells. The FC receptors (FCYR) also binds to phagocytes, leading to downstream signalling and bacterial phagocytosis (Blom., *et al* 2017).

Alternatively, recruitment of complement inhibitors by the pathogens to enhance their replication could be prevented by raising antibodies against these inhibitors. Thus, FH-ligands made by pathogens might be used as vaccine targets (Serruto *et al*., 2010). In this study, if binding to FH enhances H1N1pdm09 replication, then molecular determinants of FH-H1 HA

binding sites can be useful for inhibiting viral replication, as modification of H1 HA regions that are involved in the binding to FH may elicit antibodies that block binding of FH to H1 AH. Therefore, the use of mutated H1 HA that no longer bind to FH might be important in the designing of vaccines aimed to raise antibodies that block binding of FH to the virus. The efficiency of FH-ligands expressed by the pathogens used in vaccines is confirmed by the bacterial proteins fHbp of *N. meningitidis* and FHA of *B. pertussis*. Vaccination with these proteins elicits antibodies that block FH adherence to the bacterial surface (Santolaya *et al*., 2012; Locht, 2016).

Altogether, this chapter provided information about the role of FH in the modulation of IAV replication as well as investigation the mechanisms involved in virus entry. This detailed knowledge could yield fundamental insights that would be useful for developing small-molecule therapeutic agents and producing vaccines to prevent future IAV infections.

5.4 Conclusion

1. FH Inhibited haemagglutination of RBCs by interfering with HA viral protein adsorption to RBC, suggesting that HA protein could be the potential target of FH.

2. FH displayed varying effects on the replication of human and avian IAV subtypes; enhancing human H1N1pdm09 viral replication and inhibiting H3N2/99 replication in A549 and THP-1 cells whereas it had no impact on the avian H5N3 and H9N2 viral replication.

3. FH slowed down but did not completely inhibit H1N1pdm09 virus entry during the early stage of the replication cycle, while it completely prevented the entry of H3N2/99 into A549 target cells.

Chapter 6- Conclusions and future perspectives

6.1 Conclusions and future perspectives

FH is the major negative regulator protein in the complement alternative pathway that prevents extensive host tissue damage caused by complement activation. This protection is achieved by the ability of FH to discriminate between self and non-self surfaces and direct the complement system to kill only the pathogens (Józs, 2017). Many pathogens have evolved several strategies to evade complement system recognition and destruction. A common evasion strategy used by various pathogens is the hijacking of human complement regulators to their surfaces to provide protection from complement activation. One such host regulator is FH protein (Hovingh *et al*., 2016). It has been shown that FH is released by different cell types such as monocytes, fibroblasts, endothelial cells, keratinocytes, mesenchymal stem cells (MSCs), and retinal pigment epithelial cells (Koppa *et al*., 2012). Thus, local synthesis of FH and its alternate splice variant FHL-1 may be involved in local defence reactions during pathologic processes (Olivar *et al*., 2016). The focus of this study, therefore, was to investigate FH ability to bind to IAVs and what potential impact this interaction may have on IAV replication.

In this study, ELISA was performed to investigate the direct interaction between purified human FH and different strains of purified live human (A/England/195/09 (H1N1), A/Michigan/45/15 (H1N1), A/HK/1174/99 (H3N2), and A/HK/4801/14 (H3N2)) and avian (A/Duck/Singapore/3/97 (H5N3), and A/chicken/Pakistan/UDL-01/08 (H9N2)) IAVs. The results revealed a significant binding of all IAVs tested to human FH. In contrast to bacterial, parasitic, and fungal pathogens, little is known about the direct interaction of viruses with the complement FH protein. This interaction demonstrated by the West Nile virus encoding a non-structural protein (NS1) that binds to and recruits FH, leading to enhanced factor I activity and cleavage C3b convertase (C3bBb) into iC3b. This action attenuates the deposition of C3b and reduces the formation of the membrane attack complexes on cell surfaces (Chung *et al*., 2006).

To investigate which viral protein was responsible for the binding of IAV to human FH, far western blot was undertaken. This revealed that the interaction between IAVs (H1N1pdm09, H3N2 /HK//99, H5N3, and H9N2) and FH is mediated by HA surface protein, which has a key role in the attachment, entry mediated by membrane fusion. Pathogens have been shown to bind to FH by expressing surfaces proteins (Andre *et al*., 2007). Since HA is a surface protein (Kosik & Yewdell, 2019), it is a main target for FH binding. To confirm that IAV binds to FH by HA protein, different methods have been carried out. One of these ways is the use of

lentiviral pseudotype particles that display HA protein from different human and avian IAVs on their surfaces without or with NA protein. These results confirmed that binding of IAV to FH is carried out by HA protein, and this interaction is conserved over multiple subtypes. Comparison of HA-pseudotyped particles with those particles harbouring HA and NA protein did not show a statistical difference, suggesting that HA protein bears the main responsibility for binding to FH. This may be because HA protein is the most abundant protein on the viral envelope with around 400 – 500 molecules per virion (Moulès *et al*., 2011). This is to its crucial role in initiating viral replication cycle by attaching the virus to sialic acid on the surface of the host cell. (Duo *et al*., 2018). This feature may allow targeting of HA protein with FH.

These results were confirmed using different recombinant HA proteins H3, H1, H9, H7, and H5 in ELISA, which revealed a significant association with FH. Statistical analysis showed notable differences between human and avian HA proteins in their binding to FH, where human IAVs, in particular H3 HA showed the highest signal compared to HA protein of avian origin. This may be due to the considerable variations in HA protein sequences of different subtypes and strains of IAV (Air, 1981) which may influence the structure of FH binding sites on the surface of HA protein. Binding affinity or binding kinetics might be another possible cause contributing to differences between human and avian HAs in their binding to FH. Binding affinity is a measure of how tightly the protein binds to its ligand, while binding kinetics demonstrate how quickly a molecule attaches to its ligand and how quickly it dissociates from it (the rate of ligand association and dissociation) (Chackalamannil *et al*., 2017). This can be measured using surface plasmon resonance (SPR) analysis. Understanding binding affinity is important for characterising the intermolecular interactions. Hence, prospective studies are needed to measure the binding affinity and binding kinetics for the HA-FH interaction.

To verify whether other IAV proteins can bind to FH, far-western blot analysis was performed using recombinant N1 NA protein from H1N1pdm09 and recombinant M1 protein. these demonstrated that NA showed the ability to bind to FH, while no interaction between M1 protein and FH was observed. Although M1 is the most abundant protein component of the virion particles of about 3000 molecules per virion (Sato *et al*., 2003; Heldt *et al*., 2012), no interaction with FH occurred. This might be because the M1 protein localises under the viral membrane that is derived from host cells and is not exposed to FH. Further studies are needed to investigate the binding ability of NA protein from different IAV subtypes as well as for other viral proteins such as NP and M2, and RNA polymerase.

It is known that FH binds to negatively charged ions on carbohydrates on the cellular receptors, but it is unclear if FH binds to the pathogen proteins by carbohydrates (Meri *et al*., 2013). In this study, ELISA and far-western blot analysis revealed that the ability of FH to bind to deglycosylated IAV by PNGase F increased because of the removal of carbohydrates. This action may be because glycans could coat some amino acid sequences that participate in FH binding sites on the surface of HA protein. Thus, removal of HA glycans exposes binding sites on HA protein to FH surface, leading to high IAV-FH interaction. This study suggests that the disruption of FH structure by denaturation or deglycosylation can affect its biological, chemical, physical, and functional properties (Eckersall *et al*., 2008). Thus, in this study, a low association between IAV and deglycosylated or denatured FH was observed in ELISA. These results also indicated that the interaction between FH and IAV is protein to protein interaction. Determination of the site-specific glycosylation of the HA protein that interferes with FH binding may be beneficial to alter HA-FH binding by adding or removing glycans.

FH consists of 20 CCPs domains, and different pathogens have been shown to recruit FH to their surfaces by binding to the common binding site on the FH molecule (Meri *et al*., 2013). In this study, characterisation of the molecular binding sites on the surface of FH protein that are involved in the interaction with IAV revealed that CCPs 5 – 7 and 15 – 20 are involved in FH binding to purified IAV tested (H1N1pdm09, H3N2/99, H5N3, and H9N2). The results of this study agree with the results of previous research showing that several pathogens bind to FH through two common binding sites. One of the binding sites is conserved in the FH and FHL-1 and is localised in the N-terminal on CCPs 6 – 7, whereas the second site is in the C-terminal on CCP 19 – 20 (Meri *et al*., 2013). Through this binding, IAV leaves the functional site of FH CCPs 1 – 4 available to negatively regulate the AP. This pattern of interaction indicates that FH may still retain its ability to down regulate AP. Thus, the functionality of FH through its binding to IAV needs to be tested in future research.

To characterise the molecular determinants of the IAV HA protein involved in the binding with human FH, an ELISA was designed using a panel of biotinylated HA peptides from H1N1pdm09 and H3N2/99 subtypes. The results have defined that FH binding overlaps with 130-loop and the residues surrounding it, as well as with the region between 190-helix and 220-loop in the RBS pocket. Thus, these results suggest that FH may block virus attachment to a cellular receptor, sialic acid to a certain extent. The results also showed that FH binds to the fusion domain, F′ in the N- terminal region of HA1 which includes residues 34 – 63, residues

111 – 120, residues 199 – 219 and the residues 287 – 306 in C-terminal of HA1. Targeting the fusion peptide or its pocket could prevent the conformational change of HA protein and subsequently inhibit the fusion of viral and endosomal membrane (Mair *et al*., 2014). Mapping of FH binding sites on the H3 HA protein showed that FH binds to 130-loop and the residues surrounding it. FH has also demonstrated its interaction with residue Tyr98, the first three residues in 220-loop and the region between 190-helix and 220-loop. Moreover, the results showed that FH bound to residues in HA1 that involved in fusion peptide pocket structure, 85 – 90, 104 – 114 and it also bound to residues (1 – 25) of the fusion peptide in subdomain HA2. These findings suggest that FH binds with a broad range of amino acid residues in RBC and the fusion peptide. Thus, FH may block the binding site of the receptor sialic acid and virus entry into the host cells, inhibiting the virus infectivity. HA is responsible for virus attachment and entry into target cells, and it is the main target of neutralising antibodies (Maginnis, 2018). Therefore, this detailed knowledge of the molecular determinants of FH interaction with HA protein will provide more information on whether FH could inhibit any of these vital functions of HA.

To investigate whether FH can block IAV-HA attachment to sialic acid, HI assay was performed using TRBCs and different subtypes of human and avian IAVs. In this study, haemagglutination was inhibited by FH, suggesting that FH binds to H1 HA and inhibits its binding to sialic acid on the surface of TRBCs. However, this action did not prevent H1N1pdm09 replication in A549 and THP-1 cells. The results suggest that FH-pre-treated H1N1pdm09 enhanced viral replication in an FH dose-dependent manner in both A549 and THP-1 cells. The enhancement effect of FH was significant at FH concentration of 100 µg/ml, but not at the lowest concentrations (5 and 50 µg/ml). This may indicate that the interaction between FH and HA could be of low affinity. The stability of the HA-FH complex should be considered. If the affinity of binding between HA protein and human FH is low, this may suffice for dissociation of the bound FH molecule from HA. Thus, additional experiments are needed to verify the strength of the affinity of full-length FH and FH fragments that showed a binding ability to HA protein.

In this study, to explain why FH inhibited the haemagglutination of TRBC in the presence of the virus and at the same time increased virus replication, a western blot was performed to characterise the role of FH in the H1N1pdm09 entry strategy using M1 protein to detect the virus in infected A549 cells. The results revealed that FH slowed H1N1pdm09 entry during the

first hours of infection (at 4 h). However, the entry occurred, and FH promoted viral replication at a late stage of infection (8 h post-infection) compared to the FH untreated control. These results were confirmed using immunohistochemistry and immunofluorescence assays. The increased H1N1pmd09 viral replication may be due to the manipulation of the host immune response by FH. FH has been shown to inhibit the releasing of interleukin-12p70 and significantly reduce the production of TNFα, FN-γ, IL-8, and IL-6 and in the monocytes (Olivar *et al*., 2016). Thus, FH may downregulate cytokines such as IFNs or TNFs in A549 cells infected with H1N1/99, resulting in enhancing IAV replication. Therefore, more research is needed to investigate whether FH can alter host immune response to virus infection and track the impact of human FH on the attachment, entry, and replication of H1N1pdm09 in target cells at different time points during the infection cycle.

In contrast, the current results demonstrated that FH had significant dose-dependent inhibition against H3N2/99 in both A549 and THP-1. These results were confirmed using entry and immunohistochemistry assays. Thus, these results suggested that FH might hinder binding of H3 HA protein to sialic acid on the cell surface and thus, inhibit the viral life cycle. On the other hand, FH did not show significant impact on H5N3 and H9N2 avian IAV replication in A549 and THP-1 cells. This action may be due to the host specificity. The interaction of FH with diverse pathogenic bacteria was shown to be specific to human (Ngampasutadol *et al*., 2008; Granoff *et al*., 2009; Langereis *et al*., 2014). Thus, more studies are needed using avian FH. Further studies are needed to confirm the result obtained in the animal model of influenza infection. Infection of an animal model with IAV and treateing them with human FH may produce results similar to those of this study or demonstrate competition of other immune system molecules with FH for binding to HA viral protein such as FHR proteins.

Overall, this study indicates that different subtypes of human and avian IAVs can bind to human FH and modulate IAV replication. This detailed knowledge could yield fundamental insights that would be useful for developing small-molecule therapeutic agents from FH and producing vaccines to prevent future IAV infections.

References

Ablasser, A., Poeck, H., Anz, D., Berger, M., Schlee, M., Kim, S., Bourquin, C., Goutagny, N., Jiang, Z., Fitzgerald, K.A. and Rothenfusser, S., 2009. Selection of molecular structure and delivery of RNA oligonucleotides to activate TLR7 versus TLR8 and to induce high amounts of IL-12p70 in primary human monocytes. The Journal of Immunology, 182(11), pp.6824-6833.

Achila, D., Liu, A., Banerjee, R., Li, Y., Martinez-Hackert, E., Zhang, J.R. and Yan, H., 2015. Structural determinants of host specificity of complement Factor H recruitment by Streptococcus pneumoniae. Biochemical Journal, 465(2), pp.325-335.

Agarwal, V., Asmat, T.M., Luo, S., Jensch, I., Zipfel, P.F. and Hammerschmidt, S., 2010. Complement regulator Factor H mediates a two-step uptake of Streptococcus pneumoniae by human cells. Journal of Biological Chemistry, 285(30), pp.23486-23495.

Agrawal, P., Nawadkar, R., Ojha, H., Kumar, J. and Sahu, A., 2017. Complement evasion strategies of viruses: an overview. Front Microbiol 8: 1117.

Agrawal, P., Sharma, S., Pal, P., Ojha, H., Mullick, J. and Sahu, A., 2020. The imitation game: a viral strategy to subvert the complement system. FEBS Letters.

Air, G.M., 1981. Sequence relationships among the haemagglutinin genes of 12 subtypes of influenza A virus. Proceedings of the National Academy of Sciences, 78(12), pp.7639-7643.

Ajona, D., Castano, Z., Garayoa, M., Zudaire, E., Pajares, M.J., Martinez, A., Cuttitta, F., Montuenga, L.M. and Pio, R., 2004. Expression of complement factor H by lung cancer cells: effects on the activation of the alternative pathway of complement. Cancer Research, 64(17), pp.6310-6318.

Al Khatib, H.A., Al Thani, A.A., Gallouzi, I. and Yassine, H.M., 2019. Epidemiological and genetic characterization of pH1N1 and H3N2 influenza viruses circulated in MENA region during 2009–2017. BMC infectious diseases, 19(1), p.314.

Albrecht, J.C. and Fleckenstein, B., 1992. New member of the multigene family of complement control proteins in herpesvirus saimiri. Journal of virology, 66(6), pp.3937-3940.

Alexander, J.J., Hack, B.K., Cunningham, P.N. and Quigg, R.J., 2001. A protein with characteristics of factor H is present on rodent platelets and functions as the immune adherence receptor. Journal of Biological Chemistry, 276(34), pp.32129-32135.

Ali, A., Avalos, R.T., Ponimaskin, E. and Nayak, D.P., 2000. Influenza virus assembly: effect of influenza virus glycoproteins on the membrane association of M1 protein. Journal of virology, 74(18), pp.8709-8719.

Alsenz, J., Schulz, T.F., Lambris, J.D., Sim, R.B. and Dierich, M.P., 1985. Structural and functional analysis of the complement component factor H with the use of different enzymes and monoclonal antibodies to factor H. Biochemical Journal, 232(3), pp.841-850.

Amara, U., Rittirsch, D., Flierl, M., Bruckner, U., Klos, A., Gebhard, F., Lambris, J.D. and Huber-Lang, M., 2008. Interaction between the coagulation and complement system. In Current topics in complement II (pp. 68-76). Springer, New York, NY.

Andre, G.O., Converso, T.R., Politano, W.R., Ferraz, L.F., Ribeiro, M.L., Leite, L.C. and Darrieux, M., 2017. Role of Streptococcus pneumoniae proteins in evasion of complement-mediated immunity. Frontiers in microbiology, 8, p.224.

Arredondo, S.A., Cai, M., Takayama, Y., MacDonald, N.J., Anderson, D.E., Aravind, L., Clore, G.M. and Miller, L.H., 2012. Structure of the Plasmodium 6-cysteine s48/45 domain. Proceedings of the National Academy of Sciences, 109(17), pp.6692-6697.

Avirutnan, P., Fuchs, A., Hauhart, R.E., Somnuke, P., Youn, S., Diamond, M.S. and Atkinson, J.P., 2010. Antagonism of the complement component C4 by flavivirus nonstructural protein NS1. Journal of Experimental Medicine, 207(4), pp.793-806.

Ayllon, J. and García-Sastre, A., 2014. The NS1 protein: a multitasking virulence factor. In Influenza Pathogenesis and Control-Volume II (pp. 73-107). Springer, Cham.

Barnum, S.R., 2017. Complement: a primer for the coming therapeutic revolution. Pharmacology & therapeutics, 172, pp.63-72.

Barthel, D., Schindler, S. and Zipfel, P.F., 2012. Plasminogen is a complement inhibitor. Journal of Biological Chemistry, 287(22), pp.18831-18842.

Baum, A. and Garcia-Sastre, A., 2011. Preference of RIG-I for short viral RNA molecules in infected cells revealed by next-generation sequencing. VIRULENCE, 2(2), pp.166-169.

Behnsen, J., Hartmann, A., Schmaler, J., Gehrke, A., Brakhage, A.A. and Zipfel, P.F., 2008. The opportunistic human pathogenic fungus Aspergillus fumigatus evades the host complement system. Infection and immunity, 76(2), pp.820-827.

Belachew, E.B., 2018. Immune response and evasion mechanisms of Plasmodium falciparum parasites. Journal of immunology research, 2018.

Belser, J.A., Eckert, A.M., Tumpey, T.M. and Maines, T.R., 2016. Complexities in ferret influenza virus pathogenesis and transmission models. Microbiology and Molecular Biology Reviews, 80(3), pp.733-744.

Beijing Meizheng Biotechnology Co., Ltd.
http://www.meizhenggroupen.com/life_c/i=8&comContentId=8.html..Antibody purification.

Belser, J.A., Katz, J.M. and Tumpey, T.M., 2011. The ferret as a model organism to study influenza A virus infection. Disease models & mechanisms, 4(5), pp.575-579.

Bennion, B.J. and Daggett, V., 2003. The molecular basis for the chemical denaturation of proteins by urea. Proceedings of the National Academy of Sciences, 100(9), pp.5142-5147.

Berra, S. and Clivio, A., 2016. Rapid isolation of pure Complement Factor H from serum for functional studies by the use of a monoclonal antibody that discriminates FH from all the other isoforms. Molecular immunology, 72, pp.65-73.

Bhattacharjee, A., Oeemig, J.S., Kolodziejczyk, R., Meri, T., Kajander, T., Lehtinen, M.J., Iwaï, H., Jokiranta, T.S. and Goldman, A., 2013. Structural basis for complement evasion by Lyme disease pathogen Borrelia burgdorferi. Journal of Biological Chemistry, 288(26), pp.18685-18695.

Biedzka-Sarek, M., Jarva, H., Hyytiäinen, H., Meri, S. and Skurnik, M., 2008. Characterization of complement factor H binding to Yersinia enterocolitica serotype O: 3. Infection and immunity, 76(9), pp.4100-4109.

Blackmore, T.K., Fischetti, V.A., Sadlon, T.A., Ward, H.M. and Gordon, D.L., 1998. M protein of the group A Streptococcusbinds to the seventh short consensus repeat of human complement factor H. Infection and immunity, 66(4), pp.1427-1431.

Blaum, B.S., 2017. The lectin self of complement factor H. Current opinion in structural biology, 44, pp.111-118.

Blaum, B.S., Hannan, J.P., Herbert, A.P., Kavanagh, D., Uhrín, D. and Stehle, T., 2015. Structural basis for sialic acid–mediated self-recognition by complement factor H. Nature chemical biology, 11(1), p.77.A

Blom, A.M., Hallström, T., and Riesbeck, K. (2009) Complement evasion strategies of pathogens-acquisition of inhibitors and beyond. Mol Immunol 46: 2808–2817

Blom, A.M., Magda, M., Kohl, L., Shaughnessy, J., Lambris, J.D., Ram, S. and Ermert, D., 2017. Factor H–IgG chimeric proteins as a therapeutic approach against the Gram-positive bacterial pathogen Streptococcus pyogenes. The Journal of Immunology, 199(11), pp.3828-3839.

Bonaparte, R.S., Hair, P.S., Banthia, D., Marshall, D.M., Cunnion, K.M. and Krishna, N.K., 2008. Human astrovirus coat protein inhibits serum complement activation via C1, the first component of the classical pathway. Journal of virology, 82(2), pp.817-827.

Böttcher-Friebertshäuser, E., Freuer, C., Sielaff, F., Schmidt, S., Eickmann, M., Uhlendorff, J., Steinmetzer, T., Klenk, H.D. and Garten, W., 2010. Cleavage of influenza virus hemagglutinin by airway proteases TMPRSS2 and HAT differs in subcellular localization and susceptibility to protease inhibitors. Journal of virology, 84(11), pp.5605-5614.

Böttcher-Friebertshäuser, E., Klenk, H.D. and Garten, W., 2013. Activation of influenza viruses by proteases from host cells and bacteria in the human airway epithelium. Pathogens and disease, 69(2), pp.87-100.

Boulo, S., Akarsu, H., Ruigrok, R.W. and Baudin, F., 2007. Nuclear traffic of influenza virus proteins and ribonucleoprotein complexes. Virus research, 124(1-2), pp.12-21.

Brandstätter, H., Schulz, P., Polunic, I., Kannicht, C., Kohla, G. and Römisch, J., 2012. Purification and biochemical characterization of functional complement factor H from human plasma fractions. Vox sanguinis, 103(3), pp.201-212.

Brangulis, K., Petrovskis, I., Kazaks, A., Akopjana, I. and Tars, K., 2015. Crystal structures of the Erp protein family members ErpP and ErpC from Borrelia burgdorferi reveal the reason for different affinities for complement regulator factor H. Biochimica et Biophysica Acta (BBA)-Proteins and Proteomics, 1854(5), pp.349-355.

Brass AL, Huang IC, Benita Y, John SP, Krishnan MN, Feeley EM, et al. The IFITM proteins mediate cellular resistance to influenza A H1N1 virus, West Nile virus, and dengue virus. Cell (2009) 139(7):1243–54. doi:10.1016/j.cell.2009.12.017

Brauer, R. and Chen, P., 2015. Influenza virus propagation in embryonated chicken eggs. JoVE (Journal of Visualized Experiments), (97), p.e52421.

Breda, L.C., Hsieh, C.L., Valencia, M.M.C., da Silva, L.B., Barbosa, A.S., Blom, A.M., Yung-Fu, C. and Isaac, L., 2015. Fine mapping of the interaction between C4b-binding protein and outer membrane proteins LigA and LigB of pathogenic Leptospira interrogans. PLoS Negl Trop Dis, 9(10), p.e0004192.

Breijo, M., Anesetti, G., Martínez, L., Sim, R.B. and Ferreira, A.M., 2008. Echinococcus granulosus: the establishment of the metacestode is associated with control of complement-mediated early inflammation. Experimental parasitology, 118(2), pp.188-196.

Brooimans, R. A., Hiemstra, P. S., van der Ark, A. A., Sim, R. B., van Es, L. A., and Daha, M. R. (1989). Biosynthesis of complement factor H by human umbilical vein endothelial cells, regulation by T cell growth factor and IFN-gamma. J. Immunol. 142, 2024–2030.

Broxmeyer, L., 2006. Bird flu, influenza and 1918: The case for mutant Avian tuberculosis.

Bui, M., Whittaker, G. and Helenius, A., 1996. Effect of M1 protein and low pH on nuclear transport of influenza virus ribonucleoproteins. Journal of virology, 70(12), pp.8391-8401.

Büttner-Mainik, A., Parsons, J., Jérôme, H., Hartmann, A., Lamer, S., Schaaf, A., Schlosser, A., Zipfel, P.F., Reski, R. and Decker, E.L., 2011. Production of biologically active recombinant human factor H in Physcomitrella. Plant biotechnology journal, 9(3), pp.373-383.

Caesar, J.J., Johnson, S., Kraiczy, P. and Lea, S.M., 2013. ErpC, a member of the complement regulator-acquiring family of surface proteins from Borrelia burgdorferi, possesses an architecture previously unseen in this protein family. Acta Crystallographica Section F: Structural Biology and Crystallization Communications, 69(6), pp.624-628.

Caesar, J.J., Lavender, H., Ward, P.N., Exley, R.M., Eaton, J., Chittock, E., Malik, T.H., De Jorge, E.G., Pickering, M.C., Tang, C.M. and Lea, S.M., 2014. Competition between antagonistic complement factors for a single protein on N. meningitidis rules disease susceptibility. Elife, 3, p.e04008.

Cao S, Liu X, Yu M, Li J, Jia X, et al. (2012) A nuclear export signal in the matrix protein of influenza A virus is required for efficient virus replication. J Virol 86: 4883–4891.

Cao, X., 2016. Self-regulation and cross-regulation of pattern-recognition receptor signalling in health and disease. Nature Reviews Immunology, 16(1), p.35.

Carron, J.A., Bates, R.C., Smith, A.I., Tetoz, T., Arellano, A., Gordon, D.L. and Burns, G.F., 1996. Factor H co-purifies with thrombospondin isolated from platelet secretate. Biochimica et Biophysica Acta (BBA)-General Subjects, 1289(3), pp.305-311.

Carruthers, V.B., Håkansson, S., Giddings, O.K. and Sibley, L.D., 2000. Toxoplasma gondii uses sulfated proteoglycans for substrate and host cell attachment. Infection and immunity, 68(7), pp.4005-4011.

Chackalamannil, S., Rotella, D. and Ward, S., 2017. Comprehensive Medicinal Chemistry III. Elsevier.

Chauhan, S.K., El Annan, J., Ecoiffier, T., Goyal, S., Zhang, Q., Saban, D.R. and Dana, R., 2009. Autoimmunity in dry eye is due to resistance of Th17 to Treg suppression. The Journal of Immunology, 182(3), pp.1247-1252.

Chaurasiya, S. and Hitt, M.M., 2016. Adenoviral Vector Construction I: Mammalian Systems. In Adenoviral Vectors for Gene Therapy (pp. 85-112). Academic Press.

Chen, B.J., Leser, G.P., Morita, E. and Lamb, R.A., 2007. Influenza virus haemagglutinin and neuraminidase, but not the matrix protein, are required for assembly and budding of plasmid-derived virus-like particles. Journal of virology, 81(13), pp.7111-7123.

Chen, S.N., Zhang, X.W., Li, L., Ruan, B.Y., Huang, B., Huang, W.S., Zou, P.F., Fu, J.P., Zhao, L.J., Li, N. and Nie, P., 2016. Evolution of IFN-λ in tetrapod vertebrates and its functional characterization in green anole lizard (Anolis carolinensis). Developmental & Comparative Immunology, 61, pp.208-224.

Chen, X., Liu, S., Goraya, M. U., Maarouf, M., Huang, S., & Chen, J. L. (2018). Host Immune Response to Influenza A Virus Infection. Frontiers in immunology, 9, 320.

Chlanda, P., Schraidt, O., Kummer, S., Riches, J., Oberwinkler, H., Prinz, S., Kräusslich, H.G. and Briggs, J.A., 2015. Structural analysis of the roles of influenza A virus membrane-associated proteins in assembly and morphology. Journal of virology, 89(17), pp.8957-8966.

Chou, Y.Y., Heaton, N.S., Gao, Q., Palese, P., Singer, R. and Lionnet, T., 2013. Colocalization of different influenza viral RNA segments in the cytoplasm before viral budding as shown by single-molecule sensitivity FISH analysis. PLoS Pathog, 9(5), p.e1003358.

Chung, K.M., Liszewski, M.K., Nybakken, G., Davis, A.E., Townsend, R.R., Fremont, D.H., Atkinson, J.P. and Diamond, M.S., 2006. West Nile virus nonstructural protein NS1 inhibits complement activation by binding the regulatory protein factor H. Proceedings of the National Academy of Sciences, 103(50), pp.19111-19116.

Clark, S.J., Bishop, P.N. and Day, A.J., 2010. Complement factor H and age-related macular degeneration: the role of glycosaminoglycan recognition in disease pathology.

Clark, S.J., Schmidt, C.Q., White, A.M., Hakobyan, S., Morgan, B.P. and Bishop, P.N., 2014. Identification of Factor H–like Protein 1 as the Predominant Complement Regulator in Bruch's Membrane: Implications for Age-Related Macular Degeneration. The Journal of Immunology, 193(10), pp.4962-4970.

Cohen, M., Zhang, X.Q., Senaati, H.P., Chen, H.W., Varki, N.M., Schooley, R.T. and Gagneux, P., 2013. Influenza A penetrates host mucus by cleaving sialic acids with neuraminidase. Virology journal, 10(1), pp.1-13.

Cros, J.F. and Palese, P., 2003. Trafficking of viral genomic RNA into and out of the nucleus: influenza, Thogoto and Borna disease viruses. Virus research, 95(1-2), pp.3-12.

Cross, K.J., Burleigh, L.M. and Steinhauer, D.A. (2001) 'Mechanisms of cell entry by influenza virus', Expert Reviews in Molecular Medicine, 3(21), pp. 1–18. doi: 10.1017/S1462399401003453.

Crozat, K. and Beutler, B., 2004. TLR7: A new sensor of viral infection. Proceedings of the national academy of sciences, 101(18), pp.6835-6836.

Cserhalmi, M., Papp, A., Brandus, B., Uzonyi, B. and Józsi, M., 2019, October. Regulation of regulators: Role of the complement factor H-related proteins. In Seminars in immunology (Vol. 45, p. 101341). Academic Press.

Csincsi, Á.I., Kopp, A., Zöldi, M., Bánlaki, Z., Uzonyi, B., Hebecker, M., Caesar, J.J., Pickering, M.C., Daigo, K., Hamakubo, T. and Lea, S.M., 2015. Factor H–related protein 5 interacts with pentraxin 3 and the extracellular matrix and modulates complement activation. The Journal of Immunology, 194(10), pp.4963-4973.

Csincsi, Á.I., Szabó, Z., Bánlaki, Z., Uzonyi, B., Cserhalmi, M., Kárpáti, É., Tortajada, A., Caesar, J.J., Prohászka, Z., Jokiranta, T.S. and Lea, S.M., 2017. FHR-1 binds to C-reactive protein and enhances rather than inhibits complement activation. The Journal of Immunology, 199(1), pp.292-303.

da Silva, D.V., Nordholm, J., Madjo, U., Pfeiffer, A. and Daniels, R., 2013. Assembly of subtype 1 influenza neuraminidase is driven by both the transmembrane and head domains. Journal of Biological Chemistry, 288(1), pp.644-653.

Daly, P., Gustafson, R. and Kendall, P., 2007. Introduction to pandemic influenza. British Columbia Medical Journal, 49(5), p.240.

Das, K., Aramini, J.M., Ma, L.C., Krug, R.M. and Arnold, E., 2010. Structures of influenza A proteins and insights into antiviral drug targets. Nature structural & molecular biology, 17(5), pp.530-538.

Dave, S., Pangburn, M.K., Pruitt, C. and McDaniel, L.S., 2004. Interaction of human factor H with PspC of Streptococcus pneumoniae. Indian Journal of Medical Research, 119, pp.66-73.

Dawson, W.K., Lazniewski, M. and Plewczynski, D., 2018. RNA structure interactions and ribonucleoprotein processes of the influenza A virus. Briefings in functional genomics, 17(6), pp.402-414.

De Jong, M.D., Simmons, C.P., Thanh, T.T., Hien, V.M., Smith, G.J., Chau, T.N.B., Hoang, D.M., Chau, N.V.V., Khanh, T.H., Dong, V.C. and Qui, P.T., 2006. Fatal outcome of human influenza A (H5N1) is associated with high viral load and hypercytokinemia. Nature medicine, 12(10), pp.1203-1207.

De Veer, M.J., Holko, M., Frevel, M., Walker, E., Der, S., Paranjape, J.M., Silverman, R.H. and Williams, B.R., 2001. Functional classification of interferon-stimulated genes identified using microarrays. Journal of leukocyte biology, 69(6), pp.912-920.

Deutsch, D.G. and Mertz, E.T., 1970. Plasminogen: purification from human plasma by affinity chromatography. Science, 170(3962), pp.1095-1096.

Diaz, A., Ferreira, A. and Sim, R.B., 1997. Complement evasion by Echinococcus granulosus: sequestration of host factor H in the hydatid cyst wall. The Journal of Immunology, 158(8), pp.3779-3786.

Dopler, A., Guntau, L., Harder, M.J., Palmer, A., Höchsmann, B., Schrezenmeier, H., Simmet, T., Huber-Lang, M. and Schmidt, C.Q., 2019. Self versus nonself discrimination by the soluble complement regulators Factor H and FHL-1. The Journal of Immunology, 202(7), pp.2082-2094.

Dou, D., Revol, R., Östbye, H., Wang, H. and Daniels, R., 2018. Influenza A virus cell entry, replication, virion assembly and movement. Frontiers in immunology, 9, p.1581.

DuBois, R.M., Zaraket, H., Reddivari, M., Heath, R.J., White, S.W. and Russell, C.J., 2011. Acid stability of the haemagglutinin protein regulates H5N1 influenza virus pathogenicity. PLoS Pathog, 7(12), p. e1002398.

Dunkelberger, J.R. and Song, W.C., 2010. Complement and its role in innate and adaptive immune responses. Cell research, 20(1), pp.34-50.

Duthy, T.G., Ormsby, R.J., Giannakis, E., Ogunniyi, A.D., Stroeher, U.H., Paton, J.C. and Gordon, D.L., 2002. The human complement regulator factor H binds pneumococcal surface protein PspC via short consensus repeats 13 to 15. Infection and immunity, 70(10), pp.5604-5611.

Eckersall, P.D., 2008. Proteins, proteomics, and the dysproteinemias. Clinical biochemistry of domestic animals, 6, pp.114-155.

Edinger, T.O., Pohl, M.O. and Stertz, S., 2014. Entry of influenza A virus: host factors and antiviral targets. Journal of General Virology, 95(2), pp.263-277.

Eisen, M.B., Sabesan, S., Skehel, J.J. and Wiley, D.C., 1997. Binding of the influenza A virus to cell-surface receptors: structures of five haemagglutinin–sialyloligosaccharide complexes determined by X-ray crystallography. Virology, 232(1), pp.19-31.

Eisfeld, A.J., Neumann, G. and Kawaoka, Y., 2015. At the centre: influenza A virus ribonucleoproteins. Nature Reviews Microbiology, 13(1), pp.28-41.

Eliopoulos, A.G., Gallagher, N.J., Blake, S.M., Dawson, C.W. and Young, L.S., 1999. Activation of the p38 mitogen-activated protein kinase pathway by Epstein-Barr virus-encoded latent membrane protein 1 coregulates interleukin-6 and interleukin-8 production. Journal of Biological Chemistry, 274(23), pp.16085-16096.

Fan, J., Chaturvedi, V. and Shen, S.H., 2002. Identification and phylogenetic analysis of a glucose transporter gene family from the human pathogenic yeast Candida albicans. Journal of molecular evolution, 55(3), pp.336-346.

Fenaille, F., Le Mignon, M., Groseil, C., Ramon, C., Riandé, S., Siret, L. and Bihoreau, N., 2007. Site-specific N-glycan characterization of human complement factor H. Glycobiology, 17(9), pp.932-944.

Ferreira, V.P., Pangburn, M.K. and Cortés, C., 2010. Complement control protein factor H: the good, the bad, and the inadequate. Molecular immunology, 47(13), pp.2187-2197.

Fleury, C., Su, Y.C., Hallström, T., Sandblad, L., Zipfel, P.F. and Riesbeck, K., 2014. Identification of a Haemophilus influenzae factor H–binding lipoprotein involved in serum resistance. The Journal of Immunology, 192(12), pp.5913-5923.

Fodor, E., 2013. The RNA polymerase of influenza a virus: mechanisms of viral transcription and replication. Acta Virol, 57(2), pp.113-122.

Franci, G., Palomba, L., Falanga, A., Zannella, C., D'Oriano, V., Rinaldi, L., Galdiero, S. and Galdiero, M., 2016. Influenza virus infections: clinical update, molecular biology, and therapeutic options. In the Microbiology of Respiratory System Infections (pp. 1-32). Academic Press.

Frank, H.S. and Franks, F., 1968. Structural approach to the solvent power of water for hydrocarbons; urea as a structure breaker. The Journal of Chemical Physics, 48(10), pp.4746-4757.

Friedrich, N., Santos, J.M., Liu, Y., Palma, A.S., Leon, E., Saouros, S., Kiso, M., Blackman, M.J., Matthews, S., Feizi, T. and Soldati-Favre, D., 2010. Members of a novel protein family containing microneme adhesive repeat domains act as sialic acid-binding lectins during host cell invasion by apicomplexan parasites. Journal of biological chemistry, 285(3), pp.2064-2076.

Frieman, M., Ratia, K., Johnston, R.E., Mesecar, A.D. and Baric, R.S., 2009. Severe acute respiratory syndrome coronavirus papain-like protease ubiquitin-like domain and catalytic domain regulate antagonism of IRF3 and NF-κB signaling. Journal of virology, 83(13), pp.6689-6705.

Friese, M.A., Hellwage, J., Jokiranta, T.S., Meri, S., Peter, H.H., Eibel, H. and Zipfel, P.F., 1999. FHL-1/reconectin and factor H: two human complement regulators which are encoded by the same gene are differently expressed and regulated. Molecular immunology, 36(13-14), pp.809-818.

Gao, R., Cao, B., Hu, Y., Feng, Z., Wang, D., Hu, W., Chen, J., Jie, Z., Qiu, H., Xu, K. and Xu, X., 2013. Human infection with a novel avian-origin influenza A (H7N9) virus. New England Journal of Medicine, 368(20), pp.1888-1897.

Garman, E. and Laver, G., 2005. The structure, function, and inhibition of influenza virus neuraminidase. In Viral Membrane Proteins: Structure, Function, and Drug Design (pp. 247-267). Springer US.

Gerl, M.J., Sampaio, J.L., Urban, S., Kalvodova, L., Verbavatz, J.M., Binnington, B., Lindemann, D., Lingwood, C.A., Shevchenko, A., Schroeder, C. and Simons, K., 2012. Quantitative analysis of the lipidomes of the influenza virus envelope and MDCK cell apical membrane. Journal of Cell Biology, 196(2), pp.213-221.

Gerloff, D.L., Creasey, A., Maslau, S. and Carter, R., 2005. Structural models for the protein family characterized by gamete surface protein Pfs230 of Plasmodium falciparum. Proceedings of the National Academy of Sciences, 102(38), pp.13598-13603.

Glezen, W.P. and Couch, R.B., 1997. Influenza viruses. In Viral infections of humans (pp. 473-505). Springer US.

Gong, J., Xu, W. and Zhang, J., 2007. Structure and functions of influenza virus neuraminidase. Current medicinal chemistry, 14(1), pp.113-122.

Goubau, D., Schlee, M., Deddouche, S., Pruijssers, A.J., Zillinger, T., Goldeck, M., Schuberth, C., Van der Veen, A.G., Fujimura, T., Rehwinkel, J. and Iskarpatyoti, J.A., 2014. Antiviral immunity via RIG-I-mediated recognition of RNA bearing 5′-diphosphates. Nature, 514(7522), pp.372-375.

Granoff, D.M., Welsch, J.A. and Ram, S., 2009. Binding of complement factor H (fH) to Neisseria meningitidis is specific for human fH and inhibits complement activation by rat and rabbit sera. Infection and immunity, 77(2), pp.764-769.

Griffiths, M.R., Neal, J.W., Fontaine, M., Das, T. and Gasque, P., 2009. Complement factor H, a marker of self protects against experimental autoimmune encephalomyelitis. The Journal of Immunology, 182(7), pp.4368-4377.

Guerry, P., Ewing, C.P., Hickey, T.E., Prendergast, M.M. and Moran, A.P., 2000. Sialylation of lipooligosaccharide cores affects immunogenicity and serum resistance of Campylobacter jejuni. Infection and immunity, 68(12), pp.6656-6662.

Ha, Y., Stevens, D.J., Skehel, J.J. and Wiley, D.C., 2001. X-ray structures of H5 avian and H9 swine influenza virus haemagglutinins bound to avian and human receptor analogs. Proceedings of the National Academy of Sciences, 98(20), pp.11181-11186.

Ha, Y., Stevens, D.J., Skehel, J.J. and Wiley, D.C., 2002. H5 avian and H9 swine influenza virus haemagglutinin structures: possible origin of influenza subtypes. The EMBO journal, 21(5), pp.865-875.

Haapasalo, K., Jarva, H., Siljander, T., Tewodros, W., Vuopio-Varkila, J. and Jokiranta, T.S., 2008. Complement factor H allotype 402H is associated with increased C3b opsonization and phagocytosis of Streptococcus pyogenes. Molecular microbiology, 70(3), pp.583-594.

Haapasalo, K., van Kessel, K., Nissilä, E., Metso, J., Johansson, T., Miettinen, S., Varjosalo, M., Kirveskari, J., Kuusela, P., Chroni, A. and Jauhiainen, M., 2015. Complement factor H binds to human serum apolipoprotein E and mediates complement regulation on high density lipoprotein particles. Journal of Biological Chemistry, 290(48), pp.28977-28987.

Hair, P.S., Gronemus, J.Q., Crawford, K.B., Salvi, V.P., Cunnion, K.M., Thielens, N.M., Arlaud, G.J., Rawal, N. and Krishna, N.K., 2010. Human astrovirus coat protein binds C1q and MBL and inhibits the classical and lectin pathways of complement activation. Molecular immunology, 47(4), pp.792-798.

Hakobyan, S., Harris, C.L., Tortajada, A., De Jorge, E.G., García-Layana, A., Fernández-Robredo, P., De Cordoba, S.R. and Morgan, B.P., 2008. Measurement of factor H variants in plasma using variant-specific monoclonal antibodies: application to assessing risk of age-related macular degeneration. Investigative ophthalmology & visual science, 49(5), pp.1983-1990.

Hale, B.G., Randall, R.E., Ortín, J. and Jackson, D., 2008. The multifunctional NS1 protein of influenza A viruses. Journal of general virology, 89(10), pp.2359-2376.

Hallström, T., Siegel, C., Mörgelin, M., Kraiczy, P., Skerka, C. and Zipfel, P.F., 2013. CspA from Borrelia burgdorferi inhibits the terminal complement pathway. MBio, 4(4), pp. e00481-13.

Hallström, T., Zipfel, P.F., Blom, A.M., Lauer, N., Forsgren, A. and Riesbeck, K., 2008. Haemophilus influenzae interacts with the human complement inhibitor factor H. The Journal of Immunology, 181(1), pp.537-545.

Hamilton, B.S., Chung, C., Cyphers, S.Y., Rinaldi, V.D., Marcano, V.C. and Whittaker, G.R., 2014. Inhibition of influenza virus infection and haemagglutinin cleavage by the protease inhibitor HAI-2. Biochemical and biophysical research communications, 450(2), pp.1070-1075.

Hammerschmidt, S., Agarwal, V., Kunert, A., Haelbich, S., Skerka, C. and Zipfel, P.F., 2007. The host immune regulator factor H interacts via two contact sites with the PspC protein of Streptococcus pneumoniae and mediates adhesion to host epithelial cells. The Journal of Immunology, 178(9), pp.5848-5858.

Han, T. and Marasco, W.A., 2011. Structural basis of influenza virus neutralization. Annals of the New York Academy of Sciences, 1217(1), pp.178-190.

Hannoun, C., 2013. The evolving history of influenza viruses and influenza vaccines. Expert review of vaccines, 12(9), pp.1085-1094.

Harvey, R., Wheeler, J.X., Wallis, C.L., Robertson, J.S. and Engelhardt, O.G., 2008. Quantitation of haemagglutinin in H5N1 influenza viruses reveals low haemagglutinin content of vaccine virus NIBRG-14 (H5N1). Vaccine, 26(51), pp.6550-6554.

Haupt, K., Reuter, M., van den Elsen, J., Burman, J., Hälbich, S., Richter, J., Skerka, C. and Zipfel, P.F., 2008. The Staphylococcus aureus protein Sbi acts as a complement inhibitor and forms a tripartite complex with host complement Factor H and C3b. PLoS pathogens, 4(12).

He, X.L., Grigg, M.E., Boothroyd, J.C. and Garcia, K.C., 2002. Structure of the immunodominant surface antigen from the Toxoplasma gondii SRS superfamily. Nature structural biology, 9(8), pp.606-611.

Heinekamp, T., Schmidt, H., Lapp, K., Pähtz, V., Shopova, I., Köster-Eiserfunke, N., Krüger, T., Kniemeyer, O. and Brakhage, A.A., 2015, March. Interference of Aspergillus fumigatus with the immune response. In Seminars in immunopathology (Vol. 37, No. 2, pp. 141-152). Springer Berlin Heidelberg.

Heldt, F.S., Frensing, T. and Reichl, U., 2012. Modeling the intracellular dynamics of influenza virus replication to understand the control of viral RNA synthesis. Journal of virology, 86(15), pp.7806-7817.

Hellwage, J., Meri, T., Heikkilä, T., Alitalo, A., Panelius, J., Lahdenne, P., Seppälä, I.J. and Meri, S., 2001. The complement regulator factor H binds to the surface protein OspE of Borrelia burgdorferi. Journal of Biological Chemistry, 276(11), pp.8427-8435.

Herbert, A.P., Makou, E., Chen, Z.A., Kerr, H., Richards, A., Rappsilber, J. and Barlow, P.N., 2015. Complement evasion mediated by enhancement of captured factor H: implications for protection of self-surfaces from complement. The Journal of Immunology, 195(10), pp.4986-4998.

Herfst, S., Imai, M., Kawaoka, Y. and Fouchier, R.A.M., 2014. Avian influenza virus transmission to mammals. In Influenza Pathogenesis and Control-Volume I (pp. 137-155). Springer International Publishing.

Herfst, S., Schrauwen, E.J., Linster, M., Chutinimitkul, S., de Wit, E., Munster, V.J., Sorrell, E.M., Bestebroer, T.M., Burke, D.F., Smith, D.J. and Rimmelzwaan, G.F., 2012. Airborne transmission of influenza A/H5N1 virus between ferrets. science, 336(6088), pp.1534-1541.

Hessing, M., Vlooswijk, R.A., Hackeng, T.M., Kanters, D. and Bouma, B.N., 1990. The localization of heparin-binding fragments on human C4b-binding protein. The Journal of Immunology, 144(1), pp.204-208.

Hiscott, J., Lin, R., Nakhaei, P. and Paz, S., 2006. Outstanding questions. Trends in Molecular Medicine, 2(12), pp.53-56.

Horstmann, R.D. and Müller-Eberhard, H.J., 1985. Isolation of rabbit C3, Factor B, and Factor H and comparison of their properties with those of the human analog. The Journal of Immunology, 134(2), pp.1094-1100.

Hovingh, E.S., van den Broek, B. and Jongerius, I., 2016. Hijacking complement regulatory proteins for bacterial immune evasion. Frontiers in microbiology, 7, p.2004.

Huang S, Chen J, Chen Q, Wang H, Yao Y, et al. (2013) A second CRM1-dependent nuclear export signal in the influenza A virus NS2 protein contributes to the nuclear export of viral ribonucleoproteins. J Virol 87: 767–778.

Hutchinson, E.C., von Kirchbach, J.C., Gog, J.R. and Digard, P., 2010. Genome packaging in influenza A virus. Journal of general virology, 91(2), pp.313-328.

Hyams, C., Trzcinski, K., Camberlein, E., Weinberger, D.M., Chimalapati, S., Noursadeghi, M., Lipsitch, M. and Brown, J.S., 2013. Streptococcus pneumoniae capsular serotype invasiveness correlates with the degree of factor H binding and opsonization with C3b/iC3b. Infection and immunity, 81(1), pp.354-363.

Irigoín, F., Laich, A., Ferreira, A.M., Fernández, C., Sim, R.B. and Díaz, A., 2008. Resistance of the Echinococcus granulosus cyst wall to complement activation: analysis of the role of InsP6 deposits. Parasite immunology, 30(6-7), pp.354-364.

Izaguirre, G., 2019. The proteolytic regulation of virus cell entry by furin and other proprotein convertases. Viruses, 11(9), p.837.

Janulczyk, R., Iannelli, F., Sjöholm, A.G., Pozzi, G. and Björck, L., 2000. Hic, a novel surface protein of Streptococcus pneumoniae that interferes with complement function. Journal of Biological Chemistry, 275(47), pp.37257-37263.

Jarva, H., Janulczyk, R., Hellwage, J., Zipfel, P.F., Björck, L. and Meri, S., 2002. Streptococcus pneumoniae evades complement attack and opsonophagocytosis by expressing the pspC locus-encoded Hic protein that binds to short consensus repeats 8–11 of factor H. The Journal of Immunology, 168(4), pp.1886-1894.

Jayasekera, J.P., Moseman, E.A. and Carroll, M.C., 2007. Natural antibody and complement mediate neutralization of influenza virus in the absence of prior immunity. Journal of virology, 81(7), pp.3487-3494.

Jegaskanda, S., Job, E.R., Kramski, M., Laurie, K., Isitman, G., de Rose, R., Winnall, W.R., Stratov, I., Brooks, A.G., Reading, P.C. and Kent, S.J., 2013. Cross-reactive influenza-specific antibody-dependent cellular cytotoxicity antibodies in the absence of neutralizing antibodies. The Journal of Immunology, 190(4), pp.1837-1848.

Jokiranta, T.S., Cheng, Z.Z., Seeberger, H., Jozsi, M., Heinen, S., Noris, M., Remuzzi, G., Ormsby, R., Gordon, D.L., Meri, S. and Hellwage, J., 2005. Binding of complement factor H to endothelial cells is mediated by the carboxy-terminal glycosaminoglycan binding site. The American journal of pathology, 167(4), pp.1173-1181.

Józsi, M., 2017. Factor H family proteins in complement evasion of microorganisms. Frontiers in Immunology, 8, p.571.

Józsi, M., and Zipfel, P.F. (2008) Factor H family proteins and human diseases. Trends Immunol 29: 380–387.

Józsi, M., Schneider, A.E., Kárpáti, É. and Sándor, N., 2019, January. Complement factor H family proteins in their non-canonical role as modulators of cellular functions. In Seminars in Cell & Developmental Biology (Vol. 85, pp. 122-131). Academic Press.

Jung, C., Lee, C.Y.F. and Grigg, M.E., 2004. The SRS superfamily of Toxoplasma surface proteins. International journal for parasitology, 34(3), pp.285-296.

Kaiser, L., Fritz, R.S., Straus, S.E., Gubareva, L. and Hayden, F.G., 2001. Symptom pathogenesis during acute influenza: interleukin-6 and other cytokine responses. Journal of medical virology, 64(3), pp.262-268.

Kaiser, L., Fritz, R.S., Straus, S.E., Gubareva, L. and Hayden, F.G., 2001. Symptom pathogenesis during acute influenza: interleukin-6 and other cytokine responses. Journal of medical virology, 64(3), pp.262-268.

Kajander, T., Lehtinen, M.J., Hyvärinen, S., Bhattacharjee, A., Leung, E., Isenman, D.E., Meri, S., Goldman, A. and Jokiranta, T.S., 2011. Dual interaction of factor H with C3d and glycosaminoglycans in host–nonhost discrimination by complement. Proceedings of the National Academy of Sciences, 108(7), pp.2897-2902.

Karakus U, Crameri M, Lanz C, Yángüez E. Propagation and Titration of Influenza Viruses. Methods Mol Biol. 2018; 1836:59-88. doi: 10.1007/978-1-4939-8678-1_4. PMID: 30151569.

Kapadia, S.B., Molina, H., Van Berkel, V., Speck, S.H. and Virgin, H.W., 1999. Murine gammaherpesvirus 68 encodes a functional regulator of complement activation. Journal of Virology, 73(9), pp.7658-7670.

Kauzmann, W., 1959. Some factors in the interpretation of protein denaturation. In Advances in protein chemistry (Vol. 14, pp. 1-63). Academic Press.

Kawai, T. and Akira, S., 2011. Toll-like receptors and their crosstalk with other innate receptors in infection and immunity. Immunity, 34(5), pp.637-650.

Kenedy, M.R., Vuppala, S.R., Siegel, C., Kraiczy, P. and Akins, D.R., 2009. CspA-mediated binding of human factor H inhibits complement deposition and confers serum resistance in Borrelia burgdorferi. Infection and immunity, 77(7), pp.2773-2782.

Kennedy, A.T., Schmidt, C.Q., Thompson, J.K., Weiss, G.E., Taechalertpaisarn, T., Gilson, P.R., Barlow, P.N., Crabb, B.S., Cowman, A.F. and Tham, W.H., 2016. Recruitment of factor H as a novel complement evasion strategy for blood-stage Plasmodium falciparum infection. The Journal of Immunology, 196(3), pp.1239-1248.

Kennedy, P.G. and Rodgers, J., 2019. Clinical and neuropathogenetic aspects of human African trypanosomiasis. Frontiers in immunology, 10, p.39.

Kenno, S., Speth, C., Rambach, G., Binder, U., Chatterjee, S., Caramalho, R., Haas, H., Lass-Flörl, C., Shaughnessy, J., Ram, S. and Gow, N.A., 2019. Candida albicans Factor H Binding Molecule Hgt1p–A Low Glucose-Induced Transmembrane Protein Is Trafficked to the Cell Wall and Impairs Phagocytosis and Killing by Human Neutrophils. Frontiers in microbiology, 9, p.3319.

Khattab, A., Barroso, M., Miettinen, T. and Meri, S., 2015. Anopheles midgut epithelium evades human complement activity by capturing factor H from the blood meal. PLoS neglected tropical diseases, 9(2).

Khatua, B., Ghoshal, A., Bhattacharya, K., Mandal, C., Saha, B., Crocker, P.R. and Mandal, C., 2010. Sialic acids acquired by Pseudomonas aeruginosa are involved in reduced complement deposition and siglec mediated host-cell recognition. FEBS letters, 584(3), pp.555-561.

Killick, J., Morisse, G., Sieger, D. and Astier, A.L., 2018, January. Complement as a regulator of adaptive immunity. In Seminars in immunopathology (Vol. 40, No. 1, pp. 37-48). Springer Berlin Heidelberg.

Klimov, Alexander, Amanda Balish, Vic Veguilla, Hong Sun, Jarad Schiffer, Xiuhua Lu, Jacqueline M. Katz, and Kathy Hancock. "Influenza virus titration, antigenic characterization, and serological methods for antibody detection." In Influenza Virus, pp. 25-51. Humana Press, 2012.

Kohler, S., Hallström, T., Singh, B., Riesbeck, K., Spartà, G., Zipfel, P.F. and Hammerschmidt, S., 2015. Binding of vitronectin and Factor H to Hic contributes to immune evasion of Streptococcus pneumoniae serotype 3. Thrombosis and haemostasis, 113(01), pp.125-142.

Kopp, A., Hebecker, M., Svobodová, E. and Józsi, M., 2012. Factor h: a complement regulator in health and disease, and a mediator of cellular interactions. Biomolecules, 2(1), pp.46-75.

Kordyukova, L.V., Shtykova, E.V., Baratova, L.A., Svergun, D.I. and Batishchev, O.V., 2019. Matrix proteins of enveloped viruses: a case study of Influenza A virus M1 protein. Journal of Biomolecular Structure and Dynamics, 37(3), pp.671-690.

Korotaevskiy, A.A., Hanin, L.G. and Khanin, M.A., 2009. Non-linear dynamics of the complement system activation. Mathematical biosciences, 222(2), pp.127-143.

Kosik, I. and Yewdell, J.W., 2019. Influenza haemagglutinin and neuraminidase: Yin–Yang proteins coevolving to thwart immunity. Viruses, 11(4), p.346.

Kraiczy, P. and Würzner, R., 2006. Complement escape of human pathogenic bacteria by acquisition of complement regulators. Molecular immunology, 43(1-2), pp.31-44.

Kraiczy, P., Hartmann, K., Hellwage, J., Skerka, C., Kirschfink, M., Brade, V., Zipfel, P.F., Wallich, R. and Stevenson, B., 2004. Immunological characterization of the complement regulator factor H-binding CRASP and Erp proteins of Borrelia burgdorferi. International Journal of Medical Microbiology Supplements, 293, pp.152-157.

Krammer, F., Smith, G.J., Fouchier, R.A., Peiris, M., Kedzierska, K., Doherty, P.C., Palese, P., Shaw, M.L., Treanor, J., Webster, R.G. and García-Sastre, A., 2018. Influenza (Primer). Nature Reviews: Disease Primers.

Krejcova, L., Michalek, P., Hynek, D., Adam, V. and Kizek, R., 2015. Structure of influenza viruses, connected with influenza life cycle. Journal of Metallomics and Nanotechnologies, 1, pp.13-19.

Kristensen, T. and Tack, B.F., 1986. Murine protein H is comprised of 20 repeating units, 61 amino acids in length. Proceedings of the National Academy of Sciences, 83(11), pp.3963-3967.

Kühn, S., Skerka, C. and Zipfel, P.F., 1995. Mapping of the complement regulatory domains in the human factor H-like protein 1 and in factor H1. The Journal of Immunology, 155(12), pp.5663-5670.

Kulkarni, H.S., Liszewski, M.K., Brody, S.L. and Atkinson, J.P., 2018. The complement system in the airway epithelium: An overlooked host defense mechanism and therapeutic target?. Journal of Allergy and Clinical Immunology, 141(5), pp.1582-1586.

Kuszewski, K. and Brydak, L., 2000. The epidemiology and history of influenza. Biomedicine & pharmacotherapy, 54(4), pp.188-195.

La Gruta, N.L., Kedzierska, K., Stambas, J. and Doherty, P.C., 2007. A question of self-preservation: immunopathology in influenza virus infection. Immunology and cell biology, 85(2), pp.85-92.

Lam, T.T., Nguyen, T.P., Montgomery, R.R., Kantor, F.S., Fikrig, E. and Flavell, R.A., 1994. Outer surface proteins E and F of Borrelia burgdorferi, the agent of Lyme disease. Infection and immunity, 62(1), pp.290-298.

Lamb, R.A. and Lai, C.J., 1980. Sequence of interrupted and uninterrupted mRNAs and cloned DNA coding for the two overlapping nonstructural proteins of influenza virus. Cell, 21(2), pp.475-485.

Langereis, J.D., de Jonge, M.I. and Weiser, J.N., 2014. Binding of human factor H to outer membrane protein P 5 of non-typeable H aemophilus influenzae contributes to complement resistance. Molecular microbiology, 94(1), pp.89-106.

Lawrenz, M., Wereszczynski, J., Amaro, R., Walker, R., Roitberg, A. and McCammon, J.A., 2010. Impact of calcium on N1 influenza neuraminidase dynamics and binding free energy. Proteins: Structure, Function, and Bioinformatics, 78(11), pp.2523-2532.

Lazniewski, M., Dawson, W.K., Szczepińska, T. and Plewczynski, D., 2018. The structural variability of the influenza A haemagglutinin receptor-binding site. Briefings in functional genomics, 17(6), pp.415-427.

Le Goffic, R., Pothlichet, J., Vitour, D., Fujita, T., Meurs, E., Chignard, M. and Si-Tahar, M., 2007. Cutting Edge: Influenza A virus activates TLR3-dependent inflammatory and RIG-I-dependent antiviral responses in human lung epithelial cells. The Journal of Immunology, 178(6), pp.3368-3372.

Lee, H.S., Qi, Y. and Im, W., 2015. Effects of N-glycosylation on protein conformation and dynamics: Protein Data Bank analysis and molecular dynamics simulation study. Scientific reports, 5, p.8926.

Lenartowicz, E., Kesy, J., Ruszkowska, A., Soszynska-Jozwiak, M., Michalak, P., Moss, W.N., Turner, D.H., Kierzek, R. and Kierzek, E., 2016. Self-folding of naked segment 8 genomic RNA of influenza A virus. PLoS One, 11(2), p.e0148281.

Lesiak-Markowicz, I., Vogl, G., Schwarzmüller, T., Speth, C., Lass-Flörl, C., Dierich, M.P., Kuchler, K. and Würzner, R., 2011. Candida albicans Hgt1p, a Multifunctional Evasion Molecule: Complement Inhibitor, CR3 Analogue, and Human Immunodeficiency Virus–Binding Molecule. Journal of Infectious Diseases, 204(5), pp.802-809.

Lewis, L.A., Ngampasutadol, J., Wallace, R., Reid, J.E., Vogel, U. and Ram, S., 2010. The meningococcal vaccine candidate neisserial surface protein A (NspA) binds to factor H and enhances meningococcal resistance to complement. PLoS pathogens, 6(7).

Li, C., Xu, K., Hashem, A., Shao, M., Liu, S., Zou, Y., Gao, Q., Zhang, Y., Yuan, L., Xu, M. and Li, X., 2015. Collaborative studies on the development of national reference standards for potency determination of H7N9 influenza vaccine. Human vaccines & immunotherapeutics, 11(6), pp.1351-1356.

Li, J., Yu, M., Zheng, W. and Liu, W., 2015. Nucleocytoplasmic shuttling of influenza A virus proteins. Viruses, 7(5), pp.2668-2682.

Liao, Q., Qian, Z., Liu, R., An, L. and Chen, X., 2013. Germacrone inhibits early stages of influenza virus infection. Antiviral research, 100(3), pp.578-588.

Licht, C., Weyersberg, A., Heinen, S., Stapenhorst, L., Devenge, J., Beck, B., Waldherr, R., Kirschfink, M., Zipfel, P.F. and Hoppe, B., 2005. Successful plasma therapy for atypical hemolytic uremic syndrome caused by factor H deficiency owing to a novel mutation in the complement cofactor protein domain 15. American journal of kidney Diseases, 45(2), pp.415-421.

Lin, B., Qing, X., Liao, J. and Zhuo, K., 2020. Role of Protein Glycosylation in Host-Pathogen Interaction. Cells, 9(4), p.1022.

Lin, Y.P., Xiong, X., Wharton, S.A., Martin, S.R., Coombs, P.J., Vachieri, S.G., Christodoulou, E., Walker, P.A., Liu, J., Skehel, J.J. and Gamblin, S.J., 2012. Evolution of the receptor binding properties of the influenza A (H3N2) haemagglutinin. Proceedings of the National Academy of Sciences, 109(52), pp.21474-21479.

Lingwood, D. and Simons, K., 2010. Lipid rafts as a membrane-organizing principle. science, 327(5961), pp.46-50.

Liszewski, M.K., Farries, T.C., Lublin, D.M., Rooney, I.A. and Atkinson, J.P., 1996. Control of the complement system. Advances in immunology, 61, pp.201-283.

Liszewski, M.K., Leung, M.K., Hauhart, R., Buller, R.M.L., Bertram, P., Wang, X., Rosengard, A.M., Kotwal, G.J. and Atkinson, J.P., 2006. Structure and regulatory profile of the monkeypox inhibitor of complement: comparison to homologs in vaccinia and variola and evidence for dimer formation. The Journal of Immunology, 176(6), pp.3725-3734.

Luczo, J.M., Tachedjian, M., Harper, J.A., Payne, J.S., Butler, J.M., Sapats, S.I., Lowther, S.L., Michalski, W.P., Stambas, J. and Bingham, J., 2018. Evolution of high pathogenicity of H5 avian influenza virus: haemagglutinin cleavage site selection of reverse-genetics mutants during passage in chickens. Scientific reports, 8(1), pp.1-13.

Locht, C., 2016. Pertussis: where did we go wrong and what can we do about it? Journal of Infection, 72, pp. S34-S40.

Longping, V.T. and Whittaker, G.R., 2015. Modification of the haemagglutinin cleavage site allows indirect activation of avian influenza virus H9N2 by bacterial staphylokinase. Virology, 482, pp.1-8.

Longping, V.T., Marcano, V.C., Huang, W., Pocwierz, M.S. and Whittaker, G.R., 2013. Plasmin-mediated activation of pandemic H1N1 influenza virus haemagglutinin is independent of the viral neuraminidase. Journal of virology, 87(9), pp.5161-5169.

Losse, J., Zipfel, P.F. and Józsi, M., 2010. Factor H and factor H-related protein 1 bind to human neutrophils via complement receptor 3, mediate attachment to Candida albicans, and enhance neutrophil antimicrobial activity. The journal of immunology, 184(2), pp.912-921.

Lund JM, Alexopoulou L, Sato A, Karow M, Adams NC, Gale NW, et al. Recognition of single-stranded RNA viruses by toll-like receptor 7. Proc Natl Acad Sci U S A (2004) 101(15):5598–603. doi:10.1073/pnas.0400937101

Macleod, O.J., Bart, J.M., MacGregor, P., Peacock, L., Savill, N.J., Hester, S., Ravel, S., Sunter, J.D., Trevor, C., Rust, S. and Vaughan, T.J., 2020. A receptor for the complement regulator factor H increases transmission of trypanosomes to tsetse flies. Nature communications, 11(1), pp.1-12.

Macleod, O.J., Bart, J.M., MacGregor, P., Peacock, L., Savill, N.J., Hester, S., Ravel, S., Sunter, J.D., Trevor, C., Rust, S. and Vaughan, T.J., 2020. A receptor for the complement regulator factor H increases transmission of trypanosomes to tsetse flies. Nature communications, 11(1), pp.1-12.

McAuley, J.L., Gilbertson, B.P., Trifkovic, S., Brown, L.E. and McKimm-Breschkin, J.L., 2019. Influenza virus neuraminidase structure and functions. Frontiers in microbiology, 10, p.39.

Madico, G., Welsch, J.A., Lewis, L.A., McNaughton, A., Perlman, D.H., Costello, C.E., Ngampasutadol, J., Vogel, U., Granoff, D.M. and Ram, S., 2006. The meningococcal vaccine candidate GNA1870 binds the complement regulatory protein factor H and enhances serum resistance. The Journal of Immunology, 177(1), pp.501-510.

Maginnis, M.S., 2018. Virus–receptor interactions: the key to cellular invasion. Journal of molecular biology, 430(17), pp.2590-2611.

Maher, J.A. and DeStefano, J., 2004. The ferret: an animal model to study influenza virus. Lab animal, 33(9), pp.50-53.

Mair, C.M., Ludwig, K., Herrmann, A. and Sieben, C., 2014. Receptor binding and pH stability—how influenza A virus haemagglutinin affects host-specific virus infection. Biochimica et Biophysica Acta (BBA)-Biomembranes, 1838(4), pp.1153-1168.

Mair, C.M., Ludwig, K., Herrmann, A. and Sieben, C., 2014. Receptor binding and pH stability—how influenza A virus haemagglutinin affects host-specific virus infection. Biochimica et Biophysica Acta (BBA)-Biomembranes, 1838(4), pp.1153-1168.

Makou, E., Herbert, A.P. and Barlow, P.N., 2013. Functional anatomy of complement factor H. Biochemistry, 52(23), pp.3949-3962.

Makou, E., Herbert, A.P. and Barlow, P.N., 2013. Functional anatomy of complement factor H. Biochemistry, 52(23), pp.3949-3962.

Malhotra, R., Ward, M., Sim, R.B. and Bird, M.I., 1999. Identification of human complement Factor H as a ligand for L-selectin. Biochemical Journal, 341(1), pp.61-69.

Mandal, N.A. and Ayyagari, R., 2006. Complement factor H: spatial and temporal expression and localization in the eye. Investigative ophthalmology & visual science, 47(9), pp.4091-4097.

Mandal, N.A. and Ayyagari, R., 2006. Complement factor H: spatial and temporal expression and localization in the eye. Investigative ophthalmology & visual science, 47(9), pp.4091-4097.

Marc, D., 2014. Influenza virus non-structural protein NS1: interferon antagonism and beyond. Journal of General Virology, 95(12), pp.2594-2611.

Martinez, A., Pio, R., Zipfel, P.F. and Cuttitta, F., 2003. Mapping of the adrenomedullin-binding domains in human complement factor H. Hypertension Research, 26(Suppl), pp. S55-S59.

Matrosovich, M., Stech, J. and Dieter Klenk, H., 2009. Influenza receptors, polymerase and host range. Revue scientifique et technique, 28(1), p.203.

Matrosovich, M.N., Gambaryan, A.S., Teneberg, S., Piskarev, V.E., Yamnikova, S.S., Lvov, D.K., Robertson, J.S. and Karlsson, K.A., 1997. Avian influenza A viruses differ from human viruses by recognition of sialyloligosaccharides and gangliosides and by a higher conservation of the HA receptor-binding site. Virology, 233(1), pp.224-234.

Matrosovich, M.N., Matrosovich, T.Y., Gray, T., Roberts, N.A. and Klenk, H.D., 2004. Neuraminidase is important for the initiation of influenza virus infection in human airway epithelium. Journal of virology, 78(22), pp.12665-12667.

McAuley, J.L., Gilbertson, B.P., Trifkovic, S., Brown, L.E. and McKimm-Breschkin, J.L., 2019. Influenza virus neuraminidase structure and functions. Frontiers in microbiology, 10, p.39.

Meischel, T., Villalon-Letelier, F., Saunders, P.M., Reading, P.C. and Londrigan, S.L., 2020. Influenza A virus interactions with macrophages: Lessons from epithelial cells. Cellular Microbiology, 22(5), p.e13170.

Melin M, Di Paolo E, Tikkanen L, Jarva H, Neyt C, Käyhty H, Meri S, Poolman J, Väkeväinen M. Interaction of pneumococcal histidine triad proteins with human complement. Infection and immunity. 2010 May 1;78(5):2089-98.

Memorandums, M.L., 1980. A revision of the system of nomenclature for influenza viruses: a WHO memorandum. Bulletin ofthe World Health Organization, 58(4), pp.585-591.

Meri, S., Jördens, M. and Jarva, H., 2008. Microbial complement inhibitors as vaccines. Vaccine, 26, pp.I113-I117.

Meri, T., Amdahl, H., Lehtinen, M.J., Hyvärinen, S., McDowell, J.V., Bhattacharjee, A., Meri, S., Marconi, R., Goldman, A. and Jokiranta, T.S., 2013. Microbes bind complement inhibitor factor H via a common site. PLoS pathogens, 9(4).

Meri, T., Blom, A.M., Hartmann, A., Lenk, D., Meri, S. and Zipfel, P.F., 2004. The hyphal and yeast forms of Candida albicans bind the complement regulator C4b-binding protein. Infection and immunity, 72(11), pp.6633-6641.

Meri, T., Hartmann, A., Lenk, D., Eck, R., Würzner, R., Hellwage, J., Meri, S. and Zipfel, P.F., 2002. The yeast Candida albicans binds complement regulators factor H and FHL-1. Infection and immunity, 70(9), pp.5185-5192.

Misasi, R., Huemer, H.P., Schwaeble, W., Sölder, E., Larcher, C. and Dierich, M.P., 1989. Human complement factor H: An additional gene product of 43kDa isolated from human plasma shows cofactor activity for the cleavage of the third component of complement. European journal of immunology, 19(9), pp.1765-1768.

Miyake, Y., Ishii, K. and Honda, A., 2017. Influenza virus infection induces host pyruvate kinase M which interacts with viral RNA-dependent RNA polymerase. Frontiers in microbiology, 8, p.162.

Mögling, R., Richard, M.J., van der Vliet, S., van Beek, R., Schrauwen, E.J., Spronken, M.I., Rimmelzwaan, G.F. and Fouchier, R.A., 2017. Neuraminidase-mediated haemagglutination of recent human influenza A (H3N2) viruses is determined by arginine 150 flanking the neuraminidase catalytic site. The Journal of general virology, 98(6), p.1274.

Monteiro, V.G., Soares, C.P. and De Souza, W., 1998. Host cell surface sialic acid residues are involved on the process of penetration of Toxoplasma gondii into mammalian cells. FEMS microbiology letters, 164(2), pp.323-327.

Moreno-Navarrete, J.M., Martínez-Barricarte, R., Catalán, V., Sabater, M., Gómez-Ambrosi, J., Ortega, F.J., Ricart, W., Blüher, M., Frühbeck, G., de Cordoba, S.R. and Fernández-Real, J.M., 2010. Complement factor H is expressed in adipose tissue in association with insulin resistance. Diabetes, 59(1), pp.200-209.

Morse, S.S., 2007. Pandemic influenza: studying the lessons of history. Proceedings of the National Academy of Sciences, 104(18), pp.7313-7314.

Mostafa, A., Abdelwhab, E.M., Mettenleiter, T.C. and Pleschka, S., 2018. Zoonotic potential of influenza A viruses: a comprehensive overview. Viruses, 10(9), p.497.

Moulès, V., Terrier, O., Yver, M., Riteau, B., Moriscot, C., Ferraris, O., Julien, T., Giudice, E., Rolland, J.P., Erny, A. and Bouscambert-Duchamp, M., 2011. Importance of viral genomic composition in modulating glycoprotein content on the surface of influenza virus particles. Virology, 414(1), pp.51-62.

Moulton, E.A., Bertram, P., Chen, N., Buller, R.M.L. and Atkinson, J.P., 2010. Ectromelia virus inhibitor of complement enzymes protects intracellular mature virus and infected cells from mouse complement. Journal of virology, 84(18), pp.9128-9139.

Mullick, J., Bernet, J., Singh, A.K., Lambris, J.D. and Sahu, A., 2003. Kaposi's sarcoma-associated herpesvirus (human herpesvirus 8) open reading frame 4 protein (kaposica) is a functional homolog of complement control proteins. Journal of Virology, 77(6), pp.3878-3881.

Mullick, J., Kadam, A. and Sahu, A., 2003. Herpes and pox viral complement control proteins:'the mask of self'. Trends in immunology, 24(9), pp.500-507.

Munir, M., 2010. TRIM proteins: another class of viral victims. Science signaling, 3(118), pp.jc2-jc2.

Muñoz Carrillo, J.L., Castro García, F.P., Gutiérrez Coronado, O., Moreno García, M.A. and Contreras Cordero, J.F., 2017. Physiology and pathology of innate immune response against pathogens.

Nakaya, Y., Fukuda, T., Ashiba, H., Yasuura, M. and Fujimaki, M., 2020. Quick assessment of influenza a virus infectivity with a long-range reverse-transcription quantitative polymerase chain reaction assay. BMC Infectious Diseases, 20(1), pp.1-10.

Nasreen, S., Khan, S.U., Azziz-Baumgartner, E., Hancock, K., Veguilla, V., Wang, D., Rahman, M., Alamgir, A.S.M., Sturm-Ramirez, K., Gurley, E.S. and Luby, S.P., 2013. Seroprevalence of antibodies against highly pathogenic avian influenza A (H5N1) virus among poultry workers in Bangladesh, 2009. PLoS One, 8(9), p.e73200

Nathan, K.G. and Lal, S.K., 2020. The multifarious role of 14-3-3 family of proteins in viral replication. Viruses, 12(4), p.436.

Neumann G, Hughes MT, Kawaoka Y (2000) Influenza A virus NS2 protein mediates vRNP nuclear export through NES-independent interaction with hCRM1. EMBO J 19: 6751–6758. 84.

Ngampasutadol, J., Ram, S., Gulati, S., Agarwal, S., Li, C., Visintin, A., Monks, B., Madico, G. and Rice, P.A., 2008. Human factor H interacts selectively with Neisseria gonorrhoeae and results in species-specific complement evasion. The Journal of Immunology, 180(5), pp.3426-3435.

Nicholls, J.M., Chan, R.W., Russell, R.J., Air, G.M. and Peiris, J.M., 2008. Evolving complexities of influenza virus and its receptors. Trends in microbiology, 16(4), pp.149-157.

Noda T. Native morphology of influenza virions. Frontiers in microbiology. 2012 Jan 3; 2:269.

Noton, S.L., Medcalf, E., Fisher, D., Mullin, A.E., Elton, D. and Digard, P., 2007. Identification of the domains of the influenza A virus M1 matrix protein required for NP binding, oligomerization and incorporation into virions. The Journal of general virology, 88(Pt 8), p.2280.

Okemefuna, A.I., Nan, R., Miller, A., Gor, J. and Perkins, S.J., 2010. Complement factor H binds at two independent sites to C-reactive protein in acute phase concentrations. Journal of Biological Chemistry, 285(2), pp.1053-1065.

Olivar, R., Luque, A., Cárdenas-Brito, S., Naranjo-Gómez, M., Blom, A.M., Borràs, F.E., De Córdoba, S.R., Zipfel, P.F. and Aran, J.M., 2016. The complement inhibitor factor H generates an anti-inflammatory and tolerogenic state in monocyte-derived dendritic cells. The Journal of Immunology, 196(10), pp.4274-4290.

Olivar, R., Luque, A., Cárdenas-Brito, S., Naranjo-Gómez, M., Blom, A.M., Borràs, F.E., De Córdoba, S.R., Zipfel, P.F. and Aran, J.M., 2016. The complement inhibitor factor H generates an anti-inflammatory and tolerogenic state in monocyte-derived dendritic cells. The Journal of Immunology, 196(10), pp.4274-4290.

Oppermann, M., Manuelian, T., Józsi, M., Brandt, E., Jokiranta, T.S., Heinen, S., Meri, S., Skerka, C., Götze, O. and Zipfel, P.F., 2006. The C-terminus of complement regulator Factor H mediates target recognition: evidence for a compact conformation of the native protein. Clinical & Experimental Immunology, 144(2), pp.342-352.

Ortega-Barria, E. and Boothroyd, J.C., 1999. A Toxoplasma lectin-like activity specific for sulfated polysaccharides is involved in host cell infection. Journal of Biological Chemistry, 274(3), pp.1267-1276.

Ouyang J, Zhu X, Chen Y, Wei H, Chen Q, Chi X, et al. NRAV, a long noncoding RNA, modulates antiviral responses through suppression of interferon-stimulated gene transcription. Cell Host Microbe (2014) 16(5):616–26. doi:10.1016/j.chom.2014.10.001

Oxford, J.S., Corcoran, T., Knott, R., Bates, J., Bartolomei, O., Major, D., Newman, R.W., Yates, P., Robertson, J., Webster, R.G. and Schild, G.C., 1987. Serological studies with influenza A (H1N1) viruses cultivated in eggs or in a canine kidney cell line (MDCK). Bulletin of the World Health Organization, 65(2), p.181.

Oxford, J.S., Newman, R., Corcoran, T., Bootman, J., Major, D., Yates, P., Robertson, J. and Schild, G.C., 1991. Direct isolation in eggs of influenza A (H1N1) and B viruses with haemagglutinins of different antigenic and amino acid composition. Journal of general virology, 72(1), pp.185-189.

Pangburn, M.K., 2000. Host recognition and target differentiation by factor H, a regulator of the alternative pathway of complement. Immunopharmacology, 49(1-2), pp.149-157.

Pangburn, M.K., 2002. Cutting edge: localization of the host recognition functions of complement factor H at the carboxyl-terminal: implications for hemolytic uremic syndrome. The Journal of Immunology, 169(9), pp.4702-4706.

Pangburn, M.K., Atkinson, M.A. and Meri, S., 1991. Localization of the heparin-binding site on complement factor H. Journal of Biological Chemistry, 266(25), pp.16847-16853.

Parente, R., Clark, S.J., Inforzato, A. and Day, A.J., 2017. Complement factor H in host defense and immune evasion. Cellular and Molecular Life Sciences, 74(9), pp.1605-1624.

Parente, R., Clark, S.J., Inforzato, A. and Day, A.J., 2017. Complement factor H in host defense and immune evasion. Cellular and Molecular Life Sciences, pp.1-20.

Paterson, D. and Fodor, E., 2012. Emerging roles for the influenza A virus nuclear export protein (NEP). PLoS Pathog, 8(12), p.e1003019.

Pawer, S.D., Parkhi, S.S., Koratkar, S.S. and Mishra, A.C., 2012. Receptor specificity and erythrocyte binding preferences of avian influenza viruses isolated from India. Virology journal, 9(1), p.251.

Payne, S., 2017. Methods to study viruses. Viruses, p.37.

Peiris, J.S.M., Cheung, C.Y., Leung, C.Y.H. and Nicholls, J.M., 2009. Innate immune responses to influenza A H5N1: friend or foe?. Trends in immunology, 30(12), pp.574-584.

Peng, X., Alföldi, J., Gori, K., Eisfeld, A.J., Tyler, S.R., Tisoncik-Go, J., Brawand, D., Law, G.L., Skunca, N., Hatta, M. and Gasper, D.J., 2014. The draft genome sequence of the ferret (Mustela putorius furo) facilitates study of human respiratory disease. Nature biotechnology, 32(12), pp.1250-1255.

Perkins, S.J., Fung, K.W. and Khan, S., 2014. Molecular interactions between complement factor H and its heparin and heparan sulfate ligands. Frontiers in immunology, 5, p.126.

Perkins, S.J., Okemefuna, A.I., Nan, R., Li, K. and Bonner, A., 2009. Constrained solution scattering modelling of human antibodies and complement proteins reveals novel biological insights. Journal of The Royal Society Interface, 6(suppl_5), pp. S679-S696.

Pflug, A., Guilligay, D., Reich, S. and Cusack, S., 2014. Structure of influenza A polymerase bound to the viral RNA promoter. Nature, 516(7531), pp.355-360.

Pflug, A., Lukarska, M., Resa-Infante, P., Reich, S. and Cusack, S., 2017. Structural insights into RNA synthesis by the influenza virus transcription-replication machine. Virus research, 234, pp.103-117.

Phung, T.T., Luong, S.T., Kawachi, S., Nunoi, H., Nguyen, L.T., Nakayama, T. and Suzuki, K., 2011. Interleukin 12 and myeloperoxidase (MPO) in Vietnamese children with acute respiratory distress syndrome due to Avian influenza (H5N1) infection. Journal of Infection, 62(1), pp.104-106.

Phung, T.T.B., Sugamata, R., Uno, K., Aratani, Y., Ozato, K., Kawachi, S., Thanh Nguyen, L., Nakayama, T. and Suzuki, K., 2011. Key role of regulated upon activation normal T-cell expressed and secreted, nonstructural protein1 and myeloperoxidase in cytokine storm induced by influenza virus PR-8 (A/H1N1) infection in A549 bronchial epithelial cells. Microbiology and immunology, 55(12), pp.874-884.

Pichlmair, A., Schulz, O., Tan, C.P., Näslund, T.I., Liljeström, P., Weber, F. and e Sousa, C.R., 2006. RIG-I-mediated antiviral responses to single-stranded RNA bearing 5'-phosphates. Science, 314(5801), pp.997-1001.

Pío, R., Martínez, A., Unsworth, E.J., Kowalak, J.A., Bengoechea, J.A., Zipfel, P.F., Elsasser, T.H. and Cuttitta, F., 2001. Complement factor H is a serum-binding protein for adrenomedullin, and the resulting complex modulates the bioactivities of both partners. Journal of Biological Chemistry, 276(15), pp.12292-12300.

Ponte-Sucre, A., 2016. An overview of Trypanosoma brucei infections: an intense host–parasite interaction. Frontiers in microbiology, 7, p.2126.

Potter, C.W., 2001. A history of influenza. Journal of applied microbiology, 91(4), pp.572-579.

Pouw, R.B., Brouwer, M.C., Geissler, J., van Herpen, L.V., Zeerleder, S.S., Wuillemin, W.A., Wouters, D. and Kuijpers, T.W., 2016. Complement factor H-related protein 3 serum levels are low compared to factor H and mainly determined by gene copy number variation in CFHR3. PLoS One, 11(3).

Pouw, R.B., Vredevoogd, D.W., Kuijpers, T.W. and Wouters, D., 2015. Of mice and men: the factor H protein family and complement regulation. Molecular immunology, 67(1), pp.12-20.

Pradel, G., 2007. Proteins of the malaria parasite sexual stages: expression, function and potential for transmission blocking strategies. Parasitology, 134(14), pp.1911-1929.

Principato, S., Pizza, M. and Rappuoli, R., 2020. Meningococcal factor H binding protein as immune evasion factor and vaccine antigen. FEBS letters.

Pyle, G.F., 1986. The diffusion of influenza: patterns and paradigms. Rowman & Littlefield.

Rachakonda, P.S., Veit, M., Korte, T., Ludwig, K., Böttcher, C., Huang, Q., Schmidt, M.F. and Herrmann, A., 2007. The relevance of salt bridges for the stability of the influenza virus haemagglutinin. The FASEB Journal, 21(4), pp.995-1002.

Rehwinkel, J., Tan, C.P., Goubau, D., Schulz, O., Pichlmair, A., Bier, K., Robb, N., Vreede, F., Barclay, W., Fodor, E. and e Sousa, C.R., 2010. RIG-I detects viral genomic RNA during negative-strand RNA virus infection. Cell, 140(3), pp.397-408.

Reich, S., Guilligay, D. and Cusack, S., 2017. An in vitro fluorescence based study of initiation of RNA synthesis by influenza B polymerase. Nucleic acids research, 45(6), pp.3353-3368.

Ricklin, D., Hajishengallis, G., Yang, K. and Lambris, J.D., 2010. Complement: a key system for immune surveillance and homeostasis. Nature immunology, 11(9), pp.785-797.

Ripoche, J., Al Salihi, A., Rousseaux, J. and Fontaine, M., 1984. Isolation of two molecular populations of human complement factor H by hydrophobic affinity chromatography. Biochemical Journal, 221(1), pp.89-96.

Ripoche, J., Day, A.J., Harris, T.J. and Sim, R.B., 1988. The complete amino acid sequence of human complement factor H. Biochemical Journal, 249(2), pp.593-602.

Robertson, J.S., Bootman, J.S., Newman, R., Oxford, J.S., Daniels, R.S., Webster, R.G. and Schild, G.C., 1987. Structural changes in the haemagglutinin which accompany egg adaptation of an influenza A (H1N1) virus. Virology, 160(1), pp.31-37.

Rogers, G.N., Paulson, J.C., Daniels, R.S., Skehel, J.J., Wilson, I.A. and Wiley, D.C., 1983. Single amino acid substitutions in influenza haemagglutinin change receptor binding specificity. Nature, 304(5921), pp.76-78.

Rosa, T.F., Flammersfeld, A., Ngwa, C.J., Kiesow, M., Fischer, R., Zipfel, P.F., Skerka, C. and Pradel, G., 2016. The Plasmodium falciparum blood stages acquire factor H family proteins to evade destruction by human complement. Cellular microbiology, 18(4), pp.573-590.

Rosengard, A.M., Liu, Y., Nie, Z. and Jimenez, R., 2002. Variola virus immune evasion design: expression of a highly efficient inhibitor of human complement. Proceedings of the National Academy of Sciences, 99(13), pp.8808-8813.

Rossman, J.S. and Lamb, R.A., 2011. Influenza virus assembly and budding. Virology, 411(2), pp.229-236.

Rossman, J.S. and R.A. Lamb, Viral membrane scission. Annu Rev Cell Dev Biol, 2013. 29: p. 551-69.

Rossman, J.S., Jing, X., Leser, G.P. and Lamb, R.A., 2010. Influenza virus M2 protein mediates ESCRT-independent membrane scission. Cell, 142(6), pp.902-913.

Roy, A.M.M., Parker, J.S., Parrish, C.R. and Whittaker, G.R., 2000. Early stages of influenza virus entry into Mv-1 lung cells: involvement of dynamin. Virology, 267(1), pp.17-28.

Ruiz-Sáenz, J., Goez, Y., Tabares, W. and López-Herrera, A., 2009. Cellular receptors for foot and mouth disease virus. Intervirology, 52(4), pp.201-212.

Sahu, A., Isaacs, S.N., Soulika, A.M. and Lambris, J.D., 1998. Interaction of vaccinia virus complement control protein with human complement proteins: factor I-mediated degradation of C3b to iC3b1 inactivates the alternative complement pathway. The Journal of Immunology, 160(11), pp.5596-5604.

Sakai, T., Nishimura, S.I., Naito, T. and Saito, M., 2017. Influenza A virus haemagglutinin and neuraminidase act as novel motile machinery. Scientific reports, 7, p.45043.

Salvi, G., De Los Rios, P. and Vendruscolo, M., 2005. Effective interactions between chaotropic agents and proteins. Proteins: Structure, Function, and Bioinformatics, 61(3), pp.492-499.

Samji, T., 2009. Influenza A: understanding the viral life cycle. The Yale journal of biology and medicine, 82(4), p.153.

Sánchez-Corral, P., Pouw, R.B., López-Trascasa, M. and Józsi, M., 2018. Self-damage caused by dysregulation of the complement alternative pathway: relevance of the factor H protein family. Frontiers in immunology, 9, p.1607.

Santolaya, M.E., O'Ryan, M.L., Valenzuela, M.T., Prado, V., Vergara, R., Muñoz, A., Toneatto, D., Graña, G., Wang, H., Clemens, R. and Dull, P.M., 2012. Immunogenicity and tolerability of a multicomponent meningococcal serogroup B (4CMenB) vaccine in healthy adolescents in Chile: a phase 2b/3 randomised, observer-blind, placebo-controlled study. The Lancet, 379(9816), pp.617-624.

Sato, Y., Yoshioka, K., Suzuki, C., Awashima, S., Hosaka, Y., Yewdell, J. and Kuroda, K., 2003. Localization of influenza virus proteins to nuclear dot 10 structures in influenza virus-infected cells. Virology, 310(1), pp.29-40.

Schmidt, C.Q., Hipgrave Ederveen, A.L., Harder, M.J., Wuhrer, M., Stehle, T. and Blaum, B.S., 2018. Biophysical analysis of sialic acid recognition by the complement regulator Factor H. Glycobiology, 28(10), pp.765-773.

Schneider, A.E., Sándor, N., Kárpáti, É. and Józsi, M., 2016. Complement factor H modulates the activation of human neutrophil granulocytes and the generation of neutrophil extracellular traps. Molecular Immunology, 72, pp.37-48.

Schneider, M.C., Exley, R.M., Chan, H., Feavers, I., Kang, Y.H., Sim, R.B. and Tang, C.M., 2006. Functional significance of factor H binding to Neisseria meningitidis. The Journal of Immunology, 176(12), pp.7566-7575.

Schrödinger, LLC. The PyMOL Molecular Graphics System, Version 2.4.0a0, 2020.

Schulz, O., Diebold, S.S., Chen, M., Näslund, T.I., Nolte, M.A., Alexopoulou, L., Azuma, Y.T., Flavell, R.A., Liljeström, P. and e Sousa, C.R., 2005. Toll-like receptor 3 promotes cross-priming to virus-infected cells. Nature, 433(7028), pp.887-892.

Scott, S., Molesti, E., Temperton, N., Ferrara, F., Böttcher-Friebertshäuser, E. and Daly, J., 2012. The use of equine influenza pseudotypes for serological screening. Journal of molecular and genetic medicine: an international journal of biomedical research, 6, p.304.

Seib, K.L., Brunelli, B., Brogioni, B., Palumbo, E., Bambini, S., Muzzi, A., DiMarcello, F., Marchi, S., Van der Ende, A., Aricó, B. and Savino, S., 2011. Characterization of diverse subvariants of the meningococcal factor H (fH) binding protein for their ability to bind fH, to mediate serum resistance, and to induce bactericidal antibodies. Infection and immunity, 79(2), pp.970-981.

Seib, K.L., Scarselli, M., Comanducci, M., Toneatto, D. and Masignani, V., 2015. Neisseria meningitidis factor H-binding protein fHbp: a key virulence factor and vaccine antigen. Expert review of vaccines, 14(6), pp.841-859.

Seo, S.H. and Webster, R.G., 2002. Tumor necrosis factor alpha exerts powerful anti-influenza virus effects in lung epithelial cells. Journal of virology, 76(3), pp.1071-1076.

Serruto, D., Rappuoli, R., Scarselli, M., Gros, P. and Van Strijp, J.A., 2010. Molecular mechanisms of complement evasion: learning from staphylococci and meningococci. Nature Reviews Microbiology, 8(6), pp.393-399.

Severi, E., Hood, D.W. and Thomas, G.H., 2007. Sialic acid utilization by bacterial pathogens. Microbiology, 153(9), pp.2817-2822.

Shahab S.Z., Glezen W.P. (1994) Influenza Virus. In: Gonik B. (eds) Viral Diseases in Pregnancy. Clinical Perspectives in Obstetrics and Gynecology. Springer, New York, NY. pp 215-216

Shao, S., Sun, X., Chen, Y., Zhan, B. and Zhu, X., 2019. Complement evasion: An effective strategy that parasites utilize to survive in the host. Frontiers in Microbiology, 10.

Shao, W., Li, X., Goraya, M.U., Wang, S. and Chen, J.L., 2017. Evolution of influenza a virus by mutation and re-assortment. International journal of molecular sciences, 18(8), p.1650.

Sharp, J.A., Echague, C.G., Hair, P.S., Ward, M.D., Nyalwidhe, J.O., Geoghegan, J.A., Foster, T.J. and Cunnion, K.M., 2012. Staphylococcus aureus surface protein SdrE binds complement regulator factor H as an immune evasion tactic. PloS one, 7(5).

Shaughnessy, J., Gulati, S., Agarwal, S., Unemo, M., Ohnishi, M., Su, X.H., Monks, B.G., Visintin, A., Madico, G., Lewis, L.A. and Golenbock, D.T., 2016. A Novel Factor H–Fc Chimeric Immunotherapeutic Molecule against Neisseria gonorrhoeae. The Journal of Immunology, 196(4), pp.1732-1740.

Shaughnessy, J., Vu, D.M., Punjabi, R., Serra-Pladevall, J., DeOliveira, R.B., Granoff, D.M. and Ram, S., 2014. Fusion protein comprising factor H domains 6 and 7 and human IgG1 Fc as an antibacterial immunotherapeutic. Clin. Vaccine Immunol., 21(10), pp.1452-1459.

Shaw ML, Palese P (2013) Orthomyxoviridae, In: Bernard N. Fields and David M. Knipe (ed.), Fields virology 6th edition. Philadelphia, Pa. [u.a.]: Wolters Kluwer Lippincott Williams & Wilkins, volume I, chapter 40. pp. 1151–1185.

Shaw, M.L. and Palese, P., 2013. Orthomyxoviridae. Fields virology, 1, pp.1151-1185.

Shaw, M.L., Stone, K.L., Colangelo, C.M., Gulcicek, E.E. and Palese, P., 2008. Cellular proteins in influenza virus particles. PLoS Pathog, 4(6), p.e1000085.

Shtykova, E.V., Baratova, L.A., Fedorova, N.V., Radyukhin, V.A., Ksenofontov, A.L., Volkov, V.V., Shishkov, A.V., Dolgov, A.A., Shilova, L.A., Batishchev, O.V. and Jeffries, C.M., 2013. Structural analysis of influenza A virus matrix protein M1 and its self-assemblies at low pH. PloS one, 8(12), p. e82431.

Shtyrya, Y.A., Mochalova, L.V. and Bovin, N., 2009. Influenza virus neuraminidase: structure and function. Acta Naturae (англоязычная версия), 1(2 (2)).

Sieczkarski, S.B. and Whittaker, G.R., 2002. Influenza virus can enter and infect cells in the absence of clathrin-mediated endocytosis. Journal of virology, 76(20), pp.10455-10464.

Sikorski, P.M., Commodaro, A.G. and Grigg, M.E., 2020. Toxoplasma gondii Recruits Factor H and C4b-Binding Protein to Mediate Resistance to Serum Killing and Promote Parasite Persistence in vivo. Frontiers in Immunology, 10, p.3105.

Sikorski, P.M., Commodaro, A.G. and Grigg, M.E., 2020. Toxoplasma gondii recruits factor H and C4b-binding protein to mediate resistance to serum killing and promote parasite persistence in vivo. Frontiers in Immunology, 10, p.3105.

Sim, E., Palmer, M.S., Puklavec, M. and Sim, R.B., 1983. Monoclonal antibodies against the complement control protein Factor H (β1 H). Bioscience reports, 3(12), pp.1119-1131.

Sim, R.B. and DiScipio, R.G., 1982. Purification and structural studies on the complement-system control protein β1H (factor H). Biochemical Journal, 205(2), pp.285-293.

Sim, R.B., Day, A.J., Moffatt, B.E. and Fontaine, M., 1993. [1] Complement factor I and cofactors in control of complement system convertase enzymes. In Methods in enzymology (Vol. 223, pp. 13-35). Academic Press.

Simon, N., Lasonder, E., Scheuermayer, M., Kuehn, A., Tews, S., Fischer, R., Zipfel, P.F., Skerka, C. and Pradel, G., 2013. Malaria parasites co-opt human factor H to prevent complement-mediated lysis in the mosquito midgut. Cell host & microbe, 13(1), pp.29-41.

Skehel, J.J. and Wiley, D.C., 2000. Receptor binding and membrane fusion in virus entry: the influenza haemagglutinin. Annual review of biochemistry, 69(1), pp.531-569.

Skehel, J.J., Stevens, D.J., Daniels, R.S., Douglas, A.R., Knossow, M., Wilson, I.A. and Wiley, D.C., 1984. A carbohydrate side chain on haemagglutinins of Hong Kong influenza viruses inhibits recognition by a monoclonal antibody. Proceedings of the National Academy of Sciences, 81(6), pp.1779-1783.

Skerka, C., Kühn, S., Günther, K., Lingelbach, K. and Zipfel, P.F., 1993. A novel short consensus repeat-containing molecule is related to human complement factor H. Journal of Biological Chemistry, 268(4), pp.2904-2908.

Smith, B.J., Huyton, T., Joosten, R.P., McKimm-Breschkin, J.L., Zhang, J.G., Luo, C.S., Lou, M.Z., Labrou, N.E. and Garrett, T.P., 2006. Structure of a calcium-deficient form of influenza virus neuraminidase: implications for substrate binding. Acta Crystallographica Section D: Biological Crystallography, 62(9), pp.947-952.

Spiller, O.B., Robinson, M., O'Donnell, E., Milligan, S., Morgan, B.P., Davison, A.J. and Blackbourn, D.J., 2003. Complement regulation by Kaposi's sarcoma-associated herpesvirus ORF4 protein. Journal of virology, 77(1), pp.592-599.

Sreenivasan, C.C., Thomas, M., Kaushik, R.S., Wang, D. and Li, F., 2019. Influenza A in bovine species: a narrative literature review. Viruses, 11(6), p.561.

Sriwilaijaroen, N. and Suzuki, Y., 2012. Molecular basis of the structure and function of H1 haemagglutinin of influenza virus. Proceedings of the Japan Academy, Series B, 88(6), pp.226-249.

Stevenson, B., Casjens, S., van Vugt, R.E.N.É., Porcella, S.F., Tilly, K., Bono, J.L. and Rosa, P., 1997. Characterization of cp18, a naturally truncated member of the cp32 family of Borrelia burgdorferi plasmids. Journal of Bacteriology, 179(13), pp.4285-4291.

Stevenson, B., El-Hage, N., Hines, M.A., Miller, J.C. and Babb, K., 2002. Differential binding of host complement inhibitor factor H by Borrelia burgdorferi Erp surface proteins: a possible mechanism underlying the expansive host range of Lyme disease spirochetes. Infection and immunity, 70(2), pp.491-497.

Stoermer, K.A. and Morrison, T.E., 2011. Complement and viral pathogenesis. Virology, 411(2), pp.362-373.

Straus, M.R. and Whittaker, G.R., 2017. A peptide-based approach to evaluate the adaptability of influenza A virus to humans based on its haemagglutinin proteolytic cleavage site. PloS one, 12(3), p.e0174827.

Su, S., Fu, X., Li, G., Kerlin, F. and Veit, M., 2017. Novel Influenza D virus: Epidemiology, pathology, evolution and biological characteristics. Virulence, 8(8), pp.1580-1591.

Sun, S., Wang, Q., Zhao, F., Chen, W. and Li, Z., 2011. Glycosylation site alteration in the evolution of influenza A (H1N1) viruses. PloS one, 6(7), p.e22844.

Suthar, M.S., Diamond, M.S. and Gale Jr, M., 2013. West Nile virus infection and immunity. Nature Reviews Microbiology, 11(2), pp.115-128.

Suzuki, Y., Ito, T., Suzuki, T., Holland, R.E., Chambers, T.M., Kiso, M., Ishida, H. and Kawaoka, Y., 2000. Sialic acid species as a determinant of the host range of influenza A viruses. Journal of virology, 74(24), pp.11825-11831.

Svoboda, E., Schneider, A.E., Sándor, N., Lermann, U., Staib, P., Kremlitzka, M., Bajtay, Z., Barz, D., Erdei, A. and Józsi, M., 2015. Secreted aspartic protease 2 of Candida albicans inactivates factor H and the macrophage factor H-receptors CR3 (CD11b/CD18) and CR4 (CD11c/CD18). Immunology letters, 168(1), pp.13-21.

Swinkels, M., Zhang, J.H., Tilakaratna, V., Black, G., Perveen, R., McHarg, S., Inforzato, A., Day, A.J. and Clark, S.J., 2018. C-reactive protein and pentraxin-3 binding of factor H-like protein 1 differs from complement factor H: implications for retinal inflammation. Scientific reports, 8(1), pp.1-12.

Takeda, M., Leser, G.P., Russell, C.J. and Lamb, R.A., 2003. INAUGURAL ARTICLE by a Recently Elected Academy Member: Influenza virus haemagglutinin concentrates in lipid raft microdomains for efficient viral fusion. Proceedings of the National Academy of Sciences of the United States of America, 100(25), p.14610.

Takeshita, F., Tanaka, T., Matsuda, T., Tozuka, M., Kobiyama, K., Saha, S., Matsui, K., Ishii, K.J., Coban, C., Akira, S. and Ishii, N., 2006. Toll-like receptor adaptor molecules enhance DNA-raised adaptive immune responses against influenza and tumors through activation of innate immunity. Journal of virology, 80(13), pp.6218-6224.

Takeuchi, O. and Akira, S., 2010. Pattern recognition receptors and inflammation. Cell, 140(6), pp.805-820.

Tan, M., Cui, L., Huo, X., Xia, M., Shi, F., Zeng, X., Huang, P., Zhong, W., Li, W., Xu, K. and Chen, L., 2018. Saliva as a source of reagent to study human susceptibility to avian influenza H7N9 virus infection. Emerging Microbes & Infections, 7(1), pp.1-10.

Tate, M.D., Job, E.R., Deng, Y.M., Gunalan, V., Maurer-Stroh, S. and Reading, P.C., 2014. Playing hide and seek: how glycosylation of the influenza virus haemagglutinin can modulate the immune response to infection. Viruses, 6(3), pp.1294-1316.

Temperton, N.J., Hoschler, K., Major, D., Nicolson, C., Manvell, R., Hien, V.M., Ha, D.Q., De Jong, M., Zambon, M., Takeuchi, Y. and Weiss, R.A., 2007. A sensitive retroviral pseudotype assay for influenza H5N1-neutralizing antibodies. Influenza and other respiratory viruses, 1(3), pp.105-112.

Thangavel, R.R. and Bouvier, N.M., 2014. Animal models for influenza virus pathogenesis, transmission, and immunology. Journal of immunological methods, 410, pp.60-79.

Tong, S., Li, Y., Rivailler, P., Conrardy, C., Castillo, D.A.A., Chen, L.M., Recuenco, S., Ellison, J.A., Davis, C.T., York, I.A. and Turmelle, A.S., 2012. A distinct lineage of influenza A virus from bats. Proceedings of the National Academy of Sciences, 109(11), pp.4269-4274.

Treanor, J.J., 2014. Influenza viruses. In Viral Infections of Humans (pp. 455-478). Springer US.

Trombetta, C.M., Ulivieri, C., Cox, R.J., Remarque, E.J., Centi, C., Perini, D., Piccini, G., Rossi, S., Marchi, S. and Montomoli, E., 2018. Impact of erythrocyte species on assays for influenza serology. Journal of preventive medicine and hygiene, 59(1), p. E1.

Tsiftsoglou, S.A., Arnold, J.N., Roversi, P., Crispin, M.D., Radcliffe, C., Lea, S.M., Dwek, R.A., Rudd, P.M. and Sim, R.B., 2006. Human complement factor I glycosylation: structural and functional characterisation of the N-linked oligosaccharides. Biochimica et Biophysica Acta (BBA)-Proteins and Proteomics, 1764(11), pp.1757-1766.

van Beek, A.E., Sarr, I., Correa, S., Nwakanma, D., Brouwer, M.C., Wouters, D., Secka, F., Anderson, S.T., Conway, D.J., Walther, M. and Levin, M., 2018, July. Complement Factor H levels associate with Plasmodium falciparum malaria susceptibility and severity. In Open forum infectious diseases (Vol. 5, No. 7, p. ofy166). US: Oxford University Press.

van der Maten, E., Westra, D., van Selm, S., Langereis, J.D., Bootsma, H.J., van Opzeeland, F.J., de Groot, R., Ruseva, M.M., Pickering, M.C., van den Heuvel, L.P. and van de Kar, N.C., 2016. Complement factor H serum levels determine resistance to pneumococcal invasive disease. The Journal of infectious diseases, 213(11), pp.1820-1827.

Van Epps, H.L., 2006. Influenza: exposing the true killer. The Journal of experimental medicine, 203(4), p.803.

van Riel, D., Munster, V.J., de Wit, E., Rimmelzwaan, G.F., Fouchier, R.A., Osterhaus, A.D. and Kuiken, T., 2007. Human and avian influenza viruses target different cells in the lower respiratory tract of humans and other mammals. The American journal of pathology, 171(4), pp.1215-1223.

Varki A, Gagneux P. Biological Functions of Glycans. 2017. In: Varki A, Cummings RD, Esko JD, et al., editors. Essentials of Glycobiology [Internet]. 3rd edition. Cold Spring Harbor (NY): Cold Spring Harbor Laboratory Press; 2015-2017. Chapter 7. Available from: https://www.ncbi.nlm.nih.gov/books/NBK453034/ doi: 10.1101/glycobiology.3e.007

Vasin, A.V., Temkina, O.A., Egorov, V.V., Klotchenko, S.A., Plotnikova, M.A. and Kiselev, O.I., 2014. Molecular mechanisms enhancing the proteome of influenza A viruses: an overview of recently discovered proteins. Virus research, 185, pp.53-63.

ViralZone Alpha-influenza virus, Molecular biology. www.expasy.org/viralzone, Swiss Institute of Bioinformatics.

Virgin, H.4., Latreille, P., Wamsley, P., Hallsworth, K., Weck, K.E., Dal Canto, A.J. and Speck, S.H., 1997. Complete sequence and genomic analysis of murine gammaherpesvirus 68. Journal of virology, 71(8), pp.5894-5904.

Vogl, G., Lesiak, I., Jensen, D.B., Perkhofer, S., Eck, R., Speth, C., Lass-Flörl, C., Zipfel, P.F., Blom, A.M., Dierich, M.P. and Würzner, R., 2008. Immune evasion by acquisition of complement inhibitors: the mould Aspergillus binds both factor H and C4b binding protein. Molecular immunology, 45(5), pp.1485-1493.

Walker, A.P. and Fodor, E., 2019. Interplay between influenza virus and the host RNA polymerase II transcriptional machinery. Trends in microbiology, 27(5), pp.398-407.

Wang, F.M., Yu, F. and Zhao, M.H., 2013. A method of purifying intact complement factor H from human plasma. Protein expression and purification, 91(2), pp.105-111.

Wang, F.M., Yu, F. and Zhao, M.H., 2013. A method of purifying intact complement factor H from human plasma. Protein expression and purification, 91(2), pp.105-111.

Webster, R.G., Bean, W.J., Gorman, O.T., Chambers, T.M. and Kawaoka, Y., 1992. Evolution and ecology of influenza A viruses. Microbiology and molecular biology reviews, 56(1), pp.152-179.

Weiler, J.M., Daha, M.R., Austen, K.F. and Fearon, D.T., 1976. Control of the amplification convertase of complement by the plasma protein beta1H. Proceedings of the National Academy of Sciences, 73(9), pp.3268-3272.

Weis, W., Brown, J.H., Cusack, S., Paulson, J.C., Skehel, J.J. and Wiley, D.C., 1988. Structure of the influenza virus haemagglutinin complexed with its receptor, sialic acid. Nature, 333(6172), pp.426-431.

Whaley, K.E.I.T.H. and Ruddy, S.H.A.U.N., 1976. Modulation of the alternative complement pathways by beta 1 H globulin. The Journal of experimental medicine, 144(5), pp.1147-1163.

White, J.M. and Whittaker, G.R., 2016. Fusion of enveloped viruses in endosomes. Traffic, 17(6), pp.593-614.

Wille, M., Latorre-Margalef, N. and Waldenström, J., 2017. Of ducks and men: ecology and evolution of a zoonotic pathogen in a wild reservoir host. In Modeling the transmission and prevention of infectious disease (pp. 247-286). Springer, Cham.

Winn, E.S., Hu, S.P., Hochschwender, S.M. and Laursen, R.A., 1980. Studies on the lysine-binding sites of human plasminogen: the effect of ligand structure on the binding of lysine analogs to plasminogen. European journal of biochemistry, 104(2), pp.579-586.

Wong, S.M., Shaughnessy, J., Ram, S. and Akerley, B.J., 2016. Defining the binding region in factor H to develop a therapeutic factor H-Fc fusion protein against non-typeable Haemophilus influenzae. Frontiers in cellular and infection microbiology, 6, p.40.

Wu, W.W., Weaver, L.L. and Panté, N., 2007. Ultrastructural analysis of the nuclear localization sequences on influenza A ribonucleoprotein complexes. Journal of molecular biology, 374(4), pp.910-916.

Wu, Y., Wu, Y., Tefsen, B., Shi, Y. and Gao, G.F., 2014. Bat-derived influenza-like viruses H17N10 and H18N11. Trends in microbiology, 22(4), pp.183-191.

Xu, R., Ekiert, D.C., Krause, J.C., Hai, R., Crowe, J.E. and Wilson, I.A., 2010. Structural basis of preexisting immunity to the 2009 H1N1 pandemic influenza virus. Science, 328(5976), pp.357-360.

Xu, R., McBride, R., Nycholat, C.M., Paulson, J.C. and Wilson, I.A., 2012. Structural characterization of the haemagglutinin receptor specificity from the 2009 H1N1 influenza pandemic. Journal of virology, 86(2), pp.982-990.

Yang, J., Li, H., Jia, L., Lan, X., Zhao, Y., Bian, H. and Li, Z., 2019. High expression levels of influenza virus receptors in airway of the HBV-transgenic mice. Epidemiology & Infection, 147.

Yang, X., Steukers, L., Forier, K., Xiong, R., Braeckmans, K., Van Reeth, K. and Nauwynck, H., 2014. A beneficiary role for neuraminidase in influenza virus penetration through the respiratory mucus. PloS one, 9(10), p.e110026.

Yoneyama, M., Onomoto, K., Jogi, M., Akaboshi, T. and Fujita, T., 2015. Viral RNA detection by RIG-I-like receptors. Current opinion in immunology, 32, pp.48-53.

York, A., Hengrung, N., Vreede, F.T., Huiskonen, J.T. and Fodor, E., 2013. Isolation and characterization of the positive-sense replicative intermediate of a negative-strand RNA virus. Proceedings of the National Academy of Sciences, 110(45), pp.E4238-E4245.

Youn, S., Ambrose, R.L., Mackenzie, J.M. and Diamond, M.S., 2013. Non-structural protein-1 is required for West Nile virus replication complex formation and viral RNA synthesis. Virology journal, 10(1), p.339.

Yu, B.B., Moffatt, B.E., Fedorova, M., Villiers, C.G., Arnold, J.N., Du, E., Swinkels, A., Li, M.C., Ryan, A. and Sim, R.B., 2014. Purification, quantification, and functional analysis of Complement Factor H. In The Complement System (pp. 207-223). Humana Press, Totowa, NJ.

Zhang, J., Leser, G.P., Pekosz, A. and Lamb, R.A., 2000. The cytoplasmic tails of the influenza virus spike glycoproteins are required for normal genome packaging. Virology, 269(2), pp.325-334.

Zhang, J., Li, G., Liu, X., Wang, Z., Liu, W. and Ye, X., 2009. Influenza A virus M1 blocks the classical complement pathway through interacting with C1qA. Journal of general virology, 90(11), pp.2751-2758.

Zhang, J.J., Jiang, L., Liu, G., Wang, S.X., Zou, W.Z., Zhang, H. and Zhao, M.H., 2009. Levels of urinary complement factor H in patients with IgA nephropathy are closely associated with disease activity. Scandinavian journal of immunology, 69(5), pp.457-464.

Zhang, L., Wang, J., Muñoz-Moreno, R., Kim, M., Sakthivel, R., Mo, W., Shao, D., Anantharaman, A., García-Sastre, A., Conrad, N.K. and Fontoura, B.M., 2018. Influenza virus NS1 protein-RNA interactome reveals intron targeting. Journal of virology, 92(24).

Zhang, W., Shi, Y., Lu, X., Shu, Y., Qi, J. and Gao, G.F., 2013. An airborne transmissible avian influenza H5 haemagglutinin seen at the atomic level. Science, 340(6139), pp.1463-1467.

Zhang, Y., Wu, M., Hang, T., Wang, C., Yang, Y., Pan, W., Zang, J., Zhang, M. and Zhang, X., 2017. Staphylococcus aureus SdrE captures complement factor H's C-terminus via a novel ‘close, dock, lock and latch'mechanism for complement evasion. Biochemical Journal, 474(10), pp.1619-1631.

Zhao, M., Wang, L. and Li, S., 2017. Influenza A Virus–Host Protein Interactions Control Viral Pathogenesis. International journal of molecular sciences, 18(8), p.1673.

Zipfel, P.F. and Skerka, C., 2009. Complement regulators and inhibitory proteins. Nature Reviews Immunology, 9(10), pp.729-740.

Zipfel, P.F. and Skerka, C., 2014. Staphylococcus aureus: the multi headed hydra resists and controls human complement response in multiple ways. International Journal of Medical Microbiology, 304(2), pp.188-194.

Zipfel, P.F., Hallström, T., and Riesbeck, K. (2013) Human complement control and complement evasion by pathogenic microbes-tipping the balance. Mol Immunol 56: 152–160.

Zipfel, P.F., Hallström, T., Hammerschmidt, S., and Skerka, C. (2008) The complement fitness factor H: role in human diseases and for immune escape of pathogens, like pneumococci. Vaccine 26(Suppl 8): I67–74.

Zipfel, P.F., Hellwage, J., Friese, M.A., Hegasy, G., Jokiranta, S.T. and Meri, S., 1999. Factor H and disease: a complement regulator affects vital body functions. Molecular immunology, 36(4-5), pp.241-248.

Zipfel, P.F., Würzner, R., and Skerka, C. (2007) Complement evasion of pathogens: common strategies are shared by diverse organisms. Mol Immunol 44: 3850–3857.

Zurcher, T., Luo, G. and Palese, P., 1994. Mutations at palmitylation sites of the influenza virus haemagglutinin affect virus formation. Journal of virology, 68(9), pp.5748-5754.

Appendices

Appendix A. H1 HA - Influenza A virus (A/England/195/09 (H1N1))

```
        10         20         30         40         50
MKAILVVLLY TFATANADTL CIGYHANNST DTVDTVLEKN VTVTHSVNIL
        60         70         80         90        100
EDKHNGKLCK LRGVAPLHLG KCNIAGWILG NPECESLSTA SSWSYIVETS
       110        120        130        140        150
SSDNGTCYPG DFIDYEELRE QLSSVSSFER FEIFPKTSSW PNHDSNKGVT
       160        170        180        190        200
AACPHAGAKS FYKNLIWLVK KGNSYPKLSK SYINDKGKEV LVLWGIHHPS
       210        220        230        240        250
TSADQQSLYQ NADAYVFVGS SRYSKKFKPE IAIRPKVRDQ EGRMNYYWTL
       260        270        280        290        300
VEPGDKITFE ATGNLVVPRY AFAMERNAGS GIIISDTPVH DCNTTCQTPK
       310        320        330        340        350
GAINTSLPFQ NIHPITIGKC PKYVKSTKLR LATGLRNVPS IQSRGLFGAI
       360        370        380        390        400
AGFIEGGWTG MVDGWYGYHH QNEQGSGYAA DLKSTQNAID EITNKVNSVI
       410        420        430        440        450
EKMNTQFTAV GKEFNHLEKR IENLNKKVDD GFLDIWTYNA ELLVLLENER
       460        470        480        490        500
TLDYHDSNVK NLYEKVRSQL KNNAKEIGNG CFEFYHKCDN TCMESVKNGT
       510        520        530        540        550
YDYPKYSEEA KLNREEIDGV KLESTRIYQI LAIYSTVASS LVLVVSLGAI
       560
SFWMCSNGSL QCRICI
```

Appendix B. H3 HA - Influenza A virus (A/Hong Kong/1774/99(H3N2)

```
        10         20         30         40         50
MKTIIALSYI LCLVFAQKLP GNDNSTATLC LGHHAVPNGT LVKTITNDQI
        60         70         80         90        100
EVTNATELVQ SSSTGRICDS PHQILDGENC TLIDALLGDP HCDGFQNKEW
       110        120        130        140        150
NLFVERSKAY SNCYPYDVPD YASLRSLVAS SGTLEFNNEN FNWTGVAQNG
       160        170        180        190        200
TSSACKRRSI KSFFSRLNWL HQLKYRYPAL NVTMPNNDKF DKLYIWGVHH
       210        220        230        240        250
PSTDSDQTSL YAQASGRVTV STKRSQQTVI PNIGSGPWVR GVSSRISIYW
       260        270        280        290        300
TIVKPGDILL INSTGNLIAP RGYFKIRSGK SSIMRSDAPI GKCNSECITP
       310        320        330        340        350
NGSIPNDKPF QNVNRITYGA CPRYVKQNTL KLATGMRNVP EKQTRGIFGA
       360        370        380        390        400
IAGFIENGWE GMMDGWYGFR HQNSEGTGQA ADLKSTQAAI NQINGKLNRL
       410        420        430        440        450
IEKTNEKFHQ IEKEFSEVEG RIQDLEKYVE DTKIDLWSYN AELLVALENQ
       460        470        480        490        500
HTIDLTDSEM NKLFERTRKQ LRENAEDMGN GCFKIYHKCD NACIGSIRNG
       510        520        530        540        550
TYDHDVYRDE ALNNRFQIKG VELKSGYKDW ILWISFAISC FLLCVVLLGF
       560
IMWACQKGNI RCNICI
```